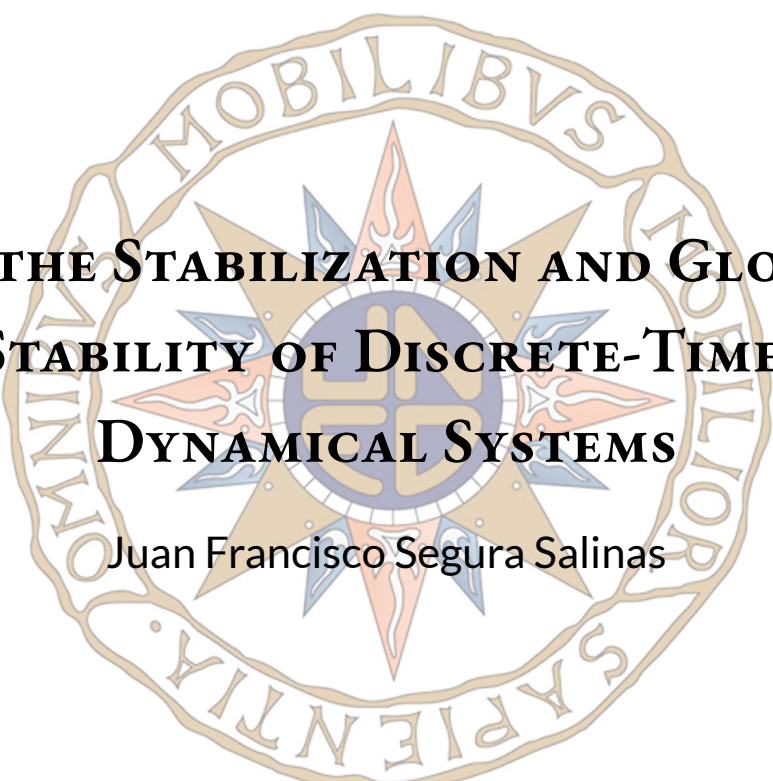# TESIS DOCTORAL

2020

On the Stabilization and Global Stability of Discrete-Time Dynamical Systems

Juan Francisco Segura Salinas

PROGRAMA DE DOCTORADO EN TECNOLOGÍAS INDUSTRIALES

Departamento de Matemática Aplicada

Directores: Daniel Franco Leis y Juan Perán Mazón

Autor: Juan Francisco Segura Salinas

Directores: Daniel Franco Leis y Juan Perán Mazón

To my sister Loli, who will always be in my heart

A mi hermana Loli, a quien llevaré siempre en mi corazón

Acknowledgments

First and foremost I wish to thank my supervisors Daniel Franco and Juan Perán who restlessly provided me with guidance and advice. They have been extremely generous with their time and support, which allowed me to develop research competencies with critical thinking. For these reasons, and many others, I am very grateful.

Alongside my supervisors I wish to express sincere gratitude to Prof. Frank Hilker. I really appreciate his support, hospitality and generosity. Discussing with him various aspects of my research helped me grow as a scientist. My sincere thanks also go to the research group and administration staff of the Institute of Environmental Systems Research at Osnabrück University for their great hospitality during my research stays.

On a more personal note, I firstly want to thank my daughter for her unwavering support and love. Invaluable support was also provided by all the rest of my family, to whom I extend my gratitude. I should like to apologize to all of them for the family time that my research stole. Finally, I dedicate this thesis to my sister Loli. Although she passed away before this research started, she is the main reason for it. Apart from her unconditional love, she always trusted in me more than I trusted myself and encouraged me to continue my studies. As the dedication at the beginning of this thesis reads, *I will always have her in my heart*.

Agradecimientos

P𝚛𝚒𝚖𝚎𝚛𝚘 𝚢 𝚊𝚗𝚝𝚎 𝚝𝚘𝚍𝚘 deseo agradecer a mis directores, Daniel Franco y Juan Perán, los consejos y la orientación que de forma incansable me han brindado. Han sido extremadamente generosos con su tiempo y apoyo, lo que me permitió desarrollar mi capacidad investigadora con pensamiento crítico. Por estas razones, y por muchas otras, les estoy muy agradecido.

Junto a mis supervisores, deseo expresar mi sincero agradecimiento al Prof. Frank Hilker. Aprecio enormemente su apoyo, hospitalidad y generosidad. Discutir con él varios aspectos de mi investigación me ayudó a crecer como científico. Vaya también mi sincero agradecimiento para el grupo de investigación y el personal de administración del Instituto de Investigación de Sistemas Ambientales de la Universidad de Osnabrück por su gran hospitalidad durante mis estancias de investigación.

En una nota más personal, en primer lugar quiero agradecer a mi hija su apoyo y amor inquebrantables. También he recibido apoyo inestimable del resto de mi familia, a quienes extiendo mi gratitud. Me gustaría disculparme con todos ellos por el tiempo familiar que robó mi investigación. Finalmente, dedico esta tesis a mi hermana Loli. Aunque falleció antes de que comenzara esta investigación, ella es la razón principal por la que ésta se ha llevado a cabo. Además de su amor incondicional, siempre confió en mí más que yo mismo y me animó a continuar mis estudios. Como dice la dedicatoria al comienzo de esta tesis, *siempre la tendré en mi corazón*.

Abstract

This thesis studies the stability of one-dimensional discrete-time dynamical systems, which can exhibit very complicated dynamics. In the case of ecological systems, which are the focus of the research conducted, this is in line with the well known fact that for biological populations fluctuations in size are ubiquitous. A major concern in management programs is how to control these fluctuations when they have undesired effects. Ecological systems have the added difficulty that it is not possible to alter the dynamics by modifying the system parameters in real time. As a consequence, many of the techniques for chaos control developed in the last three decades are not suitable for the control of biological populations.

In this thesis, we present two new control strategies that instead of modifying the system parameters directly affect the state variable. We provide analytical results showing that these techniques reduce the oscillations in the population size, and thus their application improves the stability of the managed populations. Nevertheless, the complexity of nature complicates the analysis. Biological populations can exhibit counter-intuitive behaviors, e.g., increased population size when harvested or higher risk of extinction when restocked. In view of this complexity, we investigate the performance of the two techniques introduced in this thesis in different scenarios including biological realities, e.g., noise, lattice effect or Allee effect.

The analysis of these control strategies leads us to a problem about piecewise smooth dynamical systems. We study a degenerate bifurcation structure of a family of piecewise linear maps and introduce a new type of bifurcation for these maps. We provide theoretical results that constitute a complete description of both the bifurcation structure and the dynamics of the system at the bifurcation points. In particular, these results allow us to complete the solution of a recent problem proposed in the field of economics. This is a clear illustration that discrete dynamical systems play an important role in a wide range of fields, and that the results presented in this thesis have potential interest in fields different from population dynamics, e.g., in engineering.

Another focus of this thesis is on the global stability of one-dimensional discrete-time systems. This stability property is the most desirable one, since it allows to predict the long-rung behavior of the system with independence of the initial condition. How-

ever, proving that a system possesses this property is in general a difficult task. In the case of exploited populations, several aspects may affect their global stability. It is well known that harvesting can stabilize populations that have a unique positive equilibrium by converting this equilibrium into a global attractor. Yet, as aforementioned, ecological systems are tremendously complex. In the last years, great controversy has emerged about the effect of harvest timing on the populations stability. In this thesis, we investigate the combined effect of harvesting effort and harvest timing on the global stability. We prove that for general overcompensatory models the moment of intervention has no effect on the global stability of the positive equilibrium when the harvesting effort is high enough. We also show that harvest timing can be both stabilizing and destabilizing by itself. With the latter, we disprove a conjecture recently appeared in the literature. In the case of the Ricker model, which is one of the most relevant models in population dynamics, we prove that delaying harvesting has no effect on the global stability of the system for any harvesting effort. We also introduce an innovative method that provides similar results for a broad family of compensatory models common in population dynamics, e.g., the Bellows, the Maynard-Smith-Slatkin or the Hassell model. This study allows us to obtain new global stability results for some of these models even in absence of control.

The last problem addressed in this thesis is about the global stability of generic one-dimensional discrete systems. We introduce a new method for the study of the global stability, which complements and extends existing results in the literature in several directions. Finally, we provide several examples showing the applicability of this method.

Resumen

Esta tesis estudia la estabilidad de sistemas dinámicos unidimensionales discretos, los cuales pueden presentar dinámicas muy complejas. En el caso de los sistemas ecológicos, los cuales son el foco de la investigación llevada a cabo, esto está en línea con el hecho bien conocido de que las fluctuaciones en el tamaño de las poblaciones biológicas son ubicuas. Cómo reducir estas fluctuaciones cuando su efecto es no deseado es una de las mayores preocupaciones en programas de gestión de poblaciones. Los sistemas ecológicos tienen la dificultad añadida de que no es posible alterar su dinámica modificando directamente los parámetros del sistema en tiempo real. Como consecuencia, muchas de las técnicas para el control del caos desarrolladas en las últimas tres décadas no son aplicables en el control de poblaciones biológicas.

En esta tesis presentamos dos nuevas estrategias de control que en lugar de modificar los parámetros del sistema afectan directamente a la variable de estado. Proporcionamos resultados analíticos que muestran que estas técnicas reducen las oscilaciones en el tamaño de las poblaciones y, por tanto, su aplicación mejora la estabilidad de las poblaciones controladas. Sin embargo, la complejidad de la naturaleza complica el análisis. Las poblaciones biológicas pueden mostrar comportamientos aparentemente ilógicos, como puede ser un mayor tamaño de población cuando se eliminan individuos o un mayor riesgo de extinción cuando éstos son repuestos. En vista de esta complejidad, investigamos el desempeño de las dos técnicas introducidas en esta tesis en diferentes escenarios que incluyen realidades biológicas como ruido, efecto retícula o efecto Allee.

El análisis de estas dos estrategias de control nos lleva a un problema sobre sistemas dinámicos diferenciables a trozos. Estudiamos una estructura de bifurcación degenerada de una familia de funciones lineales a trozos e introducimos un nuevo tipo de bifurcación para estas funciones. Proporcionamos resultados teóricos que brindan una completa descripción tanto de la estructura de bifurcación como de la dinámica del sistema en los puntos de bifurcación. En particular, estos resultados nos permiten completar la solución de un problema aparecido recientemente en el campo de la economía. Esto constituye una muestra clara de que los sistemas dinámicos discretos juegan un papel importante en gran variedad de áreas, y de que los resultados presentados en esta

tesis son de potencial interés en campos distintos a la dinámica de poblaciones, e.g., en ingeniería.

Otro foco de esta tesis se halla en la estabilidad global de sistemas unidimensionales discretos. Esta propiedad de estabilidad es la más deseable, dado que permite predecir el comportamiento a largo plazo del sistema con independencia de la condición inicial. Sin embargo, probar que un sistema posee esta propiedad es en general una tarea difícil. En el caso de la gestión de poblaciones, varios aspectos pueden afectar a la estabilidad global de las poblaciones controladas. Es bien conocido que la reducción de población puede estabilizar poblaciones que posean un único equilibrio positivo convirtiendo a este equilibrio en un atractor global. Sin embargo, como ya se ha mencionado, los sistemas ecológicos son tremendamente complejos. En los últimos años se ha generado gran controversia sobre el efecto del momento de captura de individuos en la estabilidad de las poblaciones explotadas. En esta tesis investigamos el efecto combinado de la intensidad de captura y del momento en que ésta se realiza sobre la estabilidad global. Probamos que para modelos sobrecompensatorios generales el momento de intervención no tiene efecto sobre la estabilidad global del equilibrio positivo cuando la intensidad de captura es suficientemente alta. También probamos que el momento de captura puede ser tanto estabilizante como desestabilizante por él mismo. Esto último nos permite probar la falsedad de una conjetura recientemente aparecida en la literatura. En el caso del modelo de Ricker, el cual es uno de los modelos más relevantes en dinámica de poblaciones, probamos que retardar la captura no tiene efecto alguno sobre la estabilidad global del sistema para ninguna intensidad de captura. Introducimos asimismo un novedoso método que proporciona resultados similares para una amplia familia de modelos compensatorios usuales en dinámica de poblaciones, e.g., los modelos de Bellows, de Maynard-Smith-Slatkin o de Hassell. Este estudio nos permite obtener nuevos resultados de estabilidad global para algunos de estos modelos incluso en ausencia de control.

El último problema considerado en esta tesis trata de la estabilidad global de sistemas unidimensionales discretos genéricos. Proponemos un nuevo método para el estudio de la estabilidad global, el cual complementa y extiende resultados existentes en la literatura en varias direcciones. Finalmente, proporcionamos varios ejemplos que muestran la aplicabilidad de este método.

Contents

RESEARCH LINE II.   HARVEST TIMING AND GLOBAL STABILITY
OF ONE-DIMENSIONAL DISCRETE DYNAMICAL
SYSTEMS   123

Conclusions and future prospects   213

References   219

List of figures

Introduction

Motivation

One of the most powerful tools to model natural phenomena are dynamical systems. Since the pioneering work of Poincaré in the late nineteenth century [171], the study of these systems has emerged as a rich discipline from both theoretical and practical points of view. From physics up to economics, dynamical systems transversely appear in almost all branches of science and engineering.

The focus of this thesis is on nonlinear one-dimensional discrete-time dynamical systems and, in particular, on their applications to population dynamics. In spite of their apparent simplicity and contrary to the continuous-time case, these systems can present an incredibly complex behavior [154], and their understanding is far from complete. Given one of these systems, the main concern is about the long-run behavior of its solutions.

Chaotic dynamics corresponds to the worse case scenario. Even though the evolution of chaotic deterministic systems is fully determined by the initial condition, small uncertainties are amplified enormously fast. In this case, long-term predictions become impossible. In practice, this unpredictability can also be extended to many systems with periodic dynamics [207]. After the seminal work of Ott *et al.* [164], numerous control methods have been proposed aimed at avoiding this unpredictability by guaranteeing that the system behaves as desired [7]. Most of these techniques are based on the modification of the system parameters in real time. Unfortunately, this is not possible for most ecological systems, which are characterized by intrinsic uncertainty and inaccessibility of parameters such as life-history traits. One of the goals of this thesis is to propose new techniques that allow to control biological populations exhibiting erratic fluctuations.

Global stability is the best case scenario for discrete one-dimensional dynamical systems. It occurs when the system has a unique positive equilibrium and all nonzero solutions are attracted towards it. In this case, the dynamics are stable under perturbations of the state variable and it is possible to predict the fate of the system with independence of the initial condition. However, proving the global stability of a system is in general a hard task. Another goal of this thesis is to provide sufficient conditions for this property.

Research lines and contributions

The contributions of this thesis follow two different research lines. With the first of them, two new techniques for the control of biological populations are proposed and analyzed. Given that modifying parameters in real time is unfeasible for most ecological systems, these techniques directly modify the state variable.

The analytical results that are obtained constitute a complete theoretical basis for these two strategies. Moreover, both theoretical results and numerical simulations are provided showing how these strategies might help to improve certain aspects of the managed populations, e.g., by reducing the risk of extinction in the case of endangered species or by reducing the risk of population outbreaks in the case of pest species.

The theoretical analysis performed for one of these techniques leads us to define a type of bifurcation of piecewise smooth dynamical systems which, to the best of our knowledge, has not been previously reported. Besides, this analysis allows us to complete the solution of a problem previously appeared in the field of economics and to provide a complete description of a bifurcation structure for a family of piecesiwe-smooth dynamical systems.

The second research line of this thesis is aimed at studying the global stability of certain dynamical systems in the field of population dynamics and to provide sufficient conditions for this property in a general framework. In particular, the combined effect of harvesting intensity and harvesting time on the stability of discrete populations is

studied. For general overcompensatory population models, we prove that the system is globally stable if the harvesting intensity is high enough. To the best of our knowledge, this is the first global stability result involving harvesting timing and harvesting effort valid for a general family of models. For the Ricker model [176], which is one of the most relevant models in discrete-time population dynamics, the global stability of the system is proved for all possible harvesting times. By means of an innovative method, such a result is also obtained for a broad family of compensatory models common in population dynamics. Prominent among them are the Bellows, Maynard-Smith-Slatkin and Thieme models. For some of them, new results for the global stability in absence of harvesting are also provided.

Finally, a new method to study the stability of general one-dimensional discrete-time models is proposed. This method complements and extends some existing conditions for the global stability. In particular, we provide a global stability condition improving the condition of negative Schwarzian derivative.

We want to highlight that discrete dynamical systems play an important role in a wide range of fields, particularly in engineering. Therefore, the results presented in this thesis have potential interest in fields different from population dynamics.

STRUCTURE OF THIS THESIS AND RELATED PAPERS

This thesis is organized into two parts, which correspond to the aforementioned two research lines. Chapters of these parts correspond to research papers as follows:

Research line I: Control of fluctuations through adaptive limiters

Chapter 1. A new method for the control of biological populations is introduced and analyzed. This is an adaptive limiter strategy that consists in removing individuals when in a given generation the population grows disproportionately with respect to the previous generation.

J. Segura, F. M. Hilker and D. Franco. Adaptive threshold harvesting and the suppression of transients. *Journal of Theoretical Biology*, 395:103–114, 2016.

Chapter 2. The effect of adaptive limiter control methods is studied in presence of biological mechanisms causing extinctions and pest outbreaks.

J. Segura, F. M. Hilker and D. Franco. Population control methods in stochastic extinction and outbreak scenarios. *PloS One*, 12(2):e0170837, 2017.

Chapter 3. A new adaptive limiter strategy that combines harvesting and restocking is introduced and studied. The focus is on the advantages that the combination of harvesting and restocking may have over only harvesting or only restocking.

J. Segura, F. M. Hilker and D. Franco. Enhancing population stability with combined adaptive limiter control and finding the optimal harvesting-restocking balance. *Theoretical Population Biology*, 130:1–12, 2019.

Chapter 4. A bifurcation structure for a family of piecewise smooth maps is studied and a new type of degenerate bifurcations for these maps is presented and analyzed.

J. Segura, F. M. Hilker and D. Franco. Degenerate period adding bifurcation structure of 1D bimodal piecewise linear maps. *Under review in SIAM Journal on Applied Mathematics*.

Research line II: Harvest timing and global stability of one-dimensional discrete dynamical systems

Chapter 5. The combined effect of harvesting intensity and harvesting time on the global stability of discrete-time populations is studied.

D. Franco, H. Logemann, J. Perán and J. Segura. Dynamics of the discrete Seno population model: Combined effects of harvest timing and intensity on population stability. *Applied Mathematical Modelling*, 48:885–898, 2017.

Chapter 6. The global stability of populations governed by the Ricker model and harvested at any time during the reproductive season is studied.

D. Franco, J. Perán and J. Segura. Effect of harvest timing on the dynamics of the Ricker–Seno model. *Mathematical Biosciences*, 306:180–185, 2018.

Chapter 7. A new method to study the local and global stability of populations subject to delayed harvesting is proposed.

D. Franco, J. Perán and J. Segura. Global stability of discrete dynamical systems via exponent analysis: applications to harvesting population models. *Electronic Journal of Qualitative Theory of Differential Equations*, 101:1–22, 2018.

Chapter 8. A new method to study the global stability of general one-dimensional discrete-time models is proposed.

D. Franco, J. Perán and J. Segura. Stability for one-dimensional discrete dynamical systems revisited. *Discrete and Continuous Dynamical Systems–B*, 25(2):635-650, 2020.

Research line I

Control of fluctuations

through adaptive limiters

There is no branch of mathematics, however abstract, which may
not some day be applied to phenomena of the real world.

Nikolai Lobachevsky

o

1

Adaptive threshold harvesting and the suppression of transients

1.1   Introduction

In the last decades, the concern about the consequences of population oscillations for ecosystems has grown [15]. These fluctuations are ubiquitous [72, 150, 172] and have multiple causes [15, 116, 180, 215]. Although they may have positive effects, e.g., increased biodiversity [9, 110] or enhanced persistence in metapopulations because of desynchronization [2], their consequences can also be negative, e.g., more variable yield of exploited populations [219], the occurrence of pest outbreaks [70], increased extinction risk [178] or the loss of genetic variability and increased inbreeding [4, 24].

Potential management strategies to deal with population fluctuations have recently come into focus [15]. They can be aimed at maintaining oscillations because of their positive effects but at avoiding some undesirable aspects [109], or at inducing certain responses at targeted points in time [107]. Many management strategies, however, are

concerned with reducing fluctuations to avoid some of their negative consequences. Here, we propose and analyze one of these strategies. It is a harvesting control method that takes effect only if the population size has grown by at least a certain factor in comparison to the previous census. This conditional strategy differs from textbook strategies like constant-effort and constant-yield harvesting, as it responds only to population increases sufficiently large. We shall refer to this strategy as *adaptive threshold harvesting (ATH)* and the *harvesting version of adaptive limiter control (h-ALC)*, because it is closely related to threshold harvesting, also known as limiter control (LC), on the one hand and to adaptive limiter control (ALC) on the other hand.

Threshold harvesting removes individuals from a population whenever the population size exceeds a fixed threshold value [83, 132]. This harvest control rule is equivalent to limiter control, which is a method originating from physics [48, 195, 217] and has been applied to problems as diverse as computer architecture design [65], cardiac rhythms [88], commodity markets [101], and population dynamics [105, 106]. Limiter control methods have the advantage that no detailed information of the system is required, which is why they are easy and fast to implement. Similarly to some other population control methods, e.g., [59, 81, 141, 157, 168, 197, 212], they directly affect the state variables, i.e., the population size, by restocking (adding) or harvesting (removing) individuals. This approach seems particularly apt for ecological systems that are characterized by intrinsic uncertainty and 'inaccessibility' of parameters such as life-history traits.

Adaptive limiter control was proposed by Sah *et al.* [184]. The idea of ALC is to add individuals to the population whenever the population size falls below a certain fraction of its value in the previous generation. The term 'adaptive' follows form the fact that the threshold value of the population size triggering control is a fraction of the previous population size, and as such variable over time. The efficacy of ALC to stabilize biological populations has been shown in laboratory experiments on populations and metapopulations of the fruit fly *Drosophila melanogaster* [184] as well as by analytical results [77] and numerical simulations [77, 183, 184, 212].

However, from the application point of view, ALC has a major caveat. As a restocking strategy, it requires the availability of a versatile source of individuals which can be used to augment the population if needed. Such a pool of individuals may be difficult or even impossible to create or to maintain in practice. For instance, some organisms cannot be kept in captivity or do not reproduce in such conditions. Moreover, there may be issues of translocation and releasing individuals. Maintaining and managing a stock may be costly, labor-intensive, logistically challenging, and time-consuming. These drawbacks are due to the restocking component and thus intrinsically linked with ALC.

By contrast, removing individuals as an intervention method can offer various advantages. It may be easier or cheaper than restocking or simply possible when augmenting a population is out of the question. In practice, one could draw upon experience from a wide range of established harvesting, hunting, exploitation, and culling methods. Removal methods may be difficult to implement as well and may raise ethical concerns about killing animals. Yet, it is easy to imagine that reducing population size seems, in many circumstances, more obvious than augmenting population size.

Being based on harvesting rather than restocking, the harvest control rule presented in this chapter is the harvesting version of adaptive limiter control. That is, whenever the population size exceeds a certain proportion of its value in the preceding generation, harvesting takes place and reduces the population size to the preceding value. In contrast to threshold harvesting, the critical population size above which interventions take place is not fixed, but is adaptive in response to the previous population size.

While replacing restocking by harvesting appears straightforward and sensible from a biological and practical point of view, there is no reason to believe that the dynamical behavior induced by ALC on the one hand and by its harvesting version ATH on the other hand is similar. This becomes clear when considering other control strategies that have harvesting and restocking variants. For instance, proportional feedback control [92] is able to stabilize a population towards a positive equilibrium when a constant proportion of the population is harvested [141], but the restocking variant adding a

constant proportion of the population fails to stabilize the equilibrium [38]. Constant feedback control provides another dramatic example. While both adding or removing a constant number of individuals each generation can stabilize chaotic dynamics [93, 157, 200], the latter form of intervention can drive the population extinct at small removal rates, even when the population is able to persist for higher removal rates [189, 196]. These examples arise in the simplest case of single-species models given by unimodal maps that we also consider here.

In the next section, we introduce the mathematical model describing adaptive threshold harvesting. We then analyze in Section 1.3 its effect on the constancy stability in terms of two different measures, namely the fluctuation range and the fluctuation index. Since ATH is a harvesting strategy and the individuals removed may be actually of economic interest (e.g., in fisheries), Section 1.4 considers the mean yield per generation, both in the long-run and the short-run. Section 1.5 focuses on the short-term dynamics generated by the interventions. Transients are often ignored in theoretical studies of ecological systems, which is why we discuss in some detail how to deal with them. In particular, we propose adjusted versions of both ATH and ALC that reduce the length of transients and thus accelerate the approach to the long-term dynamics. Finally, Section 1.6 summarizes the results obtained and draws conclusions.

1.2 Adaptive threshold harvesting

1.2.1 Population growth model

The effect of a control method on a biological population depends on the underlying population dynamics, so we start by describing the model of the uncontrolled system. We assume that the population dynamics are described by a first-order one-dimensional difference equation

$$x_{t+1} = f(x_t), \ x_0 \in [0, +\infty), \ t \in \mathbb{N}, \tag{1.1}$$

where x_t denotes the population size at time step t. The population production map f is assumed to satisfy the following conditions:

(A1) $f : [0, b] \to [0, b]$ ($b = +\infty$ is allowed) is continuously differentiable and such that $f(0) = 0$, $f(x) > 0$ for all $x \in (0, b)$ and $f'(0^+), f'(b^-) \in \mathbb{R}$.

(A2) f has two non-negative fixed points $x = 0$ and $x = K > 0$, with $f(x) > x$ for $0 < x < K$ and $f(x) < x$ for $x > K$.

(A3) f has a unique critical point $d \in (0, K)$ in such a way that $f(d) \leq b$, $f'(x) > 0$ for all $x \in (0, d)$ and $f'(x) < 0$ for all $x \in (d, b)$.

(A4) f is concave downward on $[0, d]$.

These conditions describe a unimodal population production function peaking at $x = d$ and are standard assumptions in the study of discrete-time population dynamics, e.g., [38, 54, 77, 154, 189, 194]. Biologically speaking, the population has two fixed points (namely, the extinction state $x = 0$ and a positive equilibrium $x = K$), and the dynamics are overcompensatory with no demographic Allee effect. Examples include the frequently considered population dynamics models in their overcompensatory regimes, e.g., the Ricker [176], Hassell [98], and generalized Beverton–Holt [19] maps.

1.2.2 Modeling adaptive threshold harvesting

Adaptive threshold harvesting exerts control on a population when the population size x_t at time step t exceeds a certain proportion of its value in the preceding generation. The control then restates the population size back to that threshold by harvesting the surplus individuals. Thus, ATH takes action if the population has grown beyond a certain proportion within a time step, which is why ATH can be seen as aiming to prevent population booms.

As ALC, this new limiter method is 'adaptive' because the magnitude of the intervention is nonconstant and depends on the system state at the previous time step. Fig-
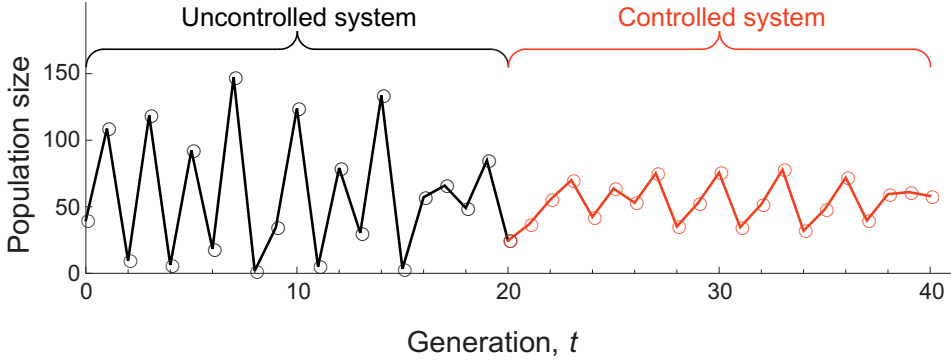
Figure 1.1: Stabilizing effect of ATH. During the first 20 generations, the population is uncontrolled and follows Eq. (1.1) for the Ricker map $f(x) = x \exp(r(1 - x/K))$ with growth parameter $r = 3$ and carrying capacity $K = 60$. In the next 20 generations, the population is controlled by adaptive threshold harvesting with intensity $h = 2/3$.

ure 1.1 shows how ATH modifies the dynamics of the population and, in particular, how the fluctuation range of the population size is reduced.

When applying ATH, there are two different population sizes at time step t, namely b_t, the population size before ATH intervention and a_t, the population size after intervention. In particular, $b_t \geq a_t$ because ATH never adds individuals to the population. With these notations, the dynamics of ATH are determined by the following equations:

$$b_{t+1} = f(a_t) \quad \text{and} \quad a_{t+1} = \begin{cases} b_{t+1}, & b_{t+1} \leq a_t/h, \\ a_t/h, & b_{t+1} > a_t/h, \end{cases} \tag{1.2}$$

where $h \in (0, 1)$ is a control parameter. Notice that we have denoted the proportion of a_t that determines when individuals are removed by a_t/h, with $0 < h < 1$, instead of $h \cdot a_t$, with $h > 1$. This allows us to interpret h as a *harvesting intensity*, since higher values of h correspond to lower values of $1/h$, and thus to higher removal efforts.

Substituting the value for b_{t+1} from the first equation of (1.2) into the second one, we obtain that the population dynamics are determined by the first-order difference equation

$$a_{t+1} = \begin{cases} f(a_t), & f(a_t) \leq a_t/h, \\ a_t/h, & f(a_t) > a_t/h, \end{cases} \tag{1.3}$$

which is piecewise smooth and can be written in one line by using the minimum function,

$$a_{t+1} = \min\{f(a_t), a_t/h\}.$$

According to conditions (A1)–(A4), ATH never takes place if $h \leq 1/f'(0^+)$, so in the remainder of this chapter we will always assume values of the intervention intensity greater than that.

Similarly, the dynamics of populations managed by ALC are given by the first-order difference equation

$$a_{t+1} = \max\{f(a_t), c \cdot a_t\}, \tag{1.4}$$

where $c \in (0, 1)$ is a control parameter measuring the ALC intensity [77].

1.2.3 ACTIVATION THRESHOLD

As previously stated, ATH only takes effect when the population size exceeds a proportion of its magnitude in the preceding generation. However, it is not necessary for the controller to wait until measuring the population size in generation t to decide about the need for intervention. Fortunately, the analysis of (1.3) reveals the existence of a 'hidden' threshold level A_H such that the intervention is triggered in generation t only if the population size in the preceding generation is below this value. In analogy to ALC, this threshold is called the activation threshold [77]. Geometrically, the activation threshold corresponds to the first component of the intersection point of the graph of f and the straight line $y = x/h$ (see Figure 1.2). Proposition 1.1 shows the existence of A_H, for control intensities $h > 1/f'(0^+)$. For intensities $h \leq 1/f'(0^+)$ the control is

never triggered and, according to conditions (A1)–(A4), the activation threshold A_H does not exist because the straight line $y = x/h$ only intersects $y = f(x)$ at $x = 0$. Obviously, the knowledge of A_H can be useful in practical situations because it allows the controller to know early on when an intervention is necessary in the next generation.

Proposition 1.1. *Assume that (A1)–(A4) hold. Then, for any $h \in (1/f'(0^+), 1)$ there exists a unique point $A_H > 0$ such that $f(A_H) = A_H/h$.*

Proof. We must prove that the function $h(x) = f(x) - x/h$ has a unique zero in $(0, b]$. As $d < K$ and f is strictly decreasing for $x > d$, we have that $f(d) > f(K) = K > d$, and therefore $f(d)/d > 1$. According to this, we consider two cases depending on the value of the control intensity h. For $h \in (d/f(d), 1)$ we have

$$
\begin{aligned}
h(d) &= f(d) - d/h > 0, \\
h(K) &= f(K) - K/h = K - K/h = (1 - 1/h) \cdot K < 0,
\end{aligned}
$$

and hence, according to Bolzano's Theorem, there exists a point $A_H \in (d, K)$ such that $f(A_H) = A_H/h$. Let us now prove the uniqueness of A_H. Since f is strictly decreasing on (d, b), and the straight line $y = x/h$ is strictly increasing, they intersect only once (at the point A_H, which existence has been proved). We must prove that there is no intersection outside the aforementioned interval. First, the hypograph of f is convex on $[0, d]$ because f is concave downward on that interval, and thereby the curve $f(x)$ is above the straight line $y = (f(d)/d) \cdot x$ (they intersect at the endpoints of this interval). Given that $h > d/f(d)$, we have that $x/h < (f(d)/d) \cdot x$ for all $x \in (0, d]$, and thus the only intersection between $f(x)$ and the straight line $y = x/h$ on $[0, d]$ is $x = 0$. This concludes the uniqueness of A_H in this case.

Second, for $h \in [1/f'(0^+), d/f(d)]$ we have that $h(d) = f(d) - d/h \leq 0$. Moreover, given that

$$
1/h < f'(0^+) = \lim_{x \to 0^+} \frac{f(x)}{x},
$$

there exists $\epsilon > 0$ such that $f(x) > x/h$ (i.e., $h(x) > 0$) for all $x \in (0, \epsilon)$. According to Bolzano's Theorem, there exists $A_H \in (0, d]$ such that $f(A_H) = A_H/h$. With regard to the uniqueness, due to the concavity of f on $[0, d]$, there are only two intersection points between f and the straight line $y = x/h$ on this interval, namely $x = 0$ and $x = A_H$. Furthermore, these two curves do not intersect on (d, b) because f is strictly decreasing on that interval; $y = x/h$ is strictly increasing; and $f(d) < d/h$. $\qquad\square$

Corollary 1.2. *Assume that (A1)–(A4) hold and $h \in (0, 1)$ is such that the activation threshold A_H exists. Then, the map describing the dynamics of a_t for the controlled system under ATH with intensity h,*

$$H(x) = \min\{f(x), x/h\},$$

can be rewritten as

$$H(x) = \begin{cases} x/h, & x \leq A_H, \\ f(x), & x > A_H. \end{cases}$$

Corollary 1.3. *Assume that (A1)–(A4) hold and $h \in (0, 1)$ is such that the activation threshold A_H exists. Then, ATH acts in generation t if and only if $a_{t-1} < A_H$.*

1.3 STABILIZATION OF FLUCTUATIONS

Here we describe how adaptive threshold harvesting affects constancy stability, i.e., the propensity of the population size to stay essentially unchanged [90]. We start by showing that ATH is not able to stabilize oscillations towards an equilibrium point. This is a property that ATH shares with ALC [77].

Proposition 1.4. *Assume that (A1)–(A3) hold and that the fixed point K is unstable for the uncontrolled system (1.1). Then, independently of the magnitude of ATH, $h \in (0, 1)$, the controlled system has no asymptotically stable equilibria.*
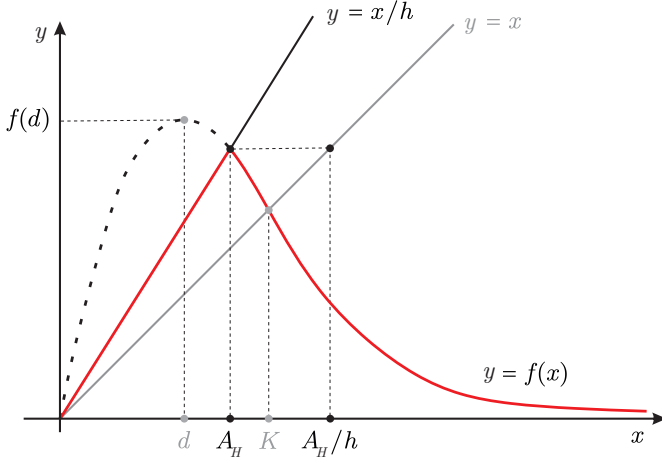
Figure 1.2: ATH map. Adaptive threshold harvesting only takes place when the straight line $y = x/h$ is under the graph of the population production map f. The activation threshold A_H is defined by their intersection. The bold red curve represents the ATH map (1.3).

Proof. ATH corresponds to the dynamical system given by

$$
\begin{cases}
b_{t+1} = f(a_t), \\
a_{t+1} = \min\{f(a_t), a_t/h\},
\end{cases}
\tag{1.5}
$$

for which a point (x, y) is a fixed point if and only if

$$
\begin{cases}
y = f(x), \\
x = \min\{f(x), x/h\}.
\end{cases}
$$

For $h \leq 1/f'(0^+)$, the control by ATH is never triggered, and the dynamics of the uncontrolled and controlled systems are the same. By condition (A2), this system has only two fixed points $x = 0$ and $x = K$. Since $f(x) > x$ for $0 < x < K$, $x = 0$ is an unstable equilibrium. Under the assumption that K is also unstable, we conclude that the controlled system has no asymptotically stable equilibria.

For control intensities larger than $1/f'(0^+)$, the dynamics of the system controlled by ATH are different from the ones for the uncontrolled system and are given by (1.5). Looking at these equations, it becomes clear that $(x, y) = (0, 0)$ is a fixed point. Since $h < 1$, we have that fixed points with $x > 0$ must verify $x = y = f(x)$, and thus $(x, y) = (K, K)$. Hence, the system controlled by ATH with intensity $h > 1/f'(0^+)$ has only two fixed points, namely $(0, 0)$ and (K, K).

We are going to prove that none of them is asymptotically stable. According to Proposition 1.1, the activation threshold A_H exists. Moreover, the neighborhood $U = (0, A_H) \times (0, A_H)$ of $(0, 0)$ is well-defined. We are going to prove that all orbits starting in U will eventually leave U. Assume $(a_t, b_t) \in U$ for all $t \geq 0$. Since $f(x) > x/h$ for $x \in (0, A_H)$, according to the second equation of (1.5), it is $a_{t+1} = a_t/h$ for all $t \geq 0$, and thus $a_t = (1/h)^t \cdot a_0$. This leads to $a_t \to +\infty$, which contradicts our hypothesis and proves that $(0, 0)$ is an unstable fixed point.

Let us now prove that (K, K) is also unstable. As f is continuous and $f(K) = K < K/h$, there exists a neighborhood V of K such that $f(x) < x/h$ for all $x \in V$. Assume $(a_t, b_t) \in V \times V$ for all $t \geq 0$. According to the second equation of (1.5), it is $a_{t+1} = f(a_t)$ for all $t \geq 0$, and thus $a_t = f^t(a_0)$. Since K is an unstable fixed point for the uncontrolled system, this last equality contradicts our hypothesis and allows us to conclude that (K, K) is an unstable fixed point for the system controlled by ATH. $\square$

In the remainder of this section, we consider two different measures of constancy stability, namely the fluctuation range and the fluctuation index.

1.3.1 FLUCTUATION RANGE

The fluctuation range gives the upper and lower bounds of the population size, in-between which the oscillations take place. It has been employed in [77] to study stability properties of ALC. The smaller the fluctuation range, the more stable the population dynamics from the constancy point of view.
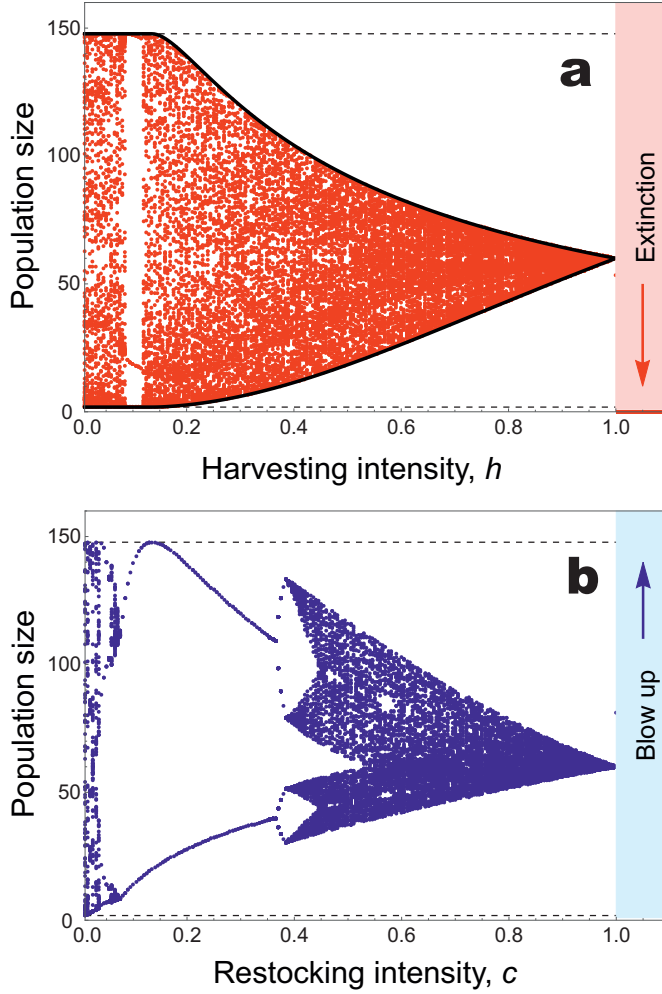
Figure 1.3: Bifurcation diagrams for ATH and ALC. (a) Bifurcation diagram for ATH. Red dots represent population sizes for the system (1.3) controlled by ATH. The bold black curves mark the limits of the intervals given by Eq. (1.6). (b) Bifurcation diagram for ALC. Blue dots represent population sizes for the system (1.4) controlled by ALC. In both panels, the horizontal dashed lines mark the limits of the fluctuation range for the uncontrolled system. The diagrams are based on the Ricker map $f(x) = x \exp(r(1 - x/K))$ with $r = 3$ and $K = 60$, after removing transients. The initial population size is chosen as a pseudorandom number in $(0, f(d)]$.

The ATH method can reduce the fluctuation range compared to the uncontrolled system. We illustrate this in Figure 1.3a, where the fluctuation range decreases as the control intensity is increased. The figure suggests that ATH confines the population size within a region around the positive but unstable equilibrium K. The following theorem states that such a 'trapping region' indeed exists and is completely determined by the map f and the control parameter h.

Theorem 1.5. *Assume that (A1)–(A4) hold and $h \in (0,1)$ is such that the activation threshold A_H exists. Then, applying ATH with intensity h confines the population sizes a_t for any $a_0 \in (0,b]$ within an interval $I_a = [l(h), u(h)]$ around the positive equilibrium K, with endpoints given by the expressions*

$$l(h) = \begin{cases} f(A_H/h), & d \le A_H, \\ f(f(d)), & d > A_H, \end{cases} \quad \text{and} \quad u(h) = \begin{cases} A_H/h, & d \le A_H, \\ f(d), & d > A_H. \end{cases}$$
(1.6)

Proof. In order to cover all possible expressions for I_a, we must consider two cases.

We start considering the case $d \le A_H$, for which $I_a = [f(A_H/h), A_H/h]$. We have that $d \le A_H < A_H/h$, and thus $f(d) \ge f(A_H) > f(A_H/h)$ because $h < 1$ and f is strictly decreasing in (d, b). From this, we conclude that the interval I_a has a nonempty interior because $f(A_H) = A_H/h$ and therefore $A_H/h > f(A_H/h)$. To prove that orbits enter I_a after a transient, we consider exhaustive and disjoint subcases depending on the initial population size $a_0 \in (0, b]$.

1. First, we assume that $a_0 \in [A_H, A_H/h]$. In this subcase,

$$d \le A_H \le a_0 \le A_H/h,$$

and thanks to the strict decrease of f on (d, b) we conclude that

$$f(d) \ge f(A_H) \ge f(a_0) \ge f(A_H/h).$$

Moreover, according to Corollary 1.2, it is $a_1 = H(a_0) = f(a_0)$. With this, given that $f(A_H) = A_H/h$, we have that $A_H/h \geq a_1 \geq f(A_H/h)$ and thus $a_1 \in I_a$.

2. Next, we assume $a_0 \in (0, A_H)$. We are going to show that there exists $t_0 \in \mathbb{N}$ such that $a_{t_0} \in [A_H, A_H/h]$. Assume $a_t \notin [A_H, A_H/h]$ for all t. Let us prove by induction on t that $a_t \in (0, A_H)$ for all t. For $t = 0$ this condition is straightforward from the hypothesis of the subcase. Suppose $a_t \in (0, A_H)$ for certain $t \geq 1$. Since $a_t < A_H$, we have that $a_{t+1} = H(a_t) = a_t/h$ by Corollary 1.2, and therefore

$$a_{t+1} = a_t/h < A_H/h.$$

As $a_{t+1} \notin [A_H, A_H/h]$ by hypothesis, we conclude that $a_{t+1} \in (0, A_H)$. In conclusion, $a_t \in (0, A_H)$ for all t and thus $a_t = H^t(a_0) = (1/h)^t \cdot a_0$ by Corollary 1.2. This leads to $a_t \to +\infty$ because $h < 1$, which is impossible because $a_t < A_H < K$. In summary, we conclude that there exists $t_0 \in \mathbb{N}$ such that $a_{t_0} \in [A_H, A_H/h]$ and thus $a_{t_0+1} \in I_a$ by the first subcase.

3. Finally, we assume $a_0 \in (A_H/h, b]$. We have that $a_0 > A_H/h > A_H \geq d$ and, according to Corollary 1.2, $a_1 = H(a_0) = f(a_0)$. From the strict decrease of f on (d, b) we have that

$$a_1 = f(a_0) < f(A_H/h) < f(A_H) = A_H/h,$$

which leads to one of the previous subcases and proves that orbits eventually enter I_a.

So far, we have proved that orbits enter the trapping region after a finite number of generations. To prove that they never leave it, we must establish that $a_{t+1} \in I_a$ for $a_t \in I_a$. Assume $a_t \in I_a$ for certain t. If $f(A_H/h) \geq A_H$ we have that $A_H \leq f(A_H/h) \leq a_t \leq A_H/h$, and therefore $a_{t+1} \in I_a$ by the previous subcase 1. For $f(A_H/h) < A_H$ we consider two cases. If $a_t < A_H$, it is $a_{t+1} = H(a_t) = a_t/h$ (Corollary 1.2) and thus $A_H/h > a_t/h = a_{t+1} > a_t \geq f(A_H/h)$, which implies

$a_{t+1} \in I_a$. If $a_t \geq A_H$; $a_t \in [A_H, A_H/h]$; and therefore $a_{t+1} \in I_a$ by the previous subcase 1.

Next, we consider the case $d > A_H$, for which $I_a = [f(f(d)), f(d)]$. If $f(f(d)) = f(d)$ then $f(d) > K$ is a fixed point for f, in contradiction with condition (A2). Hence, I_a has a nonempty interior, and we can proceed to prove that orbits enter this interval after a finite number of generations. To do this, we must distinguish some subcases as before.

1. First, we assume that $a_0 \in [d, f(d)]$. As $a_0 \geq d > A_H$, it is $a_1 = H(a_0) = f(a_0)$ by Corollary 1.2. Given that f is strictly decreasing on (d, b), from the inequality $d \leq a_0 \leq f(d)$ we deduce that $f(f(d))(d) \leq f(a_0) = a_1 \leq f(d)$, which implies $a_1 \in I_a$.

2. Next, we assume $a_0 \in (0, d)$. We are going to see that there exists $t_0 \in \mathbb{N}$ such that $a_{t_0} \in [d, f(d)]$. Suppose $a_t \notin [d, f(d)]$ for all t. Given that f reaches its absolute maximum at $x = d$, for all $x \in [0, b]$ we have that $H(x) = \min\{f(x), x/h\} \leq f(x) \leq f(d)$. Hence, $a_t = H(a_{t-1}) \leq f(d)$ for all t, which together with $a_t \notin [d, f(d)]$ leads to conclude that $a_t \in (0, d)$ for all t. The hypograph of f on $(0, d)$ is convex because f is concave downward on this interval, and therefore the curve $f(x)$ is above the straight line $y = (f(d)/d) \cdot x$ (they intersect at the endpoints of this interval). On the other hand, $h < d/f(d)$ when $d > A_H$. This allows us to conclude that $H(x) = \min\{f(x), x/h\} > (f(d)/d) \cdot x$ for all $x \in (0, d)$. With this, given that $a_t \in (0, d)$ for all t, we have that $a_t = H(a_{t-1}) > (f(d)/d) \cdot a_{t-1}$ for all $t \geq 1$ and thus

$$a_t = H^t(a_0) > (f(d)/d)^t \cdot a_0.$$

Given that $f(d) > d$ we have that $a_t \to +\infty$, which is impossible since $a_t < d$ for all t. We conclude that there exists $t_0 \in \mathbb{N}$ such that $a_{t_0} \in [d, f(d)]$ and, with this, $a_{t_0+1} \in I_a$ by the previous subcase.

3. Finally, we assume $a_0 \in (f(d), b]$. In this subcase, we have that $a_1 = H(a_0) \leq f(d)$ because $H(x) \leq f(d)$ for all $x \in (0, b]$. This brings us back to one of the

previous subcases and allows us to assert that orbits eventually enter the trapping region.

Now we proceed to prove the invariance of the trapping region under ATH. To do this, we assume $a_t \in I_a$ for a certain t and prove $a_{t+1} \in I_a$. We have seen that $a_{t+1} = H(a_t) \leq f(d)$ for all t, so it suffices to prove that $a_{t+1} \geq f(f(d))(d)$. For $a_t \geq d$ this condition is straightforward from the previous subcase 1. If $a_t < d$, we have that $f(a_t) > a_t$ by condition (A2), and then

$$a_{t+1} = H(a_t) = \min\{f(a_t), a_t/h\} \geq \min\{a_t, a_t/h\} = a_t \geq f(f(d)).$$

$\square$

If a specific goal is to be achieved, such as suppressing the population size below an upper limit; beyond a lower limit; or within two limits, the control intensity to achieve these goals can be determined with Theorem 1.5. This is possible because the trapping region is completely determined by the map f and the control parameter.

The trapping region given in Theorem 1.5 is global, that is, the reduction of the fluctuation range does not depend on the initial condition. Figure 1.3a shows a bifurcation diagram for ATH together with the limits of the intervals defining the trapping region given by Eq. (1.6). These intervals are sharp over a wide range of control parameters, which means that they cannot be improved for those parameter values.

ATH and ALC reduce the fluctuation range in different ways. On the one hand, ALC asymptotically provides, for almost all control intensities, a lower limit for the population size that is clearly higher than the one observed for the uncontrolled system. The upper limit, however, is significantly reduced for medium and high intensities only (see Figure 1.3b). On the other hand, ATH asymptotically induces, for a wide range of control intensities, an upper limit for the population size that is clearly smaller than the one observed for the uncontrolled population. However, the lower limit is significantly increased for medium and high intensities only.

Figure 1.3a also shows the case when the control intensity h is greater than unity. This corresponds to harvesting a population that has decreased below rather than increased above a fraction of its previous size. Such a choice of control leads to extinction. The reason is that the harvesting always forces the population size to a fraction $1/h < 1$; as a consequence, there is no positive fixed point. Choosing a control intensity $c > 1$ for ALC leads the population to blow up (Figure 1.3b). This is because the control forces the number of individuals to increase in each generation to at least the proportion $c > 1$ of its previous value.

1.3.2   FLUCTUATION INDEX

In Figure 1.3, we have seen that constancy stability measured in terms of the fluctuation range is always enhanced when ATH (or ALC) is applied to the Ricker model considered here. Looking at another measure of constancy stability, namely the fluctuation index (FI), we will show that ATH does not always have a stabilizing effect.

The fluctuation index is a dimensionless measure of the average one-step variation of the population size scaled by the average population size in a certain period. It was introduced in [63], and employed in [184] and [77] to study stability properties of ALC. Mathematically, the FI is given by

$$\text{FI} = \frac{1}{T\,\overline{a}} \sum_{t=0}^{T-1} \left| a_{t+1} - a_t \right|, \tag{1.7}$$

where $\overline{a}$ is the mean population size over a period of T time steps.

Figure 1.4 shows that for small values of the control parameter, the FI of the system controlled by ATH can be greater than the FI of the uncontrolled system. The same holds true for ALC. For small values of the control intensity, the FI behaves quite erratically for both ATH and ALC, with pronounced peaks as well as sporadic drops below the baseline level set by the uncontrolled system. This sudden changes are due to attrac-
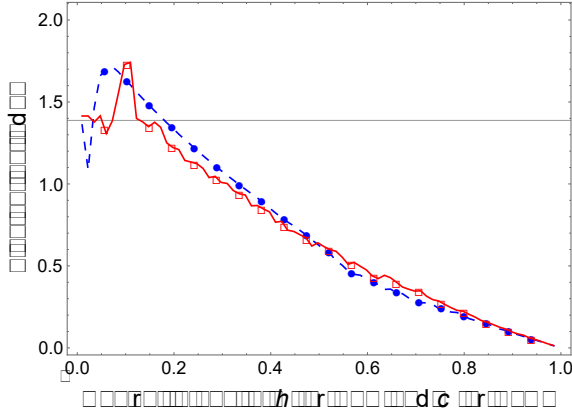
Figure 1.4: Fluctuation indices (FIs) for ATH and ALC. Red squares correspond to the FI for the system controlled by ATH and blue dots for the system controlled by ALC. The horizontal line marks the FI for the uncontrolled population. The dynamics of the uncontrolled population are described by the Ricker map $f(x) = x \exp(r(1 - x/K))$ with $r = 3$ and $K = 60$. The initial population size is chosen as a pseudorandom number in $(0, f(d)]$, and the FI is obtained over 1000 generations after removing transients.

tor transitions, e.g. from chaos to periodic oscillations or between cycles of different periods (cf. Figure 1.3).

For medium and high control intensities both ATH and ALC reduce the FI compared to the uncontrolled system. With a fixed value of the control intensity in this range, the effects of ATH and ALC on the FI are not only qualitatively but also quantitatively similar.

1.4 YIELD

Control strategies usually come at a price. Previous papers measure this cost in terms of the 'effort', i.e., the number of individuals added to or removed from a population [59, 77, 105, 184, 212]. Here, we take a slightly different viewpoint and interpret the number of individuals removed as the yield. This seems to suggest itself since ATH is
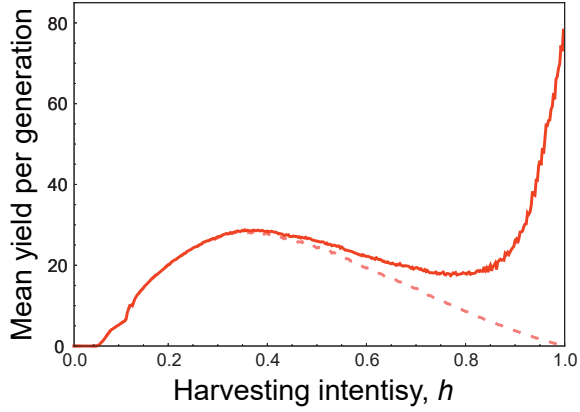
Figure 1.5: Mean yield per generation obtained by ATH. The dashed curve represents the asymptotic yield after discarding transients, and the solid curve represents the short-term yield including transients. Both yield values are averaged over 50 generations and over 1000 replicates with different initial conditions. The dynamics of the uncontrolled population are described by the Ricker map $f(x) = x \exp(r(1 - x/K))$ with $r = 3$ and $K = 60$. The initial population size is chosen as a pseudorandom number in $(0, f(d)]$ for the transient yield, and in the trapping region I_a for the asymptotic yield.

a harvesting method, provided that the managed population is of some value. If the population is a pest, however, the term effort may be more fitting. In any case, we will consider two different ways of calculating the yield; one is based on the long-term dynamics and ignores transient effects (asymptotic yield), while the other is based on the short-term dynamics only and thus takes into account transients (transient yield). The reason for considering two measures of the yield is the following. For ALC, on the one hand, the asymptotic effort has been shown to decrease to zero if the control intensity approaches its maximum value [184]. On the other hand, including transients can radically alter this observation and make the effort increase drastically [77].

Figure 1.5 shows the mean asymptotic yield per generation as a function of the ATH intensity. The curve has a hump-shaped form, reaching a maximum at some intermediate value of the control intensity. For too small control intensities, the yield is zero

but then increases with h until the maximum is reached. For large control intensities beyond the maximum, the yield declines to zero as $h \to 1$.

Figure 1.5 also shows the mean transient yield per generation, which is similar to the asymptotic yield for small and intermediate control intensities and reaches a local maximum, which is the same as for the asymptotic yield (Figure 1.5). For large control intensities ($h > 0.85$), however, the transient yield increases steeply, blowing up as $h \to 1$.

The reason for this sharp increase in the yield are prolonged transients of the population dynamics if the control intensity is large. This has the effect that the population is repeatedly harvested—and, as a matter of fact, to a large degree. This not only increases the yield, but also extends the time it takes the system to reach the trapping region. The following section considers this in more detail.

1.5 Short-term behavior

In the previous section, we have seen that, in the short term, the mean yield per generation can differ greatly from the one in the long term. In certain circumstances, there is a long transient period before the population reaches its asymptotic behavior. During this transient, the short-term dynamics can be markedly different from the long-term dynamics with the desired properties (e.g., the mean yield or population size). Here, we show that ATH induces prolonged transient periods for rather large values of the control parameter. In the second part of this section, we propose an adjustment to the control rules that suppress prolonged transients and accelerate the controlled population to reach its long-term dynamics.

1.5.1 Transients in the controlled system

In order to quantify transients, we consider a value t_{max} that represents the maximum number of generations needed for the population size to enter the trapping region, measured over all possible integer initial conditions in the interval $(0, f(d)]$. By taking the
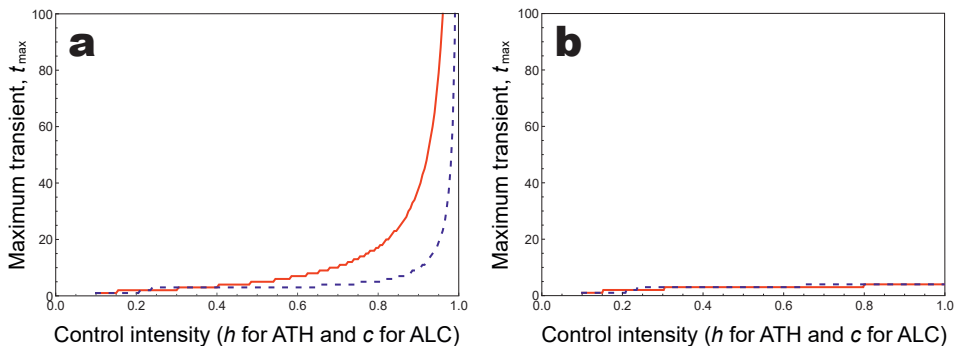
Figure 1.6: Transients in systems controlled by ATH and ALC (a) Maximum transients for ATH in solid red curve and for ALC in dashed blue curve. (b) Maximum transients for the adjusted version of ATH given by Eq. (1.8) in solid red curve and for the adjusted version of ALC given by Eq. (1.9) in dashed blue curve. The value $t_{\max}$ represents the maximum transient among all orbits with integer initial population size in the interval $(0, f(d)]$. The dynamics of the uncontrolled population are described by the Ricker map $f(x) = x \exp(r(1 - x/K))$ with $K = 60$ and $r = 3$.

maximum, we take into account that transients depend on the initial condition, and we consider the 'worst case', i.e., the longest time it takes to reach the trapping region.

Figure 1.6a shows that the maximum transient increases with the control intensity for both ATH and ALC. This increase is such that the maximum transients blow up near the maximum value of the control intensity. For medium and high control intensities ATH exhibits a longer maximum transient than ALC.

Example 1.6. For the Ricker map $f(x) = x \exp(r(1 - x/K))$ with $K = 60$ and $r = 3$ the maximum transient t_{max} for ALC with intensity $c = 0.97$ is 31 generations, whereas the corresponding value for ATH with intensity $h = 0.97$ rises up to 134 generations.

Analyzing the causes of this behavior can help us to devise techniques for the cancellation of transients induced by ATH. Numerical simulations show that the maximum transients for ATH correspond to the largest values of the initial population size, a_0. The reason is that, due to the overcompensation in the population dynamics, the value

$a_1 = f(a_0)$ is very small for large values of a_0 (see Figure 1.2); the population size must then increase until entering the trapping region. However, the control slows down the population growth. In fact, for a sufficiently large value of a_0, we have $a_1 < A_H$. That is, harvesting control will be triggered in the next and successive generations during this transient period. In summary, the prolonged transients are due to repeated high-intensity harvesting of small population sizes. Since small population sizes can have a large production, the repeated high-intensity harvesting is also the reason why the transient yield increases sharply for large control intensities (cf. Figure 1.5).

1.5.2 HOW TO REDUCE TRANSIENTS

As the transient dynamics may last for a long time, an important question from the practical point of view is whether the system can be manipulated to reach its long-term behavior faster. One of the simplest solutions is probably to apply a perturbation such that the population size directly enters the trapping region. However, depending on the current population size, this requires that both restocking and culling can be implemented promptly and to a possibly large extent. Here we consider the situation that restocking is impossible (or very costly), so that, corresponding to ATH, culling is the only possibility. We will propose an adjusted ATH method that cancels the prolonged transients without changing the asymptotic dynamics.

In the first part of this section, we have seen that the long transients are caused by repeated harvesting at small population sizes. The higher the control intensity, the more the population growth is slowed down and the longer it takes the population size to reach the trapping region. This effect can be avoided by the following two considerations.

1. We could stop harvesting small populations, say when the population size is below the trapping region. The lower limit of the trapping region is $l(h)$, but since the activation threshold A_H is always inside the trapping region, it would be actually sufficient to stop harvesting when the population size is smaller than

$h \cdot l(h) < l(h)$. For any $a_t > h \cdot l(h)$, the population size in the next generation is $a_{t+1} = a_t/h > l(h)$.

2. However, a complete cessation of the harvesting might cause the population size to 'jump' from one side of the trapping region to the other without entering it. Therefore, instead of completely canceling the harvesting of the small population sizes identified, we allow control but only to such a degree that the population size is not reduced below the trapping region.

All this leads to an adjusted ATH strategy with restricted harvesting at small population sizes, described by the following equation:

$$a_{t+1} = \begin{cases} \min\{f(a_t), a_t/h\}, & a_t > h \cdot l(h), \quad \text{(original ATH of large enough pop}^{\underline{ns}}\text{)} \\ \min\{f(a_t), l(h)\}, & a_t \leq h \cdot l(h). \quad \text{(restricted harvesting of small pop}^{\underline{ns}}\text{)} \end{cases}$$
(1.8)

This adjustment does not alter the asymptotic behavior of the controlled population because harvesting is only restricted when the population size is below the trapping region. Once it enters this region, the control follows the original ATH. We illustrate the improvement due to the adjustment (1.8) in Figure 1.6b, which shows a significant reduction in maximum transients.

Example 1.7. The maximum transient in the system from Example 1.6 controlled by ATH with intensity $h = 0.97$ lasts for 134 generations. With the adjustment given by (1.8), this transient decreases to only 4 generations.

The same kind of adjustment can be used to cancel prolonged transients generated by ALC. In that case, the restocking action of the control lengthens transients when the population size is above the trapping region. For $a_t > u(c)$, where $u(c)$ denotes the upper limit of this region, the transient lasts until the population size decreases and enters the trapping region. Since the activation threshold is always inside the trapping region, restocking takes place in every generation of this stage, thus slowing down the decrease of the population size. The higher the control intensity, the more the population is restocked and the longer it takes for the population to decrease to the trapping

region. As before, if the restocking control for population sizes above the trapping region were completely stopped, the population size could jump from one side of the trapping region to the other without entering it. The proper adjustment is therefore to restrict restocking to the upper limit $u(c)$. This leads to an adjusted version of ALC with restricted restocking at large population sizes described by the system

$$a_{t+1} = \begin{cases} \max\{f(a_t), c \cdot a_t\}, & a_t < c \cdot u(c), \quad \text{(original ALC of small enough pop}^{\text{ns}}) \\ u(c), & a_t \geq c \cdot u(c). \quad \text{(restricted restocking of large pop}^{\text{ns}}) \end{cases} \tag{1.9}$$

As for ATH, this adjustment does not alter the asymptotic behavior of the controlled population because the restocking is only reduced when the population size is above the trapping region. Once the system is in the trapping region, the control follows the original ALC scheme.

Example 1.8. We consider the same uncontrolled population as in Examples 1.6 and 1.7. Applying ALC with restocking intensity $c = 0.97$ and for initial conditions a_0 that are integer values in $(0, f(d)]$, the maximum transient lasts 31 generations. With the adjustment given by (1.9), the maximum transient decreases to only 4 generations.

1.6 DISCUSSION AND CONCLUSIONS

The original version of adaptive limiter control (ALC) as proposed by [184] is based on restocking the population as control intervention. We have shown that adaptive threshold harvesting (ATH), i.e., the harvesting version of adaptive limiter control (h-ALC), can also stabilize fluctuating populations. This extends the applicability of adaptive limiters to situations when culling is the only possible form of intervention. Moreover, adaptive limiters may also be used as a harvesting strategy, thus widening the approach of threshold harvesting.

Commonalities between ATH and ALC

ATH and ALC have the following properties in common. We begin by considering stabilization aspects. First, the fluctuations are confined in a trapping region, for which we provide analytical expressions for the lower and upper bounds. This trapping region can be proven to reduce with increased control intensity. Hence, constancy stability tends to improve. Second, the fluctuation index also becomes smaller with increased control intensity, provided the control is at least of intermediate strength. Hence, constancy stability improves. However, for smaller control intensities both ATH and ALC may increase the fluctuation index compared to the uncontrolled population. Third, the fixed point itself does not become stabilized. It is only the fluctuation that reduces in magnitude or amplitude. Yet, for the Ricker model the mean population size is, asymptotically, remarkably constant at the level of the carrying capacity (which corresponds to the unstable fixed point), for all values of the control parameter.

Hence, the stabilization properties of ATH are analogous to the ones of ALC, previously investigated in [77, 184]. This is not a straight-forward result; as pointed out in the introduction to this chapter, there are other control strategies which can greatly differ in the behavior they trigger, depending on whether interventions either add or remove individuals.

Moreover, the length of transients and the yield (or effort, respectively) behave similarly as a function of the control intensity for ATH and ALC. For the latter, again, this has been previously investigated in [77, 184].

Differences between ATH and ALC

While both ATH and ALC reduce the fluctuation range, they affect the lower and upper bounds of the trapping region in different ways. For lower and intermediate control intensities, ATH tends to reduce the upper bound, whereas ALC tends to increase the lower bound (see Figure 1.3). Hence, ATH appears more effective in avoiding outbreaks and ALC in preventing extinctions. For large control intensities, however, both

control methods seem equally effective in assuring minimum and maximum population sizes.

There are other differences between ATH and ALC. They occur when the control intensities exceed values of unity. Note that this parameter range has not been considered before for ALC. Basically, control intensity larger than unity means restocking the population to levels larger than before a crash (ALC) and harvesting the population to a level smaller than before the increase in population size (ATH). As such, these are neither unrealistic parameter regimes nor insensible strategies. However, we find that these high control intensities drive the population extinct (ATH) or lead to unbounded population growth (ALC). Neither of which seems a desirable goal for the strategy considered.

Comparison with threshold harvesting

In contrast to adaptive limiters, threshold harvesting can actually stabilize the population dynamics to a stable equilibrium for sufficiently large control values [88, 195]. However, this comes at the cost of applying the intervention in every generation. Adaptive threshold harvesting, by contrast, comes with an intervention frequency of about 40% in the simulations corresponding to the Ricker map example used in this chapter (not shown here for the sake of brevity).

In control parameter regimes, where population fluctuations are reduced, but remain chaotic, the intervention frequency of threshold harvesting is lower than the one for ATH. This makes sense, as a population tends to peak less often beyond a high threshold value than a possibly rather small size in the previous generation. However, the yield that can be obtained from threshold harvesting in this regime [105] is lower than the one obtained from ATH.

Yields and transients

While the primary goal of ATH is the stabilization of the fluctuations, it may also be applied as a harvesting strategy when the aim is to gain economic benefit from the ex-

ploited population. ATH may therefore represent an alternative to other harvesting strategies such as constant-effort, constant-yield, or threshold harvesting.

It turns out that we have to distinguish two situations, namely the long-term (asymptotic) and the short-term (transient) yield. Interestingly, the short-term yield gained by ATH rises sharply for values of high control intensities. That is, the yield becomes largest just before the population goes extinct for $h > 1$. The transition from a sustained population (with improved constancy stability and large yield) to extinction happens abruptly. In contrast to overexploitation with constant-effort harvesting, the collapse of the population does not take place gradually.

Trying to maximize the short-term gain is therefore risky in terms of sustainability. This bears some analogy to the observation that focusing on short-term gains can lead to dramatic consequences. One of the most prominent examples is probably the collapse of the cod stocks off of Newfoundland. Harvesting theory has therefore developed strategies for a sustainable catch, which can be considered as one of the cornerstones of mathematical bioeconomics [45]. In fisheries, particular attention is paid to the maximum sustainable yield (MSY). Even though there are many concerns regarding the concept of MSY [e.g., 133, 149], it remains a 'key paradigm in fisheries management' [152, p. 2295].

As a consequence, the harvesting literature has focused almost exclusively on long-term behavior and asymptotic yields. This is in contrast to the realization that harvesting represents additional perturbations to the population, and that the population rarely reaches its equilibrium state [76]. While transient dynamics are well-known to be important [99], there is little work that aims to optimize harvest taking into account transient regimes [100, 111, 120, 121]. In stochastic population models, where population extinction is inevitable in the long run, Lande *et al.* [131, p. 122] addressed this by considering the 'expected cumulative yield over all time before eventual extinction of the population or reduction to a specific size'. However, the time to stochastic population extinction may be quite long.

We have shown that the yield can be markedly different, depending on whether we consider a short or long time scale. The dramatic increase in the short-term yield for large control intensities can be readily explained by the time it takes the population to reach the trapping region. During this time, the population is always harvested; the intervention frequency approaches 1 (not shown). That is, during this time the population effectively follows $a_{t+1} = a_t/h$ with h close to one, which corresponds to geometric growth with a rather slow per capita production. Hence, due to the high yield from harvesting the population growth is significantly reduced and almost stopped.

Here, we have calculated the transient yield over a time horizon of 50 generations. This is arbitrary and could be varied.

Dealing with transients

The long transients that occur for high control intensities may appear quite desirable on the one hand because they increment the transient yield and simultaneously reduce the asymptotic fluctuation range. On the other hand, however, the prolonged transient period keeps the population size at low levels and prevents it from reaching the trapping region. In many practical situations, e.g., when it comes to supporting endangered species, it is imperative to reduce the transients.

A major drawback of adaptive limiters is that they trigger control actions whenever the population size exceeds (or falls below) a proportion of its magnitude in the preceding generation—regardless of whether this magnitude is close to zero (or on a high level, respectively). This can happen when the control intensity in both ATH and ALC is large. Yet, it does not seem to make sense to harvest a population that has increased in size when this size is still small and far below the trapping region. Similarly, for ALC, it seems unreasonable to restock a population that has declined but is still above the trapping region.

Based on this observation, we propose adjustments to both ATH and ALC that suppress prolonged transients, while retaining the asymptotic behavior. These adjustments concern only population sizes outside the trapping region and are such that the popula-

tion size in the next generation does not 'overshoot' or 'undershoot' the trapping region. This is achieved by restricting the harvesting or restocking intervention for ATH and ALC, respectively. If the population size is within the trapping region, there is no need to alter the original control schemes because the population does not leave the trapping region. The adjustments work well (Figure 1.6a, Examples 1.7 and 1.8) and are therefore effective in speeding up the transition from a transient period to the asymptotic regime.

As mentioned previously, transients are rarely taken into account or studied [but see 39, 71, 77, 82, 128], even though they are ubiquitous in nature and may be actually more important than long-term dynamics [e.g., 99]. The problem of directing an unstable or perturbed population in an efficient way to a desired state, such as the equilibrium, bears some analogy to the idea of targeting in chaos control [107, 122]. In the ecological literature, we could not find many studies that investigate how to deal with transients. Harley and Manson [97] suggested an 'intermediate harvesting policy' for the transient period that accelerated the transition to the equilibrium state of a structured population. Another, yet completely different approach is based on utilizing available time series; learning from 'trajectories from the past' one could steer the system to a desired state efficiently [107, 109].

This time-series-based approach has the advantage of not requiring any knowledge of the underlying laws of dynamics. As pointed out by Sah *et al.* [184] for ALC, one of the main advantages of adaptive limiters over other strategies for controlling biological populations is that they can be implemented even when a good estimation of the population production map f for the uncontrolled system is not available. In this situation, the lack of knowledge about the system behavior makes it very difficult to reduce the length of transients. The adjusted methods presented here do require information on the upper or lower bounds of the trapping region.

2

Population control methods in stochastic extinction and outbreak scenarios

2.1 INTRODUCTION

In the previous chapter, we have seen that ALC and ATH are two control strategies that aim to reduce oscillations in population size. Both methods have similar stabilizing properties, yet they can be expected to be implemented in different biological contexts. As a restocking strategy, ALC is likely to be applied in biological conservation, species re-introduction programs and the release of biocontrol agents, while ATH as a harvesting strategy is expected to be implemented in pest containment programs or in the management of species with commercial value (e.g., fisheries). However, on the one hand harvesting strategies can have the counter-intuitive effect of increasing population size, see the review [1]. On the other hand, adding individuals could promote extinction. For example, such an intervention can shift a bistable system to another attractor with larger extinction risk, see e.g., [177], which may be especially the case when the al-

ternative attractor oscillates and the trough values come close to an extinction threshold [108, 190, 216]. It is therefore not straightforward to assume that harvesting reduces outbreaks risk nor that restocking reduces extinction risk.

Moreover, all of the models of ALC and ATH have made use of unimodal production curves such as the Ricker map. In reality, control is likely to be necessary when populations are subject to biological mechanisms that put them at risk or promote recurrent population outbreaks. These situations are characterized by bistability such that the population can jump stochastically between two attractors, one of which is less desirable than the other from a control point of view (for nuisance species we want to avoid the high-density attractor and for endangered species we want to avoid the small-density attractor or extinction state). Biological mechanisms inducing bistability have been largely ignored, however, with the exception of ALC models setting small populations to zero with a fixed probability [183, 184].

In this chapter, we study ALC and ATH systematically in two different population contexts. In the first one, populations are vulnerable to extinction due to a strong Allee effect. The Allee effect is a positive density dependence at low population sizes that occurs when the individual fitness increases with the number of individuals [198]. If the Allee effect is strong, there is bistability and small populations go extinct due to a lack of conspecifics (which may be caused by difficulties in finding mates or in cooperation, for instance). We will consider three different extinction scenarios. In the first one, populations monotonically decline before going extinct. In the second one, populations grow to a large population size and then collapse due to overcompensation. In the third one, a strong Allee effect interacts with population cycles and causes essential extinction [108, 190, 216]. This happens when the fluctuating population drops below the minimum viable population size set by the Allee effect. The transition to essential extinction occurs through a boundary collision, and thus environmental changes may cause abrupt population collapses. As ALC and ATH reduce the fluctuation range, their stabilizing properties are particularly interesting in this extinction scenario.

Allee effects have been empirically found in many species including mammals and birds [51], plants [91], insects [127] and marine invertebrates [201], and their relevance is particularly recognized in conservation biology [49, 50, 60, 198]. However, Allee effects have also been detected in a large number of invasive species like the gypsy moth *Lymantria dispar* [112, 139], the zebra mussel *Dreissena polymorpha* [136] or the pine sawyer *Monochamus alternatus* [221]. Thus, Allee effects are relevant not only for the survival of endangered populations but also in the prevention of outbreaks.

Outbreaks are the second population context considered in this chapter. Here, we study two different outbreak scenarios. The first one is based on a strong Allee effect model, with extinction being the non-outbreak state. In the second scenario the non-outbreak state is positive. It is based on a gypsy moth outbreak model that combines density-dependent regulation by predation with host–pathogen dynamics [70]. This causes multistability between a high-density and a low-density attractor, the latter of which may be more complex and even chaotic. With stochastic perturbations ubiquitous in nature, the model population jumps rather unpredictably between different states. Again, as ALC and ATH tend to reduce fluctuation ranges, they might abate transitions to outbreak states. The importance of stochasticity is also well recognized in biological invasions [68, 139] and for endangered species [3, 49, 61, 179].

In the next section, we introduce the mathematical models that describe the underlying population dynamics in the absence of any control. Section 2.3 analyzes the effect of the control methods on deterministic and stochastic populations in three different extinction scenarios. We then turn our attention to the two outbreak scenarios in Sections 2.4 and 2.5. Section 2.6 draws conclusion on the applicability of ALC and ATH in the biological contexts considered.

2.2 DETERMINISTIC AND STOCHASTIC POPULATION MODELS

We assume that the population dynamics are described by a first-order difference equation of the form

$$x_{t+1} = f(x_t), \qquad x_0 \in [0, +\infty), \ t \in \mathbb{N},$$

where x_t denotes the population size at generation t and $f \colon [0, +\infty) \to [0, +\infty)$ is the population production function or the stock–recruitment curve. We assume that the population has a strong Allee effect and that there are three fixed points, namely the extinction state $x = 0$, the Allee threshold $L > 0$ and an equilibrium $K > 0$ corresponding to the carrying capacity. Moreover, the population dynamics are assumed to be overcompensatory such that the stock–recruitment curve is unimodal with a long tail, peaking at $x = d$.

These biological assumptions can be expressed mathematically in the following conditions on the map f:

(B1) f is continuously differentiable and such that $f(0) = 0$, $f'(0^+) > 0$ and $f(x) > 0$ for all $x \in (0, +\infty)$.

(B2) f has three non-negative fixed points $x = 0$, $x = L > 0$ and $x = K > L$, with $f(x) > x$ for $x \in (L, K)$ and $f(x) < x$ for $x \in (0, L) \cup (K, +\infty)$.

(B3) f has a unique critical point $d \in (0, K)$ such that $f'(x) > 0$ for all $x \in (0, d)$ and $f'(x) < 0$ for all $x \in (d, +\infty)$.

For numerical simulations, we will consider a population map satisfying (B1)–(B3) that was studied in [190] as a model of mate limitation [60, 158, 188]. On the basis of the Ricker model, a strong Allee effect is induced by the introduction of density dependence in the form

$$f(x) = x \cdot \exp(r(1 - x/\widetilde{K})) \cdot I(x), \tag{2.1}$$

where $I(x) = sx/(1 + sx)$ is the probability of finding a mate, $s > 0$ measures an individual's searching efficiency and $r, \widetilde{K} > 0$ represent the growth parameter and the carrying capacity for the Ricker model in the absence of mate limitation, respectively. This model and its dynamics are described in more detail in [179, 190]. For given values of r and $\widetilde{K}$, condition (B2) is satisfied only for values of s above a certain threshold, below which the population goes asymptotically extinct for all initial conditions.

Deterministic population models like (2.1) ignore, in some sense, the unpredictability of nature. In order to take into account the effect of random events on the population dynamics, we will introduce stochasticity in the underlying model. Since Allee effects are expected to operate on small populations, we focus our attention on demographic stochasticity. One way to include this is

$$x_{t+1} = f(x_t) \cdot \exp\left(\sqrt{\frac{\sigma^2}{f(x_t)}} \cdot \varepsilon_t - \frac{\sigma^2}{2f(x_t)} \right), \qquad (2.2)$$

which was proposed in [35]. Here, f denotes the production function of the deterministic model, ε_t is a normally distributed variable with expectation 0 and variance 1, and parameter σ measures the intensity of noise.

2.3 Preventing extinction

We will study three different extinction scenarios related to the Allee effect. In the first one, populations become too small, and in the second one populations become too large (as they collapse below the Allee threshold due to overcompensation). In the third scenario, populations become too cyclic (in the sense that a boundary collision causes essential extinction).

The first two scenarios are related to bistable dynamics induced by the strong Allee effect. The existence of bistability in a deterministic population means that there is a minimum viable number of individuals L (the Allee threshold) below which the popu-

lation goes extinct and above which it persists for a set of initial conditions with positive Lebesgue measure.

2.3.1   SMALL POPULATION EXTINCTION

Small deterministic populations with a size below L eventually go extinct. This is the reason why populations with a strong Allee effect are considered particularly vulnerable to extinction. This vulnerability can be expressed in terms of different statistics, such as the extinction probability, the first passage probability or the mean time to extinction [49]. We will use the first of these measures to study the effect of ALC and ATH on population persistence.

Before doing so, we consider uncontrolled populations. In the deterministic case, the probability of extinction as a function of the initial population size has the shape of a staircase near the Allee threshold L: it equals 1 on the left-hand side of L and 0 on the right-hand side of L (Figure 2.1). When stochasticity is taken into account, populations of a small size can be 'saved' from impending extinction by random events that occasionally increase the number of individuals above L. Conversely, populations that would persist in a deterministic world can fall below L due to the effect of noise and eventually go extinct [49]. As a result, stochasticity reduces the abruptness of the deterministic Allee threshold [49, 60, 61], and the extinction probability for stochastic systems has a sigmoid decreasing shape, as shown in Figure 2.1. This has an important consequence. The concept of an Allee threshold, which for deterministic systems corresponds to the smallest positive fixed point, must be redefined in the case of stochastic populations. This will be done next.

STOCHASTIC ALLEE THRESHOLD

There are two approaches to define the Allee threshold in stochastic models, which we will refer to as stochastic Allee threshold. The first one defines the Allee threshold as the population size corresponding to the inflection point of the sigmoidally decreasing population extinction probability [60, 61]. The second approach defines the Allee
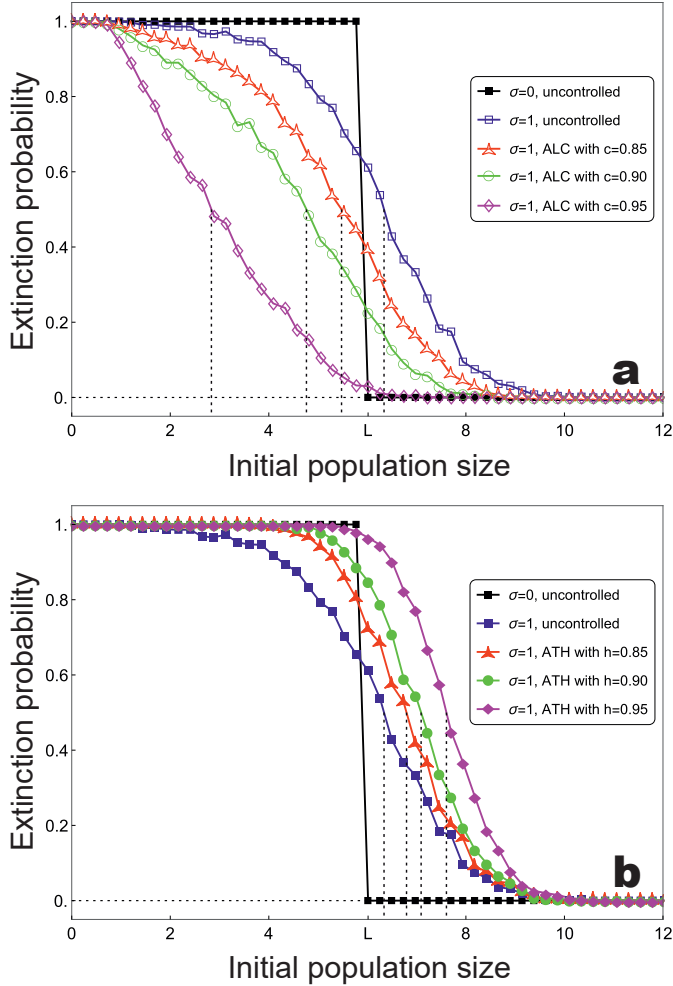
Figure 2.1: Probability of extinction of small stochastic populations. Probability of extinction in terms of the initial population size around L for deterministic ($\sigma = 0$) and demographic stochastic ($\sigma = 1$) uncontrolled populations and populations controlled with different intensities by ALC (a) and ATH (b). Calculations are based on model (2.2) for f given in (2.1), with $r = 4.5$, $\widetilde{K} = 400$ and $s = 0.002$ ($L \approx 6.015$). For a given initial population size, the probability of extinction has been obtained for the first 100 generations and over 1000 replicates.

threshold as the population size for which the probability of extinction and the probability of persistence are equal [49, 209]. This is also the definition we will use here, as it is practically easier to calculate.

It should be noted though that the two approaches yield different values for the Allee threshold, which can also be seen in Figure 2.1. Nevertheless, when we know there is always a strong Allee effect present, both approaches result in the same trends as the corresponding values are positively correlated. However, if there is weak or no demographic Allee effect, there is obviously no Allee threshold in the deterministic model and using the second approach could be misleading.

Before investigating the impact of control on the stochastic Allee thresholds, we consider the uncontrolled case. The example in Figure 2.1 shows that the stochastic Allee threshold (blue curve) is larger than the deterministic Allee threshold L. This matches the general consensus that noise renders populations with strong Allee effect more vulnerable to extinction [49, 50, 61, 179, 198].

Controlling small deterministic populations

Let us now analyze the effect of ALC and ATH on small deterministic populations. There are two questions that immediately come to mind. Firstly, can control be beneficial in the sense of saving populations that are doomed to extinction? Secondly, can control be counterproductive in the sense of inducing essential extinction of those populations that might survive otherwise? Here, we prove that neither of these situations ever happen.

Let us denote by

$$R(x) = \max\{f(x), x \cdot c\} \quad \text{and} \quad H(x) = \min\{f(x), x/h\}$$

the production function for populations controlled by ALC and ATH, respectively, and by $A_R \in (K, +\infty)$ and $A_H \in (0, K)$ the largest positive solutions of the equa-

tions $f(x) = x \cdot c$ for ALC and $f(x) = x/h$ for ATH, respectively. These values correspond to the activation thresholds for ALC [77] and ATH (Section 1.2).

For $x \in (0, L)$ the relative position of the two curves involved in $R(x)$ may vary with the control intensity, whereas for the other x-values $R(x)$ is completely defined in terms of A_R. For $x \in [L, A_R]$ the curve $y = f(x)$ is above $y = x \cdot c$ and thus $R(x) = f(x)$, whereas for $x \in (A_R, +\infty)$ the relative position of these curves is reversed and then $R(x) = x \cdot c$.

In the case of ATH, the straight line $y = x/h$ is above $y = f(x)$ for $x \in (0, L]$ and therefore $H(x) = x/h$. For $x \in [L, A_H)$ the relative position of these curves depends on the control intensity, whereas for $[A_H, +\infty)$ the curve $y = f(x)$ is above $y = x/h$ and then $H(x) = f(x)$.

Graphically, R has a bimodal shape with a local maximum at d and a local minimum at A_R. H is unimodal with a maximum at $\max\{d, A_H\}$ (cf. Figure 1.2).

The next result characterizes the dynamics of the controlled populations in case that $f(f(d)) > L$. This condition is sufficient for bistability under the assumptions (B1)–(B3). It is also necessary in case of a negative Schwarzian derivative, which is true for many population models like the generalized Beverton–Holt, Hassel, quadratic or variants of Ricker [189, 190]. In particular, it is true for the mate-finding Allee effect model considered here for numerical simulations. Recall that for a given map f, the Schwarzian derivative is defined by

$$(Sf)(x) = \frac{f'''(x)}{f'(x)} - \frac{3}{2} \left(\frac{f''(x)}{f'(x)} \right)^2. \tag{2.3}$$

Proposition 2.1. *Assume that (B1)–(B3) hold and $f(f(d)) > L$.*

1. *If $\lim\limits_{x \to +\infty} f(x) \geq L$, uncontrolled populations and populations controlled by ATH and ALC go extinct for $x_0 \in (0, L)$, and persist for $x_0 \in [L, +\infty)$.*

2. *If $\lim\limits_{x \to +\infty} f(x) < L$, there exists a unique $U > K$ such that $f(U) = L$. Uncontrolled populations and populations controlled by ATH persist for $x_0 \in [L, U]$*

and go extinct for $x_0 \in (0, L) \cup (U, +\infty)$. Populations controlled by ALC with $c \in [L/U, 1)$ persist for $x_0 \in [L, +\infty)$ and go extinct for $x_0 \in (0, L)$, while for $c \in (0, L/U)$ those initiated with $x_0 \in \bigcup_{k=0}^{+\infty} [L/c^k, U/c^k]$ persist and those with $x_0 \in (0, L) \cup \bigcup_{k=0}^{+\infty} (U/c^k, L/c^{k+1})$ go extinct.

Proof. We start by proving that small populations starting with $x_0 \in (0, L)$ go finally extinct in all cases and for all systems. This is obvious for uncontrolled populations, since $f(x) < x$ for all $x \in (0, L)$ and thus orbits correspond to strictly decreasing positive sequences. The limit of these sequences is a fixed point of the system, so must correspond to the extinction state. The same conclusion can be obtained for populations controlled by both ATH and ALC. For $x \in (0, L)$, we have $H(x) = \min\{f(x), x/h\} = f(x) < x$ since $f(x) < x < x/h$. On the other hand, $x \cdot c < x$ and $f(x) < x$ for $x \in (0, L)$, so $R(x) = \max\{f(x), x \cdot c\} < x$.

Assume now that $\lim_{x \to +\infty} f(x) \geq L$. Then, by (B1)–(B3), $f(x) \geq L$ for all $x \in [L, +\infty)$. Consequently, uncontrolled populations that start in $[L, +\infty)$ persist. This is also true for populations controlled by ALC or ATH. In the case of ALC, the conclusion follows from $R(x) = \max\{f(x), x \cdot c\} \geq f(x) \geq L$ for all $x \in [L, +\infty)$. For ATH we must distinguish two cases. For $x \in [L, A_H]$, we have $f(x) \geq L$ and $x/h \geq L/h > L$, which yields $R(x) = \min\{f(x), x/h\} \geq L$. On the other hand, $R(x) = f(x) \geq L$ for $x \in (A_H, +\infty)$.

Next, assume that $\lim_{x \to +\infty} f(x) < L$. The existence of point U follows by applying Bolzano's Theorem to $h(x) = f(x) - L$ in $(K, +\infty)$, and its uniqueness follows by (B3). Moreover, we note that $f(f(d)) > L = f(U)$ yields $f(d) < U$. We show $f([L, U]) \subset [L, U]$ by considering three different cases. Assume initially $x \in [L, d]$. Then, $L = f(L) \leq f(x) \leq f(d) < U$ because f is strictly increasing in $(0, d)$. For $x \in (d, f(d)]$ we have $L < f(f(d)) \leq f(x) < f(d) < U$, since f is strictly decreasing in $(d, +\infty)$. The same argument leads to $L = f(U) \leq f(x) <$

48

$f(f(d)) < U$ for $x \in (f(d), U]$ given that $f(f(d)) < f(d) < U$. This completes all cases and allows us to conclude that uncontrolled populations initiated in $[L, U]$ persist.

The same conclusion is true for populations controlled by ALC or ATH. For ALC, we have $R(x) = \max\{f(x), x \cdot c\} \geq f(x) > L$ for all $x \in [L, U]$. On the other hand, $f(x) \leq U$ and $x \cdot c \leq U \cdot c < U$, yielding $R(x) = \max\{f(x), x \cdot c\} \leq U$. For ATH, $H(x) = \min\{f(x), x/h\} \leq f(x) \leq U$ for all $x \in [L, U]$, and for these values $f(x) \geq L$ and $x/h \geq L/h > L$, so $H(x) = \min\{f(x), x/h\} \geq L$.

Populations starting with $x_0 \in (U, +\infty)$ go eventually extinct in the uncontrolled case because $x_1 = f(x_0) < f(U) = L$. Given that $A_H < K < U$, ATH does not alter the production function in the interval $(U, +\infty)$, and therefore the same conclusion is valid for populations controlled by this method.

Assume now $c \in [L/U, 1)$ for ALC. Given that $f(U) = L \leq U \cdot c$, we have $A_R \leq U$. For $x \in (U, +\infty)$ we have $R(x) = \max\{f(x), x \cdot c\} = x \cdot c > U \cdot c \geq L$. Since we have already shown that $R([L, U]) \subseteq [L, U]$, we obtain $R([L, +\infty)) \subseteq [L, +\infty)$, and hence controlled populations starting in $[L, +\infty)$ persist.

Finally, consider $c \in (0, L/U)$. Since $(L/c) \cdot c = L = f(U) > U \cdot c$ and f is strictly decreasing in $(d, +\infty) \supset (U, +\infty)$, we have $U < A_R < L/c$. Controlled populations initiated with $x_0 \in (U, L/c]$ go extinct because $f(x_0) < f(U) = L$ and $x_0 \cdot c < (L/c) \cdot c < L$, which yields $x_1 = \max\{f(x_0), x_0 \cdot c\} < L$. Consider now $k \geq 1$ and $x_0 \in (U/c^k, L/c^{k+1}) \subset (A_R, +\infty)$. Then, $x_k = x_0 \cdot c^k \in (U, L/c)$ and thus $x_{k+1} < L$. This proves that all controlled populations initiated in $\bigcup_{k=0}^{+\infty} (U/c^k, L/c^{k+1})$ go extinct. Assume now $x_0 \in [L/c^k, U/c^k] \subset (A_R, +\infty)$ for $k \geq 1$. Then, $x_k = x_0 \cdot c^k \in [L, U]$ and hence controlled populations starting in $\bigcup_{k=0}^{+\infty} [L/c^k, U/c^k]$ persist. $\qquad\square$

Notice that neither ALC nor ATH change the extinction probability of deterministic populations around L. Yet, there are slight differences between the effect of the two control methods in such populations. On the one hand, ATH is completely ineffec-
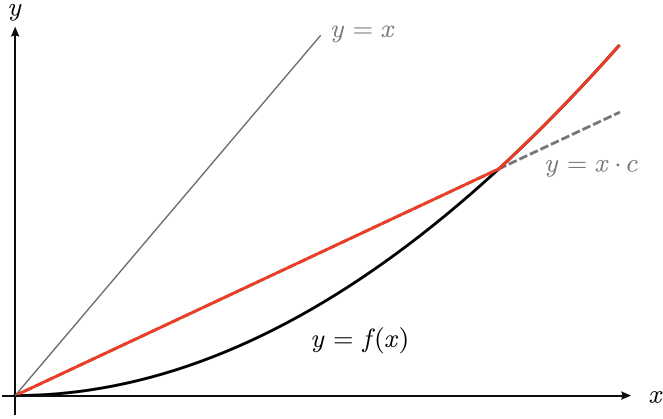
Figure 2.2: ALC can slow down the convergence to extinction of small deterministic populations. The black curve corresponds to the production function (2.1) with $r = 4.5$, $\widetilde{K} = 400$ and $s = 0.002$, and the red curve to the population controlled by ALC with intensity $c = 0.5$.

tive for small populations because it does not alter the production function around L. On the other hand, ALC does change the dynamics around the extinction state from $x_{t+1} = f(x_t)$ to $x_{t+1} = x_t \cdot c > f(x_t)$ for intensities $c > f'(0^+)$. Thus, ALC is able to slow down the extinction process, see Figure 2.2.

CONTROLLING SMALL STOCHASTIC POPULATIONS

When stochasticity is taken into account, important differences between the effect of ALC and ATH on small populations emerge. ALC with high intensities promotes population persistence by reducing both the probability of extinction and the stochastic Allee threshold (Figure 2.1a). Basically, there are two reasons for this effect. Firstly, restocking due to ALC can partially mitigate population declines that are caused by noise and that could spur extinction. Secondly, ALC prolongs for $c > f'(0^+)$ the transients to the extinction state of deterministic populations that start or drop below L (cf. Figure 2.2). These longer transients increase the chance of stochastic populations to be positively affected by noise and thus be saved for some time.

Under ATH, both the probability of extinction and the stochastic Allee threshold increase with higher harvesting intensities (Figure 2.1b). Therefore, unlike ALC, ATH seems to be counterproductive to protecting small populations. Again, two reasons help to explain this effect. Firstly, ATH is not able to slow down fortuitous declines in the size of populations that start or drop below the Allee threshold. Secondly, the harvesting of ATH tends to reduce any random growth that could move the population away from the extinction state.

Impact of stochasticity and Allee effects

We now investigate how the effect of control on population persistence depends on the level of noise, σ, and the strength of the Allee effect, s. To this end, we seek to represent the relationship between extinction probability and initial population size in a single quantity. Figure 2.1 suggests that, for given values of s and σ, the stochastic Allee threshold is positively correlated to the probability of extinction in terms of the control intensity: those control intensities with a higher extinction probability have a larger stochastic Allee threshold. Hence, we will capture the effect of the control methods on the extinction probability by analyzing the stochastic Allee threshold.

Figure 2.3a shows how the stochastic Allee threshold varies with different levels of noise in the range of bistable dynamics. When the level of noise is low, control exerted by ALC or ATH does not alter the extinction probability and, in this respect, controlled populations behave as the uncontrolled ones. For medium and high levels of noise, differences between controlled and uncontrolled populations arise: on the one hand, for small control intensities, neither ALC nor ATH alter the extinction probability; on the other hand, for medium and large control intensities, extinction probability is reduced by ALC and increased by ATH. This disparity between control methods (i) becomes more pronounced and (ii) starts to arise at smaller control intensities as the noise level increases. These observations corroborate and extend the results in Figure 2.1.

Different strengths of the Allee effect influence, of course, the quantitative level of the stochastic Allee threshold (Figure 2.3c). However, they affect neither the magnitude of disparity between ALC and ATH nor the minimum control intensity for which disparity between ALC and ATH appears.

Summary

In deterministic systems, neither ALC nor ATH are effective in changing the vulnerability of small populations to extinction associated to a strong Allee effect. The same holds true in stochastic systems with low levels of noise. If the population is sufficiently noisy, the control effect depends on the control intensity. For small control intensities, ALC and ATH are still ineffective. For medium and large control intensities, however, there is a clear difference between the control methods. While ALC decreases the stochastic Allee threshold and thus promotes population persistence, ATH decreases the stochastic Allee threshold and thus increases the risk of extinction.

2.3.2 Large population extinction

When a population is subject to a strong Allee effect, conservation concerns usually seem to focus on small populations. However, in the presence of overcompensation, also large populations can be vulnerable to extinction. Under assumptions (B1)–(B3), this happens when the limit of f for $x \to +\infty$ is below L (this is the case for the mate-finding Allee effect model (2.1) considered here, for which that limit is 0). Under these conditions, there exists a *collapse threshold* $U > K$ such that deterministic uncontrolled populations with a number of individuals above it go eventually extinct (see Figure 2.4a). By contrast, if the limit of f for $x \to +\infty$ is greater than L, all populations starting in $(L, +\infty)$ persist (see Figure 2.4b).
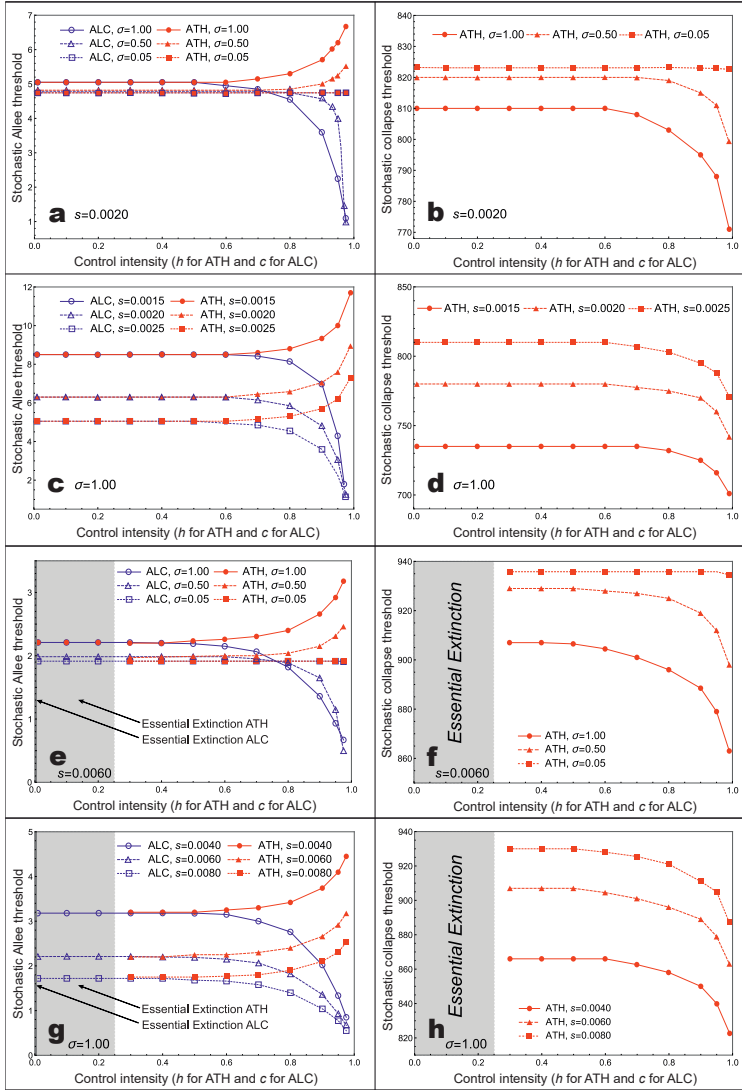
Figure 2.3: Stochastic Allee and collapse thresholds. Stochastic Allee and collapse thresholds as functions of control intensity for different levels of noise and for different strengths of the Allee effect in the range of bistable dynamics (a to d) and in the range of essential extinction (e to h). Calculations are based on model (2.2) for the production function (2.1), with $r = 4.5$ and $\widetilde{K} = 400$. For a given initial population size, the probability of extinction has been obtained for the first 100 generations and over 5000 replicates. The right-hand side panels show stochastic collapse threshold only for ATH since they exist under ALC only for extremely small intensities.
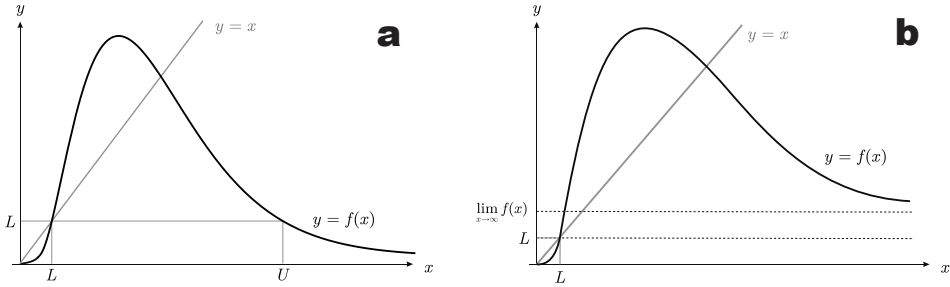
Figure 2.4: Large population extinction. Large populations can be driven to extinction if there is a collapse threshold U and population size exceeds that threshold. (a) The collapse threshold exists if $\lim_{x \to +\infty} f(x) < L$. Then there is a U such that $f(x) > L$ for all $x \in (L, U)$ and $f(x) < L$ for all $x \in (U, +\infty)$. (b) There is no collapse threshold if $\lim_{x \to +\infty} f(x) \geq L$, because then $f(x) > L$ for all $x > L$.

CONTROLLING LARGE DETERMINISTIC POPULATIONS

Assuming that a collapse threshold U exists, we now analyze how the control methods affect the extinction risk of large deterministic populations. We start by noting that ATH does not alter the production function around U. Hence, this method has no effect on the vulnerability of large deterministic populations.

By contrast, ALC can suppress that vulnerability. Proposition 2.1 shows that this happens only partially for control intensities $c < L/U$, since populations with sizes in

$$[L/c, U/c] \cup [L/c^2, U/c^2] \cup [L/c^3, U/c^3] \cup \cdots$$

persist, while populations with sizes in

$$(U, L/c) \cup (U/c, L/c^2) \cup (U/c^2, L/c^3) \cup \cdots$$

asymptotically go extinct (cf. Figure 2.5). For intensities $c > L/U$, ALC excludes extinction of large populations as all populations with sizes in $[L, +\infty)$ persist.

Regarding the critical control intensity L/U, it is remarkable that its value is less than 0.15 for the mate-finding Allee effect model considered here (for all values of s for
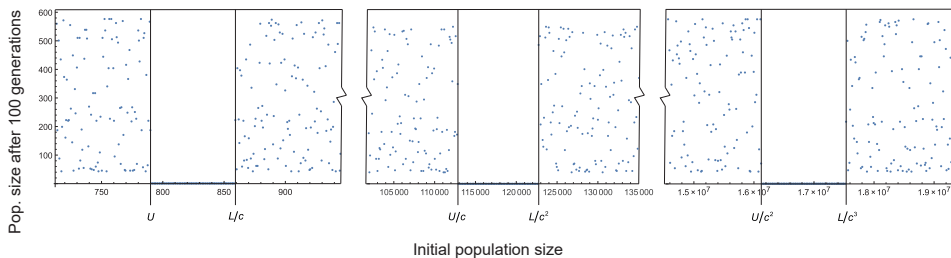
Figure 2.5: Persistence and extinction depend on the initial population size for ALC. Deterministic population sizes over the first 100 generations as a function of the initial value for ALC. Parameter values $K = 400, r = 4.5, s = 0.002, \sigma = 0$ (deterministic), and $c = 0.007$ (the value of L/U is 0.007614).

which the system exhibits bistable dynamics and for all values of r in the interval $(1, 6)$. In view of this and if the restocking intensity is greater than this value in practical implementations, one may assume that ALC totally cancels the effect of overcompensation on population persistence for the deterministic model.

Controlling large stochastic populations

Similarly to the stochastic Allee threshold, we need to extend the concept of the collapse threshold to systems that include noise. To this end, we note that, in deterministic uncontrolled systems, the extinction probability for large population sizes around U is switch-like: it equals 0 on the left-hand side of U and 1 on the right-hand side (not shown here for the sake of brevity). Noise can shift the number of individuals from one side of U to the other, thus conferring a sigmoid shape to the extinction probability around that point (not shown here). This allows us to define the *stochastic collapse threshold* as the population size for which the extinction probability equals the persistence probability.

Let us first consider the effect of ALC. Populations controlled by this method have a zero extinction probability around U (not shown here). Consequently, there is no

stochastic collapse threshold for these populations. This is consistent with the fact that ALC with large enough intensity diminishes extinction risk in the deterministic model.

By contrast, populations controlled by ATH have an extinction probability of sigmoid shape around U. Thus, we can study the effect of ATH by analyzing the stochastic collapse threshold (Figures 2.3b and 2.3d). For low levels of noise, increasing ATH intensity does not change the stochastic collapse threshold. For medium and high levels of noise, we observe the following: (i) The stochastic collapse threshold and thus population persistence become smaller with higher noise levels. (ii) There is a critical control intensity, beyond which increasing ATH intensity drastically deteriorates population persistence. (iii) This critical control intensity becomes smaller, the higher the level of noise.

Figure 2.3d shows that the stochastic collapse threshold decreases with the strength of the Allee effect. This makes sense as a collapse is more likely the stronger is the Allee effect. For low control intensities, ATH does not change the stochastic collapse threshold. For medium and high control intensities, ATH promotes population collapses. The stronger the Allee effect, the sooner the onset of the deteriorating effect of ATH.

Summary

Regarding the collapse of large populations, there is a clear difference between the control methods. ALC with high enough a restocking intensity ensures the survival of deterministic populations with a large number of individuals that would be doomed to extinction in the absence of control. In stochastic systems, ALC completely prevents collapses of large populations considered here. By contrast, ATH is either ineffective (in deterministic systems and for small control intensities in stochastic systems) or counterproductive (for medium and high control intensities in stochastic systems).

2.3.3 Essential extinction

In the previous two extinction scenarios, the deterministic uncontrolled population dynamics are bistable, i.e., the fate of the population depends on the initial condition.

Now we consider the scenario of essential extinction, where the only attractor is the extinction state. This means that populations go extinct with probability 1 for randomly chosen initial conditions.

Deterministic population dynamics

It is in the scenario of essential extinction that we find the main advantage of ALC and ATH: both methods can induce bistability and thus facilitate population persistence if the control intensity is greater than a critical threshold. With the following result we prove that the critical thresholds for the control intensities are $c_0 = L/U$ for ALC and $h_0 = d/f(d)$ for ATH. Once the critical control intensity has been exceeded and the controlled system exhibits bistability, populations behave as described in the previous two scenarios.

Proposition 2.2. *Assume that (B1)–(B3) hold and the dynamics shows essential extinction. Then, there exist $c_0, h_0 \in (0,1)$ such that the system controlled by ALC with any intensity $c > c_0$ and the system controlled by ATH with any intensity $h > h_0$ exhibit bistable dynamics.*

Proof. According to Proposition 2.1, it must be $f(f(d)) \leq L$ (otherwise, the dynamics would show bistability). Since $f(K) = K > d > L$ and $f(d) > d$, Bolzano's theorem and the strict decrease of f in $(d, +\infty)$ yield the existence of a unique $U > K$ verifying $f(U) = L$. On the other hand, $f(x) \geq L$ for all $x \in [L, U]$ because f is strictly increasing in (L, d), strictly decreasing in (d, U) and $f(L) = f(U) = L$.

Consider the restocking intensity $c_0 = L/U < 1$. For $c > c_0$ we can use the same reasoning as in Proposition 2.1 to show that orbits starting in $[L, +\infty)$ remain in this interval and the corresponding populations persist.

Let us now study the case of ATH. Consider the harvesting intensity $h = d/f(d)$, for which $A_H = d$. The peak of the stock–recruitment curve for the controlled system is $f(A_H) = A_H/h = f(d) > d$ and its image is $f(f(A_H)) = f(A_H/h) = f(f(d)) \leq L$. As h increases, the straight line $y = x/h$ tends to $y = x$ and A_H

strictly grows and approaches K for $h \to 1$. Then, given that f is strictly decreasing in $(d, +\infty)$, the term $f(A_H) = A_H/h$ strictly decreases and tends to $f(K) = K$. With the same argument, $f(A_H/h)$ strictly increases and tends to $K > L$. Hence, according to Bolzano's theorem, there must exist $h_0 \geq d/f(d)$ such that $f(A_H/h_0) = L$. Moreover, given the strict increase of $f(A_H/h)$, we have $f(A_H/h) > L$ for $h > h_0$. By arguments already used here, we obtain $H(L, U) \subset [L, U]$, and we conclude that the system controlled by ATH shows bistability for $h > h_0$. □

STOCHASTIC POPULATION DYNAMICS

While noise in bistable systems can be occasionally beneficial to populations by perturbing their size above the extinction threshold, this can never happen in the scenario of essential extinction, see also Corollary 4.3 in [179]. Deterministic populations showing essential extinction only persist for a small number of initial conditions, in particular for those that coincide with the positive fixed points. Yet, when noise is taken into account, stochastic uncontrolled populations go extinct for all possible initial sizes, including the positive fixed points, as random events perturb the population size from equilibrium. Hence, noise is in this respect counterproductive.

Let us now study the effect of ALC and ATH on stochastic systems for which the deterministic dynamics exhibits essential extinction. As in the previous two extinction scenarios, we will analyze the stochastic Allee thresholds and the stochastic collapse thresholds (Figures 2.3e to 2.3h).

As in the deterministic setting, both ALC and ATH are able to save stochastic populations that would be doomed to essential extinction in the absence of control. This can be seen in Figures 2.3e to 2.3h by the existence of a stochastic Allee or collapse threshold. The control-mediated survival occurs if the control intensity exceeds a critical value; in the case of ALC, the critical control intensity is close to (but not exactly) zero; i.e., without control there would be essential extinction. Once the control intensity of ALC or ATH exceeds the corresponding critical value, the population becomes bistable and the effect of the control methods on stochastic populations is analogous

to the case of bistable dynamics. The only remarkable difference is that the disparity between populations controlled by ALC on the one hand and ATH on the other hand arises for somewhat lower control intensities than in the bistable scenarios (cf. Figures 2.3a and 2.3c with Figures 2.3e and 2.3g).

2.4 PREVENTING POPULATION OUTBREAKS

The previous section was concerned with population extinction. Now we shift attention from vulnerable species to pests, and the aim is to contain their population size in order to avoid outbreaks. We will study bistable populations only, because under essential extinction there appears to be less need for controlling outbreaks.

2.4.1 OUTBREAKS AND PROBABILITY OF OUTBREAKS

First, we need to specify what exactly we mean by outbreaks. In the literature, there are different definitions of outbreaks, many of which concern a specific situation or population model, e.g., [22, 69, 70]. In our case, if K is stable, the concept of an outbreak does not make sense because all orbits are monotonically attracted towards this point or towards the extinction state. There are no sustained oscillations in population size, which could be controlled by ALC or ATH. Hence, we restrict our attention to K being unstable, such that all populations not attracted towards the extinction state oscillate in size around K. In this situation, an obvious definition of outbreaks is related to the amplitude of these oscillations. Hence, we will consider as *outbreak* any population size exceeding the midpoint between the unstable fixed point K and the maximum population size $f(d)$.

For uncontrolled and deterministic populations, Figure 2.6 shows that the probability of outbreaks switches at the Allee threshold L: for initial population sizes below (above) L the outbreak probability is zero (one). When stochasticity is included, we observe an effect reverse to that for the extinction probability: noise can cause booms in stochastic uncontrolled populations that start or drop below L, while populations

starting above L can remain below the outbreak threshold thanks to random declines caused by noise. This confers a sigmoid shape to the outbreak probability (but mirrored horizontally in comparison to the extinction probability). The stochastic outbreak threshold, i.e., the population size at which the probability of an outbreak equals the probability of no outbreak, increases in comparison to the deterministic outbreak threshold in Figure 2.6. Hence, stochasticity seems to render populations with a strong Allee effect more prone to outbreaks.

2.4.2 EFFECT OF ATH

Figure 2.6b shows that ATH tends to reduce the probability of outbreaks. This happens for sufficiently large control intensities ($h \gtrsim 0.55$) and can be easily explained by the harvesting action of ATH that can mitigate any fortuitous population growth due to noise. For control intensities that are too small, there is no difference in the outbreak probability between controlled and uncontrolled populations.

Moreover, Figure 2.6b shows that, for high harvesting intensities ($h \gtrsim 0.7$), ATH completely prevents population booms. This may be explained as follows. For sufficiently high harvesting intensities, ATH establishes in a deterministic system bistability between zero and a trapping region around K (see Proposition 2.2). As a consequence, the trapping region imposes an upper bound on the population size. This upper bound decreases with control intensity and tends to K when $h \to 1$. Consequently, for high enough harvesting intensities the number of individuals is asymptotically bounded by a value that is below the outbreak threshold. Hence, population booms are unlikely to happen. They can only occur if the effect of noise moves the population size above the trapping region for the deterministic system in such a way that the outbreak threshold is exceeded.

2.4.3 EFFECT OF ALC

Comparing Figure 2.6a with Figure 2.6b reveals that ALC has different impacts on outbreak probabilities than ATH has. First we note that for small and medium restocking
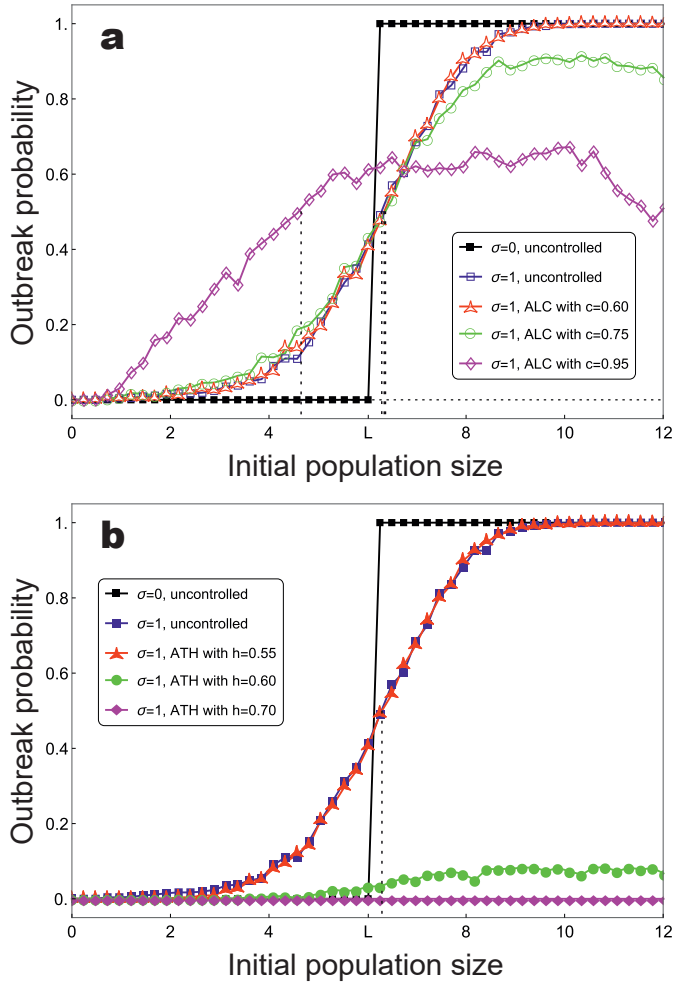
Figure 2.6: Probability of outbreak in terms of the initial population size. The population is controlled by (a) ALC and (b) ATH. Population dynamics are deterministic $(\sigma = 0)$ or with demographic stochasticity $(\sigma = 1)$. Calculations are based on model (2.2) for the production function (2.1), with $r = 4.5$, $\widetilde{K} = 400$ and $s = 0.002$ ($L \approx 6.015$). Population outbreaks are considered to occur when the number of individuals exceeds $(K + f(d))/2$. For a given initial population size, the outbreak probability has been obtained for the first 100 generations and over 1000 replicates.

intensities ($c \lesssim 0.6$), ALC seems to change outbreak probabilities only marginally. This behavior may be explained by two opposing effects of ALC. On the one hand, the restocking of ALC mitigates any random population decline, which tends to promote the risk of outbreaks. On the other hand, also ALC establishes a trapping region around K for large enough control intensities (Proposition 2.2). Then there is an asymptotic upper bound on population size, and this bound decreases with restocking intensity. For small and medium restocking intensities, the upper bound is large and potentially greater than the outbreak threshold, while the capability of ALC to restock population declines is weak.

For high control intensities, ALC has a very different effect than ATH. We have to distinguish between small and large initial population size. For initial population sizes above L, ALC significantly reduces the outbreak probability. This is probably due to the asymptotic upper bound. However, ALC cannot completely prevent outbreaks (cf. the magenta curve for $c = 0.95$) as ATH can, which is probably due to the restocking. For initial population sizes below L, ALC can have a counterproductive effect, as ALC increases extinction probability in comparison to the uncontrolled population. This happens approximately for $c \geq 0.6$ (cf. green and red curves with the uncontrolled curve in Figure 2.6a). For very large control intensities, ALC increases extinction risk of population sizes below L drastically (e.g., for $c = 0.95$ in Figure 2.6a). This may be caused by the capability of ALC to offset population declines, which becomes so strong for high control intensities such that populations are almost fully shielded against random declines. However, they benefit from all possible random growths, which inflates outbreak risk.

2.4.4 Summary

ATH reveals itself as especially suitable for the control of nuisance species as it reduces or completely prevents stochastic outbreaks of small populations. By contrast, ALC tends to be ineffective for low and medium restocking intensities and is counterproductive for high restocking intensities.

2.5 Controlling outbreaks of forest-defoliating insects

In the previous section we have considered outbreaks in a bistable population with a strong Allee effect. In this particular setting, one of the two attractors is the extinction state. That is, if the population has gone extinct, there cannot be any outbreak in the following generation unless there is immigration, invasion or some form of external perturbation. However, in bistable situations where both attractors are positive, the population can 'rest' in a low-density state until an outbreak is triggered by some mechanism and the population bursts to a higher-density attractor.

Such a situation often occurs in models of forest-defoliating insects. Here, we consider a model by Dwyer *et al.* [70] that incorporates the effect of a generalist predator to a classical host–pathogen system. The non-dimensionalized stochastic version of this model reads

$$1 - I(x_t, z_t) = \left(1 + \frac{1}{k}(x_t I(x_t, z_t) + z_t)\right)^{-k},$$

$$x_{t+1} = \lambda x_t(1 - I(x_t, z_t))\left(1 - \frac{2ABx_t}{B^2 + x_t^2}\right)\varepsilon_t, \qquad (2.4)$$

$$z_{t+1} = \phi x_t I(x_t, z_t),$$

where the two variables x_t and z_t represent the host and pathogen densities in generation t, respectively. Given these densities, $I(x_t, z_t)$ is the fraction of infected hosts. The term ε_t is a log-normal random variable with median 1 and standard deviation σ. Regarding the parameters in this model, λ represents the net defoliator fecundity, ϕ is the between-season impact of the pathogen, A is the maximum fraction of defoliators killed by the predator, B is the ratio of the density at maximum predation to the epidemic threshold and k is the inverse squared coefficient of variation of the transmission rates, which follows a gamma distribution. Parameter values have been estimated for populations of the gypsy moth *Lymantria dispar* as the host (defoliator) and a bac-

ulovirus as the pathogen, yielding $\lambda = 74.6$, $\phi = 20$, $A = 0.967$, $B = 0.14$, and $k = 1.06$ [70]. For these values, the deterministic model has three equilibria with high, intermediate and low defoliator densities. At the high-density equilibrium the defoliator is controlled by the pathogen while the predator is relatively unimportant. This equilibrium is unstable and induces an oscillatory attractor. The low-density equilibrium is stable and the control over the defoliator is exerted by the predator, with the influence of the pathogen being fairly irrelevant. Finally, the intermediate-density equilibrium is unstable. The inclusion of stochasticity makes the defoliator density move unpredictably among attractors and induces high variability in the time between insect outbreaks.

Since our goal is to diminish outbreaks of the defoliator population, we consider control actions on the state variable x_t only. Then, a model including ALC can be described by modifying the second equation of (2.4) to

$$x_{t+1} = \max \left\{ \lambda x_t (1 - I(x_t, z_t)) \left(1 - \frac{2ABx_t}{B^2 + x_t^2} \right), c \cdot x_t \right\} \varepsilon_t.$$

Similarly, for ATH we obtain

$$x_{t+1} = \min \left\{ \lambda x_t (1 - I(x_t, z_t)) \left(1 - \frac{2ABx_t}{B^2 + x_t^2} \right), x_t / h \right\} \varepsilon_t.$$

Figure 2.7a shows time series of three stochastic defoliator populations with the same initial conditions corresponding to the uncontrolled system and systems controlled by ALC and ATH with intensities $c = h = 0.9$. ATH keeps the defoliator densities close to zero for the entire time period considered. By contrast, under the control of ALC, the defoliator reaches densities much higher than in the absence of control.

In order to analyze if this is always the case, Figure 2.7b compares the maximum defoliator densities for the uncontrolled and controlled populations with different control intensities and different initial conditions for both pathogen and host. We have chosen maximum densities as they are the quantity of interest in outbreak situations. ATH
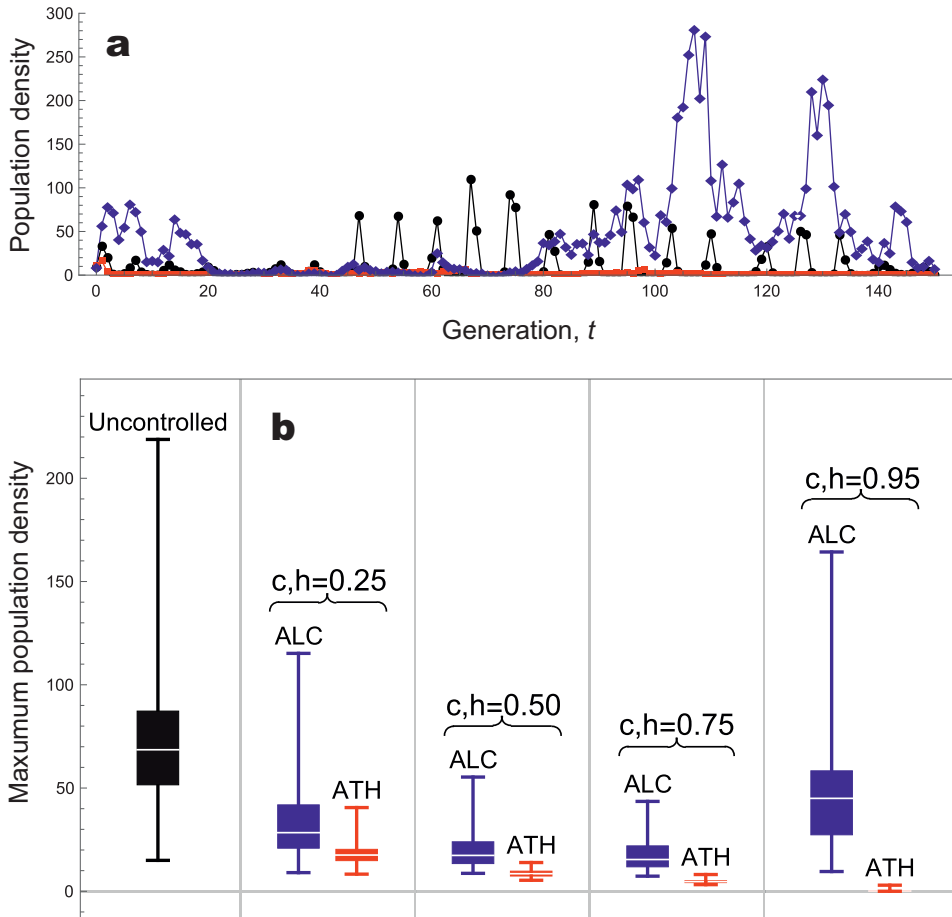
Figure 2.7: Numerical simulations for the gypsy moth model. (a) Comparison of model time series for populations of the defoliator gypsy moth. The black curve corresponds to the uncontrolled system, the blue one to the system controlled by ALC with $c = 0.9$ and the red one to ATH with $h = 0.9$. (b) Box plots of the maximum population density of defoliators for the uncontrolled system and systems controlled by ATH and ALC with different intensities. Calculations are based on model (2.4) with $\lambda = 74.6$, $\phi = 20$, $A = 0.967$, $B = 0.14$, $k = 1.06$ and $\sigma = 0.5$. Initial densities in (a) are $x_0 = 10$ for the defoliator and $z_0 = 7$ for the pathogen. Values in (b) have been obtained from 100 time series with initial population densities uniformly distributed in $[0.01, 100]$ and a time horizon of 50 generations.

clearly reduces the maximum defoliator density for the range of control intensities considered. By comparison, maximum population sizes are both higher and more variable when controlled by ALC and ATH. In particular, while ATH performs better in reducing population maxima when increasing control intensities to the values shown in Figure 2.7b, ALC loses some of its effectiveness for the control intensity of $c = 0.95$. This can also be seen in Figure 2.7a, where the maximum density of populations controlled by ALC is much larger than when the number of insects is not controlled.

2.6   DISCUSSION AND CONCLUSIONS

We have compared the impact of ALC and ATH on extinction and outbreak probabilities. In order to capture stochastic effects, we have used the concept of stochastic Allee thresholds, stochastic collapse thresholds and stochastic outbreak thresholds. Both control methods have in common that they become effective (in the sense of changing stochastic extinction or outbreak thresholds) only for sufficiently large control intensities. If their interventions do show an effect, there is a clear disparity between the two methods in each of the biological situations considered.

Regarding the control of outbreaks, we have studied how the control methods affect the outbreak probabilities. ATH proves beneficial in terms of reducing or even completely eliminating outbreak probability. It can also significantly curtail the magnitude of population booms (measured by maximum defoliator population sizes in the gypsy moth model). By contrast, ALC is either ineffective or even counterproductive. This holds for both the Allee effect and the gypsy moth model. As ATH removes individuals from and ALC adds individuals to a population, these results seem plausible because the goal is to get rid of rather than to augment pest species.

Since population fluctuations can be particularly important in driving population booms, we have defined outbreaks as the population size exceeding a value well above the carrying capacity, which can only be achieved in deterministic systems if the population cycles. Therefore, our definition of outbreak probability is not simply the inverse

of extinction probability, and it differs from related measures such as establishment, invasion or persistence probability, see, e.g., [68, 139, 179].

Regarding vulnerable species, our results are similar but reversed. Again, the control intensities of both ALC and ATH need to be high enough to change extinction risk. Once there is an effect, ALC proves beneficial for population persistence and is even able to completely eliminate the collapse risk (large population extinction). By contrast, ATH is either ineffective or counterproductive in preventing outbreaks. These results seem plausible as well because augmenting vulnerable populations appears more suitable than reducing them.

Interestingly, for deterministic population dynamics, we prove that neither ALC nor ATH have any effect on the extinction probabilities of small populations (Proposition 2.1.1). This makes sense in the case of ATH because it harvests relatively large populations and therefore does not change the production curve at small population sizes. In the case of ALC, its inefficacy may appear surprising at first sight. However, while ALC does restock small populations, it does not do so to large enough a level to exceed the Allee threshold (cf. Figure 2.2). Hence, the restocking tends to slow down the extinction process, but it cannot prevent extinction in the first place. This could only be achieved by restocking intensities $c > 1$; however, they will cause a population blow-up if implemented also at larger population sizes (Section 1.3).

In the scenario of large population extinctions, ATH has no effect on the deterministic collapse threshold, whereas ALC is either ineffective as well or can reduce extinction risk depending on the initial condition and the control intensity (Proposition 2.1.2). This is a surprising result because augmenting the population in this situation is a better option than harvesting it, even though extinction is caused by exceeding a collapse threshold. This can be explained as follows. ATH is ineffective because harvesting takes place only at population sizes below the collapse threshold. ALC can be effective because it restocks populations *after* they have collapsed. Hence, the restocking intervention 'counter-compensates' for the overcompensatory population dynamics causing

the collapse of large populations. If the order of events or census timing were changed, the quantitative results could be different [12, 27, 104].

While the two control methods have no effect in the deterministic small and large population extinction scenarios (or, in the case of ALC, only conditionally), ALC and ATH can become effective (or counterproductive) in the presence of stochasticity. In that sense, stochasticity can be a foe or a friend to management programs.

The scenario of large population extinction is particularly interesting for another reason. While conservation biology and mathematical modeling has been mostly concerned with small populations [3, 49, 60, 61, 129, 130, 179], we have shown that also large populations can be at risk of extinction, even if they have population sizes well above the Allee threshold and close to the carrying capacity. At such large population sizes, one might be tempted to expect that Allee effect could be ignored. However, in concert with overcompensatory population dynamics, the population is not safe even at those high levels.

So far, the interplay between Allee effects and overcompensation has been mostly studied in the context of essential extinction [179, 190]. However, as highlighted before, the Allee effect has been largely ignored in control methods aimed at stabilizing populations, but see [38, 44, 53]. By contrast, the fisheries literature seems to have paid more attention to the role of Allee effects in managed populations and pointed out that Allee effects curtail yield and stock levels at low population abundance, e.g., [60, 148, 218].

Allee effects have also been found to play a role in biological invasions [203] and in pest outbreaks (e.g., for the gypsy moth see [112, 208]) . In this chapter, we have studied outbreaks in two different types of models. In the model with a strong Allee effect (Section 2.4), the low-density attractor corresponds to extinction, whereas in the gypsy moth model by Dwyer *et al.* [70] the low-density attractor is positive (Section 2.5). In the latter case, noise promotes even more population variability as it can cause recurrent jumps between attractors.

3

Enhancing population stability with combined adaptive limiter control and finding the right harvesting-restocking balance

3.1   INTRODUCTION

The combination of harvesting and restocking has proved useful for the management of many populations, e.g., aqua-cultured fish [17, 18, 147], game species of birds and mammals [40], sea urchins [52] or prawns [204]. Moreover, control strategies that combine the removal and restocking of individuals of a population have been shown in mathematical models to be generally very effective, e.g., both limiter control (BLC) [212, 213, 214] or target-oriented control (TOC) [29, 59, 79, 213]. These strategies expand the range of choices for the control and allow the users to achieve management

goals that would not be possible by either only restocking or only culling the population [213].

When combined, restocking and harvesting can play a central role in population management. For instance, in the case of coastal fisheries [17], when the goal is to restock depleted populations, the release of juveniles should be combined with large reductions in culling. By contrast, when the goal is to overcome recruitment limitation, releases may be combined with relatively high culling efforts.

In this chapter, we propose a new management strategy that allows for both restocking and harvesting by combining ALC and ATH. If the population size grows beyond a certain proportion, ATH is applied to cull part of the increase, whereas if the population size declines below another proportion, ALC is applied to restock part of the diminished population. We will refer to this strategy as *combined adaptive limiter control* (CALC).

CALC avoids the state variable to become too low or too high. This is somewhat analogous to certain biological processes at the level of organism homeostasis. One example is the integral rein control [186], in which glucagon inputs prevent blood glucose from becoming too low and insulin inputs prevent blood glucose from becoming too high.

How to combine harvesting and restocking will depend on biological, economic and social factors [146, 147, 204]. In particular, the economic side seems to often play a central role. For instance, in the case of aqua-cultured fishes, the cost of hatchery fish can determine the optimal management. At a high cost, no increase in the total yield and stock abundance is expected [146]. An example of this is the management of Alaskan pink salmon, which has proved uneconomic under current conditions [26, 103]. By contrast, high efforts of both fishing and restocking can be optimal when the cost is low [146], this being the case for Japanese chum salmon [10, 161]. Another example of the relevance of the economic aspect is the release of hatchery-reared sea urchins in wild populations. In that case, restocking can recover local productivity [114, 115], but the high cost of hatchery sea urchins can make the management uneconomic [52, 134].

Here, in addition to studying the stabilizing effect that can be attained by the combination of restocking and harvesting under CALC, we analyze the trade-off between this stabilizing effect and the cost of the management interventions.

Our main goal is to show in which cases CALC may be advantageous over ALC and ATH. Optimal management strategies are commonly determined by optimizing a single objective function, e.g., the maximum sustainable yield [42, 45, 187, 199] or the maximum economic yield [6, 64, 94, 119, 174]. In our case, such an approach would provide specific values for harvesting and restocking efforts at the optimum but no information for other values. Contrary to this, our aim is to provide a more holistic view by studying the behavior of the managed populations for all possible combinations of harvesting and restocking and for different stability criteria. We are convinced that adopting such a perspective enriches the analysis. In this sense, the reader is cautioned to not expect absolute conclusions about which is the 'best' strategy.

In the next section, we describe CALC in mathematical terms and study its stabilizing properties. In Section 3.3, we introduce CALC as a management strategy in different population models. Section 3.4 studies the effect of CALC on the constancy stability of a stochastic population with overcompensation. Section 3.5 analyzes the capability of CALC to prevent outbreaks of forest-defoliating insects in a stochastic three-species model. We also consider the economic benefit that would be obtained by reducing outbreaks depending on both the restocking and harvesting costs. Section 3.6 extends the discussion of our results and draws conclusions.

3.2 Combined adaptive limiter control

3.2.1 Modeling combined adaptive limiter control

CALC aims at reducing the fluctuations in population size by avoiding crashes and outbreaks. Let x_t be the population size at time step t. If x_t drops below a certain proportion of its value in the previous generation (which we denote by $c \cdot x_{t-1}$, with $c \in (0, 1)$), individuals are restocked to that proportion. We will refer to c as the
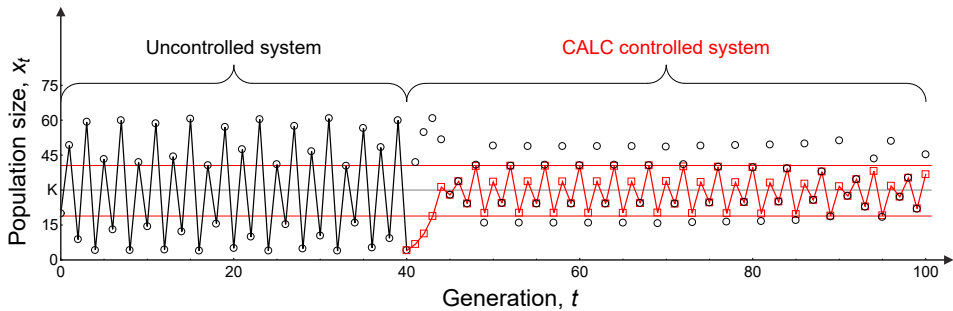
Figure 3.1: Stabilizing effect of CALC. During the first 40 generations the population is uncontrolled and its dynamics are described by the Ricker map $f(x) = x \exp(r(1 - x/K))$ with $r = 2.7$ and $K = 30$. In the next 60 generations, the population is managed by CALC with intensities $c = 0.5$ and $h = 0.6$. Black circles (red squares) correspond to the population size before (after) the control intervention. The horizontal red lines represent the limits of the interval that traps the size of populations managed according to CALC with the given control intensities (see equations (3.4) and (3.5)).

restocking intensity, since higher values of c correspond to higher restocking efforts. If x_t exceeds another proportion of x_{t-1} (which we denote by x_{t-1}/h, with $h \in (0, 1)$), the population is harvested to that proportion. We can interpret h as a *harvesting intensity*, since higher values of h correspond to lower values of $1/h$, and thus to higher removal efforts.

The control strategy described above can be seen as the combination of ALC and ATH, both of which are able to reduce the fluctuations in the population size [Chapters 1 and 2, 77, 78, 183, 184, 212]. Figure 3.1 illustrates that CALC shares this property with them. CALC differs from other strategies for which the magnitude of the intervention is also nonconstant, like proportional feedback, for which a fixed proportion of the population is harvested or restocked every generation [92]. In the case of CALC, no action is taken if the proportion between population sizes in two consecutive generations is within the stipulated limits c and $1/h$.

To further understand the effect of CALC and its relation with ALC/ATH, assume that the underlying population dynamics, i.e., in the absence of CALC, are given by

$$x_{t+1} = f(x_t), \ x_0 \in [0, +\infty), \ t \in \mathbb{N},$$

where $f : [0, b] \to [0, b]$ ($b = +\infty$ is allowed) is a continuously differentiable hump-shaped production function satisfying conditions (A1)–(A3) (see Section 1.2). Assume that b_t denotes the population size at time step t before the control intervention and a_t the population size after intervention. The dynamics of populations subject to CALC are given by the equations

$$b_{t+1} = f(a_t),$$

$$a_{t+1} = \begin{cases} c \cdot a_t, & b_{t+1} < c \cdot a_t, \\ b_{t+1}, & c \cdot a_t \leq b_{t+1} \leq a_t/h, \\ a_t/h, & b_{t+1} > a_t/h, \end{cases} \tag{3.1}$$

where $c, h \in (0, 1)$ are the restocking and harvesting intensities, respectively. Substituting the value of b_{t+1} into the second equation of (3.1), the dynamics of populations subject to CALC are described by the piecewise one-dimensional difference equation

$$a_{t+1} = \begin{cases} c \cdot a_t, & f(a_t) < c \cdot a_t, \\ f(a_t), & c \cdot a_t \leq f(a_t) \leq a_t/h, \\ a_t/h, & f(a_t) > a_t/h, \end{cases}$$

which can be rewritten in a single line as

$$a_{t+1} = \max\{\min\{f(a_t), a_t/h\}, c \cdot a_t\}. \tag{3.2}$$

We can see CALC as a general framework for adaptive limiters, including both ALC and ATH as particular cases if we allow the control parameters to be null. Given that
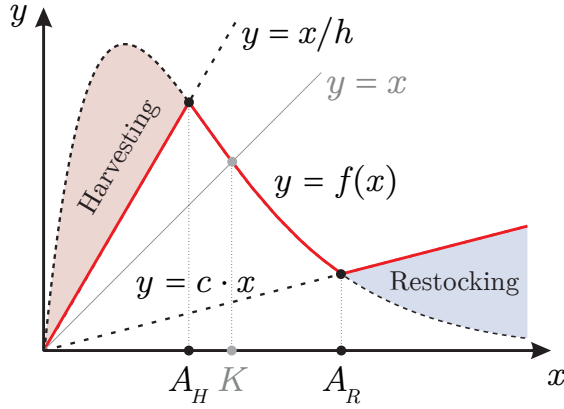
Figure 3.2: CALC map. The red solid line represents the CALC function (3.2) for a given map f in dashed line describing the underlying dynamics. The red area corresponds to the cases in which the population is harvested, and the blue to those in which it is restocked. For the meaning of the variables see the main text.

c and h respectively represent the restocking and harvesting intensities, $c = 0$ corresponds to only harvesting (ATH) and $h = 0$ to only restocking (ALC). However, the latter is not well defined in equation (3.2). To overcome this, we redefine the equation describing CALC with $h = 0$ to $a_{t+1} = \max\{f(a_t), c \cdot a_t\}$.

Figure 3.2 shows function (3.2) with $c, h \in (0, 1)$ for a certain map f describing the underlying dynamics (which is compatible, for instance, with the Ricker map). The population is harvested when the population size x is such that the graph of f is strictly above the straight line $y = x/h$. Similarly, the population is restocked when the graph of f is strictly below $y = c \cdot x$ (cf. Figure 3.2). Therefore, in case the population is controlled, the type of intervention (harvesting or restocking) depends on the population size in the previous generation, the control intensities c and h, and the production function f. It is important to highlight that restocking and harvesting cannot take place simultaneously at a given time since $c < 1/h$. Yet, for certain combinations of control intensities, the population can be restocked at some time steps and harvested at other time steps. For the sake of simplicity, we will refer to this case as the *combination* of

restocking and harvesting. Similarly, for certain values of the control intensities interventions can consist of harvesting only or restocking only.

3.2.2 CALC FOR DIFFERENT PRODUCTION FUNCTIONS

Given a production function f, we can determine for which control intensities the population will remain uncontrolled and for which control intensities the interventions used in CALC will consist of only harvesting, only restocking or a combination of harvesting and restocking. Next, we study the type of intervention (restocking, harvesting or their combination) that corresponds to CALC depending on the control parameters for different production functions of the uncontrolled population. We consider four cases.

First, we consider unimodal maps (i.e., satisfying conditions (A1)–(A3)) like the one represented in the first column of Figure 3.3a. If d denotes the abscissa of the maximum production, after the first generation the population size is always below $f(d)$. Thus, for low enough values of c (namely, $c \leq f^2(d)/f(d)$, where $f^2 = f \circ f$) and after the first generation, all possible interventions consist of harvesting only. Similarly, for low enough values of h (namely, $h \leq 1/f'(0^+)$), the graph of f is below the straight line $y = x/h$ for all values of x. Thus, in that case all possible interventions consist of restocking only. For $c > f^2(d)/f(d)$ and $h > 1/f'(0^+)$ the population can be either harvested or restocked depending on its size. Finally, for $c \leq f^2(d)/f(d)$ and $h \leq 1/f'(0^+)$, the population remains uncontrolled. The distribution of the type of intervention (uncontrolled, restocking only, harvesting only or a mixture of harvesting and restocking) is represented in the second column of Figure 3.3a.

Second, we consider maps like the one represented in Figure 3.3b, which is compatible with the Beverton-Holt model with constant immigration. In this case, CALC leads to restocking for any $c > 0$ and to harvesting for any $h > 0$. Consequently, restocking and harvesting are combined for $(c, h) \in (0, 1) \times (0, 1)$, only restocking is implemented for $(c, h) \in (0, 1) \times \{0\}$, only harvesting for $(c, h) \in \{0\} \times (0, 1)$, and the population remains uncontrolled for $(c, h) = (0, 0)$.
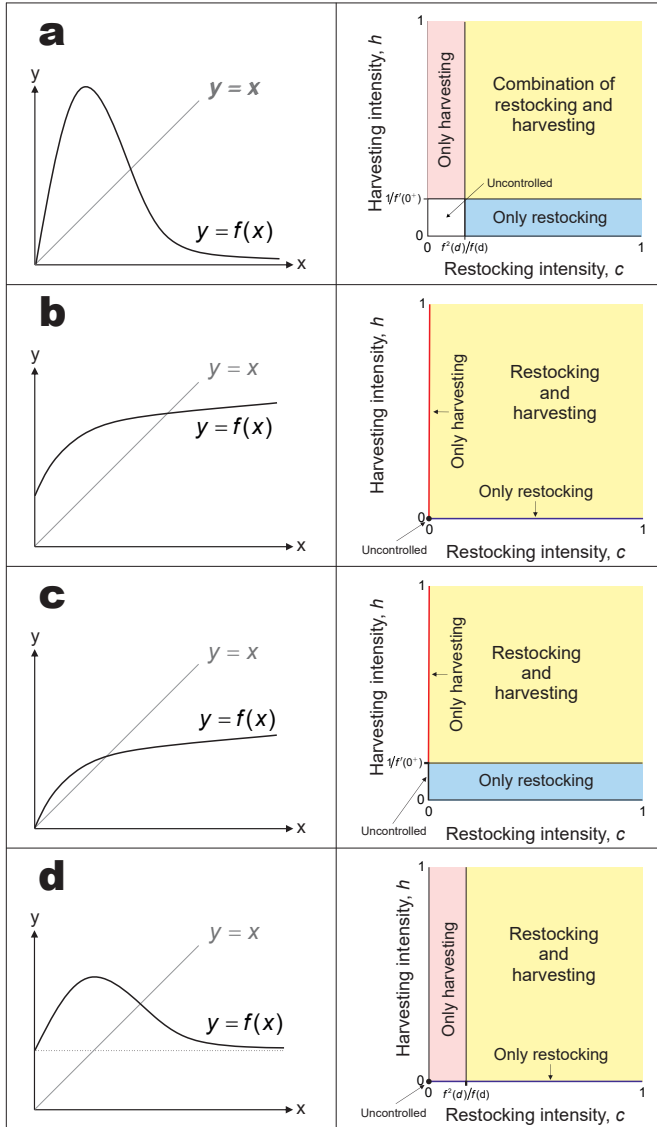
Figure 3.3: Type of intervention for CALC on different production functions. For each row, the first column shows a production function and the second column the corresponding distribution of the type of intervention (restocking, harvesting or their combination) in terms of the control intensities. In (d), the first generation was omitted in the only harvesting area.

Third, for the production function shown in Figure 3.3c, which is compatible with the Beverton-Holt model, there is a threshold for harvesting given by $h_0 = 1/f'(0^+)$, while there is no threshold for restocking. Therefore, CALC leads to a combination of restocking and harvesting for $(c, h) \in (0, 1) \times (h_0, 1)$, only restocking for $(c, h) \in (0, 1) \times [0, h_0)$, only harvesting for $(c, h) \in \{0\} \times (h_0, 1)$, and the population remains uncontrolled for $(c, h) \in \{0\} \times [0, h_0]$.

Finally, for the map shown in Figure 3.3d, which is compatible with the Ricker model (or any other unimodal map) with constant immigration, there is a restocking threshold $c_0 = f^2(d)/f(d)$ and no harvesting threshold. In this case, restocking can act in the first generation for any restocking intensity, but the population is never supplemented in subsequent generations if $c < c_0$. Consequently, after the first generation harvesting and restocking are combined for $(c, h) \in (c_0, 1) \times (0, 1)$, only restocking for $(c, h) \in (c_0, 1) \times \{0\}$, only harvesting for $(c, h) \in [0, c_0] \times (0, 1)$, and the population remains uncontrolled for $(c, h) \in [0, c_0] \times \{0\}$.

In the following subsections we prove results that also exist in similar form for ALC [77] and ATH (see Chapter 1), so we show that they translate to the two-parametric strategy of CALC.

3.2.3   ACTIVATION THRESHOLDS

As a method that combines ALC and ATH, depending on the shape of the map that describes the underlying dynamics the CALC control may induce activation thresholds in the controlled population that allow one to predict the need of intervention in the following generation. This is the case for maps satisfying conditions (A1)–(A3). For these maps, the activation threshold of harvesting (which we denote by A_H) exists for $h > \inf_{x \in (0,b)} x/f(x)$ and corresponds to the abscissa of the leftmost nonzero intersection of the curve $y = f(x)$ and $y = x/h$. No harvesting will be necessary in generation t if the population size in the preceding generation is above A_H (cf. Section 1.2). Moreover, if f is concave downward in $(0, d)$ (which is true for many unimodal maps, e.g., Ricker) the population is culled in generation t if its size in the previous generation

77
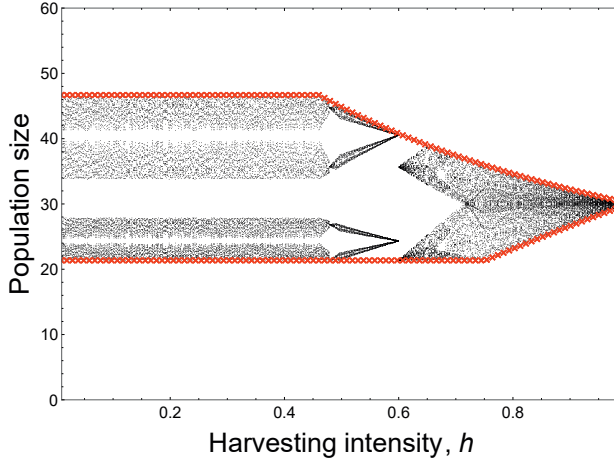
Figure 3.4: Bifurcation diagram for CALC with $c = 0.6$ and varying h. The underlying population dynamics are given by the Ricker map $f(x) = x \exp(r(1 - x/K))$ with $r = 2.7$ and $K = 30$. Initial population sizes were obtained as pseudo-random real numbers in the interval $(0, f(d)]$. For each initial condition, black dots represent 30 generations of the population subject to CALC after a transient of $10,000$ time steps. Red crosses correspond to the limits of the trapping region given by equations (3.4) and (3.5).

was below A_H (cf. Figure 3.2). Similarly, the activation threshold for restocking (which we denote by A_R) exists for $c > f(b)/b$ and corresponds to the abscissa of the unique nonzero intersection of the curve $y = f(x)$ and $y = c \cdot x$. Restocking only takes place if A_R was exceeded in the preceding generation [77]. Given that $c < 1 < 1/h$, when both A_H and A_R exist they are always different and satisfy $A_H < K < A_R$ (cf. Figure 3.2).

3.2.4 STABILIZING PROPERTIES OF CALC

The following results summarize the stabilizing properties of CALC. We start by proving that the effect of the control does not stabilize any equilibrium point.

Proposition 3.1. *Assume that (A1)–(A3) hold and that the carrying capacity K is an unstable equilibrium of the uncontrolled system. Then, independent of the magnitude*

of CALC, $(c, h) \in [0, 1) \times [0, 1)$, the controlled system has no asymptotically stable equilibria.

Proof. Denote $h_0 = \inf_{x \in (0,b)} x / f(x)$. For $(c, h) \in [0, f(b)/b] \times (h_0, 1)$, restocking is never activated and the control corresponds to ATH, which has no asymptotically stable equilibria (Proposition 1.4). The same is true for $(c, h) \in (f(b)/b, 1) \times [0, h_0]$, in which case harvesting is never activated and the control corresponds to ALC [77, Proposition 2]. For the remaining control intensities, $(c, h) \in (f(b)/b, 1) \times (h_0, 1)$, CALC combines both restocking and harvesting. Clearly, $(x, y) \in [0, b] \times [0, b]$ is an equilibrium of the controlled system (3.1) if and only if

$$
\begin{cases}
x = f(y), \\
y = \max\{\min\{x, y/h\}, c \cdot y\}.
\end{cases} \tag{3.3}
$$

Since $c, h < 1$, the second equation of (3.3) yields $y = x$, and thus $y = f(y)$. Therefore, the controlled system (3.1) only has $(0, 0)$ and (K, K) as equilibrium points. According to Proposition 1.1, for $h > h_0$ the activation threshold A_H exists. Consider the neighborhood of $(0, 0)$ given by $U = (0, A_H) \times (0, A_H)$ and assume that $(a_t, b_t) \in U$ for all $t \geq 0$. Given that $f(x) > x/h$ for $x \in (0, A_H)$, $a_{t+1} = \max\{a_t/h, c \cdot a_t\} = a_t/h$ for all $t \geq 0$, and thus $a_t = (1/h)^t \cdot x_0$. Consequently, $a_t \to +\infty$, which contradicts the hypothesis and proves that $(0, 0)$ is unstable.

Let us now prove that (K, K) is also unstable. Since f is continuous and $c \cdot K < K = f(K) < K/h$, there exists a neighborhood V of K such that $c \cdot x < f(x) < x/h$ for all $x \in V$. Assume that $(a_t, b_t) \in V \times V$ for all $t \geq 0$. Then, $a_{t+1} = f(a_t)$ for all $t \geq 0$, and thus $a_t = f^t(x_0)$. Since K is an unstable equilibrium for the uncontrolled system, this last equality contradicts the hypothesis and proves that (K, K) is unstable. □

The following result shows that the stabilizing effect of CALC is attained by asymptotically trapping the population size within an interval around the carrying capacity.

Moreover, it provides analytical expressions in terms of the control parameters for the endpoints of this interval, which are shown in Figure 3.4 together with a bifurcation diagram.

Remark 3.2. Conditions (A1)-(A3) are standard in the literature to describe unimodal maps and were also used in the study of the stabilizing properties of ALC [77]. We want to stress that imposing differentiability facilitates the description of these maps, but it is not a necessary condition in most of the results about ALC, ATH or in those that follow for CALC whenever the unimodal character of the map is not altered.

Proposition 3.3. *Assume that (A1)–(A3) hold and $(c,h) \in (0,1) \times (0,1)$ are such that the activation thresholds A_R and A_H exist. Then, applying CALC with intensities (c,h) asymptotically confines the population sizes a_t for any $a_0 \in (0,b)$ within an interval $I_a = [l(c,h), u(c,h)]$ around the positive equilibrium K, with endpoints given by the expressions*

$$l(c,h) = \begin{cases} \max\{c \cdot A_R, f(A_H/h)\}, & d \leq A_H, \\ \max\{f^2(d), c \cdot A_R\}, & d > A_H, \end{cases} \tag{3.4}$$

$$u(c,h) = \begin{cases} \min\{f(c \cdot A_R), A_H/h\}, & d \leq c \cdot A_R, d \leq A_H, \\ A_H/h, & d > c \cdot A_R, d \leq A_H, \\ f(c \cdot A_R), & d \leq c \cdot A_R, d > A_H, \\ f(d), & d > c \cdot A_R, d > A_H. \end{cases} \tag{3.5}$$

Proof. Equation (3.2) can be expressed as $a_{t+1} = \max\{F_H(a_t), c \cdot a_t\}$, where the map $F_H \colon [0,b] \to [0,b]$ is given by $F_H(x) = \max\{f(x), x/h\}$. Thus, (3.2) can be considered as a system describing the dynamics of a population with production function F_H that is controlled by only restocking (ALC). One can check that F_H satisfies conditions (A1)–(A3) except for the existence of a point where this map is not differentiable. This does not affect our conclusion since the existence of such a point does

not alter the unimodal character of the map. Moreover, one can check that there exists $T_0 > 0$ such that $F_H^2(d_H) \le a_t \le F_H(d_H)$ for all $t \ge T_0$, where d_H denotes the abscissa of the maximum of F_H. This, together with [77, Theorem 1], leads to conclude that there exists $T \ge T_0$ such that for $t \ge T$ the population size a_t for any $a_0 \in (0, b)$ is asymptotically trapped within an interval $I_a = [l(c, h), u(c, h)]$ with endpoints given by the expressions

$$l(c, h) = \max\{F_H^2(d_H), c \cdot A_R\}, \tag{3.6}$$

$$u(c, h) = \begin{cases} F_H(c \cdot A_R), & d_H \le c \cdot A_R, \\ F_H(d_H), & d_H > c \cdot A_R. \end{cases} \tag{3.7}$$

Assume that $d > A_H$. Then, $d_H = d$ and $F_H(d_H) = f(d)$. Since $f(d) > d > A_H$, it follows that $F_H^2(d_H) = F_H(f(d)) = f^2(d)$. On the other hand, if $A_H < d = d_H \le c \cdot A_R$ then $F_H(c.A_R) = f(c.A_R)$. With this, all the results given in the statement for $d > A_H$ follow.

Suppose now $d \le A_H$. Then, $d_H = A_H$ and $F_H(d_H) = A_H/h$. Since $A_H/h > A_H$, we conclude $F_H^2(d_H) = F_H(A_H/h) = f(A_H/h)$. This completes all the cases for $l(c, h)$. To derive the expression for $u(c, h)$, we consider two cases. If $d > c \cdot A_R$, then $A_H > c \cdot A_R$ and $u(c, h) = F_H(A_H) = A_H/h$. If $d \le c \cdot A_R$, then f is strictly decreasing in the interval defined by $c \cdot A_R$ and A_H, being $\min\{f(c \cdot A_R), f(A_H) = A_H/h\} = f(\max\{c \cdot A_R, A_H\})$. For $A_H > c \cdot A_R$, we have $u(c, h) = F_H(A_H) = f(A_H) = \min\{f(c \cdot A_R), A_H\}$, and for $A_H \le c \cdot A_R$ it follows that $u(c, h) = F_H(c \cdot A_R) = f(c \cdot A_R) = \min\{f(c \cdot A_R), A_H\}$. This completes the proof. $\qquad\square$

The analysis of the expressions for the endpoints of the trapping interval given in Proposition 3.3 reveals that harvesting does not affect the fluctuation range of the population when $d \ge A_H$. The reason for this is that in such a case the stock-recruitment

curves of both controlled and uncontrolled populations have a common maximum $f(d)$. Consequently, if we want harvesting to reduce the fluctuation range with respect to the uncontrolled population, the harvesting intensity must be higher than $d/f(d)$.

3.3 SIMULATIONS

To study the pros and cons of CALC versus ALC and ATH, we perform several numerical experiments with two different population models.

3.3.1 CALC OF A STOCHASTIC OVERCOMPENSATORY POPULATION

The first model is based on the Ricker map and includes environmental and demographic stochasticity as well as a lattice effect. The latter corresponds to the phenomenon whereby the dynamics of the discrete-state system can be quite different from its continuous-state version [102]. We use the negative-binomial-environmental (NBe) model introduced in [159]. This model reads $x_{t+1} \sim \text{NegBinom}(f(x_t), \alpha)$, where NegBinom denotes the negative-binomial distribution, f is the deterministic production function of the population and α is a parameter driving the shape of the distribution. Specifically, we consider for numerical simulations the equation

$$x_{t+1} = \begin{cases} \max\{\min\{z_t, x_t/h\}, c \cdot x_t\}, & h > 0, \\ \max\{z_t, c \cdot x_t\}, & h = 0, \end{cases} \tag{3.8}$$

with $z_t \sim \text{NegBinom}(x_t \exp(2.7(1 - x_t/30))), 100)$ and $(c, h) \in [0, 1) \times [0, 1)$. This describes the dynamics of a population subject to both demographic and environmental stochasticity that is managed by CALC with restocking intensity c and harvesting intensity h, and for which the uncontrolled deterministic dynamics are described by the Ricker model with growth parameter $r = 2.7$ and carrying capacity $K = 30$. Moreover, the discrete character of the statistical distribution that is considered implies the integerization of population size.

With this equation, we study the effect of CALC on the constancy stability of managed populations. We have seen in Section 1.3 that the effect of management strategies can sometimes be stabilizing or destabilizing depending on which constancy measure is used. In this sense, it is important to rely not just on one measure, because this could give results that do not hold for other measures. In view of this, we consider three different measures of the constancy stability, namely the fluctuation index (FI), the fluctuation range (FR) and the coefficient of variation (CV). The FR and FI were introduced in Section 1.3. The CV is a standardized measure of the dispersion in the population size obtained as the ratio of the standard deviation to the mean of the population size over a period of T time steps. Constancy stability of a population is inversely related to the magnitude of fluctuation in size it shows across time. Thus, decreases in any of these three measures are associated with enhancements in the constancy stability.

Given a combination of control intensities (c, h), we evaluate the above three measures for equation (3.8) averaged over series of $T = 30$ time steps and over 500 replicates with random initial conditions in $(0, f(d)]$. To study the statistical significance of the differences in the considered measures, we conduct t-tests for the comparison of their means for different combinations of control intensities. We focus on the differences between the cases in which the populations are managed by harvesting only ($c = 0$) or restocking only ($h = 0$) and the cases in which they are managed by a certain combination of harvesting and restocking ($c, h \neq 0$). We denote by $p_m((c_1, h_1), (c_2, h_2))$ the p-value of the t-test for the comparison of means of the constancy measure $m \in \{\text{FR, FI, CV}\}$ between the case in which the population is managed with control intensities (c_1, h_1) and the case in which it is managed with control intensities (c_2, h_2). The significance level is set at 0.05 and all statistical analyses are performed with IBM® SPSS Statistics 23 for Windows®.

3.3.2 CALC OF A HOST–PATHOGEN–PREDATOR MODEL

The second model is given by Eqs. (2.4), which we have used in Section 2.5 to study the effectiveness of ALC and ATH in the prevention of population outbreaks. Here, we

consider management actions of the state variable x_t only. Then, the model including CALC with control intensities $(c, h) \in [0, 1) \times [0, 1)$ is obtained by modifying the second equation of (2.4) to

$$
x_{t+1} = \begin{cases} \max\left\{\min\left\{\lambda x_t(1 - I(x_t, z_t))\left(1 - \frac{2ABx_t}{B^2 + x_t^2}\right), x_t/h\right\}, c \cdot x_t\right\}\varepsilon_t, & h > 0, \\ \max\left\{\lambda x_t(1 - I(x_t, z_t))\left(1 - \frac{2ABx_t}{B^2 + x_t^2}\right), c \cdot x_t\right\}\varepsilon_t, & h = 0. \end{cases}
$$

With this equation, we calculate the probability of defoliator outbreaks as follows. We assume that the system is in the basin of attraction of the low-density attractor of (2.4), namely $x_0 = 0.2516$ and $z_0 = 11.6420$. The maximum defoliator density for the deterministic attractors of (2.4) is approximately 44, and we will assume that an outbreak happens in generation t when the defoliator density x_t exceeds 35. The probability of these events is calculated for time series of length 50 and averaged over 5,000 replicates.

3.4 CONSTANCY STABILITY

In this section, we study if the combination of restocking and harvesting can bring any benefit in terms of the constancy stability of populations managed by CALC compared to the cases of harvesting only and restocking only. We consider stochastic overcompensatory populations that are modeled by (3.8) in two different scenarios.

3.4.1 SCENARIO 1: ADDING RESTOCKING TO HARVESTING

In this subsection, we study if the addition of restocking to harvesting reduces the FI, FR or CV of the managed populations. Let us start by studying the FR. As can be observed in Figure 3.5a, for $h \lesssim 0.45$ the FR decreases as the restocking intensity increases, while for higher values of h such a reduction is not observed for low restocking intensities ($c = 0.1$). This suggests that for a given harvesting intensity the addition

of restocking entails a significant reduction in the FR only if the restocking intensity is above a certain threshold. We will see that the same is true for both the FI and the CV. In view of this and for easy reference, we denote by $c_m(h)$ the restocking intensity threshold that must be exceeded for a given harvesting intensity h to obtain a significant reduction in the constancy measure $m \in \{FR, FI, CV\}$ with respect to the case of only harvesting ($c = 0$). The term 'significant' is used here following statistical criteria (for more details, see Section 3.2). Table 3.1 shows the statistical analysis of the aforementioned differences in the constancy measures and lists the values of $c_m(h)$ for different harvesting intensities within the ranges considered throughout this study (for other values in these ranges similar results were obtained, but they are not shown here). Table 3.1 confirms that for $h \lesssim 0.45$ and with respect to the case of only harvesting the reduction in the FR obtained with the inclusion of restocking is statistically significant even if the restocking intensity is very low, so that in this case $c_{FR}(h) \leq 0.1$. For higher values of h, reductions in the FR are only significant for higher restocking intensities since in this case $c_{FR}(h) \in (0.1, 0.4]$.

Let us now consider the FI. Figure 3.5b shows that for harvesting of low intensity $h \lesssim 0.15$ the addition of restocking of low intensity ($c = 0.1$) increases the FI. For harvesting intensities $0.15 \lesssim h \lesssim 0.3$, the inclusion of restocking significantly reduces the FI even for very low restocking intensities ($c_{FI}(h) \leq 0.1$; see Figure 3.5b and Table 3.1). For $0.3 \lesssim h \lesssim 0.9$, significant reductions in the FI are only reached at higher restocking intensities ($c_{FI}(h) \in (0.1, 0.4]$; see Figure 3.5b and Table 3.1). For very high harvesting intensities $h \gtrsim 0.9$, significant reductions in the FI are again observed from very low restocking intensities onward ($c_{FI}(h) \leq 0.1$; see Figure 3.5b and Table 3.1).

Finally, let us study the CV. For $h \lesssim 0.85$, the behavior of this measure is similar to the one observed for the FR (see Figure 3.5c and Table 3.1). Above this range, increasing the harvesting intensity increases the CV for populations managed by only harvesting. Interestingly, the inclusion of restocking nullifies this effect from low restocking intensities onward.
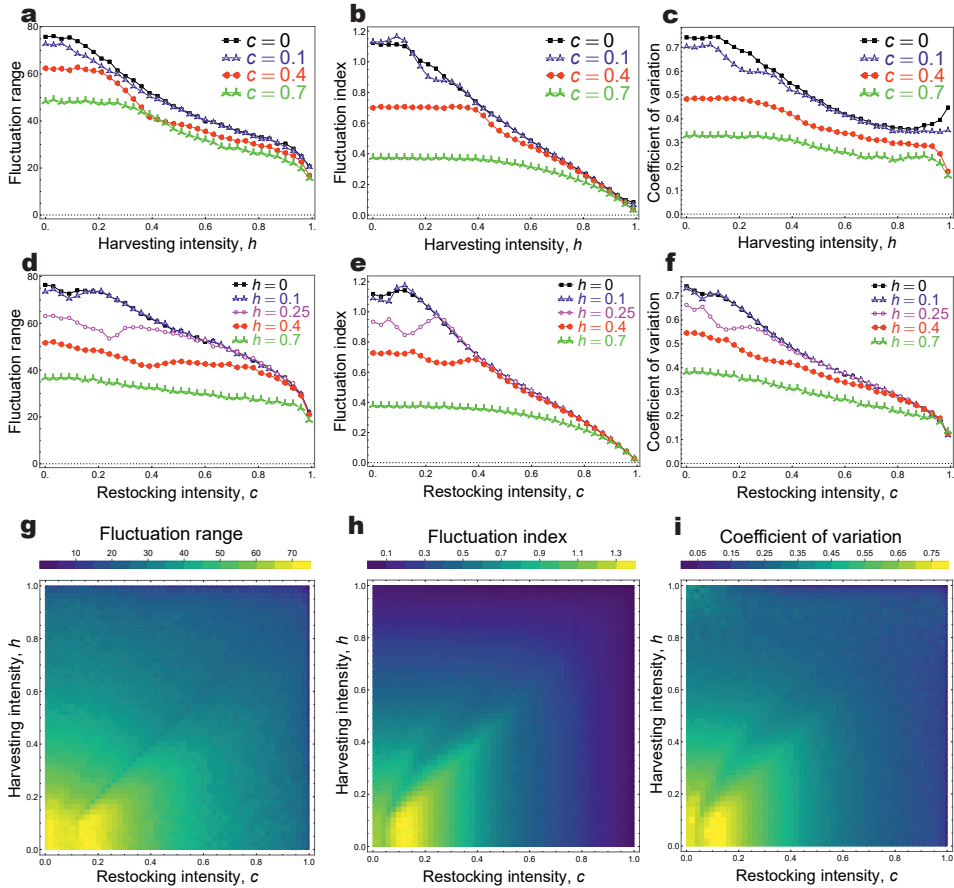
Figure 3.5: Constancy stability measures for CALC in terms of the control intensities. All values were obtained for time series of length 30 for equation (3.8) and averaged over 500 replicates (a-f) or 200 replicates (g-i) for which the population persisted. The initial population sizes were chosen as pseudo-random real numbers in $(0, f(d)]$.

	Scenario 1: adding restocking to harvesting	
h	p-values	Restocking intensity threshold
$h = 0.21$	$p_{\mathrm{FR}}((0, 0.21), (0.1, 0.21)) \approx 0^*$ $p_{\mathrm{FI}}((0, 0.21), (0.1, 0.21)) \approx 0^*$ $p_{\mathrm{CV}}((0, 0.21), (0.1, 0.21)) \approx 0^*$	$c_{\mathrm{FR}}(0.21) \leq 0.1$ $c_{\mathrm{FI}}(0.21) \leq 0.1$ $c_{\mathrm{CV}}(0.21) \leq 0.1$
$h = 0.51$	$p_{\mathrm{FR}}((0, 0.51), (0.1, 0.51)) = 0.572, p_{\mathrm{FR}}((0, 0.51), (0.4, 0.51)) \approx 0^*$ $p_{\mathrm{FI}}((0, 0.51), (0.1, 0.51)) = 0.881, p_{\mathrm{FI}}((0, 0.51), (0.4, 0.51)) \approx 0^*$ $p_{\mathrm{CV}}((0, 0.51), (0.1, 0.51)) = 0.018^*$	$c_{\mathrm{FR}}(0.51) \in (0.1, 0.4]$ $c_{\mathrm{FI}}(0.51) \in (0.1, 0.4]$ $c_{\mathrm{CV}}(0.51) \leq 0.1$
$h = 0.75$	$p_{\mathrm{FR}}((0, 0.75), (0.1, 0.75)) = 0.676, p_{\mathrm{FR}}((0, 0.75), (0.4, 0.75)) \approx 0^*$ $p_{\mathrm{FI}}((0, 0.75), (0.1, 0.75)) = 0.426, p_{\mathrm{FI}}((0, 0.75), (0.4, 0.75)) \approx 0^*$ $p_{\mathrm{CV}}((0, 0.75), (0.1, 0.75)) = 0.143, p_{\mathrm{CV}}((0, 0.75), (0.4, 0.75)) \approx 0^*$	$c_{\mathrm{FR}}(0.75) \in (0.1, 0.4]$ $c_{\mathrm{FI}}(0.75) \in (0.1, 0.4]$ $c_{\mathrm{CV}}(0.75) \in (0.1, 0.4]$
$h = 0.84$	$p_{\mathrm{FR}}((0, 0.84), (0.1, 0.84)) = 0.668, p_{\mathrm{FR}}((0, 0.84), (0.4, 0.84)) \approx 0^*$ $p_{\mathrm{FI}}((0, 0.84), (0.1, 0.84)) = 0.939, p_{\mathrm{FI}}((0, 0.84), (0.4, 0.84)) \approx 0^*$ $p_{\mathrm{CV}}((0, 0.84), (0.1, 0.84)) = 0.215, p_{\mathrm{CV}}((0, 0.84), (0.4, 0.84)) \approx 0^*$	$c_{\mathrm{FR}}(0.84) \in (0.1, 0.4]$ $c_{\mathrm{FI}}(0.84) \in (0.1, 0.4]$ $c_{\mathrm{CV}}(0.84) \in (0.1, 0.4]$
$h = 0.93$	$p_{\mathrm{FR}}((0, 0.93), (0.1, 0.93)) = 0.201, p_{\mathrm{FR}}((0, 0.93), (0.4, 0.93)) \approx 0^*$ $p_{\mathrm{FI}}((0, 0.93), (0.1, 0.93)) = 0.024^*$ $p_{\mathrm{CV}}((0, 0.93), (0.1, 0.93)) = 0.014^*$	$c_{\mathrm{FR}}(0.93) \in (0.1, 0.4]$ $c_{\mathrm{FI}}(0.93) \leq 0.1$ $c_{\mathrm{CV}}(0.93) \leq 0.1$
	Scenario 2: adding harvesting to restocking	
c	p-values	Harvesting intensity threshold
$c = 0.21$	$p_{\mathrm{FR}}((0.21, 0), (0.21, 0.1)) = 0.550, p_{\mathrm{FR}}((0.21, 0), (0.21, 0.25)) \approx 0^*$ $p_{\mathrm{FI}}((0.21, 0), (0.21, 0.1)) = 0.787, p_{\mathrm{FI}}((0.21, 0), (0.21, 0.25)) \approx 0^*$ $p_{\mathrm{CV}}((0.21, 0), (0.21, 0.1)) = 0.543, p_{\mathrm{CV}}((0.21, 0), (0.21, 0.25)) \approx 0^*$	$h_{\mathrm{FR}}(0.21) \in (0.1, 0.25]$ $h_{\mathrm{FI}}(0.21) \in (0.1, 0.25]$ $h_{\mathrm{CV}}(0.21) \in (0.1, 0.25]$
$c = 0.51$	$p_{\mathrm{FR}}((0.51, 0), (0.51, 0.1)) = 0.839, p_{\mathrm{FR}}((0.51, 0), (0.51, 0.25)) = 0.005^*$ $p_{\mathrm{FI}}((0.51, 0), (0.51, 0.25)) = 0.497, p_{\mathrm{FI}}((0.51, 0), (0.51, 0.4)) \approx 0^*$ $p_{\mathrm{CV}}((0.51, 0), (0.51, 0.25)) = 0.403, p_{\mathrm{CV}}((0.51, 0), (0.51, 0.4)) \approx 0^*$	$h_{\mathrm{FR}}(0.51) \in (0.1, 0.25]$ $h_{\mathrm{FI}}(0.51) \in (0.25, 0.4]$ $h_{\mathrm{CV}}(0.51) \in (0.25, 0.4]$
$c = 0.75$	$p_{\mathrm{FR}}((0.75, 0), (0.75, 0.25)) = 0.550, p_{\mathrm{FR}}((0.75, 0), (0.75, 0.4)) \approx 0^*$ $p_{\mathrm{FI}}((0.75, 0), (0.75, 0.25)) = 0.195, p_{\mathrm{FI}}((0.75, 0), (0.75, 0.4)) = \approx 0^*$ $p_{\mathrm{CV}}((0.75, 0), (0.75, 0.25)) = 0.972, p_{\mathrm{CV}}((0.75, 0), (0.75, 0.4)) \approx 0^*$	$h_{\mathrm{FR}}(0.75) \in (0.25, 0.4]$ $h_{\mathrm{FI}}(0.75) \in (0.25, 0.4]$ $h_{\mathrm{CV}}(0.75) \in (0.25, 0.4]$
$c = 0.84$	$p_{\mathrm{FR}}((0.84, 0), (0.84, 0.25)) = 0.874, p_{\mathrm{FR}}((0.84, 0), (0.84, 0.4)) \approx 0^*$ $p_{\mathrm{FI}}((0.84, 0), (0.84, 0.4)) = 0.092, p_{\mathrm{FI}}((0.84, 0), (0.84, 0.7)) \approx 0^*$ $p_{\mathrm{CV}}((0.84, 0), (0.84, 0.25)) = 0.306, p_{\mathrm{CV}}((0.84, 0), (0.84, 0.4)) = 0.032^*$	$h_{\mathrm{FR}}(0.84) \in (0.25, 0.4]$ $h_{\mathrm{FI}}(0.84) \in (0.4, 0.7]$ $h_{\mathrm{CV}}(0.84) \in (0.25, 0.4]$
$c = 0.93$	$p_{\mathrm{FR}}((0.93, 0), (0.93, 0.4)) = 0.145, p_{\mathrm{FR}}((0.93, 0), (0.93, 0.7)) \approx 0^*$ $p_{\mathrm{FI}}((0.93, 0), (0.93, 0.4)) = 0.681, p_{\mathrm{FI}}((0.93, 0), (0.93, 0.7)) \approx 0^*$ $p_{\mathrm{CV}}((0.93, 0), (0.93, 0.4)) = 0.729, p_{\mathrm{CV}}((0.93, 0), (0.93, 0.7)) = 0.019^*$	$h_{\mathrm{FR}}(0.93) \in (0.4, 0.7]$ $h_{\mathrm{FI}}(0.93) \in (0.4, 0.7]$ $h_{\mathrm{CV}}(0.93) \in (0.4, 0.7]$

Table 3.1: Statistical analysis of the differences in the constancy stability measures for CALC. *T*-tests and intensity thresholds for the differences in the fluctuation index (FI), fluctuation range (FR) and coefficient of variation (CV) of (3.8) in the two different scenarios and for various combinations of control intensities. Values marked with * are statistically significant at level 0.05. See Section 3.2 for more details.

3.4.2 SCENARIO 2: ADDING HARVESTING TO RESTOCKING

Now we study the same measures of constancy stability in the case in which harvesting is added to restocking. As in the previous scenario, significant reductions in the FR, FI or CV are reached only when the harvesting intensity is above a certain threshold $h_m(c)$, which depends on the constancy measure $m \in \{\text{FR, FI, CV}\}$ and the restocking intensity c (see Figure 3.5d-f and Table 3.1). Yet, the behavior of the three constancy measures is in this case similar—cutbacks in any of them due to the inclusion of harvesting require higher harvesting intensities for higher restocking intensities.

In summary, the combination of harvesting and restocking enhances the constancy stability of the managed populations in comparison to the cases of restocking only or harvesting only whenever the control intensities are high enough. This is further supported by the two-parameter diagrams in Figure 3.5g-i, where we vary both restocking and harvesting intensities. Here we can observe that if c (respectively h) is large enough, all three constancy stability measures are enhanced in comparison to the absence of restocking (respectively harvesting) for all h (respectively c).

3.5 POPULATION OUTBREAKS

In this section we study the capability of CALC to prevent outbreaks in the population size. Moreover, we analyze the trade-off between the reduction in the risk of population outbreaks and the cost of the intervention. We consider the host-pathogen-predator model (2.4).

3.5.1 OUTBREAK RISK

Population outbreaks are inherent to forest-defoliating insects, for which the population size may rest in a low-density state for several generations until some perturbation makes it burst to a higher-density attractor. Usually, management strategies aimed at avoiding pest outbreaks are based on only harvesting the population. In this section, we study if in the case of CALC the combination of such strategies with restocking may

enhance the capability of the control to contain the population size. Specifically, we study the effect of CALC on the probability of outbreak for model (2.4). The results are shown in Figure 3.6. For low harvesting intensities ($h \lesssim 0.3$) restocking defoliators reduces the probability of outbreaks whenever the restocking intensity is not too high ($c \lesssim 0.8$). Therefore, in that case harvesting and restocking defoliators is more effective for the prevention of outbreaks than the strategy based only on their removal. Yet, this is not always the case. For medium and high harvesting intensities ($h \gtrsim 0.3$), restocking defoliators is never beneficial for the prevention of outbreaks in their population density. Interestingly, which is also somehow counter-intuitive, for high removal intensities restocking even a small proportion of the density of defoliators in the previous generation promotes outbreaks in their population. A potential explanation for this behavior lies in the fact that new uninfected defoliators would be added and a large number of infected defoliators would be removed from the defoliator population at high harvesting intensities, which could be highly destabilizing.

In summary, if we can manage the defoliator with only a low harvesting intensity, then it is beneficial to combine harvesting with restocking. On the contrary, if we are able to implement harvesting with a high intensity, then it seems better to not restock the defoliator.

3.5.2 Intervention cost

The previous analysis does not take into account that interventions always have a cost. In this sense, from a management perspective, the control strategies that are the most effective at reaching a specific goal may not be the best option if they come at a higher cost. Thus, a trade-off between the goals that are reached and the cost of the intervention must be considered. Here, we study the benefit that is obtained with CALC in terms of the reduction of the risk of outbreaks. Undoubtedly, this is an extremely ambiguous concept that requires the monetization of both the goal that is reached and the cost of the intervention, which could be done in many different ways. We consider a proxy in which the cost is measured in terms of the restocking and harvesting frequen-
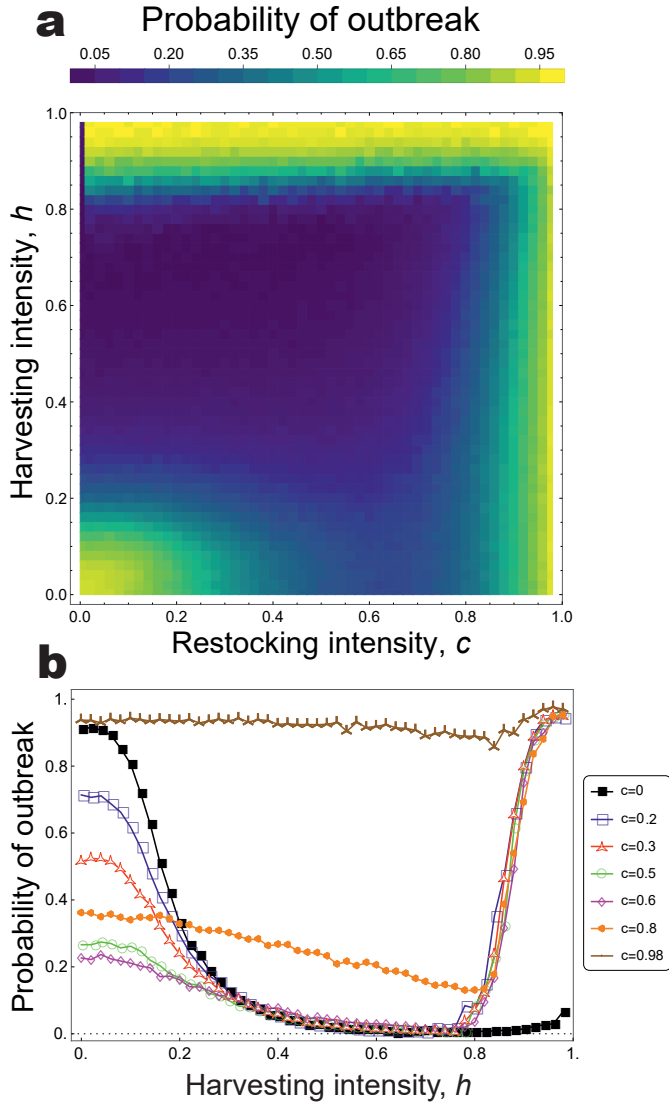
Figure 3.6: Probability of outbreak for CALC. Outbreaks for equation (2.4) are assumed to occur when the defoliator density exceeds 35, and their probability is calculated by estimating the frequency of their occurrence in time series of length 50 over 5000 replicates. The initial conditions for defoliator and pathogen are $x_0 = 0.2516$ and $z_0 = 11.6420$, respectively.

cies. In the following analysis we consider that management has a fixed 'budget' for control interventions, which can be partitioned into harvesting and restocking. The sum of harvesting and restocking intensities is thus constant—here we assume $c + h = 1$. With $c = \lambda$ and $h = 1 - \lambda$, where $\lambda \in [0, 1]$, we see that $\lambda = 0$ means only harvesting, $\lambda = 1$ only restocking and intermediate values some combination. We therefore refer to λ as the *harvesting-restocking balance*. Note that due to this assumption we have reduced the number of free control parameters from two to one, which simplifies the analysis.

Under the above assumption, we consider the function

$$B(\lambda, v_1, v_2, v_3) = \underbrace{v_1((P_u - P_c(\lambda))}_{\text{revenue}} - \underbrace{(v_2 \cdot F_R(\lambda) + v_3 \cdot F_H(\lambda))}_{\text{cost}}, \qquad (3.9)$$

where B is the benefit function and P_u, $P_c(\lambda)$, $F_R(\lambda)$ and $F_H(\lambda)$ respectively represent the probability of outbreak for the uncontrolled and controlled populations and the restocking and harvesting intervention frequencies of CALC for control intensities $c = \lambda$ and $h = 1 - \lambda$, with $\lambda \in [0, 1]$. Parameter v_1 represents the unitary revenue that corresponds to the monetization of the reduction in the probability of outbreak, while v_2 and v_3 represent the unitary cost of harvesting and restocking interventions, respectively.

We rescale (3.9) by setting $v_1 = 1$. Our goal is to study which combination of parameters yields the maximum benefit, which naturally depends on which type of intervention (restocking or harvesting) is more costly. In this sense, we can set v_2 at a fixed value (for instance, $v_2 = 1$) and study the benefit for $v_3 > 1$ (harvesting more costly than restocking), $v_3 = 1$ (harvesting and restocking equally costly) and $v_3 < 1$ (restocking more costly than harvesting). For these values, Figure 3.7 shows the graphical representation of (3.9) in terms of v_3. When harvesting is less costly than restocking ($v_3 = 1/4$), the maximum benefit is reached when the harvesting intensity is higher than the restocking intensity ($\lambda < 0.5$). As the cost of harvesting increases, the peak of the benefit curve moves to the right, which means increasing the restocking intensity
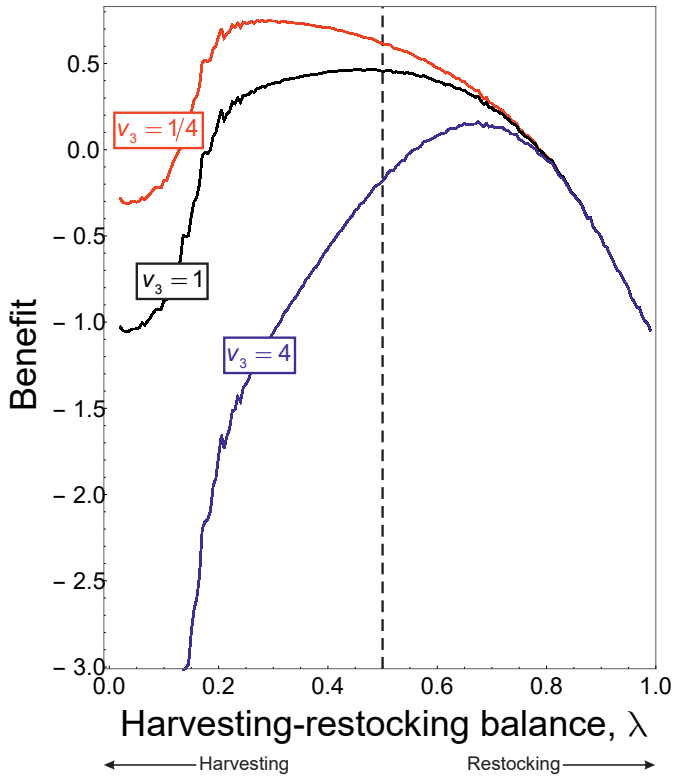
Figure 3.7: Benefit function for CALC in terms of the harvesting-restocking balance. Graphical representation of the benefit given by (3.9) in terms of the restocking-harvesting balance λ, with $c = \lambda, h = 1 - \lambda$ and $\lambda \in [0, 1]$. For all curves, v_1 and v_2 are set at 1. Parameter v_3 represents the proportion of the cost of harvesting to the cost of restocking. The vertical dashed line corresponds to $\lambda = 0.5$.

and decreasing the harvesting intensity. When restocking and harvesting are equally costly ($v_3 = 1$), the maximum benefit is reached when the two control intensities are approximately equal, i.e., $\lambda \approx 0.5$. Finally, when harvesting is more costly than restocking the maximum benefit is reached for a restocking intensity higher than the harvesting intensity ($v_3 = 4$). The same behavior is observed when v_2 is set at other values different from 1 (not shown here).

As already mentioned, similar analyses could be performed by considering different criteria for the definition of the benefit of the intervention. A similar analysis could also be performed for model (3.8) by considering the trade-off between the reduction in either the FI, FR or CV and the intervention costs. The example considered here does not pretend to be representative of all of them, but shows that choosing the values of the control intensities depends on the formulation of the cost function, and in the cases considered here the intervention costs play a role.

3.6 Discussion and conclusions

We have introduced CALC as a strategy for the management of biological populations that combines restocking and harvesting according to two already known techniques, namely ALC and ATH. This new strategy has not been previously considered in the literature and constitutes a general framework for adaptive limiters, since it includes the methods ALC and ATH as particular cases.

Our main goal has been to study the advantages that combining restocking and harvesting may have over restocking only and harvesting only. To that end, we have considered two different population models. The first is a stochastic overcompensatory model, for which we have analyzed the constancy stability of the managed populations by considering three different measures of this property, namely the fluctuation index, the fluctuation range and the coefficient of variation. In our case, all these measures showed the same trend: the constancy stability of the managed populations is improved when harvesting and restocking are combined, provided the harvesting and restocking

intensities are high enough. More specifically, complementing restocking (respectively harvesting) with harvesting (respectively restocking) enhances the constancy stability of the managed populations if the harvesting (respectively restocking) intensity is above a certain critical value, which depends on the constancy measure and the restocking (respectively harvesting) intensity that are considered. Below this critical value, the impact of combining restocking and harvesting on the constancy stability is in most cases negligible and in rare cases negative. The latter is the case of the FI, whose value can be increased by the combination of harvesting and restocking when the intensities of each are low. Such a behavior in the FI for low intensities was previously reported for both ALC [77] and ATH (Section 1.3). Interestingly, contrary to other methods that combine harvesting and restocking like BLC or TOC [213], the improvement in the constancy stability obtained by that combination is in the case of CALC observed for relatively low control intensities. This case is especially interesting because achieving high control intensities may be unfeasible due to the cost of the intervention, to logistical issues or to the unavailability of a high number of individuals to be restocked.

When the goal is to prevent outbreaks in the population size, we have shown that combining harvesting with restocking under CALC can also be beneficial. Yet, again, this depends on the control intensities. If outbreaks are to be controlled by harvesting of low intensity ($h \lesssim 0.3$), combining this strategy with restocking of not very high intensity ($c \lesssim 0.8$) helps to contain the population size. On the contrary, if outbreaks are to be controlled by harvesting of intermediate or high intensity ($h \gtrsim 0.3$), restocking individuals with any intensity is either ineffective or counterproductive. Special care must be taken in the case of harvesting of high intensity ($h \gtrsim 0.8$), for which the combination with restocking, even of very low intensity, clearly promotes population outbreaks. We wish to stress that we are not aware of an example where pest species have been actually restocked in the field and that we would expect resistance to this approach in real applications. We only know of the laboratory experiments in [213].

As a method that combines ATH and ALC, the stabilizing properties of CALC could be expected to be similar to those already observed separately for ATH and ALC.

In fact, we have extended the stability results for ATH and ALC to CALC (Section 3.2). We have shown that for unimodal maps the stabilizing effect of CALC is attained by asymptotically trapping the population size in an interval around the carrying capacity of the population. We have provided analytical expressions for the endpoints of this interval in terms of the harvesting and restocking intensities. Moreover, we have shown that when CALC combines restocking and harvesting with high enough intensities there exist activation thresholds that inform us in advance of the need of intervention in the following time step.

Several papers put forward the idea that the advantage of combining restocking and harvesting depends on multiple factors, especially on the economic side [17, 18, 146, 147]. With a particular example, we have studied the trade-off between the stabilizing goals that are reached with the application of CALC and the cost of the intervention. This allows us to conclude that the decision about appropriate control intensities for CALC cannot be exclusively based on stability criteria. In this sense, we draw attention to the fact that we should not only focus on theoretical or numerical results predicting a certain stabilizing effect, but on the benefit that is expected to be obtained with the intervention. While allowing us to conclude that the decision about the 'best' combination of control intensities is not trivial, our approach is simplistic. For instance, in coastal fisheries, there is great controversy about the appropriateness of combining fishing and restocking. It is known that few restocking or stock enhancement programs have succeeded because many other aspects different from stability issues have not been taken into account, as can be the necessity of the intervention or the integration of technology with the participation and understanding of the stakeholders by means of an appropriate management scheme [17].

4

Degenerate period adding bifurcation structure of one-dimensional bimodal piecewise linear maps

4.1   INTRODUCTION

Management in many areas involves making decisions. Decision making in turn is often based on thresholds. For instance, when pests or nuisance species are too abundant, start culling them. If endangered species or game species become too rare, start restocking them. If environmental pollution becomes too severe, take actions against it. If a pharmaceutical concentration is too high or low, then start a regimen working against it. These threshold-based management actions lead to dynamical systems that usually are nonsmooth at the thresholds, as we have seen in previous chapters; see also [21, 105, 125, 184, 212, 214].

When parameters of a smooth system are varied in a certain direction in the parameter space, transitions between regular dynamics and chaos generally occur through a *route to chaos*, which consists of a certain sequence of bifurcations (for a review of these mechanisms see, for instance, [8]). However, in the case of nonsmooth systems these transitions may occur through a single bifurcation [20]. In this chapter, we restrict ourselves to the case of one-dimensional piecewise smooth (PWS) maps. These maps are characterized by the fact that the state space consists of several partitions separated by points at which the map is not differentiable, to which we will refer as *break points* or *kink points*. As parameters are varied, abrupt changes in the dynamics of PWS maps may occur when an invariant set collides with one of the break points (e.g., the transition from an attracting fixed point to a chaotic attractor). These changes are known as *border collision bifurcations* (BCB), a term originally introduced by Nusse and Yorke [163]. This type of bifurcation can give rise to many structures that are completely different from scenarios occurring in smooth systems [13]. Several papers have studied these structures for certain families of maps (see, for instance, [86]).

CALC is modeled by maps with two break points that split the state space into three partitions and make the maps bimodal (cf. Figure 3.2). The outermost branches of these maps are determined by the adaptive limiters (and hence by the control parameters) and are linear. In the central partition of the state space, the limiters play no role and the maps are given by the production function of the population, which may have any functional form. In view of this, we focus on bimodal PWS maps with the outermost branches linear and study the bifurcation structure associated with the collision between the kink points and invariant sets lying in the outermost partitions of the state space.

We show that the bifurcations observed for these maps correspond to a rather degenerate case of a bifurcation structure associated with one-dimensional bimodal piecewise linear (PWL) maps (i.e., PWS with affine branches) with two break points. The degeneracy of this case is twofold. First, the bifurcations that are observed constitute a degenerate case of BCBs that, to our knowledge, has not been studied yet. Second,

the bifurcation structure (i.e., the number and location of the bifurcation points in the parameter space) also constitutes a degenerate case of the bifurcation structure of the general family of bimodal PWL maps. This degeneracy in the bifurcation structure (but not in the type of bifurcation) was previously reported by Foroni *et al.* in [74] for a similar dynamical system, whose study was motivated by an economic model. Foroni *et al.* succeeded in providing a partial result for the determination of bifurcation points. That is, only a necessary but not sufficient condition for the occurrence of bifurcations was reported. This leaves the problem undetermined, since with just the condition provided in [74] the number of combinations of parameters for which a bifurcation could potentially occur is extremely high. In the ecological framework considered in this thesis, this indeterminacy would imply serious difficulties for the application of CALC to the control of real populations. In this sense, it is of practical interest to exactly determine which combinations of parameter values correspond to bifurcation points and which ones do not.

Of course, this requires to find a necessary and sufficient condition for the occurrence of the considered bifurcations. We provide and prove such a condition not only for CALC and for the problem considered in [74], but for a broader family of maps that covers all the cases in which the degenerate bifurcations under study take place. By using that condition, we fully determine the bifurcation structure of CALC and complete the analytical description of the bifurcation structure of the family of maps considered in [74]. Regarding the degenerate bifurcations studied here, we provide a complete theoretical description. We prove that a continuum of cycles lying on the outermost partitions of the state space emerge at the bifurcation points, while in the non-degenerate case a unique cycle satisfying that condition exists. We also show that no cycles of this kind exist at either side of the bifurcation points.

As an application of the above results, we provide numerical simulations of populations managed by CALC for some relevant models in discrete-time population dynamics, namely the Ricker and Hassell model. These simulations show that at the bifurcation points the continuum of cycles appear to attract all possible orbits except

those corresponding to fixed points. This has important implications from the practical point of view. In case that managers are interested in keeping populations away from bifurcation points but this is not possible, the results provided here allow them to know in advance which dynamical behavior can be expected for the managed populations. Additionally, these examples show that the bifurcation structure for CALC strongly depends on the underlying dynamics and ranges from very simple to very intricate.

4.2 Transitions induced by the combination of harvesting and restocking

The analysis of the stabilizing properties of CALC carried out in the previous chapter brought to light special dynamical features of populations managed by this strategy that are the focus of this chapter. As shown in Figure 4.1, which reproduces Figure 3.4 with more detail, for certain combinations of the control parameters (e.g., $c = h = 0.6$) sudden jumps between different attractors are observed. This suggests that around the critical points in the parameter space for which these phenomena occur, slight variations in the control intensities may have dramatic consequences in the managed populations. Interestingly, such a behavior is inherent to the combination of restocking and harvesting, since it is observed neither for ATH nor for ALC.

From the ecological point of view, the population size undergoes a sharp change. As Figure 4.1 shows, the attractors on different sides of the critical points may correspond to significantly different population sizes. This is also reflected in the average population size (cf. Figure 4.2). Such a transition can seriously affect the stability and persistence of the managed populations in certain situations. This would be the case, for instance, of populations at risk of extinction. In such a case, a sudden shift from an attractor to another corresponding to lower population sizes could threaten the population persistence.
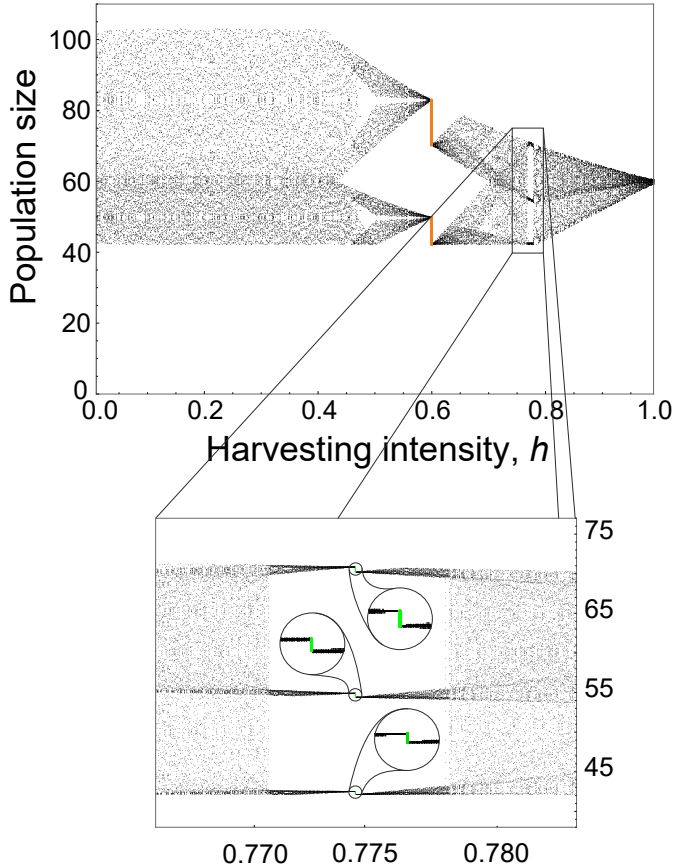
Figure 4.1: Bifurcation diagram for CALC with $c = 0.6$ and varying h. The underlying population dynamics are given by the Ricker map $f(x) = x \exp(r(1 - x/K))$ with $r = 3$ and $K = 60$. For each value of h, black dots represent 30 iterates of the state variable after a transient of $10,000$ iterates with initial conditions obtained as pseudo-random real numbers in the interval $(0, f(d)]$. For $h = 0.6$ and $h = \sqrt{0.6}$, iterates were obtained for $1,000$ different initial conditions, which are respectively represented by orange and green dots.

There are several implications that these abrupt changes in the dynamics may have from a management point of view. As can be observed in Figure 4.2, the transition between different attractors entails a sharp change in the number of individuals that are restocked/harvested. On one side of the critical point in the parameter space the intervention is essentially based on restocking and few individuals are harvested. By contrast, on the other side, only few individuals are restocked and harvesting prevails. Logically, such a transition may have severe consequences on the cost and yield of the intervention. For instance, in the case of exploited populations, shifting from mostly harvesting to mostly restocking drastically reduces the yield and increases the cost of the exploitation. Of course, this would also imply serious problems with respect to the organization, planning and preparation of the intervention, since it would have to be completely overhauled in a short period of time, provided that the necessary resources were available.
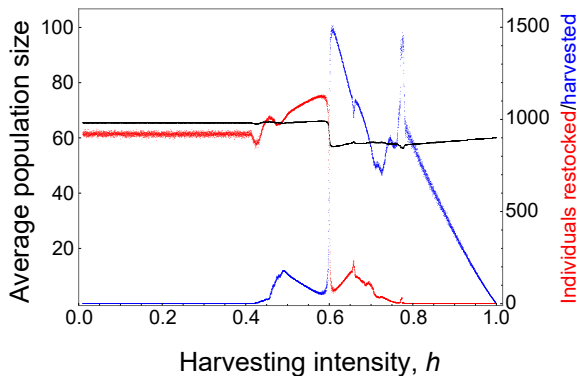
Figure 4.2: Effect of sharp transitions in the dynamics of CALC on the average population size and the intervention magnitude. For CALC with a fixed restocking intensity $c = 0.6$ and varying the harvesting intensity, the black dots represent the asymptotic average population size during 100 generations, the red dots represent the asymptotic number of restocked individuals and the blue dots the asymptotic number of harvested individuals. All values are averaged over 50 replicates. The underlying population dynamics are given by the Ricker map $f(x) = x \exp(r(1 - x/K))$ with $r = 3$ and $K = 60$.

4.3 BIFURCATION STRUCTURE

In this section we study the bifurcation structure associated with the abrupt changes in the dynamics of populations managed by CALC that were observed in the previous section. We provide necessary and sufficient conditions for the occurrence of these bifurcations in terms of the control intensities. Moreover, we study the dynamics of the managed populations at the bifurcation points.

4.3.1 BORDER COLLISION BIFURCATIONS AND PERIOD ADDING STRUCTURE OF 1D CONTINUOUS BIMODAL PIECEWISE LINEAR MAPS

The dynamics of populations satisfying (A1)–(A4) (see Section 1.2) with unbounded size (i.e., $b = +\infty$) subject to CALC are described by the difference equation $x_{t+1} = F(x_t)$, where $F\colon [0, +\infty) \to [0, +\infty)$ is the piecewise function given by

$$F(x) = \begin{cases} x/h, & 0 \leq x \leq A_H, \\ f(x), & A_H < x < A_R, \\ cx, & x > A_R. \end{cases} \tag{4.1}$$

Function F is bimodal since it increases until $\max\{d, A_H\}$, then decreases until A_R and increases again on the rest of the domain. Moreover, the functional form of the two outermost branches of F (the first ranging from 0 to A_H and the last from A_R to $+\infty$) are independent of the underlying population production function and are determined by the control intensities. Yet, the map f defines the length of each of these branches.

Given the linearity of the outermost branches of (4.1), we focus on piecewise linear (PWL) maps, which are characterized by all their branches being affine. They play a distinctive role among PWS maps and naturally appear in applied problems of a wide range of fields, e.g., circuit theory [75, 124, 222], economics [14, 85, 211] or cellular neural networks [41, 113, 138]. Reducing the problem to this type of maps simplifies

the analysis and allows to obtain complete analytical results. More specifically, we consider continuous bimodal PWL maps written in the form

$$F(x) = \begin{cases} F_{\mathcal{L}}(x) = a_{\mathcal{L}}x + \mu_{\mathcal{L}}, & 0 \le x \le d_{\mathcal{L}}, \\ F_{\mathcal{M}}(x) = a_{\mathcal{M}}x + \mu_{\mathcal{M}}, & d_{\mathcal{L}} < x < d_{\mathcal{R}}, \\ F_{\mathcal{R}}(x) = a_{\mathcal{R}}x + \mu_{\mathcal{R}}, & x \ge d_{\mathcal{R}}, \end{cases} \tag{4.2}$$

with $a_{\mathcal{M}}, \mu_{\mathcal{L}}, \mu_{\mathcal{M}}, \mu_{\mathcal{R}} \in \mathbb{R}$ and $d_{\mathcal{L}}, d_{\mathcal{R}}, a_{\mathcal{L}}, a_{\mathcal{R}} \in (0, +\infty)$. In what follows, we will denote the outermost partitions of the domain of F by $I_{\mathcal{L}} = [0, d_{\mathcal{L}}]$ and $I_{\mathcal{R}} = [d_{\mathcal{R}}, +\infty)$.

Notice that (4.2) depends on eight parameters, but two of them can always be obtained from the others by imposing continuity. Since the commonality between CALC and (4.2) is in the outermost branches, we will assume that $a_{\mathcal{M}}$ and $\mu_{\mathcal{M}}$ are determined in terms of $a_{\mathcal{L}}, a_{\mathcal{R}}, \mu_{\mathcal{L}}, \mu_{\mathcal{R}}, d_{\mathcal{L}}$ and $d_{\mathcal{R}}$. In what follows, we will denote by $\mathcal{F}$ the resulting six-parametric family of maps. Considering only the outermost partitions of the state space, the CALC map (4.1) in terms of the control intensities c and h can be considered as a biparametric subfamily $\mathcal{F}_1 \subset \mathcal{F}$ under certain parameter restrictions. First, the linearity of the outermost branches of (4.1) implies $\mu_{\mathcal{L}} = 0$ and $\mu_{\mathcal{R}} = 0$. Second, the two kink points $d_{\mathcal{L}} = A_H$ and $d_{\mathcal{R}} = A_R$ of (4.1) are uniquely determined in terms of c and h by the equalities $f(d_{\mathcal{L}}) = a_{\mathcal{L}}d_{\mathcal{L}}$ and $f(d_{\mathcal{R}}) = a_{\mathcal{R}}d_{\mathcal{R}}$, where $a_{\mathcal{L}} = 1/h$ and $a_{\mathcal{R}} = c$.

As parameters are varied, periodic orbits of (4.2) can collide with either $d_{\mathcal{L}}$ or $d_{\mathcal{R}}$. This gives rise to three different bifurcation structures depending on which partitions of the state space contain points of these cycles [167]:

- *Skew tent map structure (STMS):* the points of the cycles are located on two adjacent partitions of the state space.

- *Period adding structure (PAS):* the points of the cycles are located on the outermost partitions of the state space.

- *Fin structure (FS):* the points of the cycles are located on all three partitions of the state space.

As mentioned above, for the general case of CALC we must restrict our study to border collisions caused by invariant sets lying in the outermost partitions of the state space, and thus we focus on BCBs associated with the PAS. The elements of this structure are called *periodicity regions* (also known as *Arnold tongues* or *mode-locking tongues*) and are regions in the parameter space for which there exist cycles with all their points lying in $I_{\mathcal{L}} \cup I_{\mathcal{R}}$. Two periodicity regions differ in the number of points of their cycles in $I_{\mathcal{L}}$ and $I_{\mathcal{R}}$.

The PAS for $\mathcal{F}$ can be determined in terms of the *rotation numbers* of the associated cycles [167]. If a cycle lying in $I_{\mathcal{L}} \cup I_{\mathcal{R}}$ has m points in $I_{\mathcal{L}}$ and n points in $I_{\mathcal{R}}$, we define its rotation number as the rational number $\rho = {}^{m}/{(n+m)}$, (i.e., the number of points in the leftmost partition of the state space divided by the period of the cycle). Two rotation numbers $\rho_1 = {}^{m_1}/{p_1}$ and $\rho_2 = {}^{m_2}/{p_2}$ are Farey neighbors when $|m_1 p_2 - m_2 p_1| = 1$, and their Farey sum is defined as $\rho_1 \oplus \rho_2 = {}^{(m_1+m_2)}/{(p_1+p_2)}$. Using these definitions, the order and existence of the periodicity regions of $\mathcal{F}$ are completely determined by the following rule: if two periodicity regions are associated with cycles with Farey neighbor rotation numbers ρ_1 and ρ_2, then in the parameter space between them there exists another periodicity region related to cycles with rotation number $\rho_1 \oplus \rho_2$. Based on this principle, the PAS of $\mathcal{F}$ was iteratively determined in [167] by using Leonov's approach [86, 135]. Given a rotation number, the corresponding periodicity region is a portion of the six-dimensional parameter space bounded by two different manifolds, which are derived by imposing the collision of each of the kink points of (4.2) with cycles of that rotation number.

4.3.2 DETERMINING BORDER COLLISION BIFURCATION POINTS UNDER CERTAIN HOMOGENEITY CONDITIONS

Since $\mathcal{F}_1 \subset \mathcal{F}$, it would be logical to think that one could obtain a complete description of the PAS of $\mathcal{F}_1$ by substituting the parameter restrictions defining this subfam-

ily into the already known expressions for the periodicity regions of $\mathcal{F}$. Unfortunately, we will see that this is not the case. This idea was used in [74] for another biparametric subfamily of maps $\mathcal{F}_2 \subset \mathcal{F}$ given by the parameter restrictions $\mu_{\mathcal{L}} = 0$, $\mu_{\mathcal{R}} = 0$, $a_{\mathcal{L}} + a_{\mathcal{R}} = 2$ and $2d_{\mathcal{L}}d_{\mathcal{R}} - d_{\mathcal{L}} - d_{\mathcal{R}} = 0$. Notice that two of these restrictions, $\mu_{\mathcal{L}} = 0$ and $\mu_{\mathcal{R}} = 0$, are common with $\mathcal{F}_1$. If we consider only these two restrictions, we obtain a four-parametric subfamily $\mathcal{F}_0 \subset \mathcal{F}$ that includes both $\mathcal{F}_1$ and $\mathcal{F}_2$ as strict subfamilies. Consider a rotation number $m/(n+m)$. It could be expected that when the two restrictions for $\mathcal{F}_0$ were substituted into the equations of the two manifolds $\xi_{\mathcal{L}}$ and $\xi_{\mathcal{R}}$ bounding the corresponding periodicity region of $\mathcal{F}$ (which, recall, lie in a six-dimensional space), they would lead to another two manifolds in the four-dimensional parameter space of $\mathcal{F}_0$. In that case, the periodicity region of $\mathcal{F}_0$ for the given rotation number would be the parameter space between these two manifolds. However, when $\mu_{\mathcal{L}} = 0$ and $\mu_{\mathcal{R}} = 0$ are substituted into the equations of $\xi_{\mathcal{L}}$ and $\xi_{\mathcal{R}}$ not only $\mu_{\mathcal{L}}$ and $\mu_{\mathcal{R}}$ vanish, but also $d_{\mathcal{L}}$ and $d_{\mathcal{R}}$ drop from the equations. As a consequence, when restricted, $\xi_{\mathcal{L}}$ and $\xi_{\mathcal{R}}$ yield a unique manifold in the four-dimensional parameter space of $\mathcal{F}_0$, which is given by $a_{\mathcal{L}}^m a_{\mathcal{R}}^n = 1$ for the considered rotation number. This means that the PAS of $\mathcal{F}_0$ is rather degenerate with respect to the one of $\mathcal{F}$, since all periodicity regions of $\mathcal{F}_0$ have null Lebesgue measure in its parameter space. In particular, all points in a periodicity region of $\mathcal{F}_0$ are bifurcation points, i.e., for all of them at least one of the kink points is in a cycle with all its points in the outermost partitions of the state space.

The main inconvenience of the fact that $d_{\mathcal{L}}$ and $d_{\mathcal{R}}$ drop from the equations of $\xi_{\mathcal{L}}$ and $\xi_{\mathcal{R}}$ when the restriction $\mu_{\mathcal{L}} = \mu_{\mathcal{R}} = 0$ is imposed is that the condition that is obtained after substitution, $a_{\mathcal{L}}^m a_{\mathcal{R}}^n = 1$, is necessary but not sufficient for the occurrence of BCBs of the PAS of $\mathcal{F}_0$. Indeed, $d_{\mathcal{L}}$ and $d_{\mathcal{R}}$ actually play a central role in the problem. Assume that the four parameters defining $\mathcal{F}_0$ are set at values satisfying $d_{\mathcal{L}} < \min\{a_{\mathcal{R}}d_{\mathcal{R}}, d_{\mathcal{R}}/a_{\mathcal{L}}\}$, $a_{\mathcal{L}} > 1$, $0 < a_{\mathcal{R}} < 1$ and $a_{\mathcal{L}}^m a_{\mathcal{R}}^n = 1$ for certain $n, m \in \mathbb{N}$. According to the last equality, we could expect that a BCB of the PAS of $\mathcal{F}_0$ occurred for these values, i.e., that either $d_{\mathcal{L}}$ or $d_{\mathcal{R}}$ were in a cycle with all its points

in $I_{\mathcal{L}} \cup I_{\mathcal{R}}$. However, this is not possible since $d_{\mathcal{L}} < F_{\mathcal{L}}(d_{\mathcal{L}}) = a_{\mathcal{L}} d_{\mathcal{L}} < d_{\mathcal{R}}$ and $d_{\mathcal{L}} < F_{\mathcal{R}}(d_{\mathcal{R}}) = a_{\mathcal{R}} d_{\mathcal{R}} < d_{\mathcal{R}}$.

If the PAS of $\mathcal{F}_0$ cannot be completely determined by direct substitution of its parameter restrictions into the PAS of $\mathcal{F}$, neither can be the PAS of any subfamily of $\mathcal{F}_0$ like the $\mathcal{F}_1$ considered here or the $\mathcal{F}_2$ considered in [74]. This was implicitly observed for $\mathcal{F}_2$ in [74] when it was shown that in some specific cases no BCB can occur even if the condition $a_{\mathcal{L}}^m a_{\mathcal{R}}^n = 1$ is met. Yet, no complete description of the PAS of $\mathcal{F}_2$ in terms of the parameters was obtained. With the following result, which yields a necessary and sufficient condition for the occurrence of BCBs of the PAS of $\mathcal{F}_0$, we will complete this description and fully determine the PAS of CALC.

Proposition 4.1. *A BCB of the PAS of* (4.2) *with* $\mu_{\mathcal{L}} = \mu_{\mathcal{R}} = 0$ *occurs if and only if there exist* $\lambda \in (0,1)$ *and* $m, n \in \mathbb{N}$ *with* $\gcd(m, n) = 1$ *such that* $a_{\mathcal{L}} = \lambda^{-n}$, $a_{\mathcal{R}} = \lambda^m$ *and* $\lambda d_{\mathcal{R}} \leq d_{\mathcal{L}}$. *Moreover, the two kink points* $d_{\mathcal{L}}$ *and* $d_{\mathcal{R}}$ *are* $(m+n)$-*periodic and their orbits have* m *points in* $I_{\mathcal{L}}$ *and* n *points in* $I_{\mathcal{R}}$.

Proof. Assume that a BCB of the PAS of (4.2) with $\mu_{\mathcal{L}} = \mu_{\mathcal{R}} = 0$ occurs. Then, either $d_{\mathcal{L}}$ or $d_{\mathcal{R}}$ must be in a cycle $\mathcal{O}$ with all its points in $I_{\mathcal{L}} \cup I_{\mathcal{R}}$. Assume that this cycle has m points in $I_{\mathcal{L}}$ and n points in $I_{\mathcal{R}}$. Since $F_{\mathcal{L}}(x) = a_{\mathcal{L}} x$ and $F_{\mathcal{R}}(x) = a_{\mathcal{R}} x$ commute under composition, if $d_{\mathcal{L}} \in \mathcal{O}$ then $a_{\mathcal{L}}^m a_{\mathcal{R}}^n d_{\mathcal{L}} = d_{\mathcal{L}}$. Similarly, $d_{\mathcal{R}} \in \mathcal{O}$ leads to $a_{\mathcal{L}}^m a_{\mathcal{R}}^n d_{\mathcal{R}} = d_{\mathcal{R}}$. Given that $0 < d_{\mathcal{L}} < d_{\mathcal{R}}$, the terms $d_{\mathcal{L}}$ and $d_{\mathcal{R}}$ can be canceled from these equalities, after which both of them lead to the same condition $a_{\mathcal{L}}^m a_{\mathcal{R}}^n = 1$. In case that $a_{\mathcal{L}} < 1$, all orbits starting in $I_{\mathcal{L}}$ would stay in $I_{\mathcal{L}}$ and monotonically converge to 0, which contradicts the occurrence of a BCB. Therefore, it must be $a_{\mathcal{L}} > 1$ and $0 < a_{\mathcal{R}} < 1$. Then, if we set $\lambda = a_{\mathcal{R}}^{1/m} \in (0,1)$ it follows that $a_{\mathcal{L}} = \lambda^{-n}$ and $a_{\mathcal{R}} = \lambda^m$. On the other hand, if $\gcd(m,n) = d > 1$ then $m/d \in \mathbb{N}, n/d \in \mathbb{N}$ and $a_{\mathcal{L}}^{-m/d} a_{\mathcal{R}}^{n/d} = 1$, and thus $m + n$ is not the prime period of $\mathcal{O}$. Consequently, we can assume $\gcd(m,n) = 1$.

Suppose that $d_{\mathcal{R}} \in \mathcal{O}$. Since $\mathcal{O} \subset (I_{\mathcal{L}} \cup I_{\mathcal{R}})$, any point of $\mathcal{O}$ can be obtained by starting at $d_{\mathcal{R}}$ and successively applying $F_{\mathcal{R}}(x) = \lambda^m x$ a certain number p of times and $F_{\mathcal{L}}(x) = \lambda^{-n} x$ another certain number q of times in a specific order, with $p \in$

$\{0, \ldots, n-1\}$ and $q \in \{0, \ldots, m-1\}$. Given that $F_{\mathcal{R}}$ and $F_{\mathcal{L}}$ commute under composition, all the points of $\mathcal{O}$ can be expressed in the form $\lambda^{pm-qn} d_{\mathcal{R}}$ for certain p and q in the aforementioned ranges. Since m and n are coprime, using Bezout's lemma we can find p and q such that $pm - qn = 1$. Thus, $\lambda d_{\mathcal{R}} \in \mathcal{O}$. On the other hand, given that $\lambda d_{\mathcal{R}} < d_{\mathcal{R}}$ and $\mathcal{O} \subset (I_{\mathcal{L}} \cup I_{\mathcal{R}})$, it follows that $\lambda d_{\mathcal{R}} \in I_{\mathcal{L}}$, and thus $\lambda d_{\mathcal{R}} \leq d_{\mathcal{L}}$. The same condition is derived when repeating these arguments for the case $d_{\mathcal{L}} \in \mathcal{O}$.

Assume now that there exist $\lambda \in (0,1)$ and $m, n \in \mathbb{N}$ with $\gcd(m, n) = 1$ such that $a_{\mathcal{L}} = \lambda^{-n}$, $a_{\mathcal{R}} = \lambda^m$ and $\lambda d_{\mathcal{R}} \leq d_{\mathcal{L}}$. We will prove that the set $\mathcal{U} = \{\lambda^i d_{\mathcal{R}}\}_{i=1-n}^{m}$ is a $(m+n)$-cycle that has m points in $I_{\mathcal{L}}$ and n points in $I_{\mathcal{R}}$. Consider $\mathcal{U}_{\mathcal{L}} = \{\lambda^i d_{\mathcal{R}}\}_{i=1}^{m}$ and $\mathcal{U}_{\mathcal{R}} = \{\lambda^i d_{\mathcal{R}}\}_{i=1-n}^{0}$. With these notations, $\mathcal{U} = \mathcal{U}_{\mathcal{L}} \cup \mathcal{U}_{\mathcal{R}}$, $\mathcal{U}_{\mathcal{L}} \subset I_{\mathcal{L}}$ and $\mathcal{U}_{\mathcal{R}} \subset I_{\mathcal{R}}$. Given that $\lambda < 1$, $F(x) = F_{\mathcal{L}}(x) = \lambda^{-n} x > x$ for $x \in \mathcal{U}_{\mathcal{L}}$ and $F(x) = F_{\mathcal{R}}(x) = \lambda^m x < x$ for $x \in \mathcal{U}_{\mathcal{R}}$. Besides, $F(\max \mathcal{U}_{\mathcal{L}}) = F(\lambda d_{\mathcal{R}}) = \lambda^{1-n} d_{\mathcal{R}} = \max \mathcal{U}$ and $F(\min \mathcal{U}_{\mathcal{R}}) = F(d_{\mathcal{R}}) = \lambda^m d_{\mathcal{R}} = \min \mathcal{U}$. This proves that $\mathcal{U}$ is an invariant set for F.

Suppose now that $F^q(x) = x$ for certain $x \in \mathcal{U}$ and $q \in \mathbb{N}$. Since $\mathcal{U}$ is F−invariant, it follows that $\{x, F(x), \ldots, F^{q-1}(x)\} \subset (I_{\mathcal{L}} \cup I_{\mathcal{R}})$. Assume that $\tilde{m}$ of these points lie in $I_{\mathcal{L}}$ and $\tilde{n}$ in $I_{\mathcal{R}}$. Then, by the commutativity between $F_{\mathcal{L}}$ and $F_{\mathcal{R}}$, it follows that $F^q(x) = \lambda^{m\tilde{n} - n\tilde{m}} x = x$, which implies $m\tilde{n} = n\tilde{m}$. Since m and n are coprime, this equality is only possible if $\tilde{m}$ is a multiple of m and $\tilde{n}$ is a multiple of n. Assume that $\tilde{m} = km$ for a certain $k \in \mathbb{N}$. Then, $\tilde{n} = kn$ and $q = \tilde{m} + \tilde{n} = k(m+n) \geq m+n$. This implies that the $m+n$ points of the set $\mathcal{V} = \{d_{\mathcal{R}}, F(d_{\mathcal{R}}), \ldots, F^{m+n-1}(d_{\mathcal{R}})\} \subseteq \mathcal{U}$ are all different, and thus $\mathcal{V} = \mathcal{U}$. Since m points of $\mathcal{U}$ lie in $I_{\mathcal{L}}$ and n lie in $I_{\mathcal{R}}$, again by the commutativity between $F_{\mathcal{L}}$ and $F_{\mathcal{R}}$, it follows that $F^{m+n}(d_{\mathcal{R}}) = (\lambda^{-n})^m (\lambda^m)^n d_{\mathcal{R}} = d_{\mathcal{R}}$. This proves that $d_{\mathcal{R}}$ is in a $(m+n)$−cycle that has m points in $I_{\mathcal{L}}$ and n points in $I_{\mathcal{R}}$ and thus, in particular, a BCB of the PAS of (4.2) occurs for the considered parameter values. The same conclusion can be drawn for the kink point $d_{\mathcal{L}}$ by applying the same arguments to the set $\tilde{\mathcal{U}} = \{\lambda^i d_{\mathcal{L}}\}_{i=-n}^{m-1}$. $\qquad \square$

Interestingly, for the family $\mathcal{F}$ border collision bifurcations can occur for any positive values of $a_\mathcal{L}$ and $a_\mathcal{R}$ [166]. However, Proposition 4.1 shows that for the subfamily $\mathcal{F}_0$ they can only take place for $a_\mathcal{L} > 1$ and $0 < a_\mathcal{R} < 1$. On the other hand, Proposition 4.1 resolves the degeneracy in the PAS of $\mathcal{F}$ that emerges when the homogeneity of the outermost branches of the maps is imposed. In particular, this result determines the PAS of any subfamily of $\mathcal{F}$ for which the same homogeneity conditions must be satisfied, as can be $\mathcal{F}_1$ corresponding to CALC or $\mathcal{F}_2$ considered in [74].

Corollary 4.2. *Assume that (A1)–(A4) hold. A BCB of the PAS of CALC occurs if and only if there exist $\lambda \in (0,1)$ and $m, n \in \mathbb{N}$ with $\gcd(m,n) = 1$ such that $h = \lambda^n$, $c = \lambda^m$ and $\lambda A_R \leq A_H$. Moreover, both A_H and A_R are $(m+n)$-periodic and their orbits have m points in $(0, A_H]$ and n points in $[A_R, +\infty)$.*

In Section 4.4 we will use Corollary 4.2 to determine the PAS of CALC for different population growth models describing the underlying dynamics. On the remainder of this subsection, we use Proposition 4.1 to complete the study of the PAS of $\mathcal{F}_2$ started in [74]. Following the notation in that paper, after imposing the parameter restrictions defining $\mathcal{F}_2$, we write the parameters of (4.2) in terms of $r \in (0,1)$ and $\epsilon > r$ in the form $a_\mathcal{L} = 1 + r, a_\mathcal{R} = 1 - r, d_\mathcal{L} = \epsilon/(\epsilon+r)$ and $d_\mathcal{R} = \epsilon/(\epsilon-r)$.

Corollary 4.3. *Consider (4.2) for $a_\mathcal{L} = 1 + r$, $a_\mathcal{R} = 1 - r$, $d_\mathcal{L} = \epsilon/(\epsilon+r)$ and $d_\mathcal{R} = \epsilon/(\epsilon-r)$, with $r \in (0,1)$ and $\epsilon > r$. Then, a BCB of the PAS occurs if and only if there exist $m, n \in \mathbb{N}$ with $\gcd(m,n) = 1$ such that*

$$\begin{cases} (1+r)^m (1-r)^n = 1, \\ \epsilon \geq r \left(\frac{\sqrt[n]{1+r}+1}{\sqrt[n]{1+r}-1} \right). \end{cases} \tag{4.3}$$

Moreover, both $d_\mathcal{L}$ and $d_\mathcal{R}$ are $(m+n)$-periodic and their orbits have m points in the interval $(0, \epsilon/(\epsilon+r)]$ and n points in $[\epsilon/(\epsilon-r), +\infty)$.

The PAS in the $r - \epsilon$ plane that can be derived from Corollary 4.3 is shown in Figure 4.3, which reproduces Figure 5a in [74] with two important differences. First, the peri-

odicity region of rotation number $1/2$ that appears in [74] is not represented in Figure 4.3. The reason is that this region actually does not exist, since it corresponds to $r = 0$ and for that value the graph of the map reduces to the straight line $y = x$. Second, in [74] the endpoints of the periodicity regions were only determined for Leonov's first complexity level (blue lines in Figure 4.3), which in this case correspond to $n = 1$. Specifically, in [74] it was proved by using the skew tent map as normal form that the endpoints of the periodicity regions for the first complexity level are on the line $\epsilon = r + 2$. The same conclusion can be directly drawn by substituting $n = 1$ in the second condition of Corollary 4.3. For the remaining periodicity regions (i.e., $n \geq 2$), no expressions for the endpoints were provided in [74] and it was only stated that all of them are above the line $\epsilon = r + 2$. The second condition in Corollary 4.3 provides the exact values of the endpoints for all complexity levels and completes the analytical determination of the PAS of the family of maps considered in [74]. The curves containing these endpoints are represented by dashed lines in Figure 4.3 and the analytical expression of each of them is indicated.

4.3.3 Degenerate border collision bifurcations

Apart from determining the PAS of $\mathcal{F}_0$ (and, in particular, of CALC), Proposition 4.1 reveals another relevant fact: when a BCB of the PAS occurs, the two kink points of the map collide at the same time with cycles in the outermost partitions of the state space and with the same rotation number. This suggests that the BCBs for the family of maps $\mathcal{F}_0$ are different from the ones that have been previously observed for $\mathcal{F} \setminus \mathcal{F}_0$ [165, 166, 167] and constitute a rather degenerate case. For any fixed parameter point inside one of the periodicity regions of the PAS of $\mathcal{F} \setminus \mathcal{F}_0$ there exists a unique cycle associated with it, which can be attracting or not [165]. In particular, at a BCB point the unique cycle that exists may contain either $d_{\mathcal{L}}$ or $d_{\mathcal{R}}$. In the case of $\mathcal{F}_0$, by Proposition 4.1 we know that at any bifurcation point there exist, at least, two different cycles with the same rotation number when the parameters satisfy $\lambda d_{\mathcal{R}} < d_{\mathcal{L}}$, one containing $d_{\mathcal{L}}$ and another containing $d_{\mathcal{R}}$. Apart from giving us a glimpse of the degeneracy of the case,
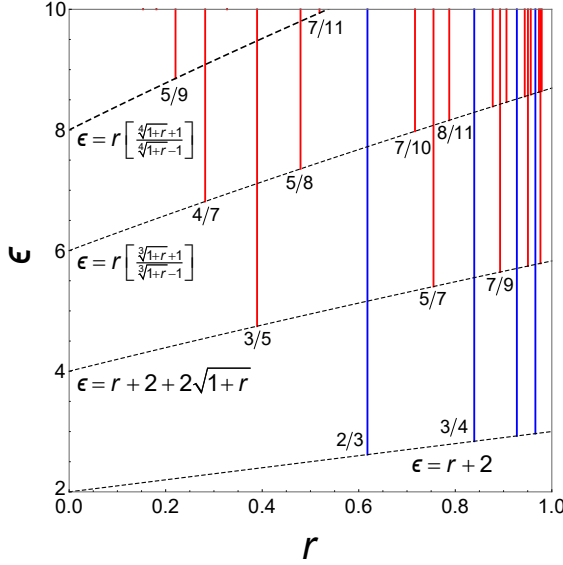
Figure 4.3: Periodic adding structure of maps in $\mathcal{F}_2$. PAS of (4.2) for $a_{\mathcal{L}} = 1 + r$, $a_{\mathcal{R}} = 1 - r$, $d_{\mathcal{L}} = \epsilon/(\epsilon+r)$ and $d_{\mathcal{R}} = \epsilon/(\epsilon-r)$, with $r \in (0, 1)$ and $\epsilon > r$. This figure is analogous to Figure 5a in [74], except that the periodicity region of rotation number $1/2$ has been omitted and the endpoints of the different regions are analytically determined by Corollary 4.3. The curves containing these points are represented by dashed lines and the expression of each of them is indicated.

this difference leads to the question about the exact number of cycles with the same rotation number that may exist at a bifurcation point of $\mathcal{F}_0$.

Beyond the theoretical interest of this question, it is also relevant from a practical point of view in the case of CALC. Managers could be particularly interested in avoiding control intensities corresponding to BCB points in light of the problems that small variations of the parameters around these points may cause. However, in case that we were faced with one of these bifurcations, it would be of practical interest to know in advance how the managed populations would behave.

To illustrate the dynamical behavior at BCB points of maps of $\mathcal{F}_0$ and compare that behavior to what is known for $\mathcal{F} \setminus \mathcal{F}_0$, we consider the maps $f_1 \in \mathcal{F} \setminus \mathcal{F}_0$ and $f_2 \in$

$\mathcal{F}_0$ given by

$$f_1(x) = \begin{cases} 2x + 2, & x \leq 1, \\ (2\alpha - 4.5)x + 8.5 - 2\alpha, & 1 < x < 2, \\ \alpha x - 0.5, & x \geq 2, \end{cases}$$

$$f_2(x) = \begin{cases} 3x, & x \leq 1, \\ (2\alpha - 3)x + 6 - 2\alpha, & 1 < x < 2, \\ \alpha x, & x \geq 2, \end{cases}$$

(4.4)

with $\alpha \in (0, 1)$. It is routine to check that a BCB of the PAS of f_1 occurs for $\alpha = 3/8$. For this value, the graph of f_1 together with its second iterate $f_1^2 = f_1 \circ f_1$ is shown in Figure 4.4a. In this case, the BCB occurs by the collision of $d_{\mathcal{L}} = 1$ with a cycle of rotation number $1/2$, while the other kink point of the map, $d_{\mathcal{R}} = 2$, is not 2-periodic. In fact, $d_{\mathcal{R}}$ collides with a cycle of the same rotation number for a lower value of α, namely $\alpha = 1/4$. The parameter interval between these two bifurcation points, $(1/4, 3/8)$, corresponds to the periodicity region of rotation number $1/2$. For all parameter values inside that interval a unique 2-cycle exists, which lies in $I_{\mathcal{L}} \cup I_{\mathcal{R}}$ and in this case is globally attracting as Figure 4.4b shows. The most important aspect, however, is that no abrupt change in the magnitude of the state variable occurs when α is varied through the bifurcation point. The situation is completely different for f_2. For this map, a BCB of the PAS associated with cycles of rotation number $1/2$ occurs for $\alpha = 1/3$. As shown in Figure 4.4c and in line with Proposition 4.1, for that parameter value the two kink points of the map collide simultaneously with cycles of that rotation number. Yet, not only the two break points of the map become periodic at the bifurcation point, but a continuum of cycles with all their points lying in $I_{\mathcal{L}} \cup I_{\mathcal{R}}$ and with the same rotation number $1/2$ exist. Two important facts about these cycles can be observed in Figure 4.4d. First, these infinitely many 2-cycles do not exist for values of parameter α on either side of the bifurcation point. Second, when α is varied through

the bifurcation point the magnitude of the state variable undergoes a sudden jump between two different attractors, which are connected by the continuum of 2-cycles. This is the same behavior that was observed for CALC in Section 4.2.

This example illustrates the differences between the BCBs for maps in $\mathcal{F}_0$ and those in $\mathcal{F} \setminus \mathcal{F}_0$. In the following result we prove that this is always the case.

Proposition 4.4. *Consider* (4.2) *for* $\mu_{\mathcal{L}} = \mu_{\mathcal{R}} = 0$. *Assume that there exist* $\lambda \in (0, 1)$ *and* $m, n \in \mathbb{N}$ *with* $\gcd(m, n) = 1$ *such that* $a_{\mathcal{L}} = \lambda^{-n}$, $a_{\mathcal{R}} = \lambda^m$ *and* $\lambda d_{\mathcal{R}} \leq d_{\mathcal{L}}$. *Then, the following holds:*

(i) *If* $\lambda d_{\mathcal{R}} < d_{\mathcal{L}}$, *all points in*

$$\mathcal{B} = \bigcup_{i=-n}^{m-1} [\lambda^{i+1} d_{\mathcal{R}}, \lambda^i d_{\mathcal{L}}]$$

are $(m + n)$-*periodic and their orbits have* m *points in* $I_{\mathcal{L}}$ *and* n *points in* $I_{\mathcal{R}}$.

(ii) *If* $\lambda d_{\mathcal{R}} = d_{\mathcal{L}}$, $d_{\mathcal{L}}$ *and* $d_{\mathcal{R}}$ *belong to the same periodic orbit of period* $m + n$ *with* m *points in* $I_{\mathcal{L}}$ *and* n *points in* $I_{\mathcal{R}}$.

Proof. Assume $\lambda d_{\mathcal{R}} < d_{\mathcal{L}}$. Under this condition, $\mathcal{B}$ is a well-defined disjoint union of non-empty intervals. For $i \in \{-n, \ldots, m-1\}$, denote $J_i = [\lambda^{i+1} d_{\mathcal{R}}, \lambda^i d_{\mathcal{L}}]$ and consider $\mathcal{B}_{\mathcal{L}} = \bigcup_{i=0}^{m-1} J_i$ and $\mathcal{B}_{\mathcal{R}} = \bigcup_{i=-n}^{-1} J_i$. With this notation, $\mathcal{B} = \mathcal{B}_{\mathcal{L}} \cup \mathcal{B}_{\mathcal{R}}$, $\mathcal{B}_{\mathcal{L}} \cap \mathcal{B}_{\mathcal{R}} = \emptyset$, $\mathcal{B}_{\mathcal{L}} \subset I_{\mathcal{L}}$ and $\mathcal{B}_{\mathcal{R}} \subset I_{\mathcal{R}}$. Given that $\lambda < 1$, $F(x) = F_{\mathcal{L}}(x) = \lambda^{-n} x > x$ for $x \in \mathcal{B}_{\mathcal{L}}$ and $F(x) = F_{\mathcal{R}}(x) = \lambda^m x < x$ for $x \in \mathcal{B}_{\mathcal{R}}$. Besides, $F(\max \mathcal{B}_{\mathcal{L}}) = F(d_{\mathcal{L}}) = \lambda^{-n} d_{\mathcal{L}} = \max \mathcal{B}$ and $F(\min \mathcal{B}_{\mathcal{R}}) = F(d_{\mathcal{R}}) = \lambda^m d_{\mathcal{R}} = \min \mathcal{B}$. With these conditions, $F(\mathcal{B}) \subset [\min \mathcal{B}, \max \mathcal{B}]$. On the other hand, F is a bijection between J_i and J_{i-n} for $i \in \{0, \ldots, m-1\}$ and between J_i and J_{i+m} for $i \in \{-n, \ldots, -1\}$. This proves that $\mathcal{B}$ is an invariant set for F and that the application of F to any point in $\mathcal{B}$ leads to another point in a different component of $\mathcal{B}$.
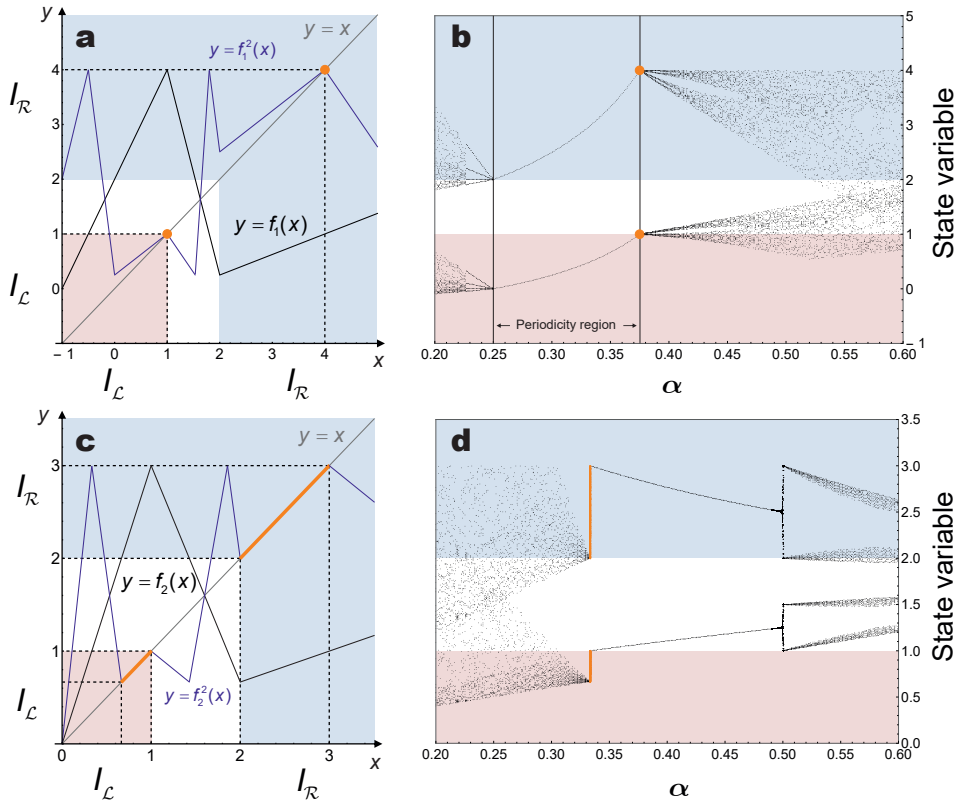
Figure 4.4: Differences in the PAS of maps in $\mathcal{F}_0$ and $\mathcal{F} \setminus \mathcal{F}_0$. (a) Graphical representation of f_1 in (4.4) and its second iterate $f_1^2 = f_1 \circ f_1$ for $\alpha = 3/8$. (b) Bifurcation diagram of f_1 in (4.4) for varying α. (c) Graphical representation of f_2 in (4.4) and its second iterate $f_2^2 = f_2 \circ f_2$ for $\alpha = 1/3$. (d) Bifurcation diagram of f_2 in (4.4) for varying α. In all panels, the orange dots correspond to 2-cycles associated with BCBs of the PAS, the red area corresponds to the interval $I_{\mathcal{L}}$ and the blue area to $I_{\mathcal{R}}$.

Suppose now that $F^q(J_i) = J_i$ for certain $i \in \{-n, \ldots, m-1\}$ and $q \in \mathbb{N}$. Since $\mathcal{B}$ is F−invariant and bijects components of $\mathcal{B}$ into different components of $\mathcal{B}$, the q intervals $J_i, F(J_i), \ldots, F^{q-1}(J_i)$ correspond to components of $\mathcal{B}$. Assume that $\tilde{m}$ of these intervals lie in $B_{\mathcal{L}}$ and $\tilde{n}$ in $B_{\mathcal{R}}$. Then, by the commutativity between $F_{\mathcal{L}}$ and $F_{\mathcal{R}}$ it follows that $F^q(J_i) = \lambda^{m\tilde{n}-n\tilde{m}} J_i = J_i$, which implies $m\tilde{n} = n\tilde{m}$. Under the coprimality condition for m and n, this equality is only possible if $\tilde{m}$ is a multiple of m and $\tilde{n}$ is a multiple of n. Assume that $\tilde{m} = km$ for a certain $k \in \mathbb{N}$. Then, $\tilde{n} = kn$ and $q = \tilde{m} + \tilde{n} = k(m+n) \geq m+n$. This means that for any $i \in \{-n, \ldots, m-1\}$ the $m+n$ intervals $J_i, F(J_i), \ldots, F^{m+n-1}(J_i)$ are different, and thus they correspond to each of the components of $\mathcal{B}$. Since $\mathcal{B}$ has m components in $B_{\mathcal{L}}$ and n components in $B_{\mathcal{R}}$, again by the commutativity of $F_{\mathcal{L}}$ and $F_{\mathcal{R}}$ we obtain $F^{m+n}(J_i) = \lambda^{mn-nm} J_i = J_i$. This proves that all the points of $\mathcal{B}$ are $(m+n)$−periodic and that their orbits have m points in $I_{\mathcal{L}}$ and n points in $I_{\mathcal{R}}$.

Assume now that $\lambda d_{\mathcal{R}} = d_{\mathcal{R}}$. According to Proposition 4.1, a BCB occurs for the control intensities given in Proposition 4.4 and both break points $d_{\mathcal{L}}$ and $d_{\mathcal{R}}$ are $(m+n)$−periodic. Moreover, in the proof of Proposition 4.1 it was shown that under the conditions in Proposition 4.4 the point $\lambda d_{\mathcal{R}}$ is in the same cycle as $d_{\mathcal{R}}$, which completes the proof. $\qquad\square$

Proposition 4.4 allows to obtain a full picture of the degenerate BCBs considered here. Since the periodicity regions of $\mathcal{F}_0$ have zero Lebesgue measure in the parameter space and coincide with the bifurcation manifolds, no cycles lying in the outermost partitions of the state space exist for parameter values outside these manifolds. Hence, when parameters are varied across a bifurcation manifold of $\mathcal{F}_0$, a continuum of cycles lying in the outermost partitions of the state space emerges at the bifurcation point and disappears afterwards. This is what was observed for the map f_2 in the previous example (cf. Figure 4.4d).

Remark 4.5. Notice that the result provided in Proposition 4.4 is independent of the expression of the map between the two kink points. Thus, in particular, it is valid for

CALC with any uncontrolled population satisfying (A1)-(A4). In that case, parameters m and n in Proposition 4.4 have a specific meaning. They represent, respectively, the number of harvesting and restocking episodes that are necessary to complete one of the cycles associated with BCBs of CALC if we consider a point of the cycle as the initial condition. This result may be helpful to predict the population behavior in case of facing such a bifurcation. On the other hand, according to Corollary 4.2, when a BCB of CALC occurs the equality $c^n = h^m$ holds. For $c > h$ we have $c^n = h^m > h^n$, and thus $m < n$. Therefore, when at a BCB point the restocking intensity is higher than the harvesting intensity, the number of restocking episodes associated with the cycles of that BCB is larger than the number of harvesting episodes. By the same argument, it can be seen that the opposite occurs for $c < h$.

4.4 EXAMPLES

In this section we use the theoretical results provided in the previous section to determine the PAS of CALC for two well known production maps. These examples show that this structure may range from very simple to very intricate depending on the map that is considered.

4.4.1 RICKER MODEL

We start by considering the Ricker map $f(x) = x \exp(r(1 - x/K))$ with $r = 3$ and $K = 60$. Using Corollary 4.2, only two BCBs can occur for this map, namely for $c = h \gtrsim 0.076$ and $c^{1/2} = h \gtrsim 0.117$. These two bifurcations can be observed in the bifurcation diagram of Figure 4.1, where c is set at 0.6 and h is varied. For $c = h = 0.6$, the inequality $cA_R < A_H$ holds and an infinite number of 2-cycles are predicted by Proposition 4.4. These cycles have one point in $I_{\mathcal{L}}$ and another point in $I_{\mathcal{R}}$, and completely fill $\mathcal{B} = [cA_R, A_H] \cup [A_R, A_H/c] \approx [42.13, 49.78] \cup [70.22, 82.97]$. They correspond to the orange dots in Fig. 4.1. The dynamics of these cycles is based on

alternating episodes of restocking and harvesting as the number of individuals switches between the two components of $\mathcal{B}$.

Similarly, for $c = h^2 = 0.6$ the inequality $\sqrt{c}A_R < A_H$ holds and a continuum of 3-cycles is predicted by Proposition 4.4. These cycles have two points in $I_{\mathcal{L}}$ and one point in $I_{\mathcal{R}}$, and fill $\mathcal{B} = [cA_R, \sqrt{c}A_H] \cup [\sqrt{c}A_R, A_H] \cup [A_R, A_H/\sqrt{c}] \cong [42.13, 42.52] \cup [54.39, 54.89] \cup [70.22, 70.86]$. They correspond to the green dots in Fig. 4.1. The dynamics of these cycles is based on a succession of three control episodes, which consist of two consecutive episodes of harvesting followed by one episode of restocking.

At the two BCB points the continuum of cycles seem to attract all orbits except those corresponding to fixed points. Thus, the managed populations asymptotically behave as has been described for these cycles.

From the practical point of view, if only two BCBs occur, as in this example, it may be possible to implement the control in such a way that sharp changes in the dynamics be avoided (and thus, the problems associated with them). However, the number of BCBs that can occur for a given production function for the uncontrolled population can be very large, as we illustrate in the following subsection. In such a case, avoiding the negative effects of BCBs can be particularly difficult.

4.4.2 Hassell model

According to Corollary 4.2, the occurrence of BCBs associated with the PAS of CALC depends on the condition $\lambda A_R \leq A_H$, which in turn depends on how steep is the production function of the uncontrolled population around the carrying capacity. The steeper the production function, the closer are A_R and A_H for a fixed λ (recall that $f(A_H) = \lambda^{-n}A_H$ and $f(A_R) = \lambda^m A_R$), and consequently there are more chances for the existence of values of λ satisfying $\lambda A_R \leq A_H$. Thus, more combinations of control intensities can correspond to bifurcation points. In view of this, we consider

the Hassell map [98]

$$x_{t+1} = \frac{\lambda x_t}{(1 + a x_t)^b}$$

with $\lambda = 1000$, $a = 0.05$ and $b = 50$. For these parameter values, the modulus of the derivative of the production function around the carrying capacity is large, namely approximately 8.20. Using Corollary 4.2, the PAS of CALC for this production function was determined and is shown in Figure 4.5. Up to period 10, a total of 29 BCBs can occur for different values of the parameters. This demonstrates that the number of BCBs associated with the PAS of CALC can be very high, as well as the period of the corresponding cycles. This may have severe consequences on the applicability of CALC, as shown in Figure 4.6, where the bifurcation diagram of CALC for this last example with $c = 0.6$ and varying h is represented. As can be observed, the distance between harvesting intensities of consecutive BCB points is short.

This last example demonstrates the practical relevance of Proposition 4.1. Without it, if only the necessary condition for the occurrence of BCBs obtained in [74] was used, the difficulties in the application of CALC would be even greater than in this last example for all population maps, included the Ricker model considered in the first example. The reason for this is that managers would not know which combinations of control intensities satisfying $c^m h^n = 1$ for coprime $m, n \in \mathbb{N}$ actually are bifurcation points and which ones are not. In that case, up to period 10, when fixing one of the control intensities a total of 31 potential bifurcation points would be obtained for the other control intensity in a unit interval. This would make it difficult to find a combination of control intensities with guarantees of placing the population away from any bifurcation point.

4.5   DISCUSSION AND CONCLUSIONS

In the analysis of CALC, sudden transitions in the dynamics of the managed populations are observed, which do not occur when only restocking or only harvesting are
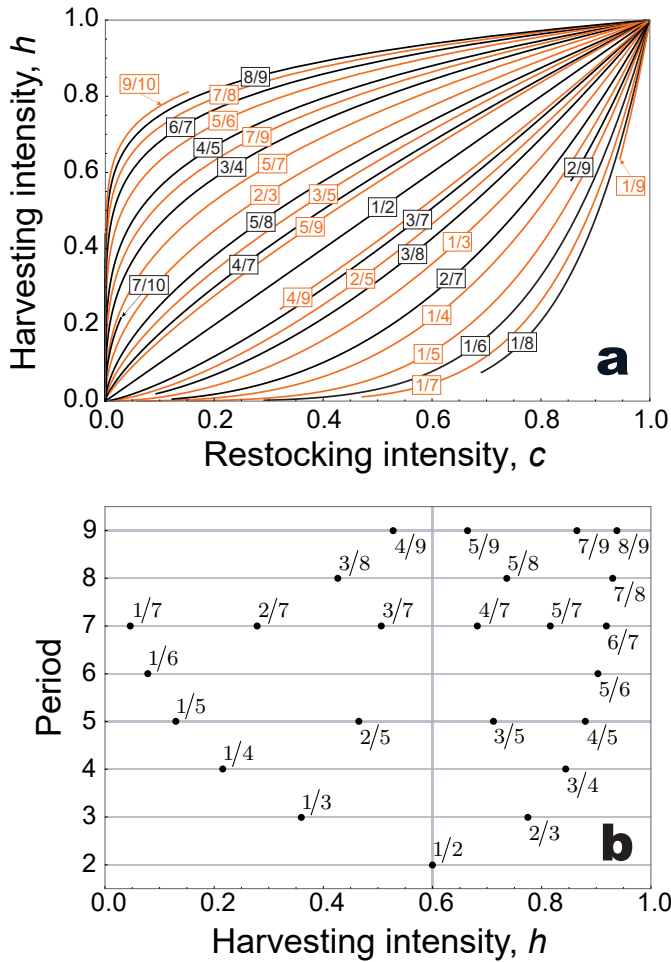
Figure 4.5: Period adding structure and its distribution of periods for CALC. (a) PAS of CALC. (b) Distribution of periods of the PAS of CALC for $c = 0.6$ and varying h. Each point is labeled in the form $m/(m+n)$, where m denotes the number of points of the cycles in $I_{\mathcal{L}}$ and n the number of points in $I_{\mathcal{R}}$. Both panels are based on the Hassell map $f(x) = \lambda x/(1+ax)^b$ with $\lambda = 1000$, $a = 0.05$ and $b = 50$. In panel (a) two colors are used to help distinguish different curves.
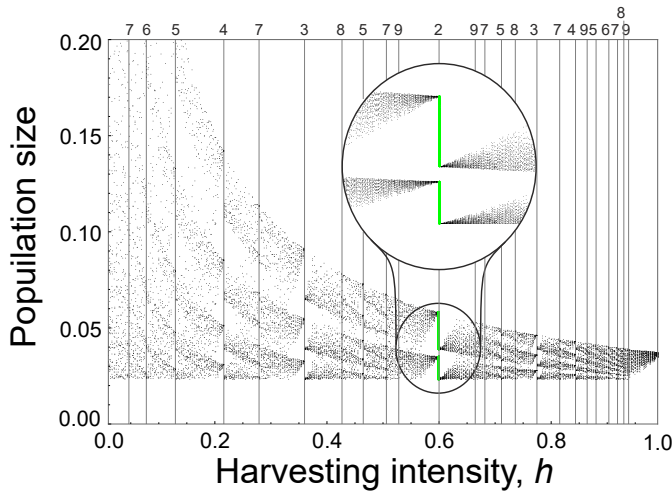
Figure 4.6: Bifurcation diagram for CALC with $c = 0.6$ and varying h for the Hassell map. For each value of h, black dots represent 30 iterates of the state variable for $f(x) = \lambda x / (1+ax)^b$ with $\lambda = 1000$, $a = 0.05$ and $b = 50$ after a transient of $10,000$ iterates with initial conditions obtained as pseudo-random real numbers in the interval $(0, f(d)]$. The vertical lines represent the harvesting intensities for which BCBs occur according to Corollary 4.2, and the numbers above them indicate the period of the cycles given by Proposition 4.4. For $h = 0.6$, iterates were obtained for $1,000$ different initial conditions, which are represented by green dots.

implemented. We have provided numerical simulations showing potential risks and opportunities associated with these abrupt changes in the dynamics. On the one hand, the number of individuals undergoes sudden jumps between different attractors that may seriously affect the stability and persistence of the population. On the other hand, these transitions are coupled with sharp changes in the type of control prevailing in the intervention (restocking or harvesting), which can seriously affect the yield and cost of exploitation as well as cause acute logistic problems.

The theoretical analysis of these phenomena leads to a mathematical problem concerning nonsmooth discrete dynamical systems. When the underlying dynamics are described by unimodal maps, we have shown that the production function of CALC

is piecewise continuous with two angular points that divide the state space into three intervals. This function is linear on the extreme partitions of its domain and is completely determined over them by the control intensities. The abrupt changes in the population dynamics are caused by the collision of periodic orbits lying in the outermost partitions of the state space with the break points of the CALC map. When only the external branches of this map are considered, it can be seen in terms of the control intensities as a biparametric family of bimodal PWL maps. We have shown that this family can be derived via certain parameter restrictions from a more generic six-parametric family of PWL maps, for which different bifurcation structures have been described in the literature [165, 166, 167]. Among these structures, the focus is on the so called period adding structure, since it corresponds to bifurcations involving events that occur only in the outermost partitions of the state space.

Similar considerations were previously done in [74] for another biparametric family of PWL maps. This family has in common with CALC that the maps are purely linear on the extreme partitions of their domain. An insightful description of the bifurcation structure of this family of maps was obtained in [74] by direct substitution of the parameter restrictions in the already known bifurcation structure for the generic six-parametric family of PWL maps. However, only partial results were obtained. We have shown that the imposition of the conditions for the homogeneity of the outermost branches of the map induces a degeneracy in the PAS that makes it impossible to relate the different structures via direct substitution of the parameter restrictions. We have proved that the inclusion of an additional condition involving the break points of the map resolves the indeterminacy in the PAS caused by this degeneracy. This allows to fully determine the PAS of any family of maps with the extreme branches purely linear, e.g., CALC or the family of maps considered in [74].

Examples of the application of these theoretical results to the determination and description of the PAS of CALC for some models common in population dynamics are provided. These examples show that the number of BCBs strongly depends on the pro-

duction function of the uncontrolled population, and thus the range of possibilities is wide.

We have also studied the degenerate BCBs that occur when homogeneity is imposed for the outermost branches of the map. We have proved that when parameters are varied through one of the bifurcation points, a continuum of cycles lying in the external partitions of the state space emerge and disappear afterwards. Moreover, we have obtained analytical results for the endpoints of the intervals filled by these cycles. These results are independent of the functional expression of the map in the middle partition of the domain, and thus are applicable to CALC with any unimodal growth model for the uncontrolled population. Numerical simulations reveal that the state variable abruptly shifts between different attractors that are connected by the continuum of cycles that exist at the bifurcation points.

Research line II

Harvest timing and global stability of one-dimensional discrete dynamical systems

A thing is right when it tends to preserve the integrity, stability and beauty of the biotic community. It is wrong when it tends otherwise.

Aldo Leopold

5

Dynamics of the discrete Seno population model: Combined effects of harvest timing and intensity on population stability

5.1 Introduction

The success of wildlife population management strongly depends on understanding the impact of harvest regulations on the capability of populations to renew themselves. The response of biological populations to the removal of individuals depends on many different aspects, such as the intensity of the control, i.e., the proportion of the population that is removed, the sex and age of the individuals that are taken, or the time of intervention. Since the population persistence can be completely conditioned by the harvest time, this factor plays a key role in the management and exploitation of biological populations and natural resources, especially for seasonally reproducing species [25, 117, 173, 185].

Many examples can illustrate the relevance of the moment of intervention in harvest programmes. In the case of large herbivores, populations are often managed during specified hunting seasons. More specifically, advancing the harvest of some migrating ungulate species has been proposed as a way to reduce the damage that they inflict on farmland and forest [144]. Another example is the management of greater sage-grouse (*Centrocercus urophasianus*) populations in North America. A major concern about the conservation of this species emerged years ago, and a certain controversy was created regarding the most appropriate moment for harvesting. Some recommendations advocated for reducing harvest of adult females and juveniles, and thus proposed delaying the harvest season in the year. Yet, recent studies have shown that this could be clearly counterproductive [25].

In light of the above, harvest timing is currently receiving an increasing attention. However, the existing literature has mostly focused on the population size [67, 84, 87, 117, 118, 191, 192, 202, 220] and few studies have analyzed the effects on the population stability. This motivated Cid *et al.* [44] to use a model proposed by Seno [191] to study the effect of harvest timing on both the size and stability of populations. Seno's model is given by a single one-dimensional difference equation based on constant effort harvesting (also known as proportional feedback) that allows for the consideration of any moment during the reproductive season for the intervention. When harvesting occurs at the beginning or at the end of the reproductive period, two topologically conjugated systems are obtained. For these systems, removing individuals can create an asymptotically stable positive equilibrium which acts as a global attractor under certain conditions [38, 43]. On the contrary, if the harvesting intensity is too high, populations starting with any initial size go eventually extinct [141]. Interestingly, when individuals are removed at an intermediate moment during the reproductive season, the stability properties of Seno's model are not so well understood.

Cid *et al.* [44] proved that for any intervention time the system has a unique positive equilibrium if the intervention effort is below a certain threshold. Moreover, the origin acts as a global attractor when that threshold is reached or exceeded. Regarding the

asymptotic stability of the positive fixed point, they obtained sharp global results for the quadratic map and a sufficient local condition for the Ricker map. This last condition states that the positive equilibrium of the Ricker-Seno model is asymptotically stable for any harvest time if harvesting at the beginning of the reproductive season guarantees stability. These results, together with numerical simulations, led Cid *et al.* [44] to conjecture that the sufficient condition proved for the Ricker-Seno model is true for any other population model described by a unimodal map.

In this chapter, we show that the moment of the intervention does not affect the stability of controlled populations when the harvesting effort is high. Moreover, we prove that for high removal intensities—below the threshold above which all populations go eventually extinct—the positive equilibrium acts as a global attractor. This result is valid for a wide family of population models described by unimodal maps and, in particular, it implies that the aforementioned conjecture in [44] is true for high harvesting intensities.

We use the Ricker-Seno model to prove that timing can be stabilizing by itself. In other words, we show that in some cases choosing an appropriate moment for removing individuals can induce an asymptotically stable positive fixed point in populations for which the same equilibrium would be unstable in case of triggering the intervention at the beginning or at the end on the reproductive season. Interestingly, timing can be destabilizing for certain maps satisfying the general conditions assumed on population production maps in [44]. We obtain specific mathematical counterexamples proving that the Conjecture 3.5 in [44] is false. Nevertheless, the implications of this destabilizing effect of timing should be considered carefully because most of the population maps considered in the ecological literature satisfy extra conditions, which could prevent this destabilizing effect to occur.

This chapter is organized as follows. In Section 5.2 we describe Seno's model and collect the conditions assumed on the population models. Section 5.3 shows that timing does not affect stability for high harvesting efforts. In Section 5.4 we show that timing can have both a stabilizing and a destabilizing effect. Section 5.5 includes biological re-

alities to check the robustness of our results. Finally, Section 5.6 summarizes the results obtained and discusses their implications and limitations.

5.2   Harvesting model with timing

Consider the discrete-time single-species population model

$$x_{t+1} = g(x_t)x_t, \tag{5.1}$$

where $x_t \in [0, +\infty)$ is the population size at the beginning of the reproductive season t and $g \colon [0, +\infty) \to \mathbb{R}$ is the per-capita production function. It is well established that harvesting a constant fraction $\gamma \in (0, 1)$ of the population at the end of every reproductive season corresponds to multiplication of the right hand side of (5.1) by the survival fraction $(1 - \gamma)$,

$$x_{t+1} = (1 - \gamma)g(x_t)x_t. \tag{5.2}$$

On the other hand, harvesting the same fraction at the beginning of the season leads to

$$x_{t+1} = g((1 - \gamma)x_t)(1 - \gamma)x_t, \tag{5.3}$$

that is, multiplies the population size x_t by the survival fraction $(1 - \gamma)$. As usual in the literature, we refer to parameter γ as harvesting effort or harvesting intensity. Note that harvesting at the beginning of the season corresponds to an application of the proportional feedback chaos control method proposed in [92] to (5.1).

In [191], Seno puts forward the following harvesting model, which encompasses the *limit* situations (5.2) and (5.3) by allowing the population to be harvested at any fixed point in time within the season. It reads

$$x_{t+1} = [\theta g(x_t) + (1 - \theta)g((1 - \gamma)x_t)](1 - \gamma)x_t, \tag{5.4}$$

where $\theta \in [0, 1]$ corresponds to the fixed harvesting moment. Model (5.4) assumes that the reproductive success at the end of the season depends on the amount of energy accumulated during it. Since the per-capita production depends on x_t before θ and on $(1 - \gamma)x_t$ afterwards, it is natural to assume that the population production is proportional to the time period before/after harvesting to arrive at (5.4). See [191, 192] for a more detailed explanation and a graphical scheme of the population dynamics of this model.

Following the notation of [44], we rewrite the right-hand side of (5.4) as

$$\theta F_1(x_t) + (1 - \theta)F_0(x_t) := F_\theta(x_t),$$

where $F_1(x) := (1 - \gamma)g(x)x$ and $F_0(x) := g((1 - \gamma)x)(1 - \gamma)x$. For every particular choice of $\theta \in [0, 1]$ the map $F_\theta(x)$ is the convex combination of the maps defining (5.2) and (5.3). Consequently, model (5.4) includes models (5.2) and (5.3) as special cases. Taking $\theta = 1$ corresponds to harvesting when the season ends, and $\theta = 0$ when it begins.

In this chapter, we are interested in populations satisfying the following conditions on g:

(i) $g'(x) < 0$ for all $x > 0$;

(ii) $g(0) > 1$;

(iii) $\lim_{x \to +\infty} g(x) = \delta < 1$;

(iii)' there exists some $d > 0$ such that $xg(x)$ is strictly increasing on $(0, d)$ and strictly decreasing on $(d, +\infty)$.

Biologically speaking, condition (i) states that the dynamics are compensatory, i.e., any increase in the population size in a generation is followed by an increase in mortality in the next generation. Condition (ii) is equivalent to $\frac{d}{dx}(xg(x))(0) > 1$, which implies that $xg(x)$ is above $y = x$ around $x = 0$. Therefore, the population grows for

small population sizes. Condition (iii)' means in particular that $xg(x)$ is a unimodal map, and implies (iii) with $\delta = 0$ — here (iii) is introduced just for easy reference to [44]. With these conditions, the system has two fixed points $x = 0$ and $x = K > 0$, and the asymptotic dynamics are overcompensatory [46]: for x large, any increase in the population size is exceeded in magnitude by the corresponding increase in mortality in the following generation, and thus the population function $xg(x)$ decreases.

Overcompensatory models can exhibit positive unstable equilibria, which leads to fluctuating dynamics [154]. Since we are interested in the combined effect of harvesting timing and harvesting effort on the stability properties of the positive equilibrium, we recall a sufficient and necessary condition for the existence of such an equilibrium regardless of the intervention moment θ.

Proposition 5.1 (from Proposition 3.1 in [44]). *Assume that conditions (i)-(iii) hold. System (5.4) has a unique positive equilibrium (denoted by $K_\gamma(\theta)$) if and only if*

$$\gamma < \gamma^* := 1 - \frac{1}{g(0)}.$$

5.3 TIMING DOES NOT AFFECT STABILITY FOR HIGH HARVESTING EFFORTS

In this section, we show that the asymptotic stability of $K_\gamma(0)$ implies the asymptotic stability of $K_\gamma(\theta)$ for $\theta \in [0, 1]$ if γ is chosen close enough to γ^* and g satisfies conditions (i)-(iii)'. Moreover, we obtain that $K_\gamma(\theta)$ is globally asymptotically stable, i.e., it attracts all solutions of (5.4) starting with a positive initial condition.

Theorem 5.2. *Assume that conditions (i)-(iii)' hold. Then, there exists $\gamma_0 < \gamma^*$ such that for $\gamma \in [\gamma_0, \gamma^*)$ the fixed point $K_\gamma(\theta)$ of (5.4) is asymptotically stable for all $\theta \in [0, 1]$ and all positive solutions of (5.4) converge to $K_\gamma(\theta)$.*

Proof. Our aim is to prove that the fixed point $K_\gamma(\theta)$ of F_θ attracts all positive solutions of (5.4), provided that γ is sufficiently close to γ^*. We do this by showing that $x <$

$F_\theta(x) < K_\gamma(\theta)$ for all $x \in (0, K_\gamma(\theta)))$ and $F_\theta(x) < x$ for all $x > K_\gamma(\theta)$; see [31, Lemma 1].

A simple calculation yields that $\frac{dF_\theta}{dx}(0) = F'_\theta(0) = (1-\gamma)g(0)$ and so, by Proposition 5.1 and condition (ii), $F'_\theta(0) > 1$ for every $\theta \in [0,1]$ and every $\gamma \in [0, \gamma^*)$. Together with the uniqueness of the positive fixed point (see Proposition 5.1) it now follows that

$$F_\theta(x) > x, \quad x \in (0, K_\gamma(\theta)),$$

for every $\theta \in [0,1]$ and every $\gamma \in [0, \gamma^*)$.

Next, the inequality $x > F_\theta(x)$ for all $x > K_\gamma(\theta)$ follows from the uniqueness of the positive fixed point and the fact that, by condition (iii)', $xg(x) < x$ for $x > K$. It is then immediate that $F_0(x) = (1-\gamma)(xg(x)) < (1-\gamma)x < x$ for $x > K$. For x large enough, $(1-\gamma)x > K$, and thus $F_1(x) = ((1-\gamma)x)g((1-\gamma)x) < (1-\gamma)x < x$. This yields $F_\theta(x) < x$ for large x.

To finish the proof, we will show that there exists $\gamma_0 < \gamma*$ such that F_θ is strictly increasing on the interval $[0, K_\gamma(\theta))$ for $\gamma \in [\gamma_0, \gamma^*)$. This combined with $K_\gamma(\theta)$ being a fixed point of F_θ implies, for every $\theta \in [0,1]$ and $\gamma \in [\gamma_0, \gamma^*)$, that $F_\theta(x) < K_\gamma(\theta)$ for $x \in (0, K_\gamma(\theta))$.

Since $F'_0(x) = F'_1((1-\gamma)x)$, the graph of F'_0 is the graph of F'_1 horizontally stretched by a factor $1 - \gamma$; see Figure 5.1. For $\gamma < \gamma^*$, both graphs are above the horizontal axis near $x = 0$. Therefore, $F'_1(x) < F'_0(x)$ around $x = 0$. On the other hand, $F'_\theta(x) = \theta F'_1(x) + (1-\theta)F'_0(x)$, implying that $0 < F'_1(x) \leq F'_\theta(x) \leq F'_0(x)$ around $x = 0$.

Let $C_\gamma(\theta)$ denote the first zero of F'_θ. Note that this zero exists because F_1 and F_0 inherit the unimodal character of $xg(x)$ assumed in condition (iii)'. Indeed, for F'_0 and F'_1 this zero is unique and corresponds to $C_\gamma(1) = d$ and $C_\gamma(0) = \frac{d}{1-\gamma}$, respectively.

From the above discussion, we have that

$$C_\gamma(1) \leq C_\gamma(\theta) \leq C_\gamma(0). \tag{5.5}$$
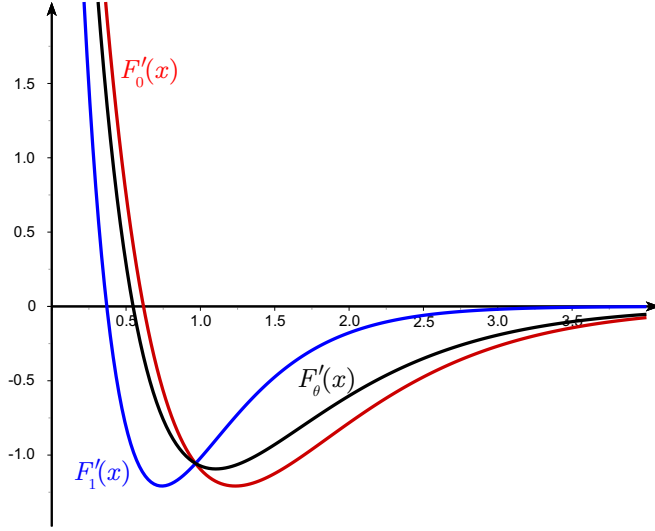
Figure 5.1: Derivatives of F_1, F_0 and F_θ. For $g(x) = e^{2.7(1-x)}$, $\gamma = 0.4$ and $\theta = 0.3$, the blue curve corresponds to F_1', the red curve to F_0' and the black curve to F_θ'.

We want to find conditions on the parameters guaranteeing that F_θ is increasing until $K_\gamma(\theta)$, i.e., $F_\theta'(x) > 0$ for all $x < K_\gamma(\theta)$. This is equivalent to impose $K_\gamma(\theta) \leq C_\gamma(\theta)$, and a sufficient condition for this is $K_\gamma(0) \leq C_\gamma(1)$. This is true because (5.5) and Proposition 3.2 in [44] yield $K_\gamma(\theta) \leq K_\gamma(0) \leq C_\gamma(1) \leq C_\gamma(\theta)$. Since $xg(x)$ is increasing on $(0, d)$, it follows that the map $j\colon [\max\{0, 1 - \frac{1}{g(d)}\}, \gamma^*) \to [0, g(d)]$ given by $j(\gamma) = K_\gamma(0)$ is strictly decreasing and satisfies $\lim_{\gamma \to \gamma^*} j(\gamma) = 0$. Hence, there exists a unique $\gamma_0 \in [\max\{0, 1 - \frac{1}{g(d)}\}, \gamma^*)$ such that $K_\gamma(0) \leq C_\gamma(1)$ for all $\gamma \geq \gamma_0$.

Finally, by construction we have that $\gamma_0 = 0$ or $K_{\gamma_0}(0) = C_{\gamma_0}(1) = d$. Since $K_{\gamma_0}(0)$ is the unique fixed point of F_0, then γ_0 is the unique solution of

$$g((1 - \gamma_0)d) = \frac{1}{1 - \gamma_0}$$

in the interval $[\max\{0, 1 - \frac{1}{g(d)}\}, \gamma^*)$. □

It is well known that harvesting can induce stability for the positive equilibrium of systems satisfying conditions (i)-(iii)', see e.g. [141]. Theorem 5.2 provides a threshold γ_0 in the removal intensity above which the positive equilibrium becomes a global attractor. The previous proof shows how to calculate γ_0, and we will illustrate this for two well known population models, namely the Hassell and the Ricker models. The per-capita production function of the former is $g(x) = \lambda(1 + a\,x)^{-b}$, where $\lambda, a, b > 0$. This model satisfies conditions (i)-(iii)' for $\lambda > 1$ and $b > 1$. In the absence of harvesting, the positive equilibrium $K = (\lambda^{\frac{1}{b}} - 1)/a$ is unstable for $b > 2$ and $\lambda > (b/(b-2))^b$. In this model, $d = 1/(a(b-1))$ and γ_0 is either null or the unique solution of

$$\lambda = \frac{1}{1-\gamma}\left(\frac{b-\gamma}{b-1}\right)^b. \tag{5.6}$$

For fixed b, the function $k(\gamma)$ given by the right-hand side of (5.6) is strictly increasing and satisfies $k \to (b/(b-1))^b$ for $\gamma \to 0$ and $k \to +\infty$ for $\gamma \to 1$. Hence, for $\lambda > (b/(b-1))^b$ the value $\gamma_0 > 0$ is implicitly given by $k(\gamma_0) = \lambda$, and $\gamma_0 = 0$ otherwise. For $\lambda = 7.7$ and $b = 50$, we obtain $\gamma_0 \approx 0.848$ and $\gamma^* \approx 0.870$. Thus, for any $\gamma \in [0.848, 0.870)$ the positive equilibrium $K_\gamma(\theta)$ is stabilized by the effect of harvesting and acts as a global attractor for all $\theta \in [0, 1]$. This can be appreciated in Figure 5.2.

In the case of the Ricker model, the per-capita production function is $g(x) = e^{r(1-x)}$, with $r > 0$. Conditions (i)-(iii)' are met for all $r > 0$. Proposition 3.4 in [44] guarantees for this model that the positive equilibrium $K_\gamma(\theta)$ of (5.4) with $\theta \in [0, 1]$ is asymptotically stable if $1 - e^{2-r} < \gamma < 1 - e^{-r}$. The curves defined by these inequalities delimit a region in the (r, γ)-parameter space shown in Figure 5.3. Theorem 5.2 provides a subregion for which the positive equilibrium is indeed a global attractor. In this case, $d = \frac{1}{r}$ and γ_0 is either zero or the unique solution of

$$r = 1 - \ln(1 - \gamma) - \gamma. \tag{5.7}$$
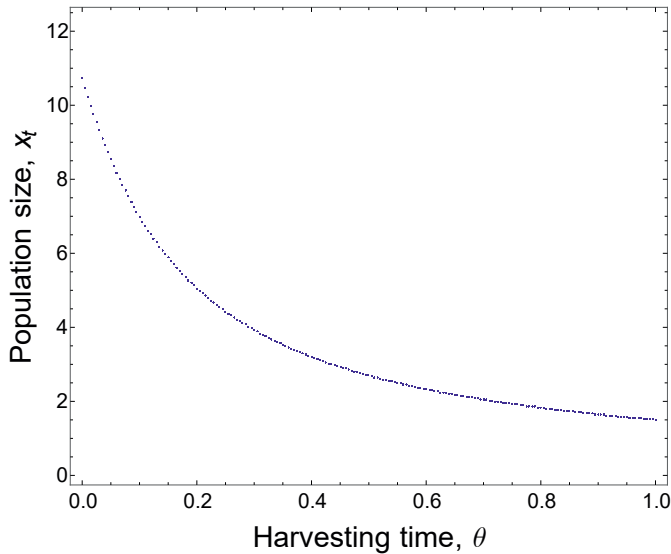
Figure 5.2: Bifurcation diagram for the Hassell-Seno model in terms of the harvest time. The underlying population dynamics is given by the Hassell map $g(x) = 7.7(1 + 10^{-3} \cdot x)^{-50}$, and the harvesting effort is $\gamma = 0.86$.

The function $h(\gamma) = 1 - \ln(1 - \gamma) - \gamma$ is strictly increasing and verifies $h \to 1$ for $\gamma \to 0$ and $h \to +\infty$ for $\gamma \to 1$. Hence, for $r > 1$ the value $\gamma_0 > 0$ is implicitly given by $h(\gamma_0) = r$, and for $r \in (0, 1]$, $\gamma_0 = 0$. The blue region in Figure 5.3 corresponds to the subregion in the (r, γ)-parameter space defined by this curve.

5.4 STABILITY DEPENDING ON TIMING

5.4.1 TIMING CAN BE STABILIZING

In this subsection, se study under which conditions timinig can be stabilizing by itself. The Ricker model has been shown to be a good descriptor of the dynamics of many populations (including bacteria, fungi, ciliates, crustaceans, fruit flies, and fishes [183]), which makes the study of the stability properties of the Ricker-Seno model appealing.
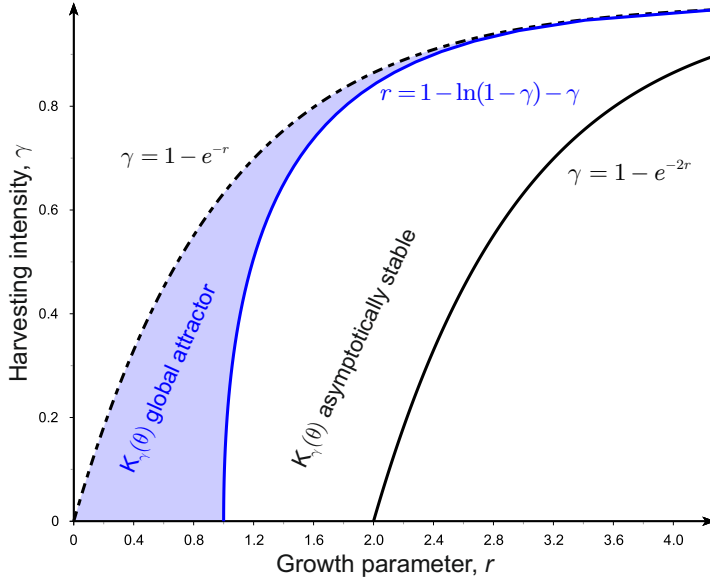
Figure 5.3: Global stability of the Ricker-Seno model for high harvesting efforts. Parameters inside the region between the black curves guarantee that $K_\gamma(\theta)$ is asymptotically stable for all $\theta \in [0, 1]$ for (5.4) in the Ricker case. The blue area specifies the region in the (r, γ)-parameter space for which Theorem 5.2 guarantees the global attraction of the positive equilibrium.

For this model, we prove that it is possible to find $\theta \in (0, 1)$ such that $K_\gamma(\theta)$ for (5.4) is stable when $K_\gamma(0)$ is unstable.

Proposition 5.3. *Assume $g(x) = e^{r(1-x)}$ and $r > 0$. Then, there exists $\gamma_c < \gamma_* :=$ $1 - e^{2-r}$ such that for any $\gamma \in (\gamma_c, \gamma_*)$ it is possible to find a timing interval (θ_0, θ_1) with the property that for each $\theta \in (\theta_0, \theta_1)$ the fixed point $K_\gamma(\theta)$ is asymptotically stable for (5.4).*

Proof. Differentiating, we obtain $F_1''(x) = (1 - \gamma)r(2 - rx)e^{r(1-x)}$, and thus F_1' is strictly decreasing to the left of $2/r$ and strictly increasing to the right. On the other hand, it is easy to check that for $\gamma = \gamma_*$ the fixed point of F_1 coincides with the above

inflection point (i.e., $K_{\gamma_*}(1) = 2/r$), and $F_1'(K_{\gamma_*}(1)) = -1$. In that case, $F_1'(x) \geq -1$ for all x.

The equalities

$$F_0(x) = F_1((1-\gamma)x)/(1-\gamma),$$
$$F_0'(x) = F_1'((1-\gamma)x),$$
$$F_0''(x) = (1-\gamma)F_1''((1-\gamma)x),$$

yield similar conclusions regarding F_0: the unique inflection point (equal to $2/(r(1-\gamma)))$ coincides with the fixed point $K_{\gamma_*}(0)$, and moreover $F_0'(K_{\gamma_*}(0)) = -1$.

For $\gamma < \gamma_*$, the fixed points $K_\gamma(0)$ and $K_\gamma(1)$ are unstable (see Proposition 3.3 in [44]) and the sets $(F_0')^{-1}(-1)$ and $(F_1')^{-1}(-1)$ contain two points (in addition to the mentioned monotonicity properties for F_1', note that $F_1'(0^+) = (1-\gamma)e^r$ and $F_1'(x) \to 0$ as $x \to +\infty$). Let denote $a = \max\{(F_1')^{-1}(-1)\}$ and $b = \min\{(F_0')^{-1}(-1)\}$. It is immediate that $a > K_\gamma(1)$ and $b < K_\gamma(0)$ because $F_0'(K_\gamma(0))$ and $F_1'(K_\gamma(1))$ are less than -1. By continuity, for $\gamma \uparrow \gamma_*$ we have

$$\max\left\{K_\gamma(1), \frac{2}{r}\right\} < a < b < \min\left\{K_\gamma(0), \frac{2}{r(1-\gamma)}\right\}. \qquad (5.8)$$

The inflection point of F_1 does not depend on γ, whereas the one of F_0 decreases as γ increases. For $\gamma \to 0$ both points coincide and hence, by continuity, there must exist some $\gamma < \gamma_*$ for which $a = b$. Let γ_c be the maximal value of γ satisfying this last condition. It is immediate that (5.8) is met for all $\gamma \in (\gamma_c, \gamma_*)$. Since F_1' is strictly increasing to the right of $2/r$ and F_0' is strictly decreasing to the left of $2/(r(1-\gamma))$, we conclude that $F_1'(x) > -1$ and $F_0'(x) > -1$ for all $x \in (a, b)$. This leads to $F_\theta'(x) > -1$ because F_θ' is a convex combination of F_0' and F_1'.

The fixed point $K_\gamma(\theta)$ strictly decreases and continuously covers $[K_\gamma(1), K_\gamma(0)] \supset (a, b)$ for varying θ. Hence, there must exist $\theta_0, \theta_1 \in (0, 1)$ such that $K_\gamma(\theta_0) = b$ and $K_\gamma(\theta_1) = a$. In particular, $K_\gamma(\theta) \in (a, b)$ for all $\theta \in (\theta_0, \theta_1)$, and thus $F_\theta'(K_\gamma(\theta)) > -1$. $\qquad \square$
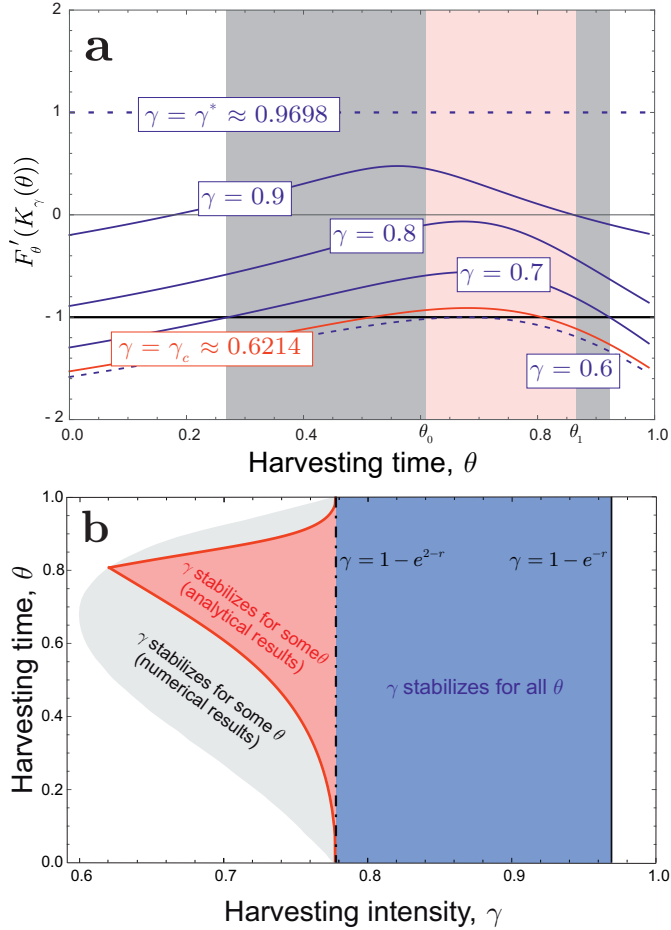
Figure 5.4: Stabilizing harvest times for the Ricker-Seno model. (a) Stability of the positive equilibrium of (5.4) in terms of the harvesting time $\theta \in [0, 1]$ for different values of the removal intensity γ. The positive equilibrium $K_\gamma(\theta)$ is stable if $-1 < F'_\theta(K_\gamma(\theta)) < 1$. The gray area corresponds to the actual range of stabilizing harvest times for $\gamma = 0.7$, and the red area to the range $[\theta_0, \theta_1]$ derived from Proposition 5.3. (b) The gray region shows numerical results for the combinations of γ and θ for which $K_\gamma(0)$ is unstable and $K_\gamma(\theta)$ is asymptotically stable. The red region corresponds to values guaranteed to be stabilizing (by Proposition 5.3). In both panels, the underlying population dynamics are given by the Ricker map $g(x) = e^{3.5(1-x)}$.
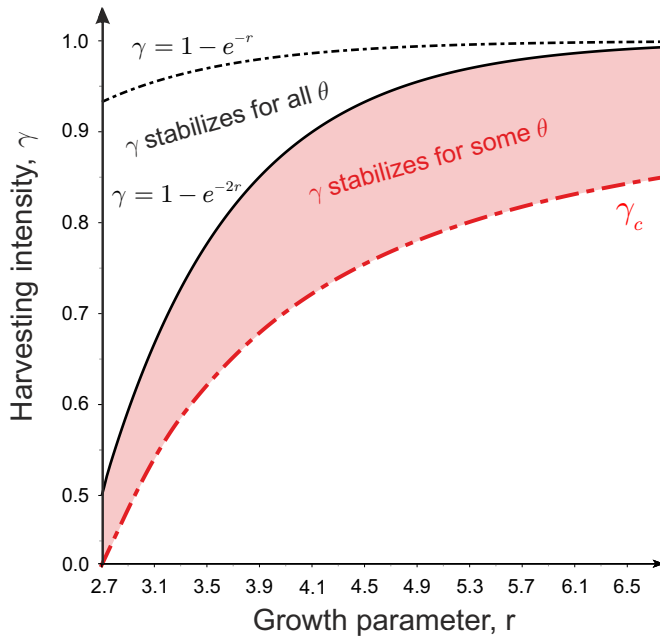
Figure 5.5: Stabilization of the Ricker-Seno model via delayed harvesting. The red region corresponds to harvesting intensities γ that are destabilizing for a given growth parameter r when individuals are removed at the beginning or at the end of the reproductive season and for which there exists a stabilizing harvesting time θ according to Proposition 5.3.

For fixed values of the growth parameter r, the proof of Proposition 5.3 yields a method for determining a range of removal intensities γ for which there exist harvest moments θ that stabilize the positive equilibrium $K_\gamma(\theta)$. Moreover, for a fixed γ it also provides a method for determining a range of stabilizing times $\theta_0 \leq \theta \leq \theta_1$. We illustrate this for the growth parameter $r = 3.5$, for which the limit of population persistence is $\gamma^* = 1 - e^{-3.5} \approx 0.9698$. Numerical simulations reveal that $\gamma_c \approx 0.6214$, and thus Proposition 5.3 guarantees the existence of stabilizing harvest times for all $\gamma \in [0.6214, 0.9698)$. Figure 5.4a shows that this range is quite accurate: there are no stabilizing times for harvesting efforts slightly below γ_c. Consider the control intensity $\gamma = 0.7 \in [\gamma_c, \gamma^*)$. It can be numerically found that $\theta_0 \approx 0.6086$ and

$\theta_1 \approx 0.8611$. The red area in Figure 5.4a corresponds to this range, and the gray area represents the actual range of times that stabilize $K_\gamma(\theta)$. Compared to the range of harvesting efforts, the range of stabilizing intervention moments given by Proposition 5.3 seems to be more conservative. However, this range is wide enough to allow for the determination of stabilizing harvest times with reasonable certainty. Figure 5.4b shows the actual range of these times and the range defined by Proposition 5.3 in terms of the removal intensity γ.

Finally, we emphasize that Proposition 5.3 implies that harvest timing can be very useful from a practical point of view since it can be used to significantly enlarge the range of harvesting efforts that are able to stabilize the population for a fixed r (see Figure 5.5).

5.4.2 TIMING CAN BE DESTABILIZING

In the previous subsection, we have seen that timing can be stabilizing by itself. In view of this, it is logical to ask the opposite question: *can timing be destabilizing?* Based on both numerical simulations and analytical results, Cid *et al.* conjectured in [44] that harvesting times θ in the interior of $[0, 1]$ cannot be destabilizing if conditions (i)-(iii)' are satisfied.

Conjecture 5.4 (Conjecture 3.5, [44]). *Assume that conditions (i)-(iii)' hold. If the positive equilibrium $K_\gamma(0)$ of (5.4) with $\theta = 0$ is asymptotically stable, then the fixed point $K_\gamma(\theta)$ is asymptotically stable for (5.4) for all $\theta \in [0, 1]$.*

Suppose that $K_\gamma(0)$ is asymptotically stable. If Conjecture 5.4 was true, then we could delay the time of intervention $\theta \in [0, 1]$ without affecting the stability of the positive equilibrium $K_\gamma(\theta)$. This freedom to choose the time of intervention is clearly desirable from a management point of view. However, the conjecture is false. We provide a counterexample. To build it, we use the map $h \colon [0, 1] \to [0, 1]$ defined by

$$h(x) = x \left(\frac{786}{100} - \frac{2331}{100}x + \frac{2875}{100}x^2 - \frac{133}{10}x^3 \right).$$
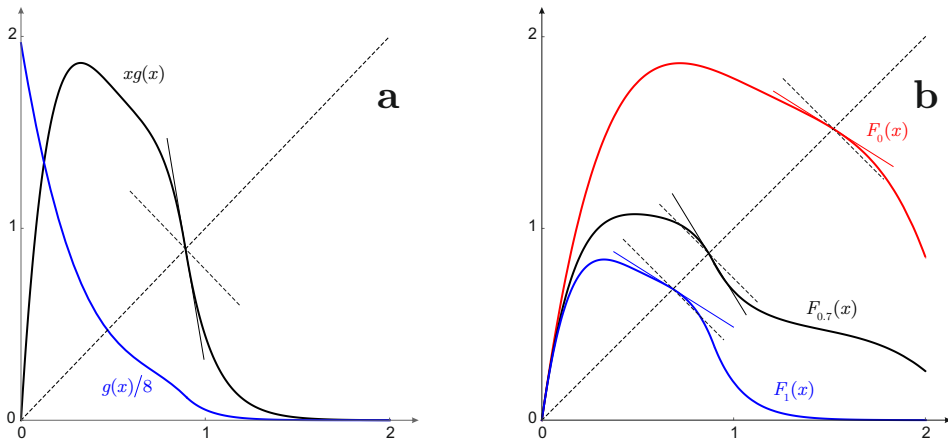
Figure 5.6: Harvest timing can destabilize the positive equilibrium. (a) The blue curve corresponds to the graph of $g(x)$, which was vertically compressed by a factor $1/8$ to improve the representation; the black curve corresponds to the graph of $xg(x)$, showing that this map satisfies (iii)' and has an unstable positive fixed point. (b) The blue, red and black curves correspond to the graphs of $F_1(x)$, $F_0(x)$ and $F_{0.7}(x)$, respectively. The harvesting effort is fixed to $\gamma = 0.55$. Observe that $K_{0.5}(0)$ is asymptotically stable whereas $K_{0.5}(0.7)$ is unstable.

This map was introduced in [194] as an example of unimodal map with negative Schwarzian derivative having two attractors. Now, we define $g \colon [0, +\infty) \to [0, +\infty)$ by

$$g(x) = \begin{cases} 2\dfrac{h(x)}{x}, & x \in [0, \tfrac{9}{10}), \\ \dfrac{591}{625}e^{-\frac{57397}{7500}\left(x - \frac{9}{10}\right)}, & x \in \left(\tfrac{9}{10}, +\infty\right). \end{cases} \tag{5.9}$$

We note that at the break point $9/10$ the function g is differentiable.

It is not hard to see that the map g satisfies conditions (i)-(iii)', see Figure 5.6a. Moreover, system (5.1) has an unstable positive equilibrium, see Figure 5.6a.

Next, we fix $\gamma = 0.55$. Figure 5.6b shows that this harvesting effort applied at the beginning or at the end of the reproductive season stabilizes a fixed point. Thus, the positive equilibrium $K_\gamma(0)$ is asymptotically stable for $\theta = 0$. However, for $\theta = 0.7$ the convex combination of F_1 and F_0 crosses the diagonal with slope greater than 1 in

absolute value (see Figure 5.6b). Thus, the positive equilibrium is unstable for $F_{0.7}$. The explanation for this effect is as follows. For this map, the intensity of the overcompensation abruptly increases for certain interval of population sizes. This makes the graph of $xg(x)$ to have a steep negative slope in that interval and such a slope is inherited by the graph of F_1, although attenuated by a $(1 - \gamma)$ factor. Since F'_θ is the convex combination of F'_1 and F'_0, when the positive equilibrium $K_\gamma(\theta)$ is in the interval where $F'_1 \ll -1$ we can have that $F'_\theta < -1$.

Actually, a bifurcation diagram taking θ as the bifurcation parameter shows that delaying the harvesting time θ leads to the emergence of bubbles (see [143, Definition 3]). This is illustrated in Figure 5.7. We point out that bubbles for (5.4) were studied in [44], but with a different approach. There it was numerically shown for the Clark-Ricker bimodal map that bubbles related to a variation in the harvesting effort for $\theta = 0$ disappear when harvesting occurs at an intermediate moment of the season, thereby demonstrating that intermediate harvesting times can have a stabilizing effect. Here, however, the bubble is related to a variation in the harvesting time θ for a unimodal map and implies that intermediate harvesting times can have a destabilizing effect.

The counterexample of Conjecture 5.4 given by (5.9) corresponds to a piecewise function obtained by extending the function $\frac{2h(x)}{x}$ to $[0, +\infty)$. We highlight that this fact has no influence on the result: the tail of the per-capita production function does not affect the stability of the positive equilibrium. On the other hand, the counterexample to Conjecture 5.4 is by non means unique. Indeed, for the analytic function

$$g(x) = e^{6 - 15x + 15x^2 - \frac{11}{2}x^3}, \qquad (5.10)$$

we have that $\frac{dF_{0.6}}{dx}(K_{0.5}(0.6)) = F'_{0.6}(K_{0.5}(0.6)) \approx -1.27786$ while $F'_0(K_{0.5}(0)) = F'_1(K_{0.5}(1)) \approx -0.206984$, and so this function provides another counterexample to Conjecture 5.4.
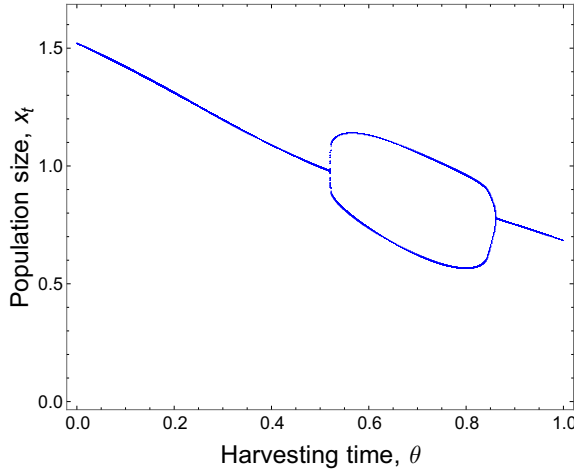
Figure 5.7: Delayed harvest can induce the emergence of bubbles. Bifurcation diagram of the population model (5.4) for varying harvesting time $\theta \in [0, 1]$. The harvest effort is fixed to 0.55, and the underlying population dynamics are described by (5.9). The positive equilibrium is asymptotically stable for $\theta = 0$ and $\theta = 1$, but for an interval of values of $\theta \in (0, 1)$ this positive equilibrium is unstable because of the presence of a bubble.

5.5 INTRODUCING BIOLOGICAL REALITIES

So far, we have analyzed how changing harvest times can affect the stability of populations described by theoretical deterministic equations. In this section, we check the robustness of our results on more realistic models. To this end, we consider the parameter estimates obtained in [63] on the basis of time series data for laboratory populations of the fruit fly *Drosophila melanogaster*. The per-capita production function is $g(x) = e^{r(1-x/K)}$, which corresponds to the non-scaled Ricker model with carrying capacity K and growth parameter r. For the different populations, the estimated growth parameter ranged from 2.7 to 3.0 (see [63], Supplementary material). We fix r in the midpoint of this range, i.e., $r = 2.85$, and the carrying capacity at $K = 60$.

We extend the above model by introducing two biological realities. The first of them is lattice effect. Individuals always come and are harvested in whole numbers and, as

previously said, the dynamics of a discrete-state system can be quite different from its continuous-state version [102]. Consequently, we integerize population sizes to make the model more realistic. The second extension to be considered is stochasticity. This is clearly more problematic, since stabilizing an equilibrium under the effect of noise is not possible unless the magnitude of the noise tends to zero as time grows. We follow the work of Braverman *et al.* [32] to generalize the notion of global stability to stochastic systems: equilibria of stochastic difference equations (blurred equilibrium) are points for which all trajectories eventually enter some interval around them. Since stochasticity is in many cases involved in the control, we propose a integerized stochastic version of (5.4) based on introducing noise in the removal intensity in the form

$$x_{t+1} = \text{int}([\theta g(x_t) + (1 - \theta)g((1 - \gamma + \sigma v_{t+1})x_t)](1 - \gamma + \sigma v_{t+1})x_t),$$
(5.11)

where σ is a parameter measuring the level of noise and $(v_t)_{t \in \mathbb{N}}$ is a sequence of independent random variables uniformly distributed in $[-1, 1]$, whereas function $\text{int}(x)$ gives the integer closest to x (if $x + 0.5 \in \mathbb{N}$, then $\text{int}(x)$ gives the even integer closest to x).

Figure 5.8a shows that the positive equilibrium of (5.4) for any intervention time θ is a global attractor for $\gamma = 0.6$, and that the same point is a blurred equilibrium of (5.11). We conclude therefore that the stabilization of populations induced by harvesting at intermediate moments during the reproductive season is robust under the effect of both noise and lattice effect. Interestingly, we observe that timing helps to damp the destabilizing effect of noise: the range of fluctuation of the population size can be significantly reduced if the intervention is conveniently delayed.

We can go further and analyze how timing can be helpful to stabilize the population size in the presence of noise around a specific value, for instance $x^* = 60$. Theorem 3.5 in [32] guarantees that if harvesting is implemented at the beginning of the reproductive season ($\theta = 0$) with an intensity $\gamma(x^*) \approx 0.9292$, the size of the population governed by the non-integerized version of (5.11) is stabilized around $x^* = 60$ with

a fluctuation range that depends on the level of noise. Numerical simulations reveal that for $\gamma = 0.6$ and $\theta = 0.6688$ the point $x^* = 60$ is a global attractor of the deterministic system (5.4). Figure 5.8b shows that the population governed by the integerized stochastic equation (5.11) is also stabilized around this point. This confirms again that the stabilizing properties of timing are not affected by neither stochasticity nor lattice effect. Moreover, we observe that stabilizing the population with delayed intervention has several advantages. Firstly, the proportion of individuals to be removed in each generation is significantly lower. This is expected to allow for the stabilization of populations that would be impossible to control due to practical limitations in case of being harvested at the beginning of the reproductive period. Secondly, the intensity of the intervention places the population far from the extinction risk associated with harvesting efforts above the persistence limit $\gamma^* \approx 0.9421$. Finally, when individuals are removed at an intermediate moment during the reproductive season, the fluctuation in the population size is lower than if they were harvested at the beginning of this period. This last fact can be evaluated in terms of the fluctuation index (see Section 1.2). We have averaged the FI over 500 time series of length 1000 with initial conditions chosen as pseudo-random numbers in $(0, dg(d)]$, ignoring the first 100 steps. If individuals are harvested with an intensity $\gamma = 0.9292$ at the beginning of the season, the FI is 0.111. If the intervention takes place at a time $\theta = 0.6688$ during the season with an intensity $\gamma = 0.6$, the FI decreases to 0.050. This is consistent with what was observed in Figure 5.8a: a delay in the intervention can reduce the fluctuations in size around the equilibrium.

5.6 Discussion and conclusions

In this chapter, we have studied the combined effect of harvesting intensity and harvesting time on the stability of a discrete population model proposed by Seno [191]. Despite the fact that this model is one of the simplest models to account for variable
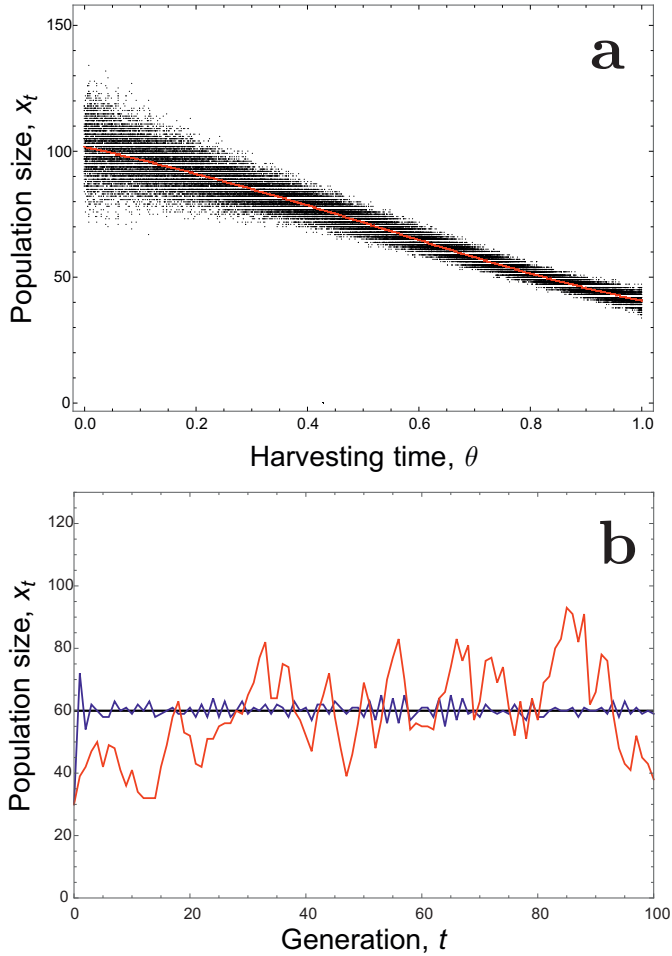
Figure 5.8: The stabilizing effect of harvest timing is robust under both stochasticity and lattice effect. (a) Bifurcation diagram of (5.4) (red dots) and (5.11) (black dots) with $\gamma = 0.6$ and $\sigma = 0.015$ for varying harvesting time $\theta \in [0, 1]$. The underlying population dynamics is given by the Ricker map $g(x) = e^{2.85(1-x/60)}$. (b) The red curve gives the size of a population governed by (5.11) with $\gamma = 0.9292$ and $\theta = 0$, and the blue curve for $\gamma = 0.6$ and $\theta = 0.6688$. In both cases, the initial population size is $x_0 = 30$ and the level of noise is $\sigma = 0.015$.

harvest timings, it is suitable to gain some basic understanding of how the timing of interventions affects the stability of controlled populations.

Under general conditions, we have shown in Theorem 5.2 that timing has no negative effect on the stability of the positive equilibrium if the harvesting intensity is close enough to γ^* (see Figure 5.3). Moreover, we have shown that the latter stability is global. To the best of our knowledge, this is the first global stability result for (5.4) valid for general overcompensatory population models, since global stability results in [44] only cover undercompensatory models (such as the Beverton-Holt model [23]) and the quadratic model.

We have rigorously shown for the Ricker-Seno model that timing can be stabilizing, that is, a harvesting intensity applied at an appropriate time of the season can asymptotically stabilize the positive equilibrium even when it cannot be stabilized at the beginning or the end of the reproductive season with the same harvesting intensity. We have also shown that timing can be destabilizing under natural conditions assumed on population production maps. This provides counterexamples for a conjecture recently published in [44]. However, these counterexamples are the result of mathematical constructions. Most of the populations maps considered in the ecological literature satisfy additional conditions, as for example to have negative Schwarzian derivative, which may prevent any destabilizing effects of timing.

Due to its simplicity, Seno's model has some important limitations that must be taken into account. First, a constant duration of the period in which individuals accumulate energy for reproduction is implicitly assumed. This may be unrealistic in practical applications since it is well established that environmental conditions affect the length of the reproductive season of some species of birds and mammals [96, 160, 205]. Second, the model fixes for all generations a harvesting moment θ during the season that can be arbitrarily chosen. Due to practical limitations, this freedom of choice may be impossible in certain situations. Third, the model is deterministic and assumes a continuum of system states. Numerical simulations indicate that timing enhances the stabilizing properties of harvesting in the presence of both noise and lattice effect.

6

Effect of harvest timing on the dynamics of the Ricker–Seno model

6.1 Introduction

The disproof of Conjecture 5.4 provided in the previous chapter illustrates the difficulty of finding stability results for Seno's model valid for all maps in a given family. To the best of our knowledge, Theorem 5.2 is the only result of this type that has been obtained so far. The relevance of this result is indisputable at a theoretical level, since it is not tied to a specific form of density dependence and is valid for one of the most important families of models in discrete-time population dynamics. However, from a practical point of view, this result has some drawbacks that call into question its applicability to real populations. On the one hand, reaching the high harvesting efforts that are referred may be impossible or too expensive in many cases. On the other hand, these high removal intensities can put the population into risk of extinction, since they are close to a certain collapse threshold. Nevertheless, the result provides interesting in-

formation from a practical point of view: the global character of the stability exhibited by the system. As previously said, global stability is always a desirable property since it allows one to predict the fate of the population independently of its initial size.

In view of all these considerations, it is of the utmost interest to obtain global stability results for the most relevant models in population dynamics under delayed harvest. Focusing on models with overcompensatory density dependence, the Ricker model is probably the most important among them. Many different reasons can be argued to support this claim. Here, we just highlight the work of Brännström and Sumpter [34] according to which time series fit the Ricker model when individuals experience scramble competition and are randomly uniformly distributed over space. These two conditions are true for a vast majority of the biodiversity found on this planet. As has already been mentioned, Cid *et al.* proved in [44] that local stability for the Ricker map is not altered by the effect of harvest time. Knowing whether the local stability is global for all possible combinations of the population parameters is an interesting open problem. In this chapter, we provide a complete answer to this question.

The stability of a population in ecology is a broad concept which encompasses several definitions addressing various biological aspects. Knowing the effect of a certain intervention on the stability of an equilibrium point, even if this stability is global, provides a partial view of the actual impact of that intervention on the population dynamics. Interestingly, we will see that although global stability is not affected by the time of intervention, the constancy stability does strongly depend on the moment of intervention.

In the next section, we show the limitations of the existing stability results for the Ricker-Seno model. In Section 6.3, we provide the main result of this chapter. Section 6.4 studies the effect of the moment of intervention on the constancy stability of the controlled populations. Section 6.5 introduces biological extensions to check the robustness of our results. Finally, Section 6.6 extends the discussion of our results and draws conclusions.

6.2 Existing results and limitations

If we focus on populations governed by the Ricker model, the per capita production function is given by $g(x) = e^{r(1-x)}$, where $r > 0$ is a growth parameter. In this case, it was proved in [44, Proposition 3.3] that equation (5.3) has an asymptotically stable positive equilibrium if and only if

$$1 - e^{2-r} \leq \gamma < 1 - e^{-r}. \tag{6.1}$$

Moreover, this positive equilibrium is globally asymptotically stable (G.A.S.), i.e., it attracts all positive orbits [141, Theorem 1]. Given that systems (5.2) and (5.3) are topologically conjugated, the positive equilibrium of (5.2) is G.A.S. as well. From a practical point of view, this implies that for these two limit cases we can predict the long-run behavior of the population independently of its initial size. In view of this, it is natural to study to what extent the same is true if individuals are removed at any intermediate time during the reproductive season. In [44, Proposition 3.4] it was proved that when condition (6.1) holds, equation (5.4) has a unique positive equilibrium $K_\gamma(\theta)$, which is locally asymptotically stable (L.A.S.). Our goal is to determine whether this equilibrium inherits for intermediate intervention moments the global stability character of the limit cases (5.2) and (5.3).

We note that providing a rigorous proof of global stability is in general a difficult task. Nevertheless, for some population models involving the Ricker map there are analytic results showing that local stability implies global stability; e.g., [30, 169, 182]. Theorem 5.2 provides a condition that guarantees the global stability of the positive equilibrium for general production functions with overcompensatory density dependence. We have seen that for the Ricker-Seno model this condition is

$$r \leq 1 - \ln(1 - \gamma) - \gamma, \tag{6.2}$$

which gives a partial answer to the open problem about global stability cited above.

To illustrate the limitations of this condition, let us consider a population governed by the Ricker model with a growth parameter $r = 3.3$. According to (6.1), if individuals are harvested at the beginning or at the end of the reproductive season, the system is globally stable if and only if the harvest effort is between $1 - e^{2-r} \approx 0.7275$ and $1 - e^{-r} \approx 0.9631$. Outside this range, the positive equilibrium is unstable. Moreover, for higher control intensities populations will go eventually extinct. Assuming that γ ranges in this interval, little can be said about the global stability for intermediate intervention times with condition (6.2): the positive equilibrium of (5.4) is globally stable for all harvest times if $\gamma \in [0.9617, 0.9631)$. From a practical point of view, knowing this is completely useless. Apart from the short length of this interval, surpassing the threshold intensity 0.9631 implies the collapse of the population. In view of this, it is natural to ask what can be said about the global stability of (5.4) for control intensities meeting (6.1) and uncovered by (6.2), i.e., those ranging from 0.7275 to 0.9617. The result provided in the following section gives the answer to this question.

6.3 GLOBAL STABILITY

In this section we prove that delaying the removal of individuals for populations governed by the Ricker model never affects the global stability of the system. To that end, as in the previous chapter, we rewrite the right-hand side of (5.4) as

$$(1 - \theta)F_0(x_t) + \theta F_1(x_t) := F_\theta(x_t),$$

where $F_0(x) := g((1 - \gamma)x)(1 - \gamma)x$ and $F_1(x) := (1 - \gamma)g(x)x$. With these notations, the multiplier of equation (5.4) is given by

$$\lambda = \frac{dF_\theta}{dx}(K_\gamma(\theta)). \tag{6.3}$$

We start by proving some auxiliary results.

Lemma 6.1. *Assume* $g(x) = e^{r(1-x)}$, $r > 0$, *and condition* (6.1) *holds. Then,* $F_0'(x) \geq -1$, $F_1'(x) \geq -1$, *and* $F_\theta'(x) > -1$ *for all* $x \in (0, +\infty)$ *and* $\theta \in (0, 1)$.

Proof. It is straightforward to see that F_0' attains its global minimum at $x = \frac{2}{(1-\gamma)r}$ and F_1' attains the same global minimum at $x = \frac{2}{r}$. Since $F_0'(\frac{2}{(1-\gamma)r}) = F_1'(\frac{2}{r}) = -(1-\gamma)e^{r-2}$, it follows from the first inequality of condition (6.1) that $F_0'(x) \geq -1$, and $F_1'(x) \geq -1$ for all $x \in (0, +\infty)$.

On the other hand, $F_\theta'(x) = (1 - \theta)F_0'(x) + \theta F_1'(x)$, so using that F_0' and F_1' attain the same global minimum greater than or equal to -1 at different points, one gets $F_\theta'(x) > -1$ for $x \in (0, +\infty)$ and $\theta \in (0, 1)$. $\qquad\square$

The next result is a particular case of Proposition 3.1 in [44].

Lemma 6.2. *Assume* $g(x) = e^{r(1-x)}$ *and* $r > 0$. *System* (5.4) *has a unique positive equilibrium (denoted by* $K_\gamma(\theta)$*) if and only if*

$$\gamma < 1 - e^{-r}.$$

Proof. The positive equilibria of equation (5.4) are the positive solutions of

$$G(x)(1 - \gamma) = 1, \tag{6.4}$$

with $G(x) = \theta e^{r(1-x)} + (1 - \theta)e^{r(1-(1-\gamma)x)}$. Since G is decreasing and $G(+\infty) = 0$, equation (6.4) has a unique solution if and only if $G(0)(1 - \gamma) > 1$. $\qquad\square$

The next result is a consequence of [57, Theorem 3]. We provide a short proof for the sake of completeness.

Lemma 6.3. *Assume* $f \colon [0, +\infty) \to [0, +\infty)$ *is continuous,* $f(0) = 0$, *and* $f(x) > 0$ *for* $x > 0$. *In addition, assume that there exists* $K > 0$ *such that*

$$|f(x) - K| < |x - K| \quad \textit{for } x > 0, \ x \neq K. \tag{6.5}$$

Then, K is a G.A.S. fixed point for the difference equation $x_{t+1} = f(x_t), t \in \mathbb{N}$.

Proof. The limit points of the bounded sequence $x_t < |x_0 - K| + K$ belong to $U = \{K + \alpha, K - \alpha\}$, where $\alpha \geq 0$ is the limit of the decreasing sequence $a_t = |x_t - K|$. By substituting $x = K \pm \alpha$ in (6.5) and taking into account that $f(U) \subset U$, we see that $\alpha = 0$. □

With these auxiliary results, we are ready to prove the main result in this chapter.

Theorem 6.4. *Assume $g(x) = e^{r(1-x)}$, $r > 0$, and $\gamma \in (0,1)$ such that condition (6.1) holds. Then, for any $\theta \in [0,1]$ the positive equilibrium of equation (5.4) is G.A.S.*

Proof. For $\theta \in \{0,1\}$, the result has been already proved in [141, Theorem 1]. Consider $\theta \in (0,1)$. We will prove (6.5) for $f = F_\theta$ and $K = K_\gamma(\theta)$. Let us start by proving

$$2K_\gamma(\theta) - x < F_\theta(x) < x \tag{6.6}$$

for all $x > K_\gamma(\theta)$. Suppose $F_\theta(z) \geq z$ for some $z > K_\gamma(\theta)$ and consider the function $h(x) = F_\theta(x) - x$, for which $h(z) \geq 0$. Since $F_\theta(x) \to 0$ for $x \to +\infty$, there must exist $x \geq z$ such that $h(x) < 0$. Therefore, h has a root in the interval $[z, +\infty) \ni K_\gamma(\theta)$, which corresponds to a positive fixed point of F_θ different from $K_\gamma(\theta)$. This leads to a contradiction according to Lemma 6.2. Suppose now $F_\theta(z) \leq 2K_\gamma(\theta) - z$ for some $z > K_\gamma(\theta)$. Then, $F_\theta(z) - K_\gamma(\theta) \leq -(z - K_\gamma(\theta))$, and thus

$$\frac{F_\theta(z) - K_\gamma(\theta)}{z - K_\gamma(\theta)} \leq -1. \tag{6.7}$$

By the mean value theorem, there must exist $u \in (K_\gamma(\theta), z)$ such that $F_\theta'(u)$ equals the left-hand side of (6.7). This is again impossible according to Lemma 6.1. With this, we have proved (6.6) for all $x > K_\gamma(\theta)$. This yields (6.5) for all $x > K_\gamma(\theta)$.

A similar argument shows that (6.5) holds for $x < K_\gamma(\theta)$, and the final conclusion follows from Lemma 6.3. □
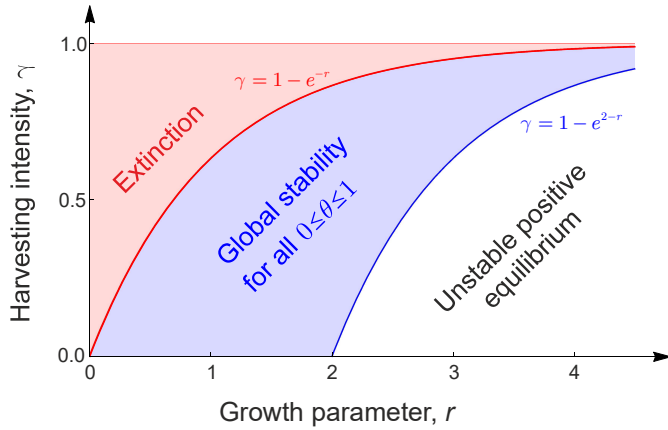
Figure 6.1: Global stability of the Ricker-Seno model for all harvest times. The blue area is the region in the (r, γ)-parameter space for which changing timing does not affect the global attraction of the positive equilibrium of model (5.4) in the Ricker case. In the red area, varying the moment of intervention does not affect the global attraction of the trivial equilibrium. For parameters in the white area, the positive equilibrium of (5.2) and (5.3) is unstable.

Remark 6.5. Condition (6.5) implies that f is enveloped by the map $\phi(x) = 2K - x$. Enveloping has been used to study the global stability of several population models (see, e.g., [56, 57]), and it is known to be a sufficient condition for the existence of a global Lyapunov function [181].

Figure 6.1 shows the area in the (r, γ)-parameter space for which Theorem 6.4 ensures that changing the harvest time does not affect the global stability of the positive equilibrium. For the example considered at the end of the previous section ($r = 3.3$), if the positive equilibrium is globally stable for $\theta = 0$ (i.e., $\gamma \in [0.7275, 0.9631)$), then there is also global stability for any other intervention moment. As said, for control efforts above 0.9631, the population is led to extinction, and for values below 0.7275 we only know that the positive equilibrium for the limit cases $\theta = 0$ and $\theta = 1$ is unstable. We have seen in the previous chapter that in the latter case for certain intervention

times θ the positive equilibrium of (5.4) can be locally stable (cf. Proposition 5.3), but knowing whether this stability is or is not global is an open problem.

Let us analyze the practical implications of Theorem 6.4. If we choose harvesting efforts satisfying (6.1), we can then postpone the intervention to any moment during the reproductive season that the population will be attracted to the positive equilibrium of the system for any initial population size. Of course, this has important implications for the management of populations. Moreover, we have seen in the previous chapter that the global stabilization of populations induced by harvesting at any intermediate moment during the reproductive season is robust not only under stochasticity but also under lattice effect.

6.4   EFFECT ON CONSTANCY STABILITY

In the previous section, we have seen that for the Ricker-Seno model delaying harvest does not affect the global stability of the positive equilibrium. However, knowing that all populations will be attracted towards the same point may not be enough in most practical situations. In this sense, there are relevant questions about the effect of timing on the population dynamics that remain unanswered. Probably, the most important is the effect that delayed harvest may have on the constancy stability of controlled populations. When the system shows global stability, the asymptotic constancy is guaranteed by the fact that all populations are attracted towards the positive equilibrium regardless of the initial population size. However, transients to the asymptotic dynamics are known to play a central role in the management of biological species. Two factors determine the constancy of populations during this transitional period. One is the type of convergence (monotonic or oscillatory) and the magnitude of fluctuations in the population size. Another factor is the length of the transient, which depends on the convergence speed to the positive attractor. Interestingly, this convergence speed can also be related to the concept of *engineering* resilience, understood as the time taken for

a system to return to its pre-disturbed stable state [170, 210], which has been frequently used in ecology (see, e.g., [11]).

To address the above questions, we start by studying the multiplier (6.3) in the Ricker case for different values of the harvest effort and the moment of intervention. For $\lambda > 0$ the convergence to the positive attractor is monotonic and for $\lambda < 0$ oscillatory. Moreover, the magnitude of $|\lambda|$ determines the speed of convergence of populations to the equilibrium: for lower values of $|\lambda|$ the convergence is quicker. The very best situation occurs when $\lambda = 0$, in which case the equilibrium point is called superstable. Figure 6.2(a) shows the multiplier (6.3) in terms of the control intensity γ and the harvest time θ for a growth parameter $r = 3.3$ (the values of γ represented are only those for which Theorem 6.4 ensures the global stability of the system). As can be observed, the moment of intervention has an impact on both the type and the speed of convergence. If we set the value of the removal effort, for example, at $\gamma = 0.85$, there are two harvest times for which the system exhibits superstability, namely $\theta_0 \approx 0.3399$ and $\theta_1 \approx 0.7851$. For $\theta \in [0, \theta_0) \cup (\theta_1, 1]$, the convergence is oscillatory, and for $\theta \in (\theta_0, \theta_1)$ monotonic. In any case, as θ approaches either θ_0 or θ_1 the convergence becomes faster. This can be observed in Figure 6.2(b). Notice that superstability cannot be attained by changing the moment of intervention for some harvesting efforts. Yet, even in those cases, the speed of convergence depends on the harvest time.

6.5 Introducing biological realities

All the results of the previous sections refer to deterministic systems with continuous-state variables. Now, we introduce some biological mechanisms to better study the effect that harvest timing may have on the constancy stability of real populations. To study the impact of lattice effect on the dynamics, we follow the work of [102] and consider the underlying dynamics to be described by the model

$$x_{t+1} = bx_t \exp\left(-\frac{c}{V}x_t\right),$$
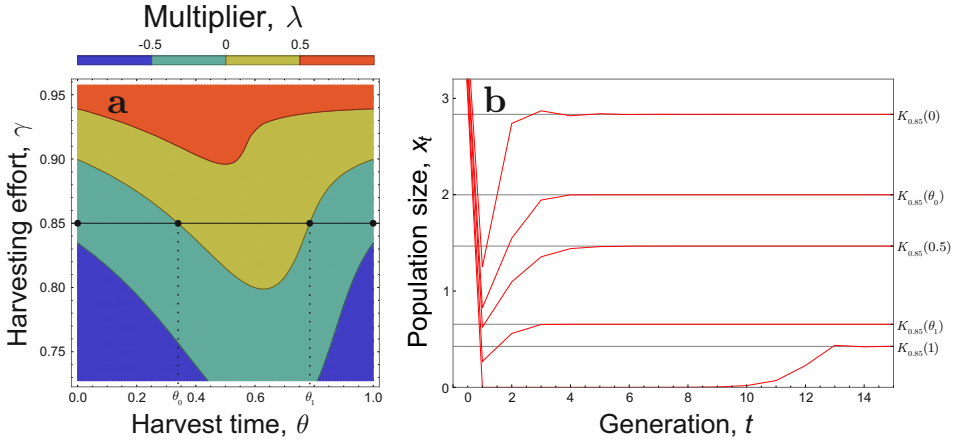
Figure 6.2: Effect of harvest timing on the constancy stability of the Ricker-Seno model.
(a) Multiplier (6.3) for $r = 3.3$ in terms of the removal intensity, γ, and the time of intervention, θ. Parameter γ ranges in the interval $[0.7275, 0.9631)$, for which (5.4) exhibits global stability according to Theorem 6.4. Values θ_0 and θ_1 in the horizontal axis represent the harvest times for which the positive equilibrium of (5.4) is superstable. for $\gamma = 0.85$. (b) The red curves represent time series of (5.4) for $r = 3.3$ and $\gamma = 0.85$ with initial condition $x_0 = 6$ and different harvest times. The horizontal black lines represent the positive equilibrium $K_{0.85}(\theta)$ of (5.4) for each intervention moment θ.

where x_t is the number of individuals in generation t in a habitat of size V, $b > 0$ is the per capita birth rate and $\exp(-cx_t/V)$ (with $c > 0$) is the fraction of offspring expected to survive one unit of time at population density x_t/V. The per capita production function for this model is therefore $g(x) = b \exp\left(-\frac{c}{V}x\right)$. For numerical simulations, we will consider $b = 17$, $c = 1$ and $V = 20$. Given that the impact of the lattice effect on the dynamics depends on the presence of noise in the system [102], we consider the discrete-state stochastic equation 5.11. To measure the constancy stability of populations governed by this equation, we consider the fluctuation index (see Section 1.2). The magnitude of the FI somehow measures the width of the blurred equilibria described in Section 5.5.
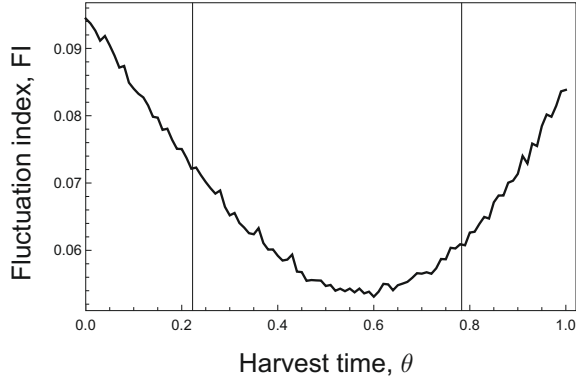
Figure 6.3: Fluctuation index for the Ricker-Seno model in terms of the harvest time. The value represented for a given θ is the average of the FI for Eq. 5.11 with $\gamma = 0.85$ and $\sigma = 0.015$ over 5000 time series of 100 generations with initial population sizes chosen as pseudorandom numbers in the interval $(0, dg(d)]$, where d is the abscissa of the maximum population production. The underlying population dynamics are given by $g(x) = b \exp\left(-\frac{c}{V} x\right)$ with $b = 17$, $c = 1$, and $V = 20$. The vertical lines correspond to the intervention moments $\theta_0 \approx 0.22258$ and $\theta_1 \approx 0.78301$ for which the positive equilibrium of equation (5.4) is superstable.

Figure 6.3 shows the FI for (5.11) with $\gamma = 0.85$ and $\sigma = 0.015$. As can be observed, the curve describing the FI for the stochastic discrete-state system is U-shaped. Globally, the FI attains lower values for harvest times corresponding to monotonic convergence in the deterministic continuous-state system (between the values θ_0 and θ_1 for which the positive equilibrium of (5.4) is superstable), and higher values when the convergence is oscillatory. This correspondence between the stochastic integerized and the deterministic non-integerized systems leads us to conclude that the results obtained in this chapter are robust under both lattice effect and noise, and reinforces the idea that choosing an appropriate moment for the intervention helps to improve the constancy stability of the controlled populations.

6.6 Discussion and conclusions

We have studied the effect of harvest timing on the global stability of populations governed by the Ricker-Seno model. We have proved that timing cannot have a destabilizing effect (neither local nor global) on the population dynamics. This extends recent results in the literature about local and global stability for the Ricker-Seno model (see [44] and Chapter 5 of this thesis), and completely characterizes the global stability of this model when the positive equilibrium of the limit case (5.3) –which corresponds to harvesting at the beginning of the reproductive season– is G.A.S. This result, together with the robustness of the global stability under both noise and lattice effect (see Section 5.5), allows to predict in practical situations the fate of populations harvested at any moment with independence of the initial number of individuals.

We have also shown that the constancy stability of controlled populations strongly depends on the moment of intervention. In the deterministic case, we have shown that harvest timing determines both the speed and the type of convergence to the positive equilibrium. This is expected to have important consequences from the practical point of view. It is known that biological populations that monotonically approach a deterministically stable equilibrium will tend to return towards it faster than populations for which the convergence is oscillatory, and for the same amount of noise will have a lower variance in the population density [155]. Moreover, in the case of oscillatory convergence, the population dynamics may seem to be persistently cyclic because the population size is easily prevented from reaching the equilibrium. This behavior has been observed in several experimental systems and is known as quasicyclicity [162]. In view of this, the impact of the moment of intervention in the population dynamics of real populations is expected to be even stronger than what has been observed for deterministic systems. We have checked this by studying the fluctuation index (FI) in presence of noise for discrete-state systems. Our analysis leads to conclude that the time of intervention plays a key role in the constancy stability of the managed populations.

On the other hand, the results in this chapter may not cover all possible cases in which the Ricker-Seno model is globally stable. Proposition 5.3 states that there exists a range of harvesting efforts γ under the threshold $\gamma^* = 1 - e^{2-r}$ for which the positive equilibrium of the limit cases (5.2) and (5.3) is unstable but it is possible to find intervention times $\theta \in (0, 1)$ such that equation (5.4) is L.A.S. Determining whether or not this stabilization is global remains as an open problem.

7

Global stability of discrete dynamical systems via exponent analysis: applications to harvesting population models

7.1 INTRODUCTION

In Chapter 5, we proved that Conjecture 5.4 is false for general compensatory population maps. Yet, in Chapter 6 we proved that harvest time does not affect the global stability in the Ricker case. Cid et al. also obtained in [44] sharp global stability results for the quadratic map [153] and the Beverton-Holt model [23]. Little is known about the effect of the moment of intervention on the stability of populations governed by equations different from the Ricker model, the Beverton-Holt model or the quadratic map (apart from Theorem 5.2, where we proved that the moment of intervention does not affect the stability when the harvesting effort is high enough). To reduce this gap, we introduce an innovative approach that is especially useful to prove the global stabil-

ity of a broad family of population models, namely those encompassed in the so called *generalized α-Ricker* model [151]. Among others, the Bellows, the Maynard-Smith-Slatkin and the discretized version of the Richards models are covered by our analysis [19, 156, 175]. Interestingly, these three models can be seen, respectively, as generalizations of the already studied Ricker, Beverton-Holt and quadratic maps where the term related to the density dependence includes a new exponent parameter α. This exponent is the focus of the proposed new method: under certain conditions, we provide sharp results of both local and global stability of the positive equilibrium of the system depending on the value of α. In particular, these results can be considered as the proof for a wide range of population models of Conjecture 5.4.

The proposed new method can be applied whenever the per capita production function g has a strictly negative derivative. The domain $(0, \rho)$ of g can be bounded or unbounded. All bounded cases can be easily reduced to the case $\rho = 1$. The range $(g(\rho), g(0))$ can also be bounded or unbounded, provided that $0 \leq g(\rho) < 1 < g(0) \leq +\infty$.

The applications that we present focus on the cases $g(0) < +\infty$ and $g(\rho) = 0$. In particular, our examples deal with the following models:

- The Bellows model, which includes the Ricker model as a particular case (Subsection 7.4.1).

- The discretization of the Richards model, which includes the quadratic model as a particular case (Subsection 7.4.2).

- The Maynard Smith-Slatkin model, which includes the Beverton-Holt model as a particular case (Subsection 7.4.3).

- The Thieme model, which includes the Hassell model as a particular case (Subsection 7.4.4).

This chapter is organized as follows. Section 7.2 lists the families of per capita production functions for which we will show that Conjecture 5.4 is true. In Section 7.3,

we state and prove the main results of the chapter. Section 7.4 is divided in several subsections, each of them consisting in an example of the applicability of the main results. In addition, and with the aim of showing the validity of Conjecture 5.4 for a broad family of maps, Section 7.4 provides new—or shorter proofs of some already known—global stability results. Finally, Section 7.5 summarizes the results obtained and draws conclusions.

7.2 PER CAPITA PRODUCTION FUNCTIONS

First-order difference equations are commonly used to describe the population dynamics of species reproducing in a short period of the year. Usually, these equations take the general form

$$x_{t+1} = x_t\, g(x_t),\ x_0 \in [0, +\infty),\ t \in \mathbb{N}, \tag{7.1}$$

where x_t corresponds to the population size at generation t and map g to the per capita production function, which naturally has to be assumed as non-negative. In addition, g is frequently assumed to be strictly decreasing, because of the negative effect of the intraspecific competition in the population size, and when that condition holds the population is said *compensatory* [33, 123]. Theoretical ecologists have developed several concrete families of per capita production functions. These families depend on one or several parameters, which are essential to fit the functions to the experimental data.

Our results in this chapter cover some of the most relevant families of compensatory population maps, which, as it was pointed out in [151], can be described in a unified way by using the map

$$g\colon \{x \in (0, +\infty) : 1 + px^\alpha > 0\} \to (0, +\infty)$$

defined by

$$g(x) = \lim_{q \downarrow p} \frac{\kappa}{(1 + qx^\alpha)^{1/q}}, \tag{7.2}$$

where $\alpha, \kappa \in (0, +\infty)$ and $p \in \overline{\mathbb{R}} \setminus \{-\infty\}$, with $\overline{\mathbb{R}} := [-\infty, +\infty]$ denoting the extended real line.

The following models are obtained for different values of the parameters:

[M1] For $p = 1$ and $\alpha = 1$, the *Beverton-Holt* model [23], in which $g(x) = \dfrac{\kappa}{1 + x}$.

[M2] For $p = -1$ and $\alpha = 1$, the *quadratic* model [153], in which $g(x) = \kappa(1 - x)$ and where $\kappa < 4$ for the difference equation (7.1) to be well-defined.

[M3] For $p = 0$ and $\alpha = 1$, the *Ricker* model [176], in which $g(x) = \kappa e^{-x}$.

Models **[M1-M3]** are compensatory. Nevertheless, **[M2-M3]** are always overcompensatory [33, 45] (the map $xg(x)$ is unimodal) and can have very rich and complicate dynamics, whereas **[M1]** is never overcompensatory (the map $xg(x)$ is increasing) and has pretty simple dynamics: all nontrivial solutions monotonically tend to the same equilibrium which, consequently, is G.A.S.

Map (7.2) also includes models that are overcompensatory or not depending on the values of the parameters:

[M4] For $p = 1$, the *Maynard-Smith-Slatkin* model [156], in which $g(x) = \dfrac{\kappa}{1 + x^\alpha}$.

[M5] For $\alpha = 1$ and $p > 0$, the *Hassell* model [98], in which $g(x) = \dfrac{\kappa}{(1 + px)^{1/p}}$.

[M6] For $p > 0$, the *Thieme* model [206], in which $g(x) = \dfrac{\kappa}{(1 + px^\alpha)^{1/p}}$.

Obviously, **[M4-M6]** include **[M1]** as a special case. Similarly, the last two models that we will mention can be considered as generalizations of **[M2]** and **[M3]**, respectively:

[M7] For $p = -1$, the discretization of the *Richards* model [175], in which $g(x) = \kappa(1 - x^\alpha)$. Since $xg(x)$ reaches its maximum value at $x = (1/(1 + \alpha))^{1/\alpha}$, the inequality $\alpha\kappa < (1 + \alpha)^{\frac{1+\alpha}{\alpha}}$ must be satisfied for the difference equation (7.1) to be well-defined.

[M8] For $p = 0$, the *Bellows* model [19], in which $g(x) = \kappa e^{-x^\alpha}$.

Models **[M7-M8]** generalize **[M2-M3]** by including a new exponent parameter α, which determines the severity of the density dependence and makes the models more flexible to describe datasets [19]. This is the announced exponent parameter playing a central role in our study.

At this point, it is convenient to make some remarks. First, we point out that the domain of g is bounded for models **[M2]** and **[M7]**, whereas it is unbounded for the rest of models. When the domain of g is bounded, there is a restriction in the parameters involved in the map for which the difference equation (7.1) is well-defined. Second, a suitable rescaling allows to obtain other frequently used expressions of these eight models depending on an extra parameter, e.g., $g(x) = \kappa(1 - mx)$ for the quadratic model or $g(x) = \kappa e^{-mx}$ for the Ricker model. This extra parameter is irrelevant for the dynamics of (7.1).

Substituting map (7.2) into Seno's equation (5.4), we obtain an intricate model depending on up to five parameters for which establishing general local or global stability results is a tricky task. For that purpose, we develop a general method in the following section.

7.3 EXPONENT ANALYSIS METHOD

Consider the difference equation

$$x_{t+1} = x_t g_s\left(x_t\right),$$

with

$$g_s(x) = c\, h(x^\alpha) + (b - c)\, h(sx^\alpha),$$

where $b, s, \alpha \in (0, +\infty)$ and $c \in [0, +\infty)$ are such that $c < b$, $s \leq 1$, and $h \colon (0, \rho) \to (\nu, \mu) \subset (0, +\infty)$ is a decreasing diffeomorphism with $\rho, \mu \in \{1, +\infty\}$ and $\nu b < 1 < \mu b$.

Notice that the domain of h can be the open bounded interval $(0,1)$ or the open unbounded interval $(0,+\infty)$, covering all the models described in the previous section. In addition, the image of h can be bounded or unbounded, although the applications presented in this paper are restricted to the bounded case.

For $\rho = 1$, it is not obvious that the difference equation $x_{t+1} = x_t g_s(x_t)$ is well-defined, i.e., $x g_s(x) \in (0,\rho)$ for $x \in (0,\rho)$. Next, we study when the difference equation $x_{t+1} = x_t g_s(x_t)$ is well-defined and has a unique positive equilibrium. We establish some notation first. Being the function

$$ x \mapsto g_s\left(x^{1/\alpha}\right) = c\,h(x) + (b-c)\,h(sx), $$

a diffeomorphism from $(0,\rho)$ to $(\nu_s b, \mu b)$, where

$$ \nu_s := \lim_{x \to \rho} g_s\left(x^{1/\alpha}\right)/b, \tag{7.3} $$

we denote by j_s its inverse diffeomorphism, i.e., the function $j_s : (\nu_s b, \mu b) \to (0,\rho)$ satisfying

$$ c\,h(j_s(z)) + (b-c)\,h(sj_s(z)) = z, \tag{7.4} $$

for all $z \in (\nu_s b, \mu b)$. Obviously, if $\rho = +\infty$, then $\nu_s = \nu$ for $s \in (0,1]$.

Lemma 7.1. *Assume $b, s, \alpha \in (0,+\infty)$ and $c \in [0,+\infty)$ are such that $c < b, s \leq 1$, and $h : (0,\rho) \to (\nu,\mu) \subset (0,+\infty)$ is a decreasing diffeomorphism with $\rho, \mu \in \{1,+\infty\}$ and $\nu b < 1 < \mu b$. In addition, let*

$$ s_* := \inf\{s \in (0,1] : \nu_s < 1/b\}, \tag{7.5} $$

where ν_s is given by (7.3). Then, the map $x g_s(x)$ has a unique fixed point in $(0,\rho)$ if and only if $s > s_*$. Moreover, this fixed point is $(j_s(1))^{1/\alpha}$.

Proof. Clearly, $x \in (0,\rho)$ is a fixed point of $x g_s(x)$ if and only if $g_s(x) = 1$, and in such case, $x = (j_s(1))^{1/\alpha}$.

Next, notice that $v_0 := \frac{cv+(b-c)\mu}{b} \geq v_{\hat{s}} \geq v_s \geq v_1 = v$, for $0 < \hat{s} < s < 1$, and that v_s depends continuously on s. Since g maps $(0, \rho)$ onto $(v_s b, \mu b)$ and $vb < 1 < \mu b$ holds, the equation $g_s(x) = 1$ for $x \in (0, \rho)$ has solution if and only if $s > s_*$. We have already stressed that $v_s = v$ for $\rho = +\infty$. Hence, $s_* = 0$ for $\rho = +\infty$. $\qquad\square$

In the conditions of Lemma 7.1, for each $s \in (0, 1]$ we define the function

$$\tau_s : \left(\tfrac{1}{\mu b}, \tfrac{1}{v_s b}\right) \to \overline{\mathbb{R}} \quad \text{by} \quad \tau_s(z) := \frac{\ln\left(j_s\left(\tfrac{1}{z}\right)\right)}{\ln z}.$$

Now, we study under which conditions the difference equation $x_{t+1} = x_t g_s(x_t)$ is well-defined.

Lemma 7.2. *Assume that the conditions of Lemma 7.1 hold with $s \in (s_*, 1]$. Then, $z g_s(z) \in (0, \rho)$ for all $z \in (0, \rho)$ if and only if $\alpha < \alpha_s$, with*

$$\alpha_s = \begin{cases} +\infty, & \rho = +\infty, \\ \min_{z \in (1/\mu b, 1)} \tau_s(z), & \rho = 1. \end{cases} \tag{7.6}$$

Moreover, if the equation $x_{t+1} = x_t g_s(x_t)$ is well-defined for $s = 1$, then it is also well-defined for $s \in (s_*, 1]$.

Proof. We consider separately the cases $\rho = +\infty$ and $\rho = 1$. The case $\rho = +\infty$ is trivial. For $\rho = 1$, we have

$$z\, g_s(z) \in (0, 1) \text{ for } z \in (0, 1) \iff g_s(z) < \frac{1}{z} \text{ for } z \in (0, 1).$$

The latter inequality always holds if $z \leq \frac{1}{\mu b}$ because $g_s\left((0,1)\right) = (\nu_s b, \mu b)$. Hence,

$$g_s\left(z\right) < \frac{1}{z} \text{ for } z \in (0,1) \iff g_s\left(z\right) < \frac{1}{z} \text{ for } z \in \left(\tfrac{1}{\mu b}, 1\right)$$

$$\iff z^\alpha > j_s\left(\tfrac{1}{z}\right) \text{ for } z \in \left(\tfrac{1}{\mu b}, 1\right)$$

$$\iff \alpha < \frac{\ln\left(j_s\left(\tfrac{1}{z}\right)\right)}{\ln z} = \tau_s(z) \text{ for } z \in \left(\tfrac{1}{\mu b}, 1\right).$$

Since $\rho = 1$, we have that $\tau_s(z) > 0$ for $z \in \left(\tfrac{1}{\mu b}, 1\right)$ and

$$\lim_{z \to 1/\mu b} \tau_s(z) = +\infty \quad \text{and} \quad \lim_{z \to 1} \tau_s(z) = +\infty,$$

which finishes the proof of the first assertion. For the second one, notice that α_s decreases as s increases, since j_s decreases with s. Therefore, $\alpha < \alpha_1$ guarantees $\alpha < \alpha_s$ for $s \in (s_*, 1]$. $\square$

Now, in the conditions of Lemma 7.1, for each $s \in (s_*, 1]$, we write

$$b_s := \min\{\mu b, \frac{1}{\nu_s b}\}$$

and define the continuous function $\sigma_s \colon \left(\tfrac{1}{b_s}, b_s\right) \subset \left(\tfrac{1}{\mu b}, \tfrac{1}{\nu_s b}\right) \to \mathbb{R}$ by

$$\sigma_s(z) := \begin{cases} \tau_s(z) + \tau_s\left(\tfrac{1}{z}\right), & z \neq 1, \\ \dfrac{-2j_s'(1)}{j_s(1)}, & z = 1. \end{cases} \tag{7.7}$$

Lemma 7.3. *The function σ_s given in (7.7) is continuous and positive. Moreover, when $\rho = 1$, it satisfies $\sigma_s(z) < \tau_s(z)$ for $z \in \left(\tfrac{1}{b_s}, 1\right)$.*

Proof. A direct application of l'Hôpital rule shows that σ_s is a continuous function:

$$\lim_{z \to 1} \sigma_s(z) = \lim_{z \to 1} \frac{\ln(j_s(1/z)) - \ln(j_s(z))}{\ln z} = \lim_{u \to 0} \frac{\ln(j_s(e^{-u})) - \ln(j_s(e^u))}{u}$$
$$= \frac{-2j_s'(1)}{j_s(1)} = \sigma_s(1).$$

On the other hand, to see that σ_s takes values on $(0, +\infty)$ note that $z \mapsto \ln(j_s(z))$ is a decreasing function and we are assuming that j_s is a diffeomorphism, so $j_s'(1) < 0$. Finally, for $\rho = 1$,

$$\tau_s(z) = \frac{\ln(j_s(1/z))}{\ln z} > 0 \quad \text{and} \quad \tau_s(1/z) = \frac{\ln(j_s(z))}{-\ln z} < 0,$$

for $z \in \left(\frac{1}{b_s}, 1\right)$. Thus, $\sigma_s(z) < \tau_s(z)$ for $z \in \left(\frac{1}{b_s}, 1\right)$. $\qquad \square$

The function σ_s, given in (7.7), is related to the fixed points of the map $f_s \circ f_s$, with $f_s(x) = xg_s(x)$, as we will see next. Assuming $\alpha < \alpha_s$, for the map $f_s \circ f_s$ to be well-defined, and rearranging for α in the fixed points equation, we have (see Lemma 7.1)

$$g_s(x)g_s(xg_s(x)) = 1 \iff j_s^{-1}(y)\,j_s^{-1}\left(y\left(j_s^{-1}(y)\right)^\alpha\right) = 1\,;\, y = x^\alpha \quad (7.8)$$
$$\iff z j_s^{-1}(j_s(z)z^\alpha) = 1\,;\, z = j_s^{-1}(x^\alpha) \quad (7.9)$$
$$\iff j_s(z)z^\alpha = j_s(1/z)\,;\, z = j_s^{-1}(x^\alpha) \quad (7.10)$$
$$\iff \alpha = \sigma_s(z) \text{ with } z = j_s^{-1}(x^\alpha)\,,\text{ or } z = 1. \quad (7.11)$$

In other words, the difference equation $x_{t+1} = x_t g_s(x_t)$ has a nontrivial period-2 orbit if and only if there exists $z \in (1/b_s, b_s) \setminus \{1\}$ and $\alpha < \alpha_s$ such that $\sigma_s(z) = \alpha$. Consequently, considering σ_s for the study of the global stability of the positive equilibrium of $x_{t+1} = x_t g_s(x_t)$ becomes natural since, by the main theorem in [47], the

absence of nontrivial period-2 orbits of $x_{t+1} = x_t g_s(x_t)$ is equivalent to the global asymptotic stability of this positive equilibrium. More specifically, we will use the following result:

Lemma 7.4. *Let* $-\infty \le a_1 < a_2 \le +\infty$, $I = (a_1, a_2)$, $f \colon I \to I$ *a continuous function and* $x_{f \circ f} \in I$ *such that* $(f \circ f)(x) \ne x$ *for all* $x \in I \setminus \{x_{f \circ f}\}$. *Then,* $x_{f \circ f}$ *is a stable equilibrium for the map* $f \circ f$ *if and only if* $x_{f \circ f}$ *is a G.A.S. equilibrium for the map* f.

Proof. Define $f^{(1)} := f$, $f^{(n)} := f \circ f^{(n-1)}$ and apply the Sharkovsky Forcing Theorem [193] to see that $f^{(n)}(x) \ne x$ for all $x \in I \setminus \{x_{f \circ f}\}, n \le 1$. If the continuous function $f^{(n)}(x) - x$ was negative in $(a_1, x_{f \circ f})$, then $x_{f \circ f}$ would not be stable for the map $f^{(2)}$ since $x_j = f^{(2nj)}(x_0)$ would be a decreasing sequence for all $x_0 \in (a_1, x_{f \circ f})$. Applying the same argument to the interval $(x_{f \circ f}, a_2)$, we conclude that $(f^{(n)}(x) - x)(x - x_{f \circ f}) < 0$ for all $n \ge 1, x \in I \setminus \{x_{f \circ f}\}$. In particular, replacing x by $f^{(m)}(x)$, it follows that $\left(f^{(n+m)}(x) - f^{(m)}(x) \right) \left(f^{(m)}(x) - x_{f \circ f} \right) < 0$ for all $n, m \ge 1$, $x \in I \setminus \{x_{f \circ f}\}$. Therefore, the subsequence $\left(f^{(n)}(x) \right)_n$ formed by the terms smaller (respectively, greater) than $x_{f \circ f}$ is increasing (respectively, decreasing). Then, $\lim_{n \to +\infty} f^{(n)}(x) = x_{f \circ f}$ for all $x \in I$. The converse is obvious. $\qquad \square$

Remark 7.5. We are considering per capita production functions from $(0, \rho)$ onto $(\nu_s b, \mu b) \subset (\nu b, \mu b)$, given by

$$g_s(x) = ch(x^\alpha) + (b - c)h(sx^\alpha),$$

where s and α run, respectively, through $(s_*, 1]$ and $(0, \alpha_s)$, these being the largest intervals within which the equation $x_{t+1} = x_t g_x(x_t)$ is well-defined and has an equilibrium (see (7.3), (7.5) and (7.6)).

Probably, the most relevant applications arise for the case in which the domain is unbounded (i.e., $\rho = +\infty$). In such a particular case, $s_* = 0$, $\nu_s = \nu$ and $\alpha_s = +\infty$

for all $s \in [0,1]$. Therefore, when $\rho = +\infty$ the equation $x_{t+a} = x_t g_x(x_t)$ is well-defined and has an equilibrium for all $s \in [0,1]$ and $\alpha > 0$.

Moreover, we point out that the following theorem (which is the main result of this chapter) can be applied under very general conditions. In particular, it holds when the per capita production function has an unbounded range.

In what follows, ρ, μ, ν, b and c will be considered as constants, while s and α will mostly be seen as parameters.

Theorem 7.6. *Let $\mu, \rho \in \{1, +\infty\}$, $0 < c < b$, $0 \le \nu b < 1 < \mu b$ and $h: (0, \rho) \to (\nu, \mu)$ be a decreasing diffeomorphism. Let $s_* := \inf\{s \in (0,1] : \nu_s < 1/b\}$, α_s given in (7.6), and consider the families of functions $\{j_s\}_{s_* < s \le 1}$ and $\{\sigma_s\}_{s_* < s \le 1}$ defined by (7.4) and (7.7), respectively. For each $s \in (s_*, 1]$ and $\alpha \in (0, \alpha_s)$ also consider the discrete equation:*

$$x_{t+1} = x_t \left(c\, h\left(x_t^\alpha\right) + (b - c) h\left(s x_t^\alpha\right)\right). \qquad (7.12)$$

(A) Then, the equation (7.12) is well-defined, it has a unique positive equilibrium and:

(i) The equilibrium of (7.12) is locally asymptotically stable (L.A.S.) when $\alpha < \sigma_s(1)$ and it is unstable for $\alpha > \sigma_s(1)$.

(ii) The equilibrium of (7.12) is globally asymptotically stable (G.A.S.) if and only if $\alpha < \sigma_s(z)$ for all $z \in (1, b_s)$.

(B) Additionally, assume that the function h satisfies the following condition

($\mathbf{H_1}$) The function $x \mapsto h'(x)/h'(sx)$ is nonincreasing for each $s \in (s_*, 1]$.

If (7.12) is well-defined and its equilibrium is G.A.S. for $s = 1$, then (7.12) is well-defined and its equilibrium is G.A.S., for the same parameters, but $s \in (s_*, 1]$.

(C) Finally, assume that the function h satisfies the following condition

($\mathbf{H_2}$) The function $x \mapsto h'(x)/h'(sx)$ is decreasing for each $s \in (s_*, 1]$.

If (7.12) is well-defined and its equilibrium is L.A.S. for $s = 1$, then (7.12) is well-defined and its equilibrium is L.A.S., for the same parameters, but $s \in (s_*, 1]$.

Proof. (A). Consider the map

$$f_s(x) = x\left(c\,h(x^\alpha) + (b - c)\,h(sx^\alpha)\right) = x j_s^{-1}(x^\alpha).$$

By Lemmas 7.1 and 7.2, equation (7.12) is well-defined and has a unique equilibrium $x_{f_s} = (j_s(1))^{1/\alpha}$. To prove *(i)*, we compute the derivative at the equilibrium,

$$f_s'(x) = j_s^{-1}(x^\alpha) + x\left(j_s^{-1}\right)'(x^\alpha)\,\alpha x^{\alpha-1}.$$

The evaluation of this expression at $x_{f_s} = (j_s(1))^{1/\alpha}$ yields

$$f_s'\left((j_s(1))^{1/\alpha}\right) = 1 + \alpha j_s(1)\left(j_s^{-1}\right)'(j_s(1)) = 1 + \alpha\frac{j_s(1)}{j_s'(1)} = 1 - \frac{2\alpha}{\sigma_s(1)},$$

and then, since $\sigma_s(1) > 0$ holds by Lemma 7.3,

$$-1 < f_s'\left((j_s(1))^{1/\alpha}\right) < 1 \iff \alpha < \sigma_s(1).$$

Similarly, if $0 < \sigma_s(1) < \alpha$ then $f_s'(x_{f_s}) < -1$, so (7.12) is unstable.

By the symmetry of σ_s and applying an analogous argument as the one presented in (7.8)–(7.11), it follows that

$$\sigma_s(z) \gtrless \alpha \quad \forall z \in (1, b_s) \iff ((f_s \circ f_s)(x) - x)(x - x_{f_s}) \gtrless 0 \quad \forall x \in (0, \rho) \setminus \{x_{f_s}\}.$$
$$(7.13)$$

To prove *(ii)*, in view of *(i)* above, (7.8)–(7.11) and Lemma 7.4, just consider the following four scenarios:

- If $\alpha < \sigma_s(z)$ for all $z \in [1, b_s)$, then, by (7.13), $(f_s \circ f_s)(x) \neq x$ for all $x \in (0, \rho) \setminus \{x_{f_s}\}$ and x_{f_s} is L.A.S. Then, x_{f_s} is G.A.S.

- If $\alpha = \sigma_s(1) < \sigma_s(z)$ for all $z \in (1, b_s)$, then, by (7.13), $((f_s \circ f_s)(x) - x)(x - x_{f_s}) < 0$ for all $x \in (0, \rho) \setminus \{x_{f_s}\}$ and $(f_s \circ f_s)'(x_{f_s}) = 1$. The equilibrium x_{f_s} is L.A.S. for $f_s \circ f_s$. Then, x_{f_s} is G.A.S. for f_s.

- If $\alpha > \sigma_s(z)$ for all $z \in (1, b_s)$, then, by (7.13), $(f_s \circ f_s)(x) < x$ for all $x \in (0, x_{f_s})$. Therefore, the equilibrium x_{f_s} is unstable.

- In any other case, the equation $x_{t+1} = f_s(x_t)$ has nonconstant periodic solutions. Hence, the equilibrium x_{f_s} is not G.A.S.

(B). We start by verifying that the function $s \mapsto \sigma_s(z)$ is nonincreasing for each $z \in (1/b_s, b_s)$. Recall that ν_s is nonincreasing in s (see (7.3)), so $(1/b_{\hat{s}}, b_{\hat{s}}) \subset (1/b_s, b_s)$ for any $0 < \hat{s} < s < 1$. Hence, $\sigma_s(z)$ is well-defined if $\sigma_{\hat{s}}(z)$ is. By differentiating with respect to s in

$$ z = c\, h(j_s(z)) + (b - c)\, h(s j_s(z)), $$

we obtain

$$ 0 = c\, h'\,(j_s(z))\, \frac{\partial j_s(z)}{\partial s} + (b - c)\, h'\,(s j_s(z)) \left(j_s(z) + s \frac{\partial j_s(z)}{\partial s} \right), $$

which implies

$$ \frac{\partial \ln\,(j_s(z))}{\partial s} = \frac{\frac{\partial j_s(z)}{\partial s}}{j_s(z)} = \frac{(c - b)\, h'\,(s j_s(z))}{c\, h'\,(j_s(z)) + (b - c)\, s\, h'\,(s j_s(z))} $$
$$ = \frac{(c - b)}{c \dfrac{h'\,(j_s(z))}{h'\,(s j_s(z))} + (b - c) s}. $$

Since condition $(\mathbf{H_1})$ holds and j_s is a decreasing diffeomorphism, we have that the function $z \mapsto \partial(\ln j_s(1/z))/\partial s$ is nondecreasing in $(1/b_s, b_s)$ for each $s \in (s_*, 1]$.

Thus,

$$\frac{\partial}{\partial s}\sigma_s(z) = \frac{\partial}{\partial s}\left(\frac{\tau_s(z) + \tau_s(1/z)}{\ln z}\right) = \frac{\frac{\partial}{\partial s}\ln j_s(1/z) - \frac{\partial}{\partial s}\ln j_s(z)}{\ln z} \leq 0,$$

for all $z \in (1/b_s, b_s) \setminus \{1\}$. Therefore, the function $s \mapsto \sigma_s(z)$ is nonincreasing for each $z \in (1/b_s, b_s)$.

Now, if (7.12) is well-defined for $s = 1$, by Lemma 7.2, we know that (7.12) is well-defined for $s \in (s_*, 1)$, and, if its equilibrium is G.A.S. for $s = 1$, *(A)-(ii)* and the fact that $\sigma_s(1/z) = \sigma_s(z)$ yield

$$\alpha \leq \sigma_1(1) < \sigma_1(z) \leq \sigma_s(z) \quad \text{for all } z \in (1/b_s, b_s) \setminus \{1\} \text{ and } s \in (s_*, 1].$$

Therefore, equation (7.12) is well-defined and its equilibrium is G.A.S. for all $s \in (s_*, 1]$.

(C). Following the same reasoning as in the previous case but using $(\mathbf{H_2})$ instead of $(\mathbf{H_1})$, it is easy to see that the function $s \mapsto \sigma_s(z)$ is decreasing for each $z \in (1/b_s, b_s)$. As a consequence, if the equilibrium of (7.12) is L.A.S. for $s = 1$, the application of *(A)-(i)* yields

$$\alpha \leq \sigma_1(1) < \sigma_s(1), \text{ for all } s \in (s_*, 1],$$

and (7.12) is well-defined and its equilibrium is L.A.S. for all $s \in (s_*, 1]$. $\qquad\square$

Remark 7.7. Notice that $\sigma_s \circ \exp$ is an even function, which makes it more suitable for graphical representations than σ_s itself.

Theorem 7.6 reduces the study of the local or global stability to the study of the relative position of the graph of σ_s with respect to α. Figure 7.1 illustrates this. For a fixed s, the relative position of $\min_{z \in (1, b_s)} \sigma_s(z)$, $\sigma_s(1)$ and α determines the local and global stability of the equilibrium of (7.12). Suppose that the graph of σ_s corresponds to the black curve Figure 7.1a. From (i) and (ii) in Theorem 7.6, we obtain that the equilibrium of (7.12) is unstable for $\alpha > \sigma_s(1)$, L.A.S. but not G.A.S. for

$\min_{z \in (1,b_s)} \sigma_s(z) < \alpha < \sigma_s(1)$, and G.A.S. for $\alpha < \min_{z \in (1,b_s)} \sigma_s(z)$. Figure 7.1b illustrates the special case when the function σ_s reaches a strict global minimum at $z = 1$. In such a situation, the range of values of α for which the equilibrium is L.A.S., thanks to (i) in Theorem 7.6, is contained in the range of values of α for which it is G.A.S., thanks to (ii) in Theorem 7.6. Hence, in this case, Theorem 7.6 completely characterizes the stability of the equilibrium of (7.12): it is G.A.S. for $\alpha \leq \sigma_s(1)$ and unstable for $\alpha > \sigma_s(1)$.
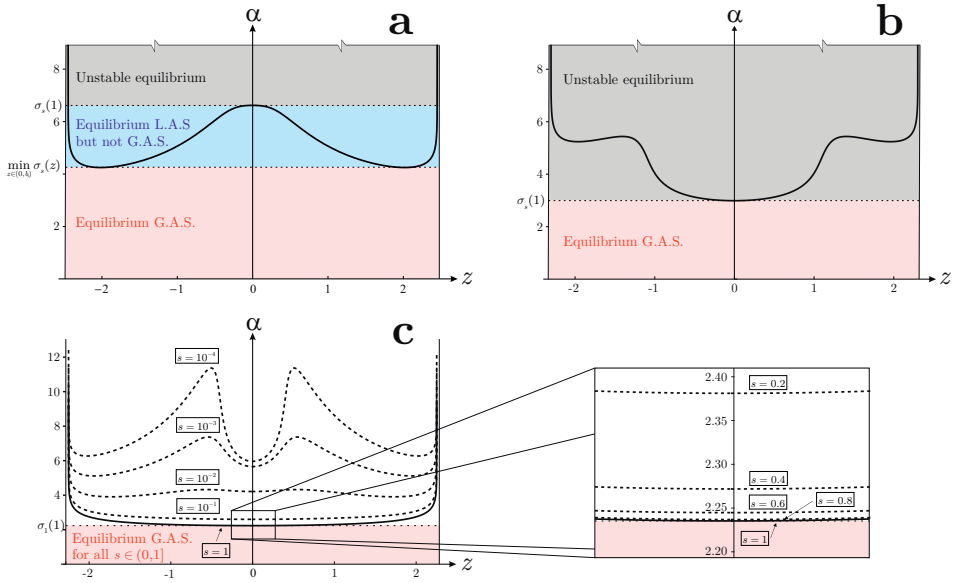
Figure 7.1: In all panels, the black curve represents the graph of $\sigma_1 \circ \exp$. **A:** For $\alpha > \sigma_s(1)$ the equilibrium of (7.12) is unstable, for $\min_{z \in (1,b_s)} \sigma_s(z) < \alpha < \sigma_s(1)$ it is L.A.S. but not G.A.S., and for $\alpha < \min_{z \in (1,b_s)} \sigma_s(z)$ it is G.A.S. **B:** Since σ_s reaches at $z = 1$ a strict global minimum, the equilibrium of (7.12) is G.A.S. for $\alpha \leq \sigma_s(1)$. **C:** The assumption that σ_1 reaches a strict global minimum at $z = 1$ and condition $(\mathbf{H_1})$ are sufficient to guarantee that the graphs of the family of functions $\{\sigma_s\}_{0 < s \leq 1}$ are above the graph of σ_1 and, consequently, the equilibrium of (7.12) is G.A.S. for each $s \in (0,1]$ and $\alpha \leq \sigma_1(1)$.

Figure 7.1c deals with the last part of Theorem 7.6. Assume that $\sigma_1(1)$ is a global minimum of $\sigma_1(z)$ and that condition $(\mathbf{H_1})$ holds. Then, all the graphs of the family

of functions $\{\sigma_s\}_{0<s\leq 1}$ are above the graph of $\sigma_1(z)$ and, therefore, the equilibrium of equation (7.12) is G.A.S. for each $\alpha \leq \sigma_1(1)$ and $0 < s \leq 1$.

Apart from condition $(\mathbf{H_1})$, Theorem 7.6-(B) assumes that (7.12) is well-defined and that its equilibrium is G.A.S. for $s = 1$. But we have already mentioned that guaranteeing the G.A.S. character of an equilibrium is a difficult task. Nevertheless, when the logarithmically scaled diffeomorphism $\phi_s(u) := \ln(j_s(e^u))$ is $\mathcal{C}^3$, we can derive a sufficient condition for $\sigma_s(1)$ to be the strict global minimum of $\sigma_s(z)$.

Corollary 7.8. *If $\phi_s(u) := \ln(j_s(e^u))$ is three times continuously differentiable with $\phi_s'''(u) < 0$ for all $u \in (-\ln b_s, \ln b_s)$, then $\sigma_s(z)$ reaches at $z = 1$ its strict global minimum value.*

Proof. It is routine to check that

$$\left[\frac{d^j \left(\sigma_s\left(e^u\right)u - \sigma_s\left(1\right)u\right)}{du^j}\right]_{u=0} = \left[\frac{d^j \left(\phi_s(-u) - \phi_s(u) - \sigma_s\left(1\right)u\right)}{du^j}\right]_{u=0} = 0,$$

for $j = 0, 1, 2$, and that

$$\frac{d^3 \left(\sigma_s\left(e^u\right)u - \sigma_s\left(1\right)u\right)}{du^3} = \frac{d^3 \left(\phi_s(-u) - \phi_s(u) - \sigma_s\left(1\right)u\right)}{du^3}$$
$$= -\phi_s'''(-u) - \phi_s'''(u) > 0,$$

for $u \in (-\ln b_s, \ln b_s)$. Therefore, $\sigma_s\left(e^u\right)u - \sigma_s(1)u > 0$ for $u \in (0, \ln b_s)$, i.e., $\sigma_s(z) > \sigma_s(1)$ for all $z \in \left(\frac{1}{b_s}, b_s\right) \setminus \{1\}$. $\square$

7.4 APPLICATION TO SOME POPULATION MODELS

The next result characterizes the elements of the family of per capita production functions (7.2) for which condition $(\mathbf{H_1})$ in Theorem 7.6 holds.

Lemma 7.9. *For any $p \in \mathbb{R}$, the function $h\colon \{x \in [0, +\infty) : 1 + px > 0\} \to (0,1)$ defined by $h(x) = \lim_{q \downarrow p} \dfrac{1}{(1 + qx)^{1/q}}$ is a decreasing diffeomorphism. Moreover, h satisfies $(\mathbf{H_1})$ for each $s \in (0,1)$ if and only if $p \geq -1$.*

Proof. Assume $p \neq 0$. Differentiating, we obtain that

$$h'(x) = - (1 + px)^{-(p+1)/p} < 0$$

for any $x \in [0, +\infty)$ such that $1 + px > 0$ and, consequently, the first statement is true.

Moreover,

$$\frac{h'(x)}{h'(sx)} = \frac{- (1 + px)^{-(p+1)/p}}{- (1 + psx)^{-(p+1)/p}} = \left(\frac{1 + psx}{1 + px} \right)^{(p+1)/p} = \left(s + \frac{1 - s}{1 + px} \right)^{(p+1)/p}$$

and

$$\frac{d}{dx} \left(\frac{h'(x)}{h'(sx)} \right) = -(p+1) \left(s + \frac{1 - s}{1 + px} \right)^{1/p} \frac{(1 - s)}{(1 + px)^2},$$

which is non-positive for each $s \in (0,1)$ if and only if $p \in [-1, +\infty) \setminus \{0\}$.

Finally, the result is straightforward for $p = 0$ since $h(x) = e^{-x}$ and $h'(x)/h'(sx) = e^{-(1-s)x}$. □

The following subsections deal with the study of the harvesting model (5.4) for the per capita production functions in Section 7.2. We use a similar procedure based in five steps.

1. First, we rewrite the difference equation that we want to study, which will depend on certain original parameters, as (7.12) with parameters $b, c, s, \alpha, \nu, \mu$ and ρ.

2. We check that h satisfies condition $(\mathbf{H_1})$, thanks to Lemma 7.9.

3. If necessary, we check that (7.12) is well-defined for $s = 1$. Next, we invoke Corollary 7.8 to guarantee that the rewritten difference equation with $s = 1$ has an equilibrium, which is G.A.S.

4. Then, we use statement (B) in Theorem 7.6 to conclude the global stability result for $s \in (s_*, 1]$.

5. Finally, we interpret the result in terms of the original parameters.

7.4.1 BELLOWS MODEL

The per capita production function of the Bellows model is given by $g(x) = \kappa e^{-x^\alpha}$, with $\kappa, \alpha > 0$. The Seno model (5.4) is in this case

$$x_{t+1} = \kappa\theta(1-\gamma)x_t e^{-x_t^\alpha} + \kappa(1-\theta)(1-\gamma)x_t e^{-(1-\gamma)^\alpha x_t^\alpha}, \quad x_0 > 0, \quad (7.14)$$

where $\theta \in [0, 1]$ and $\gamma \in [0, 1)$.

In order to apply the results in Section 7.3, we set $b = \kappa(1-\gamma) > 1, c = \kappa(1-\gamma)\theta, s = (1-\gamma)^\alpha, \rho = +\infty, \nu = 0, \mu = 1$, and $h(x) = e^{-x}$, which is a decreasing diffeomorphism from $(0, +\infty)$ to $(0, 1)$ satisfying condition $(\mathbf{H_1})$ thanks to Lemma 7.9. Notice that (7.12) with $s = 1$ is equivalent to (7.14) with $\theta = 1$. In this case, $b_s = b$ for each $s \in (0, 1]$ and $j_1(z) = \ln(b/z)$ for $z \in (0, b), \sigma_1(1) = 2/\ln b$. Moreover, $\phi_1(u) = \ln(\ln(be^{-u}))$ and $\phi_1'''(u) = -\frac{2}{(\ln(be^{-u}))^3} < 0$ for $u \in (-\ln b, \ln b)$.

Therefore, a direct application of Theorem 7.6, taking into account that $s_* = 0$, $\nu_s = \nu$ and $\alpha_s = +\infty$, for all $s \in [0, 1]$ when $\rho = +\infty$ (see Remark 7.5), yields the following result:

Proposition 7.10. *If $\kappa(1-\gamma) > 1$, then (7.14) has a unique positive equilibrium. If, in addition, $\theta = 1$, then the equilibrium of (7.14) at $x = (\ln(\kappa(1-\gamma)))^{1/\alpha}$ is unstable for $\alpha > 2/\ln(\kappa(1-\gamma))$ and G.A.S. for $\alpha \leq 2/\ln(\kappa(1-\gamma))$. Furthermore, for $\theta < 1$ and $\alpha \leq 2/\ln(\kappa(1-\gamma))$, the equilibrium is also G.A.S.*

Proposition 7.10 characterizes the global stability of the positive equilibrium for the Bellows model without harvesting. Such a result is new, as far as we know, and is interesting in itself. Moreover, Proposition 7.10 confirms that, for the Bellows model, the harvesting effort necessary for stabilization is less for $\theta \in (0,1)$ than for $\theta = 0$ and $\theta = 1$. Since the Bellows model has the Ricker model as a particular case, Proposition 7.10 generalizes [44, Proposition 3.3] and gives an alternative proof of the main result in the previous chapter of this thesis.

7.4.2 Discretization of the Richards model

The per capita production function of the discretization of the Richards model is given by $g(x) = \kappa(1 - x^\alpha)$, with $\kappa, \alpha > 0$. Hence, Seno's model (5.4) reads

$$x_{t+1} = \kappa\theta(1-\gamma)x_t(1-x_t^\alpha) + \kappa(1-\theta)(1-\gamma)x_t(1-(1-\gamma)^\alpha x_t^\alpha), \qquad (7.15)$$

with $x_0 \in (0,1)$, and where $\theta \in [0,1]$ and $\gamma \in [0,1)$.

In this case, it is natural to assume that (7.15) is well-defined for $\gamma = 0$, i.e., that the population model without harvesting makes sense. As mentioned when we presented this per capita production function in Subsection 7.2, equation (7.15) is well-defined for $\gamma = 0$ if and only if $\alpha\kappa < (1+\alpha)^{\frac{1+\alpha}{\alpha}}$.

As in the previous case, we set $b = \kappa(1-\gamma) > 1$, $c = \kappa(1-\gamma)\theta$, $s = (1-\gamma)^\alpha$, $\rho = 1$, $\nu = 0$, $\mu = 1$, and $h(x) = 1 - x$. Clearly, $h(x)$ is a decreasing diffeomorphism from $(0,1)$ to $(0,1)$ and, by Lemma 7.9, satisfies condition ($\mathbf{H_1}$).

We aim to obtain a global stability result for (7.12) with $s = 1$, which is equivalent to (7.15) with $\theta = 1$. Note that (7.12) is well-defined for $s = 1$ because $\alpha b \leq \alpha\kappa < (1+\alpha)^{\frac{1+\alpha}{\alpha}}$. We have also $j_1(z) = 1 - \frac{z}{b}$ for $z \in (0,b)$, being $\sigma_1(1) = \frac{2}{b-1}$, $\phi_1(u) = \ln\left(1 - \frac{e^u}{b}\right)$, and $\phi_1'''(u) = -\frac{be^u(b+e^u)}{(b-e^u)^3} < 0$. Then, $\sigma_1(z) > \frac{2b}{b-1}$ for $z > 1$ and the equilibrium of (7.12) is G.A.S. for $s = 1$ if $\alpha \leq \frac{2b}{b-1}$, i.e., if $b(\alpha - 2) \leq \alpha$.

In order to use Theorem 7.6, we need to impose $s > s_* = \max\{0, 1 - \frac{1}{b-c}\}$, or what is the same, $\nu_s b = (b-c)(1-s) < 1$. For the selected values of the parameters,

this is always true because

$$(b-c)(1-s) = (1-\theta)\kappa(1-\gamma)(1-(1-\gamma)^{\alpha}) \leq \kappa(1-\gamma)(1-(1-\gamma)^{\alpha}) < 1,$$

where we have used that $x_{t+1} = \kappa x_t(1-x_t^{\alpha})$, $x_0 \in (0,1)$ is well-defined.

Proposition 7.11. *If $\kappa(1-\gamma) > 1$ and $\alpha\kappa < (1+\alpha)^{\frac{1+\alpha}{\alpha}}$, then (7.15) is well-defined and has a unique positive equilibrium. If, in addition, $\theta = 1$, then the equilibrium of (7.15) is unstable for $\kappa(1-\gamma)(\alpha-2) > \alpha$ and G.A.S. for $\kappa(1-\gamma)(\alpha-2) \leq \alpha$. Furthermore, for $\theta < 1$ and $\kappa(1-\gamma)(\alpha-2) \leq \alpha$, the equilibrium of (7.15) is also G.A.S.*

To the best of our knowledge, Proposition 7.11 gives the first global stability result for the discretization of the Richards model even in the case without harvesting. Notice that the results in [140] cannot be used in this case since $\rho \neq +\infty$. In the harvesting framework, Proposition 7.11 includes [44, Proposition 3.6] as a particular result, where the quadratic model was considered.

7.4.3 Maynard-Smith-Slatkin model

If we focus on populations governed by the Maynard-Smith-Slatkin model, the per capita production function is given by $g(x) = \dfrac{\kappa}{1+x^{\alpha}}$, where $\kappa > 0$ and $\alpha > 0$. In that case, model (5.4) is

$$x_{t+1} = \kappa\theta(1-\gamma)\frac{x_t}{1+x_t^{\alpha}} + \kappa(1-\theta)(1-\gamma)\frac{x_t}{1+(1-\gamma)^{\alpha}x_t^{\alpha}}, \qquad (7.16)$$

where $\theta \in [0,1]$ and $\gamma \in [0,1)$.

In [44], following [1, Appendix S1] and [141, Theorem 1], it was stated that the equilibrium of (7.16) for $\theta = 0$ is G.A.S. if $1 < \kappa(1-\gamma) \leq \frac{\alpha}{\alpha-2}$. No result is known about global convergence for the production function (7.16), in the general case. However, this model can be easily handled by using Theorem 7.6 and Lemma 7.9.

Consider (7.12) with $b = \kappa(1-\gamma) > 1$, $c = \kappa(1-\gamma)\theta$, $s = (1-\gamma)^\alpha$, $\rho = +\infty$, $\nu = 0$, $\mu = 1$ and $h(x) = 1/(1+x)$, which satisfies condition $(\mathbf{H_1})$ by Lemma 7.9. Then, $j_1(x) = \frac{b}{x} - 1$, $\sigma_1(1) = \frac{2b}{b-1}$, $\phi_1(u) = \ln\left(be^{-u} - 1\right)$, and $\phi_1'''(u) = -\frac{be^u(b+e^u)}{(b-e^u)^3} < 0$.

Now, observe again that (7.12) with $s = 1$ corresponds to (7.16) with $\theta = 1$, and apply Theorem 7.6 taking into account that $s_* = 0$, $\nu_s = \nu$ and $\alpha_s = +\infty$ for all $s \in [0,1]$ when $\rho = +\infty$ (see Remark 7.5).

Proposition 7.12. *If $\kappa(1-\gamma) > 1$, then (7.16) has a unique positive equilibrium. If, in addition, $\theta = 1$, then the equilibrium of (7.16) is unstable for $\kappa(1-\gamma)(\alpha-2) > \alpha$ and G.A.S. for $\kappa(1-\gamma)(\alpha-2) \leq \alpha$. Furthermore, for $\theta < 1$ and $\kappa(1-\gamma)(\alpha-2) \leq \alpha$, the equilibrium is also G.A.S.*

It is interesting to note that considering the exponent parameter α in the quadratic model, i.e., studying the discretization of the Richards model, unveils the complete parallelism between the Maynard-Smith-Slatkin model and the quadratic model with respect to stability results.

7.4.4 Hassell and Thieme models

As already mentioned, topologically conjugated production functions give rise to equivalent dynamical behaviors. However, when a convex combination of the type of (5.4) is applied to two topologically conjugated production functions, the transformed systems could exhibit different dynamical behaviors.

When applying Theorem 7.6, while working in the case $s = 1$, we can replace our production function by a topologically conjugated one, for which calculations are simpler. This replacement is no longer valid when checking condition $(\mathbf{H_1})$.

In this subsection, we put into practice this approach to study the two models still left: Thieme's and Hassell's models. Since Thieme's model has Hassell's model as a particular case, we only consider the former. Besides, without loss of generality, we

assume the per capita production function of the the Thieme model to be given by

$$g(x) = \frac{\kappa}{(1 + x^\alpha)^\beta}, \quad \kappa, \alpha, \beta > 0.$$

Now, the change of variables $y_t = x_t^{1/\beta}$ shows that the dynamics of the difference equation

$$x_{t+1} = \frac{\kappa x_t}{(1 + x_t^\alpha)^\beta} \tag{7.17}$$

are identical of those of the equation

$$y_{t+1} = \frac{\kappa^{1/\beta} y_t}{1 + y_t^{\alpha\beta}},$$

whose per capita production function, $g(x) = \dfrac{\kappa^{1/\beta}}{1 + x^{\alpha\beta}}$, belongs to the Maynard-Smith-Slatkin family of maps. This provides a straightforward way to characterize the global stability of the Thieme model.

Proposition 7.13. *If $\kappa > 1$, then (7.17) has a unique equilibrium. In addition, the equilibrium of (7.17) is unstable for $\kappa^{1/\beta}(\alpha\beta - 2) > \alpha\beta$ and G.A.S. for $\kappa^{1/\beta}(\alpha\beta - 2) \leq \alpha\beta$.*

The previous result improves the global stability condition presented in [206] with a simpler proof than the one used in [140], which relies on calculating the sign of a certain Schwarzian derivative.

The Seno model (5.4) for the Thieme production function is

$$x_{t+1} = \frac{\kappa\theta(1 - \gamma)x_t}{(1 + x_t^\alpha)^\beta} + \frac{\kappa(1 - \theta)(1 - \gamma)x_t}{(1 + (1 - \gamma)^\alpha x_t^\alpha)^\beta}. \tag{7.18}$$

Again, in order to apply the results in Section 7.3, we set $b = \kappa(1 - \gamma) > 1, c = \kappa(1 - \gamma)\theta$ and $h(x) = \dfrac{1}{(1 + x)^\beta}$, which is a decreasing diffeomorphism from $(0, +\infty)$

to $(0, 1)$ satisfying condition $(\mathbf{H_1})$ thanks to Lemma 7.9. We obtain the following new result about the Thieme model under harvesting.

Proposition 7.14. *If $\kappa(1 - \gamma) > 1$, then (7.18) has a unique positive equilibrium. If, in addition, $\theta = 1$, then the equilibrium of (7.18) is unstable for $[\kappa(1 - \gamma)]^{1/\beta}(\alpha\beta - 2) > \alpha\beta$ and G.A.S. for $[\kappa(1 - \gamma)]^{1/\beta}(\alpha\beta - 2) \leq \alpha\beta$. Furthermore, for $\theta < 1$ and $[\kappa(1 - \gamma)]^{1/\beta}(\alpha\beta - 2) \leq \alpha\beta$, the equilibrium is also G.A.S.*

Altogether, we have shown that Conjecture 5.4 holds when restricted to the per capita production functions **[M1-M8]**. Indeed, we have shown that a stronger result holds since we are able to guarantee that the equilibrium is G.A.S. for $\theta \in (0, 1)$. Furthermore, using part C of Theorem 7.6 we obtain the following general local stability result in the spirit of Conjecture 5.4.

Corollary 7.15. *Assume that $g \colon (0, +\infty) \to (0, +\infty)$ satisfies $(\mathbf{H_2})$, $g'(x) < 0$ for all $x > 0$, $g(0^+) > 1$, and there exists some $d > 0$ such that $xg(x)$ is strictly increasing on $(0, d)$ and strictly decreasing on $(d, +\infty)$. Then, if the equilibrium of (5.4) with $\theta = 0$ is L.A.S., then the equilibrium of (5.4) is L.A.S. for all $\theta \in [0, 1]$.*

7.5 DISCUSSION AND CONCLUSIONS

This chapter completes and concludes the study conducted in this thesis about the effect of harvesting time on the stability of managed populations. This study revolves around Conjecture 5.4, in which Cid et al. stated that for compensatory models the moment of intervention has no effect on the local stability [44]. Cid et al. showed in [44] that this conjecture is true, even for global stability, in the case of the quadratic map and the Beverton-Holt model. Although in Chapter 5 we disproved the conjecture for general compensatory models, we expected it to be true for many models common in population dynamics, which in most cases are known to satisfy additional conditions, e.g., negative Schwarzian derivative. This led us to prove in Chapter 6 that harvest timing does not affect the global stability in the Ricker case. Apart from Theorem 5.2,

where we proved that the moment of intervention does not affect the stability when the harvesting effort is high enough, little was known about the effect of the harvest time on the stability of models different from the quadratic map or the Beverton-Holt and Ricker models.

The results presented in this chapter help to fill this gap. We have introduced an innovative approach called *exponent analysis*, which reduces the study of the local or global stability of populations subject to delayed harvesting to the analysis of the relative position of the graph of a certain function with respect to an exponent parameter. The application of this method allowed us to obtain new local and global stability results for many common compensatory population models, which are encompassed under the so called generalized α-Ricker model [151]. In other cases, shorter proofs of already known results were obtained.

In particular, the application of the exponent analysis to the Bellows model allowed us to characterize its global stability, even in the case without harvesting. To the best of our knowledge, this is a new result. The study of this case illustrates the power of the method introduced in this chapter, since the main result in Chapter 6 is directly derived, given that the Ricker model is a particular case of the Bellows model. Similarly, the application of the exponent analysis to the discretization of the Richards model allowed us to conclude a global stability result for this model even in the absence of harvesting. This is, as far as we know, the first global stability result for this model. Sharp global stability results were also obtained by the application of the method to the Maynard-Smith-Slatkin and the Thieme models under delayed harvesting (also for the Hassell model as a particular case of the latter). In particular, for the Thieme model without harvesting, the global stability condition provided in [206] was improved and a simpler proof than the one used in [140] was provided.

Finally, the study conducted in this chapter allowed us to determine additional conditions for compensatory models that yield a local stability result in the spirit of Conjecture 5.4.

8

Stability for one-dimensional discrete dynamical systems revisited

8.1 INTRODUCTION

One-dimensional discrete-time dynamical systems are used to describe a large number of processes in a wide range of fields, e.g., the population growth of species with nonoverlapping generations [206]. Usually, these processes are modeled by considering an appropriate family of maps depending on meaningful parameters and fitting them to sample data. For most of these models, parameter restrictions ensuring the existence and uniqueness of an equilibrium can be easily determined. The next step towards determining the dynamics of the model consists in studying the stability of the equilibrium. In general, conditions asserting the local stability are also easy to find. Yet, the most desirable stability property is the global stability, since it allows to know the fate of all solutions with independence of the initial condition. Unfortunately, as

already pointed out and contrary to the local stability, proving the global stability is in most cases a hard task.

The statement 'L.A.S. implies G.A.S.' meaning that the local asymptotic stability of the equilibrium implies its global asymptotic stability is common in the literature. This statement appeared for the first time in [137, 154], and has been backed up by several papers corroborating it for the most typical models in discrete-time population dynamics [16, 57, 73, 80, 89, 95, 126, 140, 142, 169]. Nevertheless, the property is not true in general; see for example [55, 145].

The above considerations highlight the relevance of finding sufficient conditions ensuring the global stability of the equilibrium. On paper, such conditions can be easily found. For instance, a well-known necessary and sufficient condition for the global stability is the absence of period two orbits. However, this condition is hard to test. It is in this sense that several papers have focused on finding sufficient conditions easier to test and, in some cases, providing methods to test them. Prominent among these are the results for S-maps (unimodal maps with negative Schwarzian derivative) independently obtained by Allwright [5] and Singer [194], or the *enveloping* method introduced by Cull and Chaffee [58].

The aim of this chapter is to provide a new method for studying the local and global stability of one-dimensional discrete-time models. These models are frequently of the form

$$x_{n+1} = x_n g(x_n), \quad x_0 \in \operatorname{dom} g, \tag{8.1}$$

with g belonging to a certain family of positive maps with $\operatorname{dom} g \subset (0, +\infty)$. Instead of directly considering such models, the proposed method considers topologically conjugated models of the form

$$\Delta y_n = h(y_n), \quad y_0 \in \operatorname{dom} h, \tag{8.2}$$

where $\Delta y_n := y_{n+1} - y_n$ and $h = \ln \circ g \circ \exp$. Notice that the change of variables $y_n = \ln(x_n)$ transforms (8.1) into (8.2).

The study of the stability of model (8.2) is reduced to the study of the graph of a certain family of functions in a similar way to the exponent analysis introduced in the previous chapter. The method introduced here allows to complement and extend some existing conditions for the global stability. In particular, it allows us to give a sufficient condition for the global stability of (8.2), namely,

$$3(h'')^2 > h'h''',$$

which, obviously, is strictly weaker than $3(h'')^2 > 2h'h'''$, i.e., than h having negative Schwarzian derivative.

The rest of this chapter is organized as follows. Section 8.2 contains some preliminary results and definitions. The method for the analysis of the global stability is introduced in Section 8.3. In Section 8.4 we illustrate the applicability of the method. Section 8.5 studies the relationship of this method with the enveloping technique. Finally, Section 8.6 discusses the implications and limitations of our results.

8.2   DEFINITIONS AND PRELIMINARY RESULTS

This section collects some preliminary results and definitions. Although all of them could be considered as standard results and concepts, they are included here for the sake of completeness and to fix notation. We use these preliminaries in the proofs of the main results presented in the next section.

Throughout this section $I \subset \mathbb{R}$ is an interval (bounded or unbounded), f is a continuous map from I to itself and $x_f \in I$ is a fixed point of f, i.e., $f(x_f) = x_f$. As usual, we denote

$$f^{(0)} := \mathrm{id}, \quad f^{(n+1)} = f \circ f^{(n)}, \quad n \geq 1, \, n \in \mathbb{N}, \tag{8.3}$$

with id denoting the identity map; i.e., $\mathrm{id}(x) = x$ for all $x \in I$.

Remark 8.1. In what follows, the domains of the identity and constant functions are assumed to be the largest sets for which the corresponding expressions make sense.

Definition 8.2. We say that x_f is:

- *Stable* if for each neighborhood V of x_f in I there exists a neighborhood U of x_f in I such that $f^{(n)}(x) \in V$ for all $x \in U$, $n \geq 1$, i.e., if the family of maps $\{f^{(n)}\}_{n \geq 1}$ is equicontinuous at x_f.

- *Unstable* if there exits a sequence $x_n \to x_f$ such that
$$\limsup_n \left| f^{(n)}(x_n) - x_f \right| > 0,$$
i.e., if x_f is not stable.

- *A local repeller* if there exists a sequence $x_m \to x_f$ such that
$$\inf_m \liminf_n |f^{(n)}(x_m) - x_f| > 0.$$

- *A global repeller* if the sequence $(f^{(n)}(x))_n$ has no accumulation points in I for any $x \in I \setminus x_f$.

- *A local attractor* if there exists a neighborhood $V \subset I$ of x_f such that
$$\lim_{n \to +\infty} f^{(n)}(x) = x_f$$
for all $x \in V$.

- *A global attractor* if
$$\lim_{n \to +\infty} f^{(n)}(x) = x_f$$
for all $x \in I$.

Proposition 8.3. *The following statements are equivalent:*

a) x_f *is a global attractor.*

b) $(f^{(n)}(x) - x)(x_f - x) > 0$ *for all* $x \in I \setminus \{x_f\}$, $n \geq 1$.

c) $(f^{(n+m)}(x) - f^{(m)}(x))(x_f - f^{(m)}(x)) > 0$ *for all* $x \in I$ *such that* $f^{(m)}(x) \neq x_f$, $n, m \geq 1$.

d) $f^{(2)}(x) \neq x$ *and* $\left[\inf_{n \geq 1} f^{(n)}(x), \sup_{n \geq 1} f^{(n)}(x) \right] \subset I$ *for all* $x \in I \setminus \{x_f\}$.

e) $f^{(2)}(x) \neq x$ *for all* $x \in I \setminus \{x_f\}$ *and there exists* $n \geq 1$ *such that* x_f *is stable for* $f^{(n)}$.

f) $(f^{(2)}(x) - x)(x_f - x) > 0$ *for all* $x \in I \setminus \{x_f\}$.

Moreover, if x_f *is a global attractor, then it is stable and* $f^{(n)} \to x_f$ *uniformly on compact subsets of* I.

Proof. First, we show that $a) \implies b) \implies c) \implies a)$.

$a) \implies b)$. Since x_f is a global attractor, there are no periodic points other than x_f. Then, for each $n \geq 1$, the difference $f^{(n)}(x) - x$ has constant sign for all $x \in I$, $x < x_f$. If this sign were negative for certain $n_0 \geq 1$, then we would have $f^{(n_0)}(x) < x$ and the sequence $(f^{(jn_0)}(x))_j$ would be strictly decreasing. But this is impossible because we are assuming that x_f is a global attractor. A similar argument works for $x > x_f$. Thus, $(f^{(n)}(x) - x)(x - x_f) < 0$ for all $x \in I \setminus \{x_f\}$, $n \geq 1$.

$b) \implies c)$. Just apply b), changing x by $f^{(m)}(x)$.

$c) \implies a)$. Let $x \in I$ with $f^{(m)}(x) \neq x_f$, $m \geq 1$ and consider the sequence $(f^{(n)}(x))_n$. By c), the subsequence of $(f^{(n)}(x))_n$ formed by the terms smaller than x_f is strictly increasing, whereas the subsequence formed by the terms greater than x_f is strictly decreasing. Besides, x_f is the only candidate to accumulation point of the sequence. Thus, $\lim_{n \to +\infty} f^{(n)}(x) = x_f$ for all $x \in I$.

Second, we show that $a) \implies d) \implies b)$, so that $a) \iff b) \iff c) \iff d)$.

$a) \implies d)$. Trivial.

$d) \implies b)$. Invoking Sharkovskii's Theorem [193], we know that $f^{(n)}(x) \neq x$ for all $x \in I \setminus \{x_f\}$. Assume that there exists $n_0 \geq 1$ such that $(f^{(n_0)}(x) - x)(x_f - x) < 0$ for all x, say, to the right of x_f. Then, the sequence $(f^{(jn_0)}(x))_j$ converges (because it is bounded and increasing) towards a point $c > x_f$ in I. But this is impossible, since by continuity c must satisfy $c = f^{(n_0)}(c)$.

Third, we prove that x_f is stable whenever it is G.A.S. Assume x_f to be G.A.S. For each $x \in I$, the subsequence of $(f^{(n)}(x))_n$ formed by the terms smaller than x_f is increasing, whereas the subsequence formed by the terms greater than x_f is decreasing. Then, the functions $h_n(x) = \sup_{m \geq n} f^{(m)}(x)$ and $j_n(x) = \inf_{m \geq n} f^{(m)}(x)$ are continuous for all $n \geq 1$. Clearly, $h_n \geq f^{(n)} \geq j_n$ and h_n, j_n both converge uniformly on compact sets to x_f as they are monotone sequences (Dini's Theorem). Therefore, $f^{(n)}$ itself converges uniformly on compact sets to x_f. A convergent sequence of functions defined on a compact metric space is equicontinuous if and only if it converges uniformly (a consequence of the Theorem of Arzelà-Ascoli). Therefore, $\{f^{(n)}\}_n$ is equicontinuous at x_f, i.e., x_f is stable.

Now, it is obvious that $a) \implies e)$. Let us prove that $e) \implies d)$ (keep in mind that it has already been proved that $a) \iff b) \iff c) \iff d)$).

Assume $f^{(2)}(x) \neq x$ for all $x \in I \setminus \{x_f\}$ to hold and suppose that neither $b)$ nor $d)$ is met. Then, there exists $n_0 \geq 1$ such that $f^{(n_0)}(x) < x$, for all $x \in I \cap (-\infty, x_f)$, or $f^{(n_0)}(x) > x$, for all $x \in I \cap (x_f, +\infty)$. Consider an arbitrary $n \geq 1$. Then, the sequence $\left(f^{(jnn_0)}(x)\right)_j$ has no convergent subsequences in I. Consequently, x_f is unstable for $f^{(n)}$, which contradicts $e)$.

Since it is obvious that $b) \implies f)$, to finish the proof it suffices to show that $f) \implies e)$.

Let U be any interval containing x_f and consider $V = U \cup f(U)$. Statement $f)$ implies that $(f(x) - x)(x_f - x) > 0$ and $(f^{(2)}(x) - f(x))(f(x) - x_f) > 0$ for

any $x \in I \setminus \{x_f\}$. Using these inequalities, we have $f(V) \subset V$. Therefore, x_f is stable for f. □

Proposition 8.4. *The following statements are equivalent:*

a) *x_f is a local attractor.*

b) *x_f belongs to the interior of a closed interval $J \subset I$ such that $f(J) \subset J$ and x_f is a global attractor for the restriction $f_{|J}$.*

In particular, if x_f is a local attractor, then it is stable and $f^{(n)} \to x_f$ uniformly on a compact interval of x_f.

Proof. $a) \implies b)$. Since f is continuous and x_f is a local attractor, $f^{(n)}(x) - x < 0$ for $x \in V \cap (-\infty, x_f)$ or $f^{(n)}(x) - x > 0$ for $x \in V \cap (-\infty, x_f)$. Assume there is $n_0 \geq 1$ such that $f^{(n_0)}(x) - x < 0$ for $x \in V \cap (-\infty, x_f)$. The set $C = \{x \in I \cap (-\infty, x_f) : f^{(n_0)}(x) = x\}$ cannot be empty, because otherwise the sequence given by $x_j = f^{(jn_0)}(x)$, $x \in I \cap (-\infty, x_f)$, would be strictly decreasing. But that is impossible because $\left(f^{(n)}(x) \right)_n$ converges to x_f provided that $x \in V \cap (-\infty, x_f)$. Define $x_0 := \sup C \cap (-\infty, x_f)$. We consider two cases. On the one hand, let us suppose that $f^{(n_0)}((x_0, x_j)) \subset (x_0, x_j)$. Then, the sequence given by $x_j = f^{(jn_0)}(x)$, $x \in I \cap (x_0, x_f)$, would be strictly decreasing—what we know is impossible. On the other hand, let us suppose that $[x_0, x_j) \subset f^{(n_0)}((x_0, x_j))$. Then, we can construct a sequence $x_m \to x_f$ in (x_0, x_f) such $x_{m-1} = f^{(n_0)}(x_m) < x_m$, for all $m > 0$. Thus, for all $n > m$, we have

$$f^{(nn_0)}(x_m) = f^{(nn_0 - n_0)}(x_{m-1}) = \cdots = f^{(nn_0 - mn_0 + n_0)}(x_1) = f^{(nn_0 - mn_0)}(x_0) = x_0.$$

But this is impossible because the sequence $\left(f^{(nn_0)}(x_m) \right)_n$ must converge to x_f if $x_m \in V$. Therefore, we have shown that $f^{(n)}(x) - x > 0$ for $x \in V \cap (-\infty, x_f)$, $n \geq 1$. And a similar argument leads to

$$(f^{(n)}(x) - x)(x_f - x) > 0, \text{ for all } x \in V \setminus \{x_f\}, \, n \geq 1. \qquad (8.4)$$

Now, choose an interval $[a, b]$ such that $x_f \in [a, b] \subset V$ and $f([a, b]) \subset V$. Using (8.4), $J := [a, b] \cup f([a, b])$ satisfies $f(J) \subset J$. Finally, (8.4) implies that $b)$ in Proposition 8.3 holds for $f_{|J}$, therefore x_f is a global attractor for $f_{|J}$.

$b) \implies a)$. Trivial. $\qquad\qquad\qquad\qquad\qquad\qquad\qquad\qquad\qquad\qquad\qquad\qquad\square$

We recall that x_f is G.A.S. if it is a stable global attractor. Similarly, x_f is L.A.S. if it is a stable local attractor. Propositions 8.3 and 8.4 show the known fact that, in the one-dimensional case, x_f is G.A.S. (L.A.S.) if and only if it is a global attractor (local attractor). As usual in the literature, in what follows we will call x_f G.A.S. (L.A.S.) instead of global attractor (local attractor).

The following two results give sufficient conditions to classify x_f.

Proposition 8.5.   *a) If $(f^{(2)}(x) - x)(x_f - x) < 0$ for all $x \in I \setminus \{x_f\}$, then x_f is a global repeller.*

    b) If $(f^{(2)}(x) - x)(x_f - x) < 0$ for all $x \in U \setminus \{x_f\}$, where U is neighborhood of x_f in I, then x_f is a local repeller.

Proof. a) For each $x \in I \setminus \{x_f\}$, the sequences $\left(f^{(2n)}(x)\right)_n$ and $\left(f^{(2n+1)}(x)\right)_n = \left(f^{(2n)}(f(x))\right)_n$ are monotone and move away from x_f. If any of these sequences had a convergent subsequence, the limit of the subsequence would be a fixed point of $f^{(2)}$. But that is impossible by our assumption. Therefore, the sequence $\left(f^{(n)}(x)\right)_n$ has not accumulation points in I.

b) If $C = \{x \in I \setminus \{x_f\} : f^{(2)}(x) = x\}$ is the empty set, we can use $a)$. In other case, define $x_0 := \inf C \cap (x_f, +\infty)$ and $y_0 := \sup C \cap (-\infty, x_f)$. On the one hand, let us suppose that

$$x_0 = \sup_{x_f < x < x_0} f^{(2)}(x) \quad \text{and} \quad y_0 = \inf_{x_f < x < y_0} f^{(2)}(x).$$

We can select a sequence $(x_m)_m$ in (x_f, x_0) such that $f(x_m) \in (y_0, x_0)$ for all m. Thus, the sequences $\left(f^{(2n)}(x_m) \right)_n$, $\left(f^{(2n+1)}(x_m) \right)_n$ in (y_0, x_0) are monotone and move away from x_f, so they do not have a subsequence converging to any point of (y_0, x_0). Consequently,

$$\inf_m \liminf_n |f^{(n)}(x_m) - x_f| \geq \min\{|x_0 - x_f|, |y_0 - x_f|\} > 0. \qquad (8.5)$$

On the other hand, let us suppose that

$$x_0 < \sup_{x_f < x < x_0} f^{(2)}(x) \quad \text{or} \quad y_0 > \inf_{x_f < x < y_0} f^{(2)}(x).$$

We assume that the first inequality holds, since in the other case the reasoning is similar. In such a case, we can define a sequence $x_m \to x_f$ in (x_f, x_0) such that $x_{m-1} = f^{(2)}(x_m) > x_m$, for all $m > 0$. Thus, for all $n > m$,

$$f^{(2n)}(x_m) = f^{(2n-2)}(x_{m-1}) = \cdots = f^{(2n-2m+2)}(x_1) = f^{(2n-2m)}(x_0) = x_0$$

and

$$f^{(2n+1)}(x_m) = f\left(f^{(2n)}(x_m) \right) = f(x_0).$$

Again, the sequences $\left(f^{(2n)}(x_m) \right)_n$ and $\left(f^{(2n+1)}(x_m) \right)_n$ in (y_0, x_0) do not have any convergent subsequence with limit in (y_0, x_0), and (8.5) holds. $\qquad \square$

Proposition 8.6. *If $f: I \to I$ is continuously differentiable, then:*

a) *$|f'(x)| < 1$ for all $x \in I$ implies that x_f is G.A.S.*

b) *$|f'(x_f)| < 1$ implies that x_f is L.A.S.*

c) *$|f'(x_f)| > 1$ implies that x_f is unstable (local repeller).*

d) *$(f^{(2)}(x) - x)(x_f - x) \geq 0$ for all x in a neighborhood of x_f implies that x_f is stable.*

Proof. *a)* We have $(f^{(2)}(x) - x)' < 0$ for all $x \in I$, and $f^{(2)}(x_f) - x_f = 0$. Integrating we obtain that $(f^{(2)}(x) - x)(x_f - x) > 0$ for all $x \in I \setminus \{x_f\}$, and it suffices to use Proposition *8.3.f)* to finish the proof of this part.

b) It is a direct consequence of Proposition *8.4.b)*.

c) We omit the proof since it follows the reasoning in part *a)*, but using Proposition 8.5.

d) Assume, without loss of generality, that $|f'(x_f)| \geq 1$. Then, $(f^{(2)})'(x_f) \geq 1$ and

$$(f^{(2)}(x) - x_f)(x_f - x) \leq 0, \qquad (f^{(2)}(x) - x)(x_f - x) \geq 0 \qquad (8.6)$$

for all x in a neighborhood of x_f. Finally, (8.6) implies $f^{(2n)}((x_f - \varepsilon, x_f + \varepsilon)) \subset (x_f - \varepsilon, x_f + \varepsilon)$, for all $n \geq 1$ and $\varepsilon > 0$ small enough. $\qquad \square$

8.3   STABILITY ANALYSIS

In this section we introduce our method for the stability analysis, which is based on models of the form

$$\Delta y_n = h(y_n), \quad h \in \mathfrak{G}_*, y_0 \in \operatorname{dom} h, \qquad (8.7)$$

where

$$\mathfrak{G}_* := \bigcup_{-\infty \leq \alpha < \beta \leq +\infty} \mathfrak{G}_*(\alpha, \beta) \qquad (8.8)$$

and

$$\mathfrak{G}_*(\alpha, \beta) := \{h \in \mathcal{C}^1(\alpha, \beta) : \alpha < \operatorname{id} + h < \beta, h' < 0, h(\beta) < 0 < h(\alpha)\}. \qquad (8.9)$$

After analyzing these models, we will see that topological conjugacy allows us to translate all the stability results obtained for them to positive models in the form of (8.1).

8.3.1 STABILITY OF SINGLE MAPS

We start our study by defining which stability properties can be associated with (8.7) for a given $h \in \mathfrak{G}_*$. It is clear that for each $h \in \mathfrak{G}_*$ there exists a unique $y_h \in \operatorname{dom} h$ such that $h(y_h) = 0$. We say that $h \in \mathfrak{G}_*$ is G.A.S. (respectively, L.A.S. or unstable) when y_h is G.A.S. (respectively, L.A.S. or unstable) for the map $\operatorname{id} + h$. To facilitate the study of these properties, we define a function from $\mathfrak{G}_*$ to $\mathfrak{C} = \bigcup_{-\infty \leq \alpha < \beta \leq +\infty} \mathcal{C}(\alpha, \beta)$

as follows.

Definition 8.7. We denote by σ the function $\sigma \colon \mathfrak{G}_* \to \mathfrak{C}$ defined by $h \to \sigma(h) := \sigma_h$, with

$$\sigma_h \colon (-b_h, b_h) \to (0, +\infty), \qquad \sigma_h(u) = \begin{cases} \frac{h^{-1}(-u) - h^{-1}(u)}{u} & \text{if} \quad u \neq 0, \\ \frac{-2}{h'(y_h)} & \text{if} \quad u = 0, \end{cases}$$

$$(8.10)$$

where $b_h := \min\{-\inf h, \sup h\}$.

The expression of σ_h in (8.10) is intricate but can be calculated explicitly for certain maps. For instance, $\sigma_{-\operatorname{id}} = 2$. If the domain of the minus identity function in the previous equality is (α, β), with $\alpha < 0 < \beta$, then the domain of the constant function $\sigma_{-\operatorname{id}}$ is $(-b, b)$, where $b = \min\{-\alpha, \beta\}$.

Some basic properties of σ are listed in the following result. In particular, it informs us that σ_h is invariant under translations of the equilibrium point for h and how it behaves under changes of scale.

Proposition 8.8. *Let $h \in \mathfrak{G}_*$. The following statements hold:*

a) *σ_h is continuous, even and positive.*

b) *If $(\operatorname{id} + h)^{(2)}(y) = y$, then $h(y) \in \operatorname{dom} \sigma_h$.*

c) *If $a, b, c \in \mathbb{R}$ are such that $bh \circ (a \operatorname{id} + c) \in \mathfrak{G}_*$, then $\sigma_{bh\circ(a \operatorname{id} + c)} = \frac{1}{ab}\sigma_h \circ \left(\frac{1}{b} \operatorname{id}\right)$.*

d) If $h \in \mathfrak{G}_* \cap C^3(\operatorname{dom} h)$, *then*

$$\sigma'_h(0) = 0$$

$$\sigma''_h(0) = -\frac{2}{3}(h^{-1})'''(0) = -\frac{6(h''(y_h))^2 - 2h'(y_h)h'''(y_h)}{3(h'(y_h))^5}.$$

Proof. *a).* It is straightforward that σ_h is an even and continuous function for $u \neq 0$. Moreover, by using L'Hôpital's rule we obtain

$$\lim_{u \to 0} \frac{h^{-1}(-u) - h^{-1}(u)}{u} = -2\left(h^{-1}\right)'(0) = \frac{-2}{h'(h^{-1}(0))} = \frac{-2}{h'(y_h)}.$$

Hence, σ_h is continuous. Finally, the positivity of σ_h follows from the fact that $h' < 0$ as $h \in \mathfrak{G}_*$.

b). Assume that $y \in \operatorname{dom} h$ satisfies $(\operatorname{id} + h)^{(2)}(y) = y$. This means that $h(y + h(y)) + h(y) = 0$, which implies $\inf h < -h(y) < \sup h$. Therefore,

$$\max\{\inf h, -\sup h\} < h(y) < \min\{-\inf h, \sup h\},$$

or what is the same, $h(y) \in (-b_h, b_h) = \operatorname{dom} \sigma_h$.

c). Operating,

$$\sigma_{bh}(u) = \frac{(bh)^{-1}(-u) - (bh)^{-1}(u)}{u} = \frac{1}{b}\frac{h^{-1}(-\frac{1}{b}u) - h^{-1}(\frac{1}{b}u)}{\frac{1}{b}u} = \frac{1}{b}\sigma_h\left(\frac{1}{b}u\right).$$

$$\sigma_{h \circ a\,\mathrm{id}}(u) = \frac{(h \circ a\,\mathrm{id})^{-1}(-u) - (h \circ a\,\mathrm{id})^{-1}(u)}{u} = \frac{\frac{1}{a}h^{-1}(-u) - \frac{1}{a}h^{-1}(u)}{u}$$

$$= \frac{1}{a}\sigma_h(u).$$

$$\sigma_{h \circ (\mathrm{id}+c)}(u) = \frac{(h \circ (\mathrm{id}+c))^{-1}(-u) - (h \circ (\mathrm{id}+c))^{-1}(u)}{u}$$

$$= \frac{(h^{-1}(-u) - c) - (h^{-1}(u) - c)}{u} = \sigma_h(u).$$

d). By using L'Hôpital's rule,

$$\sigma'_h(0) = \lim_{u \to 0} \frac{\frac{h^{-1}(-u) - h^{-1}(u)}{u} - \sigma_h(0)}{u} = \lim_{u \to 0} \frac{h^{-1}(-u) - h^{-1}(u) - u\sigma_h(0)}{u^2}$$

$$= \frac{\left(h^{-1}\right)''(0) - \left(h^{-1}\right)''(0)}{2} = 0,$$

and

$$\sigma''_h(0) = \lim_{u \to 0} \frac{\left(\frac{h^{-1}(-u) - h^{-1}(u)}{u}\right)'}{u}$$

$$= \lim_{u \to 0} \frac{\left(h^{-1}(-u) - h^{-1}(u)\right)' u - \left(h^{-1}(-u) - h^{-1}(u)\right)}{u^3}$$

$$= \frac{3\left(-\left(h^{-1}\right)'''(0) - \left(h^{-1}\right)'''(0)\right) - \left(-\left(h^{-1}\right)'''(0) - \left(h^{-1}\right)'''(0)\right)}{6}$$

$$= -\frac{2}{3}\left(h^{-1}\right)'''(0) = -\frac{6(h''(y_h))^2 - 2h'(y_h)h'''(y_h)}{3(h'(y_h))^5}.$$

$\square$

We disclose the relation between the stability of h and the map σ_h in the following result.

Theorem 8.9. *Let $h \in \mathfrak{G}_*$. The following statements hold:*

a) *h is L.A.S. if $\sigma_h(0) > 1$, and it is unstable (local repeller) if $\sigma_h(0) < 1$.*

b) *h is G.A.S. if and only if $1 < \sigma_h(u)$ for all $u \in (-b_h, b_h) \setminus \{0\}$.*

c) *If $\sigma_h(u) \geq 1$ for all u in a neighborhood of $u = 0$, then h is stable.*

d) *If $\sigma_h(u) < 1$ for all u in a punctured neighborhood of $u = 0$, then h is unstable (local repeller).*

Proof. a). It follows from Proposition 8.6.b) and 8.6.c) after noting that

$$\sigma_h(0) > 1 \iff \frac{-2}{h'(y_h)} > 1 \iff -2 < h'(y_h) < 0 \iff$$

$$-1 < 1 + h'(y_h) < 1 \iff -1 < (\mathrm{id} + h)'(y_h) < 1 \iff \left| (\mathrm{id} + h)'(y_h) \right| < 1$$

and

$$\sigma_h(0) < 1 \iff \frac{-2}{h'(y_h)} < 1 \iff -2 > h'(y_h) \iff$$

$$-1 > 1 + h'(y_h) \iff -1 > (\mathrm{id} + h)'(y_h) \iff \left| (\mathrm{id} + h)'(y_h) \right| > 1.$$

b). Let us assume that $1 < \sigma_h(u)$, $\forall u \in (-b_h, b_h) \setminus \{0\}$. On the one hand, if $u \in (0, b_h)$,

$$\begin{aligned}
1 < \sigma_h(u), \ \forall u \in (0, b_h) &\iff u < h^{-1}(-u) - h^{-1}(u), \ \forall u \in (0, b_h) \\
&\iff h(y) < h^{-1}(-h(y)) - y, \ \forall y \in \left(h^{-1}(b_h), h^{-1}(0) \right) \\
&\iff h(h(y) + y) + h(y) + y > y, \ \forall y \in \left(h^{-1}(b_h), y_h \right) \\
&\iff (\mathrm{id} + h)^{(2)}(y) - y > 0, \ \forall y \in \left(h^{-1}(b_h), y_h \right),
\end{aligned}$$

where we have written $u = h(y)$.

On the other hand, an analogous reasoning can be used if $u \in (-b_h, 0)$ to obtain

$$1 < \sigma_h(u), \ \forall u \in (-b_h, 0) \iff (\mathrm{id} + h)^{(2)}(y) - y < 0, \ \forall y \in \left(y_h, h^{-1}(-b_h) \right).$$

Therefore,

$$\begin{aligned}
1 < \sigma_h(u), \ &\forall u \in (-b_h, b_h) \setminus \{0\} \\
&\iff \left((\mathrm{id} + h)^{(2)}(y) - y \right)(y - y_h) > 0, \ \forall y \in \left(h^{-1}(b_h), h^{-1}(-b_h) \right) \setminus \{y_h\}.
\end{aligned}$$

$$(8.11)$$

Next, by Proposition 8.8.b), the right-hand side of (8.11) is equivalent to

$$((\mathrm{id} + h)^{(2)}(y) - y)(y - y_h) > 0, \ \forall y \in \mathrm{dom} \, h \setminus \{y_h\}.$$

Finally, invoking Proposition 8.3 (statements a) and f)), we reach the equivalence

$$1 < \sigma_h(u), \ \forall u \in (-b_h, b_h) \setminus \{0\} \iff h \text{ is G.A.S.}$$

c). If $u \in U \cap (0, +\infty)$,

$$\sigma_h(u) \leq 1, \ \forall u \in U \cap (0, +\infty) \iff u + h \left(u + h^{-1}(u) \right) \leq 0, \ \forall u \in U \cap (0, +\infty)$$
$$\iff y + h(y) + h \left(h(y) + y \right) - y \leq 0, \ \forall y \in h^{-1} \left(U \cap (0, +\infty) \right)$$
$$\iff (\mathrm{id} + h)^{(2)}(y) - y \leq 0, \ \forall y \in h^{-1} \left(U \right) \cap (-\infty, y_h),$$

where, as before, we have written $u = h(y)$.

Analogously, if $u \in U \cap (-\infty, 0)$,

$$\sigma_h(u) \leq 1, \forall u \in U \cap (-\infty, 0) \iff (\mathrm{id} + h)^{(2)}(y) - y \geq 0, \ \forall y \in h^{-1} \left(U \right) \cap (y_h, +\infty).$$

Thus, we obtain the equivalence

$$\sigma_h(u) \leq 1, \forall u \in U \iff \left((\mathrm{id} + h)^{(2)}(y) - y \right) (y_h - y) \geq 0, \ \forall y \in h^{-1} \left(U \right),$$

which together with Proposition 8.6.d) proves the result.

d). We omit the proof of *d)* since it is similar to the previous one, but using Proposition 8.5.b) instead of Proposition 8.6.d). □

8.3.2 STABILITY OF FAMILIES OF MAPS

In the previous subsection, we have focused on stability results valid for a specific map $h \in \mathfrak{G}_*$ (we recall that the definition of $\mathfrak{G}_*$ appears in (8.8)). Here, we are interested

in stability results valid for a family $\mathfrak{G} \subset \mathfrak{G}_*$, and thus we consider

$$\Delta y_n = h(y_n), \quad h \in \mathfrak{G}, \ y_0 \in \mathrm{dom}\, h, \ \text{where } \mathfrak{G} \subset \mathfrak{G}_*. \tag{8.12}$$

In particular, we are interested in studying in which cases the local stability of maps in $\mathfrak{G}$ implies their global stability. This leads us to define the following property.

Definition 8.10. We say that a family $\mathfrak{G} \subset \mathfrak{G}_*$ satisfies the property *stable implies G.A.S.* (with relation to model (8.12)) if $\mathfrak{G} \subset \{h \in \mathfrak{G}_* : h \text{ is G.A.S. or } h \text{ is unstable}\}$.

The following result provides some general families of maps, in terms of the function σ defined in the previous subsection, for which the *stable implies G.A.S.* property holds.

Proposition 8.11. *Let*

$$\mathfrak{R} := \{h \in \mathfrak{G}_* : \sigma_h^{-1}(\inf \sigma_h) = \{0\}\},$$

$$\mathfrak{P} := \{h \in \mathfrak{G}_* \cap \mathcal{C}^3(\mathrm{dom}\, h) : (h^{-1})''' < 0\}, \tag{8.13}$$

and

$$\mathfrak{Q} := \{h \in \mathfrak{G}_* \cap \mathcal{C}^5(\mathrm{dom}\, h) : (h^{-1})^{(v} > 0; \ \sigma_h(0) \le \sigma_h(b_h)\}. \tag{8.14}$$

Then $\mathfrak{P} \subset \mathfrak{R}$, $\mathfrak{Q} \subset \mathfrak{R}$, $\mathfrak{R}$ satisfies the property stable implies G.A.S., *and*

$$\{h \in \mathfrak{R} : |(\mathrm{id} + h)'(y_h)| \le 1\} = \{h \in \mathfrak{R} : h \text{ is G.A.S.}\}. \tag{8.15}$$

Proof. We note that $h \in \mathfrak{R}$ means that σ_h attains a strict global minimum at 0. Assume $h \in \mathfrak{P}$ and consider the function $\Psi(u) := u(\sigma_h(u) - \sigma_h(0))$. Obviously, $\Psi(0) = 0$. By differentiating and substituting at $u = 0$,

$$\Psi^{j)}(0) = \left[\frac{d^j((h^{-1})(-u) - (h^{-1})(u) - \sigma_h(0)u)}{du^j} \right]_{u=0} = 0$$

for $j = 1, 2$. Moreover,

$$\Psi'''(u) = -(h^{-1})'''(-u) - (h^{-1})'''(u) > 0.$$

Therefore $\Psi(u) > 0$ for $u > 0$, and Proposition 8.8.a) implies that σ_h attains a strict global minimum at 0. Thus, $\mathfrak{P} \subset \mathfrak{R}$.

Assume now $h \in \mathfrak{Q}$ and consider again the function Ψ. We know that

$$\Psi(0) = \Psi'(0) = \Psi''(0) = 0.$$

Moreover,
$$\Psi^{(iv)}(0) = (h^{-1})^{(iv)}(0) - (h^{-1})^{(iv)}(0) = 0.$$

and
$$\Psi^{(v)}(0) = -(h^{-1})^{(v)}(-u) - (h^{-1})^{(v)}(u) < 0.$$

If $\Psi'''(0) \leq 0$ then

$$\Psi(b_h) = \int_0^{b_h} \Psi'(u) du < 0,$$

which is impossible since $\sigma_h(b_h) \geq \sigma_h(0)$. Therefore, Ψ' is convex at $u = 0$. Besides, $\Psi''(0) = 0$ and Ψ''' is strictly decreasing in the interval $(0, b_h)$. Hence, Ψ has at most one inflection point in $(0, b_h)$. This, together with $\Psi(b_h) \geq 0$ and Proposition 8.8.a), implies that σ_h attains a strict global minimum at 0, and thus $\mathfrak{Q} \subset \mathfrak{R}$.

Now, assume $h \in \mathfrak{R}$. We consider two cases. First, if $\inf \sigma_h < 1$, then $\sigma_h(0) < 1$, because $h \in \mathfrak{R}$. And Theorem 8.9.a) implies h is unstable. Second, if $1 \leq \inf \sigma_h$, then $1 < \sigma_h(u)$ for all $u \in (-b_h, b_h) \setminus \{0\}$, again because $h \in \mathfrak{R}$. And Theorem 8.9.b) guarantees that h is G.A.S.

In particular, we have just shown $\{h \in \mathfrak{R} : \sigma_h(0) \geq 1\} = \{h \in \mathfrak{R} : h \text{ is G.A.S.}\}$, which finishes the proof after noting that for $h \in \mathfrak{G}_*$ the following holds

$$\sigma_h(0) \geq 1 \iff \frac{-2}{h'(y_h)} \geq 1 \iff -2 \leq h'(y_h) \leq 0 \iff$$

$$-1 \leq 1 + h'(y_h) \leq 1 \iff -1 \leq (\operatorname{id} + h)'(y_h) \leq 1 \iff |(\operatorname{id} + h)'(y_h)| \leq 1.$$

$\square$

The set $\mathfrak{P}$ in (8.13) satisfies

$$\mathfrak{P} = \{h \in \mathfrak{G}_* \cap \mathcal{C}^3(\operatorname{dom} h) : 3(h'')^2 > h'h'''\},$$

since $(h^{-1})'''(u) = \dfrac{3(h''(y))^2 - h'(y)h'''(y)}{(h'(y))^5}$, with $u = h(y)$ and $h' < 0$. Therefore, we have the following result.

Corollary 8.12. *If $h \in \mathfrak{G}_* \cap \mathcal{C}^3(\operatorname{dom} h)$ satisfies*

$$3(h'')^2 > h'h''', \tag{8.16}$$

then h is G.A.S. whenever it is stable.

Remark 8.13. With regard to (8.14), given that $\Psi^{(v} > 0$, functions Ψ and Ψ' are eventually monotone near b_h. Therefore, $\sigma_h(b_h)$ is well defined if we take

$$\sigma_h(b_h) = \lim_{u \to b_h} \sigma_h(u) \in [0, +\infty].$$

Also note that condition $|(\operatorname{id} + h)'(y_h)| \leq 1$ in (8.15) is equivalent to $h'(y_h) \geq -2$.

8.3.3 STABILITY OF POSITIVE MODELS

As pointed out at the beginning of this section, our results can be translated via topological conjugacy to positive models of the form (8.1). Let us denote

$$\mathfrak{C} = \bigcup_{-\infty \leq \alpha < \beta \leq +\infty} \mathcal{C}(\alpha, \beta)$$

and

$$\mathfrak{C}_+ = \bigcup_{0 \leq \alpha < \beta \leq +\infty} \mathcal{C}_+(\alpha, \beta),$$

with $\mathcal{C}_+(J) = \{g \in \mathcal{C}(J) : g > 0\}$, and define $\mathfrak{T} \colon \mathfrak{C}_+ \to \mathfrak{C}$ by

$$\mathfrak{T}(g) = \ln \circ g \circ \exp. \tag{8.17}$$

Clearly, $\mathfrak{T}$ is bijective, with $\mathfrak{T}^{-1} \colon \mathfrak{C} \to \mathfrak{C}_+$ given by $\mathfrak{T}^{-1}(h) = \exp \circ h \circ \ln$. Furthermore, $(\mathfrak{T}(g))^{-1} = \mathfrak{T}(g^{-1})$, whenever $g \in \mathfrak{C}_+$ and g is injective. Similarly, $(\mathfrak{T}^{-1}(h))^{-1} = \mathfrak{T}^{-1}(h^{-1})$, whenever $h \in \mathfrak{C}$ and h is injective.

The operator $\mathfrak{T}$ transforms model (8.1) into model (8.2). The results for model (8.2) are valid for subsets $\mathfrak{G}$ of $\mathfrak{G}_*$. Therefore, those results are valid for model (8.1) for subsets $\mathfrak{F} = \mathfrak{T}^{-1}(\mathfrak{G})$ of

$$\mathfrak{F}_* = \mathfrak{T}^{-1}(\mathfrak{G}_*) = \bigcup_{0 \leq \alpha < \beta \leq +\infty} \mathfrak{F}_*(\alpha, \beta) \tag{8.18}$$

with

$$\mathfrak{F}_*(\alpha, \beta) = \{g \in \mathcal{C}^1(\alpha, \beta) : \alpha < \mathrm{id}\, g < \beta,\, g' < 0,\, g(\beta) < 1 < g(\alpha)\},$$

or, what is the same,

$$\mathfrak{F}_*(\alpha, \beta) = \mathfrak{T}^{-1}(\mathfrak{G}_*(\ln \alpha, \ln \beta)).$$

8.4 Applications

We illustrate in this section how the above results allow one to obtain sharp global stability results for some several relevant models in discrete-time population dynamics.

Example 8.14. The Pennycuik model [37], $x_{n+1} = \dfrac{\kappa x_n}{1 + pe^{x_n}}$, corresponds to the family

$$\mathfrak{F} = \left\{ g(x) = \frac{\kappa}{1 + pe^x} : \kappa > 1 + p > 1 \right\} \subset \mathfrak{F}_*(0, +\infty) \subset \mathfrak{F}_*.$$

Then,

$$\mathfrak{G} := \mathfrak{T}(\mathfrak{F}) = \left\{ h(y) = \ln \kappa - \ln \left(1 + pe^{(e^y)} \right) : \kappa > 1 + p > 1 \right\} \subset \mathfrak{G}_*(-\infty, +\infty) \subset \mathfrak{G}_*,$$

$$3 \left(h''(y) \right)^2 - h'''(y)h'(y) = \frac{p^2 e^{2y + 2e^y} \left(3e^y + 2e^{2y} + 2p^2 e^{2e^y} + 4pe^{e^y} + pe^{2y + e^y} + 3pe^{y + e^y} + 2 \right)}{\left(pe^{e^y} + 1 \right)^4} > 0.$$

Thus, $\mathfrak{G} \subset \mathfrak{P} \subset \mathfrak{R}$, and then $\mathfrak{G}$ satisfies the property *stable implies G.A.S.* and $\{h \in \mathfrak{G} : |(\mathrm{id} + h)'(y_h)| \leq 1\} = \{h \in \mathfrak{G} : h \text{ is G.A.S.}\}$. Consequently, the equilibrium x_g of the Pennycuik model is G.A.S. if and only if $\frac{\kappa - 1}{\kappa} \ln \left(\frac{\kappa - 1}{p} \right) \leq 1$.

Next, we consider generalizations of other relevant models in population dynamics that were studied in [55, 57, 58] via the enveloping method. Some of these models are defined for all positive values of the state variable and others have bounded domains. In [140], sharp global stability results were obtained for generalizations of models in [55, 57, 58] with unbounded domains, including the Pennycuik model above. Here, we apply our method to obtain similar results for generalizations of models in [55, 58, 57] with bounded domains.

Example 8.15. Consider the model $x_{n+1} = x_n(1 + \alpha(1 - x_n))^\kappa$, with $\alpha, \kappa > 0$. This model generalizes model **II** in [55, 57, 58], which corresponds to $\kappa = 1$. Moreover,

it corresponds to the family

$$\mathfrak{F} = \left\{ f(x) = (1 + \alpha(1-x))^\kappa : \frac{(1+\alpha)^\kappa \kappa^\kappa}{(\kappa+1)^{\kappa+1}} < 1 \right\} \subset \mathfrak{F}_*(0, (\alpha+1)/\alpha) \subset \mathfrak{F}_*.$$

Then,

$$\mathfrak{G} := \mathfrak{T}(\mathfrak{F}) = \left\{ h(y) = \kappa \ln(1 + \alpha(1 - e^y)) : \frac{(1+\alpha)^\kappa \kappa^\kappa}{(\kappa+1)^{\kappa+1}} < 1 \right\} \subset$$
$$\subset \mathfrak{G}_*(-\infty, \ln(\alpha+1) - \ln(\alpha)) \subset \mathfrak{G}_*,$$

and

$$3\left(h''(y)\right)^2 - h'''(y)h'(y) = \frac{\kappa^2\alpha^2(\alpha+1)e^{2y}((2-e^y)\alpha+2)}{(1+\alpha-\alpha e^y)^4} > 0.$$

Thus, $\mathfrak{G} \subset \mathfrak{P} \subset \mathfrak{R}$, and then $\mathfrak{G}$ satisfies the property *stable implies G.A.S.* Furthermore, $\{h \in \mathfrak{G} : |(\mathrm{id}+h)'(y_h)| \le 1\} = \{h \in \mathfrak{G} : h \text{ is G.A.S.}\}$.

It is straightforward to see that the equilibrium x_g of model $x_{n+1} = x_n(1 + \alpha(1 - x_n))^\kappa$, with $\alpha, \kappa > 0$, is G.A.S. if and only if $\alpha\kappa \le 2$, which was previously reported for the particular case $\kappa = 1$ in [55, 57, 58] (see model **II** there) as an application of the enveloping method.

Example 8.16. Our next example is the model $x_{n+1} = x_n(1 - \alpha \ln(x_n))^\kappa$ with $\kappa, \alpha > 0$. This model generalizes model **III** in [55, 57, 58], which corresponds to $\kappa = 1$. Moreover, it corresponds to the family

$$\mathfrak{F} = \{g(x) = (1 - \alpha \ln(x_n))^\kappa : \kappa\alpha < e\} \subset \mathfrak{F}_*(0, e^{1/\alpha}) \subset \mathfrak{F}_*.$$

Then,

$$\mathfrak{G} := \mathfrak{T}(\mathfrak{F}) = \{h(y) = \kappa \ln(1 - \alpha y) : \kappa\alpha < e\} \subset \mathfrak{G}_*(-\infty, 1/\alpha) \subset \mathfrak{G}_*,$$

and

$$3 \left(h''(y) \right)^2 - h'''(y) h'(y) = \frac{\kappa^2 \alpha^4}{(1 - \alpha y)^4} > 0.$$

Thus, $\mathfrak{G} \subset \mathfrak{P} \subset \mathfrak{R}$, and then $\mathfrak{G}$ satisfies the property *stable implies G.A.S.* Furthermore, $\{ h \in \mathfrak{G} : |(\mathrm{id} + h)'(y_h)| \leq 1 \} = \{ h \in \mathfrak{G} : h \text{ is G.A.S.} \}$.

As in the previous example, this implies that the equilibrium x_g of model $x_{n+1} = x_n (1 - \alpha \ln(x_n))^\kappa$, with $\kappa, \alpha > 0$, is G.A.S. if and only if $\alpha \kappa \leq 2$. In particular, this generalizes the result reported in [55, 57, 58] for model **III** via the enveloping method.

The above examples show that our results are applicable to models for which the results in [140] are not applicable due to the boundedness of their domains. We end this section by showing that the method presented here is applicable, even in the case of unbounded domains, to models for which the results in [140] are inconclusive.

Example 8.17. Consider $x_{n+1} = \frac{x_n}{1 + \ln(x_n + e^{-1})}$, which corresponds to the positive map $g(x) = \frac{1}{1 + \ln(x + e^{-1})} \in \mathfrak{F}_*(0, +\infty) \subset \mathfrak{F}_*$. We have that $\mathfrak{T}(g)(y) = h(y) = -\ln(1 + \ln(e^y + e^{-1})) \in \mathfrak{G}_*(-\infty, +\infty) \subset \mathfrak{G}_*$. If we consider $h(y) = 3 \left(h''(y) \right)^2 - h'''(y) h'(y)$ then

$$h(y) = \frac{e^{2y+2} \left(e^{2y+2} + \left(e^{y+1} + 2 \right) \ln^2 \left(e^{y+1} + 1 \right) - 3 e^{y+1} \ln \left(e^{y+1} + 1 \right) \right)}{\left(e^{y+1} + 1 \right)^4 \ln^4 \left(e^{y+1} + 1 \right)}.$$

For $z = e^{y+1} > 0$,

$$h(y) = h(\ln(z) - 1) = \frac{z^2 \left(z^2 + (z + 2) \ln^2(z + 1) - 3z \ln(z + 1) \right)}{(z + 1)^4 \ln^4(z + 1)}.$$

Consider the function $u(z) = z^2 + (z + 2) \ln^2(z + 1) - 3z \ln(z + 1)$, for which $u(0) = 0$ and $u'(0) = 0$. Since $u''(z) = \frac{z(2z + 2 \ln(z+1) + 3)}{\alpha^2 (z+1)^2} > 0$ for all $z > 0$, we conclude $u'(z) > 0$ for all $z > 0$. And using the same argument, $u(z) > 0$ for all

$z > 0$. This means that $h(y) > 0$ for all $y \in (-\infty, +\infty)$. Thus, $h \in \mathfrak{P} \subset \mathfrak{R}$, and then h is G.A.S. if and only if $|(\text{id} + h)'(y_g)| \leq 1$.

We show now that Corollary 2.7 in [140] is not applicable in this case. The positive equilibrium is $x_g = 1 - e^{-1}$ and the Schwarzian derivative of $j(y) = -\ln(g(x_g e^{-y}))$ is the same as for h. Therefore, proving that the Schwarzian derivative of j is negative everywhere is equivalent to prove that $3\left(h''(y)\right)^2 - 2h'''(y)h'(y)$ is positive everywhere. However, this expression evaluated at $y = 0$ is positive (approximately 0.0482) while evaluated at $y = 3$ is negative (approximately -0.0014).

It can be argued that Corollary 2.7 in [140] refers only to per capita production functions that are bounded at the origin, while that of our example is not. However, it would suffice to replace the constant e^{-1} above with a larger one, close enough to e^{-1} so that all the reasoning would remain valid.

8.5   Pre-order and enveloping

In the previous section, we have seen that the method presented in this chapter allows to obtain sharp global stability results for generalized versions of models previously studied via the enveloping technique (see [58]). In this section, we relate our method to this technique. To that end, we introduce a pre-order in $\mathfrak{G}_*$ by

$$g \ll \hat{g} \iff b_{\hat{g}} \leq b_g \text{ and } \sigma_g \leq \sigma_{\hat{g}}. \tag{8.19}$$

Proposition 8.18. *Let $\alpha, \beta \in [-\infty, +\infty]$, with $\alpha < \beta$ and $g, \hat{g} \in \mathfrak{G}_*(\alpha, \beta)$. Then, the following statements hold:*

  a) If $(\text{id} - y_{\hat{g}})\, g \leq (\text{id} - y_{\hat{g}})\, \hat{g}$, then $g \ll \hat{g}$.

  b) If $g \ll \hat{g}$ and g is G.A.S., then $\hat{g}$ is G.A.S.

  c) If $(\text{id} - y_{\hat{g}})\, g < (\text{id} - y_{\hat{g}})\, \hat{g}$ in $(\alpha, \beta) \setminus \{y_{\hat{g}}\}$ and $\sigma_g \geq 1$, then $\hat{g}$ is G.A.S.

Proof. a). Since $g, \hat{g} \in \mathfrak{G}_*(\alpha, \beta)$, the inequality

$$(\mathrm{id} - y_{\hat{g}})\, g \leq (\mathrm{id} - y_{\hat{g}})\, \hat{g} \tag{8.20}$$

implies $y_g = y_{\hat{g}}$. Moreover, from (8.20), we have $-\inf \hat{g} \leq -\inf g$ and $\sup \hat{g} \leq \sup g$. Hence, $b_{\hat{g}} \leq b_g$.

On the other hand, (8.20) implies $\hat{g}(y) \leq g(y)$ for $y \in (\hat{g}^{-1}(b_{\hat{g}}), y_{\hat{g}})$. So $u \leq g(\hat{g}^{-1}(u))$ for $u \in (0, b_{\hat{g}})$. And it follows that

$$g^{-1}(u) \geq \hat{g}^{-1}(u) \text{ for } u \in (0, b_{\hat{g}}). \tag{8.21}$$

Analogously, we obtain that (8.20) guarantees

$$g^{-1}(u) \leq \hat{g}^{-1}(u) \text{ for } u \in (-b_{\hat{g}}, 0). \tag{8.22}$$

Using (8.21) and (8.22), we conclude that

$$\sigma_g(u) = \frac{g^{-1}(-u) - g^{-1}(u)}{u} \leq \frac{\hat{g}^{-1}(-u) - \hat{g}^{-1}(u)}{u} = \sigma_{\hat{g}}(u) \text{ for } u \in (0, b_{\hat{g}}),$$

which together with Proposition 8.8.a) and $b_{\hat{g}} \leq b_h$ shows that $g \ll \hat{g}$.

b). Since $g \ll \hat{g}$, $b_{\hat{g}} \leq b_g$ and $\sigma_g \leq \sigma_{\hat{g}}$. Besides, since g is G.A.S., applying Theorem 8.9.b) we know that $1 < \sigma_g(u)$, for all $u \in (-b_g, b_g) \setminus \{0\}$. Thus, $1 < \sigma_{\hat{g}}(u)$, for all $u \in (-b_{\hat{g}}, b_{\hat{g}}) \setminus \{0\}$. And, using again Theorem 8.9.b), $\hat{g}$ is G.A.S.

c). Following the proof of part a), $b_{\hat{g}} \leq b_g$ and $\sigma_g(u) < \sigma_{\hat{g}}(u)$ for $u \in (-b_{\hat{g}}, b_{\hat{g}}) \setminus \{y_{\hat{g}}\}$. Furthermore, since $1 \leq \sigma_g$, we arrive at $1 = \sigma_g(u) < \sigma_{\hat{g}}(u)$ for $u \in (-b_{\hat{g}}, b_{\hat{g}}) \setminus \{y_{\hat{g}}\}$, and by Theorem 8.9.b), $\hat{g}$ is G.A.S. $\qquad \square$

Proposition 8.19. *Let $\beta, \hat{\beta} \in (-\infty, +\infty]$ such that $\beta \leq \hat{\beta}$, $g \in \mathfrak{G}_*(-\infty, \beta)$ and $\hat{g} \in \mathfrak{G}_*(-\infty, \hat{\beta})$. Assume $y_{\hat{g}} < \beta$ and $g(\beta) = -\infty$, then the following statements hold:*

a) *If $(\mathrm{id} - y_{\hat{g}})\, g \leq (\mathrm{id} - y_{\hat{g}})\, \hat{g}$ in $(-\infty, \beta)$, then $g \ll \hat{g}$.*

b) If $(\mathrm{id} - y_{\hat{g}})\, g < (\mathrm{id} - y_{\hat{g}})\, \hat{g}$ *in* $(-\infty, \beta) \setminus \{y_{\hat{g}}\}$ *and* $\sigma_g \geq 1$, *then* $\hat{g}$ *is G.A.S.*

c) If $(\mathrm{id} - y_{\hat{g}})\, g < (\mathrm{id} - y_{\hat{g}})\, \hat{g}$ *in* $(-\infty, \beta) \setminus \{y_{\hat{g}}\}$ *and* $(\mathrm{id} + g)^{(2)} = \mathrm{id}$, *then*
$\hat{g}$ *is G.A.S.*

Proof. a). The condition $y_{\hat{g}} < \beta$ together with $(\mathrm{id} - y_{\hat{g}})\, g \leq (\mathrm{id} - y_{\hat{g}})\, \hat{g}$ in $(-\infty, \beta)$ guarantees that $y_{\hat{g}} = y_g$. By hypothesis, $-\inf g = +\infty$, so $-\inf \hat{g} \leq -\inf g$. The rest of the proof is identical to that of Proposition 8.18.a)

b). Using the proofs of the previous statement and Proposition 8.18.b), $g \ll \hat{g}$ with $\sigma_g(u) < \sigma_{\hat{g}}(u)$ for $u \in (-b_{\hat{g}}, b_{\hat{g}}) \setminus \{y_{\hat{g}}\}$. Furthermore, since $1 \leq \sigma_g$, it follows that $1 = \sigma_g(u) < \sigma_{\hat{g}}(u)$ for $u \in (-b_{\hat{g}}, b_{\hat{g}}) \setminus \{y_{\hat{g}}\}$, and by Theorem 8.9.b), $\hat{g}$ is G.A.S.

c). It is a consequence of the previous statement after noting that $(\mathrm{id} + g)^{(2)} = \mathrm{id}$ implies $\sigma_g = 1$. Indeed,

$$
\begin{aligned}
(\mathrm{id} + g)^{(2)} = \mathrm{id} \implies & (\mathrm{id} + g)^{(2)}(y) = y, \ \forall y \in \left(g^{-1}(b_g), g^{-1}(-b_g) \right) \\
\iff & g\left(g(y) + y \right) + g(y) + y = y, \ \forall y \in \left(g^{-1}(b_g), g^{-1}(-b_g) \right) \\
\iff & g(y) = g^{-1}(-g(y)) - y, \ \forall y \in \left(g^{-1}(b_g), g^{-1}(-b_g) \right) \\
\iff & u = g^{-1}(-u) - g^{-1}(u), \ \forall u \in (-b_g, b_g) \\
\iff & 1 = \sigma_g(u), \ \forall u \in (-b_g, b_g).
\end{aligned}
$$

$\square$

Using the operator $\mathfrak{T}$ defined in (8.17), we can see that the relation between the method presented here and the enveloping technique is as follows. Theorem 3 in [57] corresponds to Proposition 8.19.c), and Corollary 4 in [57] corresponds to Proposition 8.19.b).

Example 8.20. Our last example shows how the pre-order defined in (8.19) can be applied to study a perturbed model. Let $P, Q \in \mathfrak{F}_*(0, +\infty)$ and suppose the asymptotic

behavior of equation

$$x_{n+1} = x_n P(x_n) \tag{8.23}$$

to be known. Consider the perturbed model

$$x_{n+1} = x_n P(x_n)(Q(x_n))^{\alpha}, \tag{8.24}$$

with $\alpha \geq 0$, and denote $p := \mathfrak{T}(P), q := \mathfrak{T}(Q)$ and $g := p + \alpha q$. Assume also that $y_p = y_q$.

Clearly, $g \ll p$, and we conclude that (8.23) to be G.A.S. is a necessary condition for (8.24) to be G.A.S.

8.6 Discussion and conclusions

We have introduced a new method for the study of the global stability of one-dimensional discrete dynamical systems. Although the focus of this technique is on generic positive maps, it is based on the graphical analysis of a certain family of functions obtained for a transformed version of these maps.

The main result provided here allows one to carry out stability analysis for single maps. Moreover, we have shown that this result can be extended and applied to some general families of maps. The results obtained complement and extend some existing conditions in the literature for the global stability. In particular, Corollary 8.16 provides a strictly weaker condition than the classical condition of negative Schwarzian derivative. We have also shown how all these results can be translated to the case of generic positive maps via topological conjugacy.

We have provided examples showing the applications of our method. These examples show that the results provided here extend Corollary 2.7 in [140] in several directions, since they are applicable in certain cases in which the domain is bounded or far from the origin, the per capita production function is not bounded at the origin, or the

Schwarzian derivative is not negative. In particular, we have obtained sharp global stability results for generalizations of some relevant models in population dynamics with bounded domains studied in [55, 57, 58] via the enveloping method, which complements the work done in [140] for models with unbounded domains. We have also demonstrated with a specific example that, even in the case of models with unbounded domain, the method presented here is applicable to cases in which the results provided in [140] are inconclusive. Yet, we want to highlight that the results in [140] were recently useful to study the global stability of delay differential equations modeling economic growth [36]. Checking if the results presented here would be useful in that framework is an interesting problem.

We have related our method to the enveloping technique by introducing a certain pre-order in a generic family of maps. Using this pre-order, we have shown how our results are related to the main results in [58] via topological conjugacy. Finally, we have applied these results to study the global stability of a perturbed model.

Conclusions and future prospects

Conclusions

In this thesis, we have addressed two different problems concerning the stability of one-dimensional discrete dynamical systems. These systems play an important role in a wide range of fields, and therefore our results have potential interest in fields different from population dynamics, e.g., in engineering.

On the one hand, we have proposed new control methods aimed at reducing erratic fluctuations. These techniques are particularly suitable for the control of biological populations since they directly modify the state variable of the system. The analysis of these techniques led us to investigate bifurcation structures of piecewise smooth systems. On the other hand, we have studied the global stability of systems in two different situations. First, we have investigated the effect of the interplay of harvesting intensity and harvesting timing on the global stability of dynamical systems modeling biological populations. Second, we have proposed a new method to study the global stability of generic one-dimensional discrete dynamical systems.

Adaptive threshold harvesting (ATH) is the first control technique proposed in this thesis. It is a harvesting control method closely related to the existing techniques adaptive limiter control (ALC) and threshold harvesting (also known as limiter control). The scope of these two techniques is widened with ATH, since it extends the applicability of adaptive limiters to situations in which harvesting is the only possible form of intervention. We have proved that the stabilizing effect of ATH is attained by trapping the population size within an interval around the positive equilibrium, whose length decreases with the harvesting intensity. Analytical expressions for the endpoints of this interval were obtained, which allow one to determine the harvesting intensity necessary

to reach any stabilization goal. For populations starting outside the trapping region, reaching it takes a certain time, which is excessively long for high harvesting intensities. We have proposed modified versions of both ATH and ALC to reduce the length of these transients without altering the asymptotic dynamics of the managed populations. We have also studied the applicability of ATH as a harvesting strategy when the aim is to gain economic benefit from the exploited populations. To that end, we have investigated both the short and long term yield. In particular, we have shown that trying to maximize the short-term yield is risky in terms of sustainability.

We have studied the performance of both ATH and ALC on populations subject to biological mechanisms that put them at risk of extinction or promote recurrent population outbreaks. To that end, we have compared the impact of the two control methods on extinction and outbreak probabilities in different scenarios. We have shown that the beneficial effect of the two strategies is only observed for sufficiently large control intensities. Yet, the two methods show a clear disparity in each of the biological situations considered. With regard to the control of outbreaks, we have shown that ATH reduces the probability of their occurrence while ALC is either ineffective or counterproductive. When the goal is to prevent population extinctions, the situation is just the opposite. Contrary to what is common in conservation biology and mathematical modeling, we have investigated the risk of extinction of large populations. We have shown that these populations are not necessarily safe by their large size and that Allee effects can not be ignored if the dynamics are overcompensatory.

Combined adaptive limiter control (CALC) is the second control strategy proposed in this thesis. This is a control method that combines restocking and harvesting according to ALC and ATH, and constitutes a general framework for adaptive limiters since it includes ALC and ATH as particular cases. We have proved CALC to have stabilizing properties similar to the ones of ALC and ATH, and we have investigated the advantages of the combination of restocking and harvesting under CALC over only restocking (ALC) and only harvesting (ATH). To that end, we have studied the effect of the control interventions on the constancy stability and the outbreak risk of different

population models. We have shown that the combination of restocking and harvesting improves the constancy stability of the managed populations over only restocking or only harvesting when the control intensities are high enough. When the goal is to prevent population booms, we have shown that combining harvesting with restocking is only beneficial when the harvesting intensity is low. Since interventions always have a cost, we have studied the trade-off between the stabilizing goals that are attained with CALC and the cost of the interventions. We have demonstrated that the decision about which are the 'best' intensities for harvesting and restocking can not be only based on stability criteria.

The study of the stabilizing properties of CALC naturally leads to a problem about piecewise smooth dynamical systems. When the underlying dynamics are described by unimodal maps, the production function of CALC is piecewise continuous with two break points. If only the outermost branches of this function are considered, it can be seen in terms of the control intensities as a biparametric family of bimodal piecewise linear maps (PWL). We have studied the bifurcation structure obtained from the collision of the breakpoints of these maps with cycles contained in the outermost partitions of the domain. We have shown that this structure is a rather degenerate case of an already studied bifurcation structure of a six-parametric family of PWL maps, which includes the maps obtained from CALC as a strict subfamily. Our results allow us to completely describe the bifurcation structure of CALC and to complete the solution of a similar problem previously stated in the field of economics [74]. With regard to the type of bifurcation, we have proved that when parameters are varied through one of the bifurcation points a continuum of cycles lying in the external partitions of the state space emerge and disappear afterwards. This constitutes a case of degenerate border collision bifurcation that, as far as we know, has not been reported before. We have also demonstrated the applicability of our results to the determination of the bifurcation structure of CALC for some relevant models in population dynamics. We have shown that the bifurcation structure may range from very simple to very intricate.

Another problem addressed in this thesis is about the combined effect of harvesting intensity and harvesting time on the stability of discrete population models in the framework proposed by Hiromi Seno [191]. We have proved that for general overcompensatory models delaying the moment of intervention does not affect the global stability of the positive equilibrium if the harvesting intensity is high enough. To the best of our knowledge, this is the first global stability result for a general family of maps in Seno's framework. Moreover, we have demonstrated that the global stability that is attained with delayed harvesting is robust under both noise and lattice effect. We have also shown that timing can be stabilizing or destabilizing by itself, the latter disproving a recent conjecture published in [44]. Special attention has been paid to Ricker's model, which is one of the most relevant models in population dynamics. We have proved that harvest timing has no effect on the global stability of the positive equilibrium for any harvesting intensity. Moreover, we have studied the effect of the moment of intervention on the constancy stability of the harvested populations. In particular, we have shown that harvest time determines the speed and type of convergence to the positive equilibrium.

The method *exponent analysis* proposed in this thesis reduces the study of the local and global stability of populations subject to delayed harvesting to the analysis of the relative position of the graph of a certain function with respect to an exponent parameter. One of the important contributions of this thesis comes from the application of this method to a broad family of compensatory population models common in population dynamics. Moreover, for the Bellows model and the discretization of the Richards model, we have provided global stability results even in the absence of harvesting. So far we know, these results are new.

The last contribution of this thesis is a new method for the study of the global stability of one-dimensional discrete dynamical systems. This method complements and extends some existing conditions for the global stability, e.g., the classical condition of negative Schwarzian derivative. We have shown the applicability of the method with several examples showing that it is applicable in cases in which the domain is unbounded,

bounded or far from the origin, the per capita production function is not bounded at the origin, or the Schwarzian derivative is not negative. We have compared and related our method to other techniques previously proposed. In particular, we have shown that our results yield sharp global stability conditions for maps with unbounded domains for which the results in [140] are inconclusive. We have also related the method proposed here to the enveloping technique proposed in [58] by considering a pre-order in a certain family of maps. The applicability of these results was shown by studying the global stability of a perturbed model.

FUTURE PROSPECTS

A number of desirable extensions to the present work have been mentioned at various places in this thesis. Next, we discus these and some further ideas for future work separately for each of the research lines of this thesis.

Research line I

1. **ATH and CALC on structured populations.** All the analysis performed in this thesis for adaptive limiters has been carried out for populations without structure, neither spatial nor temporal. An interesting problem to be addressed is about the performance of ATH and CALC on metapopulations and populations with age structure. The case of metapopulations has been previously studied for other control techniques, e.g., proportional feedback [66] or ALC [183, 184]. And a similar situation occurs for populations with age structure, e.g., the in-box [62] or TOC [28] methods.

2. **Comparison of ATH and CALC with other control strategies.** Like many other strategies, the two control methods presented in this thesis are aimed at reducing fluctuations in the population size. A key question in populations management is which strategy is the most appropriate to attain each of the long list of possible stabilizing goals. In this thesis, we have compared ALC, ATH and CALC. Previously, this question was addressed for both one-parameter [e.g.,

212, 214] and two-parameter [e.g., 213] control strategies. A future research direction is to compare ATH with other one-parameter strategies like proportional feedback or threshold harvesting, and CALC with other two-parameter strategies like target oriented control or both limiter control.

3. **Effect of the order of events in ATH and ALC.** Contrary to continuous-time systems, the order of events completely determines the dynamics of discrete-time systems. The dynamics of ALC, ATH and CALC has been investigated in this thesis assuming that the population is harvested after being censused. Yet, we can define alternative control strategies by reversing the order of harvest and census. This was done in [78] for ALC. It was observed that the control method assuming census after harvest increases the population fluctuations or exhibits bistability for wide ranges of control intensities. Studying whether the same is true for ATH and CALC is a problem for future research.

4. **Application of ATH and CALC to laboratory or real populations.** ALC is one of the few control strategies that has been studied not only theoretically and numerically but also empirically on laboratory populations [183, 184]. In this thesis, we have obtained a complete description of the stabilizing properties of ATH and CALC via both theoretical and numerical results. Checking if these properties are observed in real populations is an interesting problem to be addressed.

5. **Application of ATH and CALC to other areas of knowledge.** Adaptive limiters have been already applied to areas different from population dynamics, e.g., computer architecture [65], medicine [88] or economics [101]. We can expect that the control methods presented in this thesis could as well be applied to other areas. Moreover, an interesting question is whether their adaptive character can bring any advantage with respect to other control techniques in the different fields of possible application.

Research line II

6. **Character of the stabilization attained with harvest timing.** We have seen that in some cases harvest timing can be stabilizing by itself. It is an interesting open question to determine conditions allowing to predict the local or global character of the stability attained by delaying harvesting.

7. **Applicability of the method for the global stability analysis to other problems.** In the last chapter of this thesis we have introduced a new method aimed at studying the global stability of one-dimensional discrete systems. In particular, we have shown that this method extends and complements the results in [140]. These results have been useful to study the global stability of delay-differential equations [36]. Checking if the method presented here is useful in that case and whether it can improve in any direction the results obtained in [36] is an interesting open question to be addressed in future research.

8. **Study of the effect of harvest timing on structured populations.** Seno's model allows to consider any harvesting moment during the reproductive season for populations without structure, neither temporal nor spatial. An appealing problem to be addressed is to obtain a model for structured populations similar to Seno's model and then study its qualitative properties.

References

[1] P. A. Abrams. When does greater mortality increase population size? The long history and diverse mechanisms underlying the hydra effect. *Ecology Letters*, 12(5):462–474, 2009.

[2] J. C. Allen, W. M. Schaffer, and D. Rosko. Chaos reduces species extinction by amplifying local population noise. *Nature*, 364(6434):229, 1993.

[3] L. J. S. Allen, J. F. Fagan, G. Högnäs, and H. Fagerholm. Population extinction in discrete-time stochastic population models with an Allee effect. *Journal of Difference Equations and Applications*, 11(4-5):273–293, 2005.

[4] F. W. Allendorf and G. Luikart. *Conservation and the genetics of populations*. Blackwell Publishing, Malden, 2007.

[5] D. J. Allwright. Hypergraphic functions and bifurcations in recurrence relations. *SIAM Journal on Applied Mathematics*, 34(4):687–691, 1978.

[6] L. G. Anderson. Analysis of open-access commercial exploitation and maximum economic yield in biologically and technologically interdependent fisheries. *Journal of the Fisheries Research Board of Canada*, 32(10):1825–1842, 1975.

[7] B. R. Andrievskii and A. L. Fradkov. Control of chaos: Methods and applications. I. methods. *Automation and Remote Control*, 64(5):673–713, 2003.

[8] V. S. Anishchenko, T. E. Vadivasova, and G. I. Strelkova. *Deterministic Nonlinear Systems. A Short Course*. Springer International Publishing Switzerland, 2014.

[9] R. A. Armstrong and R. McGehee. Competitive exclusion. *The American Naturalist*, 115(2):151–170, 1980.

[10] R. Arnason. *The economics of ocean ranching: experiences, outlook and theory*. FAO Fisheries Technical Paper no. 413. Rome, Italy: Food and Agriculture Organization of the United Nations, 2001.

[11] J. F. Arnoldi, M. Loreau, and B. Haegeman. Resilience, reactivity and variability: a mathematical comparison of ecological stability measures. *Journal of Theoretical Biology*, 389:47–59, 2016.

[12] M. Åström, P. Lundberg, and S. Lundberg. Population dynamics with sequential density-dependencies. *Oikos*, 75(2):174–181, 1996.

[13] V. Avrutin and I. Sushko. A gallery of bifurcation scenarios in piecewise smooth 1D maps. In *Global Analysis of Dynamic Models in Economics and Finance, G. Bischi G, C. Chiarella and Sushko, eds.* Springer, Berlin, Heidelberg, 2013.

[14] V. Avrutin, I. Sushko, and F. Tramontana. Bifurcation structure in a bimodal piecewise linear business cycle model. *Abstract and Applied Analysis*, 2014, 2014. Article ID: 401319.

[15] F. Barraquand, S. Louca, K. C. Abbott, C. A. Cobbold, F. Cordoleani, D. L. DeAngelis, B. D. Elderd, J. W. Fox, P. Greenwood, F. M. Hilker, D. L. Murray, C. R. Stieha, R. A. Taylor, K. Vitense, G. S. K. Wolkowicz, and R. C. Tyson. Moving forward in circles: challenges and opportunities in modelling population cycles. *Ecology Letters*, 20(8):1074–1092, 2017.

[16] F. A. Bartha, A. Garab, and T. Krisztin. Local stability implies global stability for the 2-dimensional Ricker map. *Journal of Difference Equations and Applications*, 19(12):2043–2078, 2013.

[17] J. D. Bell, D. M. Bartley, K. Lorenzen, and N. R. Loneragan. Restocking and stock enhancement of coastal fisheries: Potential, problems and progress. *Fisheries Research*, 80(1):1–8, 2006.

[18] J. D. Bell, K. M. Leber, H. L. Blankenship, N. R. Loneragan, and R. Masuda. A new era for restocking, stock enhancement and sea ranching of coastal fisheries resources. *Reviews in Fisheries Science*, 16(1-3):1–9, 2008.

[19] T. S. Bellows. The descriptive properties of some models for density dependence. *The Journal of Animal Ecology*, 50:139–156, 1981.

[20] M. Bernardo, C. Budd, A. R. Champneys, and P. Kowalczyk. *Piecewise-smooth dynamical systems: Theory and applications*. Springer-Verlag, London, 2008.

[21] M. Bernardo, C. Budd, A. R. Champneys, P. Kowalczyk, A. B. Nordmark, G. O. Tost, and P. T. Piiroinen. Bifurcations in nonsmooth dynamical systems. *SIAM review*, 50(4):629–701, 2008.

[22] A. A. Berryman and P. Kindlmann. *Population systems: A general introduction*. Springer, New York, 2008.

[23] R. J. H. Beverton and S. J. Holt. *Mathematical Representation of the Four Primary Factors*, pages 27–35. Springer Netherlands, 1993.

[24] R. Bijlsma, J. Bundgaard, and A. C. Boerema. Does inbreeding affect the extinction risk of small populations? Predictions from *Drosophila*. *Journal of Evolutionary Biology*, 13(3):502–514, 2000.

[25] E. J. Blomberg. The influence of harvest timing on greater sage-grouse survival: A cautionary perspective. *The Journal of Wildlife Management*, 79(5):695–703, 2015.

[26] J. Boyce, M. Herrmann, D. Bischak, and J. Greenberg. The Alaska salmon enhancement program: a cost/benefit analysis. *Marine Resource Economics*, 8(4):293–312, 1993.

[27] M. S. Boyce, A. R. E. Sinclair, and G. C. White. Seasonal compensation of predation and harvesting. *Oikos*, 87(3):419–426, 1999.

[28] E. Braverman and D. Franco. Stabilization with target oriented control for higher order difference equations. *Physics Letters A*, 379(16):1102–1109, 2015.

[29] E. Braverman and D. Franco. Stabilization of structured populations via vector target-oriented control. *Bulletin of Mathematical Biology*, 79(8):1759–1777, 2017.

[30] E. Braverman and D. D. Kinzebulatov. On linear perturbations of the Ricker model. *Mathematical Biosciences*, 202(2):323–339, 2006.

[31] E. Braverman and E. Liz. Global stabilization of periodic orbits using a proportional feedback control with pulses. *Nonlinear Dynamics*, 67(4):2467–2475, 2012.

[32] E. Braverman and A. Rodkina. Stabilization of difference equations with noisy proportional feedback control. *Discrete & Continuous Dynamical Systems-B*, 22(6):2067–2088, 2017.

[33] N. F. Britton. *Essential Mathematical Biology*. Springer, London, 2012.

[34] Å. Brännström and D. J. T. Sumpter. The role of competition and clustering in population dynamics. *Proceedings of the Royal Society of London B: Biological Sciences*, 272(1576):2065–2072, 2005.

[35] Å. Brännström and D. J. T. Sumpter. Stochastic analogues of deterministic single-species population models. *Theoretical Population Biology*, 69(4):442–451, 2006.

[36] S. Buedo-Fernández and E. Liz. On the stability properties of a delay differential neoclassical model of economic growth. *Electronic Journal of Qualitative Theory of Differential Equations*, 43:1–14, 2018.

[37] R. M. Compton C. J. Pennycuick and L. Beckingham. A computer model for simulating the growth of a population, or of two interacting populations. *Journal of Theoretical Biology*, 18(3):316–329, 1968.

[38] P. Carmona and D. Franco. Control of chaotic behaviour and prevention of extinction using constant proportional feedback. *Nonlinear Analysis: Real World Applications*, 12(6):3719–3726, 2011.

[39] H. Caswell. Sensitivity analysis of transient population dynamics. *Ecology Lettets*, 10(1):1–15, 2007.

[40] J. Champagnon, J. Elmberg, M. Guillemain, M. Gauthier-Clerc, and J. D. Lebreton. Conspecifics can be aliens too: a review of effects of restocking practices in vertebrates. *Journal for Nature Conservation*, 20(4):231–241, 2012.

[41] H. M. Chang and J. Juang. Piecewise two-dimensional maps and applications to cellular neural networks. *International Journal of Bifurcation and Chaos*, 14(07):2223–2228, 2004.

[42] D. G. Chapman, R. J. Myhre, and G. M. Southward. Utilization of Pacific halibut stocks: estimation of maximum sustainable yield, 1960. *International Pacific Halibut Commission Report 31*, 1962.

[43] N. P. Chau. Controlling chaos by periodic proportional pulses. *Physics Letters A*, 234(3):193–197, 1997.

[44] B. Cid, F. M. Hilker, and E. Liz. Harvest timing and its population dynamic consequences in a discrete single-species model. *Mathematical Biosciences*, 248:78–87, 2014.

[45] C. W. Clark. *Mathematical Bioeconomics. The optimal management of renewable resources*. John Wiley, New York, 1990.

[46] C. W. Clark. *Mathematical Bioeconomics: The Mathematics of Conservation*. John Wiley & Sons, Hoboken, 2010.

[47] W. A. Coppel. The solution of equations by iteration. *Mathematical Proceedings of the Cambridge Philosophical Society*, 51:41–43, 1955.

[48] N. J. Corron, S. D. Pethel, and B. A. Hopper. Controlling chaos with simple limiters. *Physical Review Letters*, 84:3835–3838, 2000.

[49] F. Courchamp, L. Berec, and J. Gascoigne. *Allee effects in Ecology and conservation*. Oxford University Press, New York, 2008.

[50] F. Courchamp, T. Clutton-Brock, and B. Grenfell. Inverse density dependence and the Allee effect. *Trends in Ecology & Evolution*, 14(10):405–410, 1999.

[51] F. Courchamp, B. T. Grenfell, and T. H. Clutton-Brock. Impact of natural enemies on obligately cooperative breeders. *Oikos*, 91(2):311–322, 2000.

[52] S. Couvray, T. Miard, R. Bunet, Y. Martin, J. P. Grillasca, J. L. Bonnefont, and S. Coupé. Experimental release of juvenile sea urchins (*Paracentrotus lividus*) in exploited sites along the French Mediterranean coast. *Journal of Shellfish Research*, 34(2):555–563, 2015.

[53] M. Crisan and G. Erzse. Anticipative chaos control in population models with the Allee effect. In *International Conference on Computer Engineering & Systems*, pages 216–221. IEEE, 2008.

[54] P. Cull. Global stability of population models. *Bulletin of Mathematical Biology*, 43(1):47–58, 1981.

[55] P Cull. Stability of discrete one-dimensional population models. *Bulletin of Mathematical Biology*, 50(1):67–75, 1988.

[56] P. Cull. *Difference equations: from rabbits to chaos*. Springer Science & Business Media, New York, 2005.

[57] P. Cull. Population models: stability in one dimension. *Bulletin of Mathematical Biology*, 69(3):989–1017, 2007.

[58] P. Cull and J. Chaffee. Stability in discrete population models. *AIP Conference Proceedings*, 517(1):263–276, 2000.

[59] J. Dattani, J. C. Blake, and F. M. Hilker. Target-oriented chaos control. *Physics Letters A*, 375(45):3986–3992, 2011.

[60] B. Dennis. Allee effects: population growth, critical density, and the chance of extinction. *Natural Resource Modeling*, 3(4):481–538, 1989.

[61] B. Dennis. Allee effects in stochastic populations. *Oikos*, 96:398–401, 2002.

[62] R. A. Desharnais, R. F. Costantino, J. M. Cushing, S. M. Henson, and B. Dennis. Chaos and population control of insect outbreaks. *Ecology Letters*, 4(3):229–235, 2001.

[63] S. Dey and A. Joshi. Stability via asynchrony in *Drosophila* metapopulations with low migration rates. *Science*, 312(5772):434–436, 2006.

[64] C. M. Dichmont, S. Pascoe, T. Kompas, A. E. Punt, and R. Deng. On implementing maximum economic yield in commercial fisheries. *Proceedings of the National Academy of Sciences*, 107(1):16–21, 2010.

[65] W. L. Ditto and S. Sinha. Exploiting chaos for applications. *Chaos*, 25(9):097615, 2015.

[66] M. Doebeli and G. D. Ruxton. Controlling spatial chaos in metapopulations with long-range dispersal. *Bulletin of Mathematical Biology*, 59(3):497–515, 1997.

[67] W. G. Doubleday. Harvesting in matrix population models. *Biometrics*, pages 189–200, 1975.

[68] J.M. Drake and D. M. Lodge. Allee effects, propagule pressure and the probability of establishment: risk analysis for biological invasions. *Biological Invasions*, 8:365–375, 2006.

[69] G. Dwyer, J. Dushoff, J. S. Elkinton, and S. A. Levin. Pathogen-driven outbreaks in forest defoliators revisited: building models from experimental data. *The American Naturalist*, 156(2):105–120, 2000.

[70] G. Dwyer, J. Dushoff, and S. H. Yee. The combined effects of pathogens and predators on insect outbreaks. *Nature*, 430:341–345, 2004.

[71] M. M. Ellis. Evidence for transient dynamics in plant populations based on long-term demographic data. *Journal of Ecology*, 101(3):734–742, 2013.

[72] C. S. Elton. Periodic fluctuations in the numbers of animals: their causes and effects. *Journal of Experimental Biology*, 2:119–163, 1924.

[73] M. Fisher, B. Goh, and T. Vincent. Some stability conditions for discrete-time single species models. *Bulletin of Mathematical Biology*, 41(6):861–875, 1979.

[74] I. Foroni, A. Avellone, and A. Panchuk. Sudden transition from equilibrium stability to chaotic dynamics in a cautious tâtonnement model. *Chaos, Solitons & Fractals*, 79:105–115, 2015.

[75] D. Fournier-Prunaret and P. Chargé. Route to chaos in a circuit modeled by a 1-dimensional piecewise linear map. *Nonlinear Theory and Its Applications, IEICE*, 3(4):521–532, 2012.

[76] G. A. Fox and J. Gurevitch. Population numbers count: Tools for near-term demographic analysis. *The American Naturalist*, 156(3):242–256, 2000.

[77] D. Franco and F. M. Hilker. Adaptive limiter control of unimodal population maps. *Journal of Theoretical Biology*, 337:161–173, 2013.

[78] D. Franco and F. M. Hilker. Stabilizing populations with adaptive limiters: prospects and fallacies. *SIAM Journal on Applied Dynamical Systems*, 13(1):447–465, 2014.

[79] D. Franco and E. Liz. A two-parameter method for chaos control and targeting in one-dimensional maps. *International Journal of Bifurcation and Chaos*, 23(01):1350003, 2013.

[80] D. Franco, H. Logemann, and J. Perán. Global stability of an age-structured population model. *Systems & Control Letters*, 65:30–36, 2014.

[81] D. Franco and J. Perán. Stabilization of population dynamics via threshold harvesting strategies. *Ecological Complexity*, 14:85–94, 2013.

[82] D. Franco and A. Ruiz-Herrera. To connect or not to connect isolated patches. *Journal of Theoretical Biology*, 370:72–80, 2015.

[83] J. M. Fryxell, I. M. Smith, and D. H. Lynn. Evaluation of alternate harvesting strategies using experimental microcosms. *Oikos*, 111(1):143–149, 2005.

[84] S. Gao and L. Chen. The effect of seasonal harvesting on a single-species discrete population model with stage structure and birth pulses. *Chaos, Solitons & Fractals*, 24(4):1013–1023, 2005.

[85] L. Gardini, T. Puu, and I. Sushko. A Goodwin-type model with a piecewise linear investment function. In *Business Cycle Dynamics, T. Puu and I. Sushko, eds.* Springer, Berlin, Heidelberg, 2006.

[86] L. Gardini, F. Tramontana, and I. Sushko. Border collision bifurcations in one-dimensional linear-hyperbolic maps. *Mathematics and Computers in Simulation*, 81(4):899–914, 2010.

[87] W. M. Getz and R. G. Haight. *Population harvesting: demographic models of fish, forest, and animal resources*, volume 27. Princeton University Press, 1989.

[88] L. Glass and W. Zeng. Bifurcations in flat-topped maps and the control of cardiac chaos. *International Journal of Bifurcation and Chaos*, 4(4):1061–1067, 1994.

[89] B. S. Goh. *Management and analysis of biological populations*. Elsevier, Amsterdam, 2012.

[90] V. Grimm and C. Wissel. Babel, or the ecological stability discussions: An inventory and analysis of terminology and a guide for avoiding confusion. *Oecologia*, 109(3):323–334, 1997.

[91] M. J. Groom. Allee effects limit population viability of an annual plant. *The American Naturalist*, 151(6):487–496, 1998.

[92] J. Güémez and M. A. Matías. Control of chaos in unidimensional maps. *Physics Letters A*, 181(1):29–32, 1993.

[93] S. Gueron. Controlling one-dimensional unimodal population maps by harvesting at a constant rate. *Physical Review E*, 57(3):3645, 1998.

[94] J. Guillen, C. Macher, M. Merzéréaud, M. Bertignac, S. Fifas, and O. Guyader. Estimating MSY and MEY in multi-species and multi-fleet fisheries, consequences and limits: an application to the Bay of Biscay mixed fishery. *Marine Policy*, 40:64–74, 2013.

[95] I. Györi and S. I. Trofimchuk. Global attractivity and persistence in a discrete population model. *Journal of Difference Equations and Applications*, 6(6):647–665, 2000.

[96] E. S. E. Hafez. Effects of high temperature on reproduction. *International Journal of Biometeorology*, 7(3):223–230, 1964.

[97] P. J. Harley and G. A. Manson. Harvesting strategies for age-stable populations. *Journal of Applied Ecology*, 18(1):141–147, 1981.

[98] M. P. Hassell. Density-dependence in single-species populations. *The Journal of Animal Ecology*, 44(1):283–295, 1975.

[99] A. Hastings. Transients: the key to long-term ecological understanding? *Trends in Ecology & Evolution*, 19(1):39–45, 2004.

[100] C. E. Hauser, E. G. Cooch, and J. D. Lebreton. Control of structured populations by harvest. *Ecological Modelling*, 196(3):462–470, 2006.

[101] X. He and F. H. Westerhoff. Commodity markets, price limiters and speculative price dynamics. *Journal of Economic Dynamics and Control*, 29(9):1577–1596, 2005.

[102] S. H. Henson, R. F. Costantino, J. M. Cushing, R. A. Desharnais, B. Dennis, and A. A. King. Lattice effects observed in chaotic dynamics of experimental populations. *Science*, 294(5542):602–605, 2001.

[103] R. Hilborn. The economic performance of marine stock enhancement projects. *Bulletin of Marine Science*, 62(2):661–674, 1998.

[104] F. M. Hilker and E. Liz. Harvesting, census timing and 'hidden' hydra effects. *Ecological Complexity*, 14:95–107, 2013.

[105] F. M. Hilker and F. H. Westerhoff. Control of chaotic population dynamics: Ecological and economic considerations. *Beitraege des Instituts fuer Umweltsystemforschung*, 32:1–21, 2005.

[106] F. M. Hilker and F. H. Westerhoff. Paradox of simple limiter control. *Physical Review E*, 73(5):052901, 2006.

[107] F. M. Hilker and F. H. Westerhoff. Triggering crashes in chaotic dynamics. *Physics Letters A*, 362(5):407–411, 2007.

[108] F. M. Hilker, M. Langlais, and H. Malchow. The Allee effect and infectious diseases: extinction, multistability, and the (dis-)appearance of oscillations. *The American Naturalist*, 173(1):72–88, 2009.

[109] F. M. Hilker and F. H. Westerhoff. Preventing extinction and outbreaks in chaotic populations. *The American Naturalist*, 170(2):232–241, 2007.

[110] J. Huisman and F. J. Weissing. Biodiversity of plankton by species oscillations and chaos. *Nature*, 402(6760):407, 1999.

[111] A. L. Jensen. Density-dependent matrix yield equation for optimal harvest of age-structured wildlife populations. *Ecological Modelling*, 88(1):125–132, 1996.

[112] D. M. Johnson, A. M. Liebhold, P. C. Tobin, and O. N. Bjørnstad. Allee effects and pulsed invasion by the gypsy moth. *Nature*, 444:361–363, 2006.

[113] J. Juang, C. Li, and M. Liu. Cellular neural networks: Mosaic patterns, bifurcation and complexity. *International Journal of Bifurcation and Chaos*, 16(01):47–57, 2006.

[114] M. A. Juinio-Menez, H. G. Bangi, M. C. Malay, and D. Pastor. Enhancing the recovery of depleted *Tripneustes gratilla* stocks through grow-out culture and restocking. *Reviews in Fisheries Science*, 16(1-3):35–43, 2008.

[115] M. A. Juinio-Menez, D. Pastor, and H. G. Bangi. Indications of recruitment enhancement in the sea urchin *Tripneustes gratilla* due to stock restoration efforts. In *Proceedings of the 11th International Coral Reef Symposium. Ft. Lauderdale, Forida: Nova Southeastern University*, pages 1017–1021, 2008.

[116] B. E. Kendall, C. J. Briggs, W. W. Murdoch, P. Turchin, S. P. Ellner, E. McCauley, R. M. Nisbet, and S. N. Wood. Why do populations cycle? A synthesis of statistical and mechanistic modelling approaches. *Ecology*, 80(6):1789–1805, 1999.

[117] H. Kokko. Optimal and suboptimal use of compensatory responses to harvesting: timing of hunting as an example. *Wildlife Biology*, 7(3):141–150, 2001.

[118] H. Kokko and J. Lindström. Seasonal density dependence, timing of mortality, and sustainable harvesting. *Ecological Modelling*, 110(3):293–304, 1998.

[119] T. Kompas. Fisheries management: economic efficiency and the concept of 'maximum economic yield'. *Australian Commodities: Forecasts and Issues*, 12(1):152–160, 2005.

[120] D. N. Koons, R. R. Holmes, and J. B. Grand. Population inertia and its sensitivity to changes in vital rates and population structure. *Ecology*, 88(11):2857–2867, 2007.

[121] D. N. Koons, R. F. Rockwell, and J. B. Grand. Population momentum: Implications for wildlife management. *The Journal of Wildlife Management*, 70(1):19–26, 2006.

[122] E. J. Kostelich. Targeting in chaotic dynamical systems. In H. G. Schuster, editor, *Handbook of Chaos Control*, pages 141–156. Wiley-VCH Verlag, Weinheim, 1999.

[123] M. Kot. *Elements of Mathematical Ecology*. Cambridge University Press, Cambridge, 2001.

[124] T. Kousaka and H. Asahara. Complete bifurcation analysis of a chaotic attractor in an electric circuit with piecewise-smooth characteristics. *IEEJ Transactions on Electrical and Electronic Engineering*, 9(6):656–663, 2014.

[125] M. Kunze. *Non-smooth dynamical systems*, volume 1744 of *Lecture Notes in Mathematics*. Springer-Verlag, Berlin, Heidelberg, 2000.

[126] S. A. Kuruklis and G. Ladas. Oscillations and global attractivity in a discrete delay logistic model. *Quarterly of Applied Mathematics*, 50:227–233, 1992.

[127] M. Kuussaari, I. Saccheri, M. Camara, and I. Hanski. Allee effect and population dynamics in the Glanville fritillary butterfly. *Oikos*, 82(2):384–392, 1998.

[128] F. A. Labra, N. A. Lagos, and P. A. Marquet. Dispersal and transient dynamics in metapopulations. *Ecology Letters*, 6(3):197–204, 2003.

[129] R. Lande. Risks of population extinction from demographic and environmental stochasticity and random catastrophes. *The American Naturalist*, 142(6):911–927, 1993.

[130] R. Lande. Demographic stochasticity and Allee effect on a scale with isotropic noise. *Oikos*, 83(2):353–358, 1998.

[131] R. Lande, S. Engen, and B. Sæther. *Stochastic population dynamics in Ecology and conservation*. Oxford University Press, Oxford, 2003.

[132] R. Lande, B. Sæther, and S. Engen. Threshold harvesting for sustainability of fluctuating resources. *Ecology*, 78:1341–1350, 1997.

[133] P. A. Larkin. An epitaph for the concept of maximum sustained yield. *Transactions of the American Fisheries Society*, 106(1):1–11, 1977.

[134] J. M. Lawrence. *Sea Urchins: Biology and Ecology*. Elsevier, London, 3rd edition, 2013.

[135] N. N. Leonov. Map of the line onto itself. *Radiofisica*, 3(3):942–956, 1959.

[136] B. Leung, J. M. Drake, and D. M. Lodge. Predicting invasions: propagule pressure and the gravity of Allee effects. *Ecology*, 85:1651–1660, 2004.

[137] S. A. Levin and R. M. May. A note on difference-delay equations. *Theoretical Population Biology*, 9(2):178–187, 1976.

[138] X. Li. Analysis of complete stability for discrete-time cellular neural networks with piecewise linear output functions. *Neural Computation*, 21(5):1434–1458, 2009.

[139] A. Liebhold and J. Bascompte. The Allee effect, stochastic dynamics and the eradication of alien species. *Ecology Letters*, 6(2):133–140, 2003.

[140] E. Liz. Local stability implies global stability in some one-dimensional discrete single-species models. *Discrete and Continuous Dynamical Systems. Series B*, 7(1):191–199, 2007.

[141] E. Liz. How to control chaotic behaviour and population size with proportional feedback. *Physics Letters A*, 374(5):725–728, 2010.

[142] E. Liz and S. Buedo-Fernández. A new formula to get sharp global stability criteria for one-dimensional discrete-time models. *Qualitative Theory of Dynamical Systems*, 2019. Published online, 12 pp. doi: https://doi.org/10.1007/s12346-018-00314-4.

[143] E. Liz and A. Ruiz-Herrera. The hydra effect, bubbles, and chaos in a simple discrete population model with constant effort harvesting. *Journal of Mathematical Biology*, 65(5):997–1016, 2012.

[144] L. E. Loe, I. M. Rivrud, E. L. Meisingset, S. Bøe, M. Hamnes, V. Veiberg, and A. Mysterud. Timing of the hunting season as a tool to redistribute harvest of migratory deer across the landscape. *European Journal of Wildlife Research*, 62(3):315–323, 2016.

[145] V. J. López and E. Parreño. L.A.S. and negative Schwarzian derivative do not imply G.A.S. in Clark's equation. *Journal of Dynamics and Differential Equations*, 28(2):339–374, 2016.

[146] K. Lorenzen. Population dynamics and potential of fisheries stock enhancement: practical theory for assessment and policy analysis. *Philosophical Transactions of the Royal Society B: Biological Sciences*, 360(1453):171–189, 2005.

[147] K. Lorenzen. Understanding and managing enhancement fisheries systems. *Reviews in Fisheries Science*, 16(1-3):10–23, 2008.

[148] D. Ludwig. Management of stocks that may collapse. *Oikos*, 83(2):397–402, 1998.

[149] D. Ludwig, R. Hilborn, and C. Walters. Uncertainty, resource exploitation, and conservation: lessons from history. *Science*, 260:17, 36, 1993.

[150] P. Lundberg, E. Ranta, J. Ripa, and V. Kaitala. Population variability in space and time. *Trends in Ecology & Evolution*, 15(11):460–464, 2000.

[151] A. S. Martínez, R. S. González, and L. Espíndola. Generalized exponential function and discrete growth models. *Physica A*, 388:2922–2930, 2009.

[152] M. N. Maunder. Maximum sustainable yield. In S. E. Jørgensen and B. Fath, editors, *Encyclopedia of Ecology*, pages 2292 – 2296. Academic Press, Oxford, 2008.

[153] R. M. May. Biological populations with nonoverlapping generations: stable points, stable cycles, and chaos. *Science*, 186:645–647, 1974.

[154] R. M. May. Simple mathematical models with very complicated dynamics. *Nature*, 261(5560):459–467, 1976.

[155] R. M. May and A. R. McLean. *Theoretical Ecology: Principles and Applications*. Oxford University Press, New York, 2007.

[156] J. Maynard Smith and M Slatkin. The stability of predator-prey systems. *Ecology*, 54:384–391, 1973.

[157] H. I. McCallum. Effects of immigration on chaotic population dynamics. *Journal of Theoretical Biology*, 154(3):277–284, 1992.

[158] M. A. McCarthy. The Allee effect, finding mates and theoretical models. *Ecological Modelling*, 103(1):99–102, 1997.

[159] B. A Melbourne and A. Hastings. Extinction risk depends strongly on factors contributing to stochasticity. *Nature*, 454(7200):100, 2008.

[160] A. P. Møller, E. Flensted-Jensen, K. Klarborg, W. Mardal, and J. T. Nielsen. Climate change affects the duration of the reproductive season in birds. *Journal of Animal Ecology*, 79(4):777–784, 2010.

[161] K. Morita, T. Saito, Y. Miyakoshi, M. Fukuwaka, T. Nagasawa, and M. Kaeriyama. A review of Pacific salmon hatchery programmes on Hokkaido Island, Japan. *ICES Journal of Marine Science*, 63(7):1353–1363, 2006.

[162] R. M. Nisbet and W. S. C. Gurney. Population dynamics in a periodically varying environment. *Journal of Theoretical Biology*, 56(2):59–475, 1976.

[163] H. E. Nusse and J. A. Yorke. Border-collision bifurcations including 'period two to period three' for piecewise smooth systems. *Physica D: Nonlinear Phenomena*, 57(1-2):39–57, 1992.

[164] E. Ott, C. Grebogi, and J. A. Yorke. Controlling chaos. *Physical Review Letters*, 64(11):1196–1199, 1990.

[165] A. Panchuk, I. Sushko, and V. Avrutin. Bifurcation structures in a bimodal piecewise linear map: chaotic dynamics. *International Journal of Bifurcation and Chaos*, 25(03):1530006, 2015.

[166] A. Panchuk, I. Sushko, and V. Avrutin. Bifurcation structures in a bimodal piecewise linear map. *Frontiers in Applied Mathematics and Statistics*, 3(7), 2017.

[167] A. Panchuk, I. Sushko, B. Schenke, and V. Avrutin. Bifurcation structures in a bimodal piecewise linear map: regular dynamics. *International Journal of Bifurcation and Chaos*, 23(12):1330040, 2013.

[168] S. Parthasarathy and S. Sinha. Controlling chaos in unidimensional maps using constant feedback. *Physical Review E*, 51(6):6239–6242, 1995.

[169] J. Perán and D. Franco. Global convergence of the second order Ricker equation. *Applied Mathematics Letters*, 47:47–53, 2015.

[170] S. L. Pimm. The complexity and stability of ecosystems. *Nature*, 307:321–326, 1984.

[171] H. Poincaré and R. Magini. *Les méthodes nouvelles de la mécanique céleste*. Gauthier Villars, Paris, 1899.

[172] E. Ranta, V. Kaitala, and P. Lundberg. Population variability in space and time: the dynamics of synchronous population fluctuations. *Oikos*, 83(2):376–382, 1998.

[173] I. I. Ratikainen, J. A. Gill, T. G. Gunnarsson, W. J. Sutherland, and H. Kokko. When density dependence is not instantaneous: theoretical developments and management implications. *Ecology Letters*, 11(2):184–198, 2008.

[174] C. Reid, N. Caputi, S. de Lestang, and P. Stephenson. Assessing the effects of moving to maximum economic yield effort level in the western rock lobster fishery of Western Australia. *Marine Policy*, 39:303–313, 2013.

[175] F. J. Richards. A flexible growth function for empirical use. *Journal of Experimental Botany*, 10:290–301, 1959.

[176] W. E. Ricker. Stock and recruitment. *Journal of the Fisheries Board of Canada*, 11(5):559–623, 1954.

[177] F. Roccati. Analysis of a predator-prey model with group defense and pack hunting. Master's thesis, University of Turin, Department of Mathematics, 2015.

[178] M. L. Rosenzweig. Paradox of enrichment: destabilization of exploitation ecosystems in ecological time. *Science*, 171(3969):385–387, 1971.

[179] G. Roth and S. J. Schreiber. Pushed beyond the brink: Allee effects, environmental stochasticity, and extinction. *Journal of Biological Dynamics*, 8(1):187–205, 2014.

[180] T. Royama. *Analytical population dynamics*. Chapman & Hall, London, 2012.

[181] J. Rubió-Massegú and V. Mañosa. On the enveloping method and the existence of global Lyapunov functions. *Journal of Difference Equations and Applications*, 13(11):1029–1035, 2007.

[182] B. Ryals and R. J. Sacker. Global stability in the 2D Ricker equation. *Journal of Difference Equations and Applications*, 21(11):1068–1081, 2015.

[183] P. Sah and S. Dey. Stabilizing spatially-structured populations through adaptive limiter control. *PloS One*, 9(8):e105861, 2014.

[184] P. Sah, J. P. Salve, and S. Dey. Stabilizing biological populations and metapopulations through adaptive limiter control. *Journal of Theoretical Biology*, 320:113–123, 2013.

[185] B. K. Sandercock, E. B. Nilsen, H. Brøseth, and H. C. Pedersen. Is hunting mortality additive or compensatory to natural mortality? Effects of experimental harvest on the survival and cause-specific mortality of willow ptarmigan. *Journal of Animal Ecology*, 80(1):244–258, 2011.

[186] P. T. Saunders, J. H. Koeslag, and J. A. Wessels. Integral rein control in Physiology. *Journal of Theoretical Biology*, 194:163–173, 1998.

[187] M. B. Schaefer. Fisheries dynamics and the concept of maximum equilibrium catch. *Proceedings of the Gulf and Caribbean Fisheries Institute*, 6:1–11, 1954.

[188] I. Scheuring. Allee effect increases the dynamical stability of populations. *Journal of Theoretical Biology*, 199(4):407–414, 1999.

[189] S. J. Schreiber. Chaos and population disappearances in simple ecological models. *Journal of Mathematical Biology*, 42(3):239–260, 2001.

[190] S. J. Schreiber. Allee effects, extinctions, and chaotic transients in simple population models. *Theoretical Population Biology*, 64(2):201–209, 2003.

[191] H. Seno. A paradox in discrete single species population dynamics with harvesting/thinning. *Mathematical Biosciences*, 214(1):63–69, 2008.

[192] H. Seno. Native intra-and inter-specific reactions may cause the paradox of pest control with harvesting. *Journal of Biological Dynamics*, 4(3):235–247, 2010.

[193] O. Sharkovskiĭ. Coexistence of cycles of a continuous map of the line into itself. *International Journal of Bifurcation and Chaos*, 5(5):1263–1273, 1995.

[194] D. Singer. Stable orbits and bifurcation of maps of the interval. *SIAM Journal on Applied Mathematics*, 35(2):260–267, 1978.

[195] S. Sinha. Unidirectional adaptive dynamics. *Physical Review E*, 49:4832–4842, 1994.

[196] S. Sinha and S. Parthasarathy. Unusual dynamics of extinction in a simple ecological model. *Proceedings of the National Academy of Sciences*, 93(4):1504–1508, 1996.

[197] R. V. Solé, J. G. Gamarra, M. Ginovart, and D. López. Controlling chaos in ecology: from deterministic to individual-based models. *Bulletin of Mathematical Biology*, 61(6):1187–1207, 1999.

[198] P. A. Stephens, W. J. Sutherland, and R. P. Freckleton. What is the Allee effect? *Oikos*, 87(1):185–190, 1999.

[199] D. K. Stevenson. Management of a tropical fish pot fishery for maximum sustainable yield. *Proceedings of the Gulf and Caribbean Fisheries Institute*, 30:95–114, 1978.

[200] L. Stone and D. Hart. Effects of immigration on the dynamics of simple population models. *Theoretical Population Biology*, 55(3):227–234, 1999.

[201] A. W. Stoner and M. Ray-Culp. Evidence for Allee effects in an over-harvested marine gastropod: density-dependent mating and egg production. *Marine Ecology Progress Series*, 202:297–302, 2000.

[202] S. Tang and L. Chen. The effect of seasonal harvesting on stage-structured population models. *Journal of Mathematical Biology*, 48(4):357–374, 2004.

[203] C. M. Taylor and A. Hastings. Allee effects in biological invasions. *Ecology Letters*, 8(8):895–908, 2005.

[204] M. D. Taylor. Preliminary evaluation of the costs and benefits of prawn stocking to enhance recreational fisheries in recruitment limited estuaries. *Fisheries Research*, 186(2):478–487, 2017.

[205] R. A. Taylor, A. White, and J. A. Sherratt. How do variations in seasonality affect population cycles? *Proceedings of the Royal Society B*, 280(1754):20122714, 2013.

[206] H. R. Thieme. *Mathematics in population biology*. Princeton University Press, Princeton, 2003.

[207] H. Thunberg. Periodicity versus chaos in one-dimensional dynamics. *SIAM Review*, 43(1):3–30, 2001.

[208] P. C. Tobin, L. Berec, and A. M. Liebhold. Exploiting Allee effects for managing biological invasions. *Ecology Letters*, 14(6):615–624, 2011.

[209] P. C. Tobin, S. L. Whitmire, D. M. Johnson, O. N. Bjørnstad, and A. M. Liebhold. Invasion speed is affected by geographical variation in the strength of Allee effects. *Ecology Letters*, 10(1):36–43, 2007.

[210] L. C. Todman, F. C. Fraser, R. Corstanje, L. K. Deeks, J. A. Harris, M. Pawlett, K. Ritz, and A. P. Whitmore. Defining and quantifying the resilience of responses to disturbance: a conceptual and modelling approach from soil science. *Scientific Reports*, 6:28426, 2016.

[211] F. Tramontana, L. Gardini, V. Avrutin, and M. Schanz. Period adding in piecewise linear maps with two discontinuities. *International Journal of Bifurcation and Chaos*, 22(03):1250068, 2012.

[212] S. Tung, A. Mishra, and S. Dey. A comparison of six methods for stabilizing population dynamics. *Journal of Theoretical Biology*, 356(0):163–173, 2014.

[213] S. Tung, A. Mishra, and S. Dey. Simultaneous enhancement of multiple stability properties using two-parameter control methods in *Drosophila melanogaster*. *Ecological Complexity*, 26:128–136, 2016.

[214] S. Tung, A. Mishra, and S. Dey. Stabilizing the dynamics of laboratory populations of *Drosophila melanogaster* through upper and lower limiter controls. *Ecological Complexity*, 25:18–25, 2016.

[215] P Turchin. *Complex population dynamics: a theoretical/empirical synthesis*. Princeton University Press, Princeton, 2003.

[216] G. A. K. van Voorn, L. Hemerik, M. P. Boer, and B. W. Kooi. Heteroclinic orbits indicate overexploitation in predator–prey systems with a strong Allee effect. *Mathematical Biosciences*, 209(2):451–469, 2007.

[217] C. Wagner and R. Stoop. Optimized chaos control with simple limiters. *Physical Review E*, 63(1):017201, 2000.

[218] C. Walters and A. M. Parma. Fixed exploitation rate strategies for coping with effects of climate change. *Canadian Journal of Fisheries and Aquatic Sciences*, 53(1):148–158, 1996.

[219] J. A. Wilson, R. Townsend, P. Kelban, S. McKay, and J. French. Managing unpredictable resources: traditional policies applied to chaotic populations. *Ocean and Shoreline Management*, 13(3-4):179–197, 1990.

[220] C. Xu, M. S. Boyce, and D. J. Daley. Harvesting in seasonal environments. *Journal of Mathematical Biology*, 50(6):663–682, 2005.

[221] A. Yoshimura, K. Kawasaki, F. Takasu, K. Togashi, K. Futai, and N. Shigesada. Modeling the spread of pine wilt disease caused by nematodes with pine sawyers as vector. *Ecology*, 80:1691–1702, 1999.

[222] G. Zhong and F. Ayrom. Periodicity and chaos in Chua's circuit. *IEEE Transactions on Circuits and Systems*, 32(5):501–503, 1985.